# THE ST. GEORGE GROUP (LOWER ORDOVICIAN), WESTERN NEWFOUNDLAND: SEDIMENTOLOGY, DIAGENESIS, AND CRYPTALGAL STRUCTURES

CENTRE FOR NEWFOUNDLAND STUDIES

TOTAL OF 10 PAGES ONLY
MAY BE XEROXED

(Without Author's Permission)

BRIAN RICHARD PRATT

000194

CENTRE FOR NFLD. STUDIES
OCT 5 1981
MEMORIAL UNIVERSITY
OF NEWFOUNDLAND

National Library of Canada
Collections Development Branch

Canadian Theses on
Microfiche Service

Bibliothèque nationale du Canada
Direction du développement des collections

Service des thèses canadiennes
sur microfiche

NOTICE

The quality of this microfiche is heavily dependent upon the quality of the original thesis submitted for microfilming. Every effort has been made to ensure the highest quality of reproduction possible.

If pages are missing, contact the university which granted the degree.

Some pages may have indistinct print especially if the original pages were typed with a poor typewriter ribbon or if the university sent us a poor photocopy.

Previously copyrighted materials (journal articles, published tests, etc.) are not filmed.

Reproduction in full or in part of this film is governed by the Canadian Copyright Act, R.S.C. 1970, c. C-30. Please read the authorization forms which accompany this thesis.

THIS DISSERTATION
HAS BEEN MICROFILMED
EXACTLY AS RECEIVED

AVIS

La qualité de cette microfiche dépend grandement de la qualité de la thèse soumise au microfilmage. Nous avons tout fait pour assurer une qualité supérieure de reproduction.

S'il manque des pages, veuillez communiquer avec l'université qui a conféré le grade.

La qualité d'impression de certaines pages peut laisser à désirer, surtout si les pages originales ont été dactylographiées à l'aide d'un ruban usé ou si l'université nous a fait parvenir une photocopie de mauvaise qualité.

Les documents qui font déjà l'objet d'un droit d'auteur (articles de revue, examens publiés, etc.) ne sont pas microfilmés.

La reproduction, même partielle, de ce microfilm est soumise à la Loi canadienne sur le droit d'auteur, SRC 1970, c. C-30. Veuillez prendre connaissance des formules d'autorisation qui accompagnent cette thèse.

LA THÈSE A ÉTÉ
MICROFILMÉE TELLE QUE
NOUS L'AVONS REÇUE

Ottawa, Canada
K1A 0N4

NL-339 (Rev. 8/80)

# THE ST. GEORGE GROUP (LOWER ORDOVICIAN), WESTERN NEWFOUNDLAND: SEDIMENTOLOGY, DIAGENESIS, AND CRYPTALGAL STRUCTURES

by

© Brian R. Pratt, B.Sc.

A Thesis submitted in partial fulfillment
of the requirements for the degree of
Master of Science

Department of Geology
Memorial University of Newfoundland

St. John's

September 1979

## ABSTRACT

Detailed stratigraphic examination was undertaken of the Lower Ordovician Isthmus Bay, Catoche, and Aguathuna Formations, St. George Group, in western Newfoundland. Lithologic descriptions were grouped into seven peritidal lithotopes, with additional descriptions of the effects of erosion and subaerial exposure, such as hardground formation, evaporite precipitation, and karstification. The vertical oscillation of lithotopes generates sequences rather than ideal shallowing upward cycles. These sequences show that the continental shelf in western Newfoundland, in Lower Ordovician time, was a patchwork of low-relief islands and banks whose character differed geographically and changed with time, as the shelf slowly subsided. Slight uplift and subaerial exposure of the shelf occurred at the end of the Lower Ordovician, resulting in irregular erosion.

Cryptalgal structures of very diverse character are related to environmental and biological parameters that interacted in a complex way. Laminated structures, stromatolites and cryptalgal laminites, formed in inter- and supratidal areas areas characterized by the episodic addition of sediment. Thrombolite mounds were common in the subtidal zone, where sedimentation onto algal mats resulted in unlaminated microstructure. In places, sponges, primitive corals and the 'calcareous' algae Renalcis contributed to their framework. These mounds are ecologic reefs of surprising complexity, supporting a benthic flora and fauna of all major trophic groups occupying most niches. These reefs occur in the

transition period from algal-dominated bioherms to metazoan-dominated bioherms of the later Phanerozoic. Cryptalgal microstructures can be separated into a number of recurring types and a classification is proposed that can be amended to include types not recognized in the St. George. 'Calcareous' algae such as Girvanella and Renalcis are interpreted to be diagenetic taxa resulting from the calcification of blue-green algae.

The calcareous sediments of the St. George underwent diagenetic modification beginning on the sea floor and continuing until the Upper Mississippian. Processes included synsedimentary and burial calcite cementation, neomorphism, silicate authigenesis, silicification, burial and epigenetic dolomitization. Galena and sphalerite mineralization occurred during epigenetic dolomitization and colloform vein formation. The paragenetic sequence seems typical of Lower Paleozoic peritidal shelf and epeiric carbonate sediments.

## ACKNOWLEDGEMENTS

I especially thank my supervisor and saviour Dr. N. P. James who provided the opportunity to study the rocks of western Newfoundland and who gave generously of his time in all stages for energetic and stimulating discussion and advice. PetroCanada Exploration Inc. funded the study by providing field and thesis preparation expenses, and bailing the university out for fellowship money. I am especially indebted to Drs. E. E. Pelzer and V. Schmidt for their interest. Mr. D. Furey, able and enthusiastic field dogsbody, greatly increased the efficiency and enjoyment of the field work. Mr. M. MacIsaac helped lug samples back to St. John's and spotted Bathyurus at Table Point. Paleontological advice was provided by Drs. R. A. Fortey (British Museum), R. H. Flower (New Mexico Bureau of Mines and Mineral Resources), J. E. Sorauf (State University of New York-Binghamton), and E. L. Yochelson (U.S. Geological Survey), and Messrs. S. Stouge and D. Boyce (Memorial University). Dr. J. D. Smewing (Open University) helped with authigenic feldspar identification. Mr. T. Lane (Newfoundland Zinc Corp.) discussed freely aspects of ore emplacement at Daniel's Harbour. Mr. N. Higgins (Memorial University) performed the fluid inclusion analyses and provided their interpretation. Members of the Dept. of Biology discussed aspects of blue-green algae. Dr. D. Skevington (Chairman) provided funds to attend a beneficial trace fossil short course and associated field trips. Other assorted professors, post-docs, and grad students and Memorial discussed many aspects of the study and

related Newfoundland geology. Field accommodation was aided by the Newfoundland Parks Branch, the Bay St. George Community College, and the people of western Newfoundland. Samples were stowed temporarily at the Corner Brook campus of Memorial University through the courtesy of Mr. P. Stratton. Vast numbers of thin sections were cheerfully prepared by Messrs. L. Warford and F. Thornhill. Mr. W. Marsh photographed the plates which were printed by Ms. G. Smith (Dept. of Engineering). The Educational Television section printed the line drawings. Ms. C. Talkington and Ms. B. Neame entered the fray and typed the final rough draft; the final draft was typed by the devoted Ms. C. Talkington, Ms. I. Kirkham, and B. Beepough, esq.

CONTENTS

Page

LIST OF TABLES . . . . . ix

LIST OF FIGURES . . . . . x

CHAPTER 1 - INTRODUCTION

PURPOSE . . . . . 1
METHODS . . . . . 3
REGIONAL SETTING AND STRATIGRAPHY . . . . . 4

CHAPTER 2 - SEDIMENTOLOGY

INTRODUCTION . . . . . 10
LITHOLOGIES . . . . . 12
Lithotope A . . . . . 12
Lithotope B . . . . . 13
Lithotope C . . . . . 14
Lithotope D . . . . . 16
Lithotope E . . . . . 18
Lithotope F . . . . . 19
Lithotope G . . . . . 21
SECONDARY LITHOLOGIC FEATURES . . . . . 22
Channels . . . . . 22
Ooids . . . . . 24
Evaporites . . . . . 24
Dolomitized laths . . . . . 25
Dolomitized nodules . . . . . 25
Silicified anhydrite . . . . . 25
Hardgrounds . . . . . 27
Paleokarst . . . . . 31
Solution pitting . . . . . 31
Collapse brecciation . . . . . 32
Subaerial rubble . . . . . 34
LITHOLOGICAL SUMMARY . . . . . 35
REGIONAL CORRELATION . . . . . 36
LATERAL VARIATION . . . . . 39
FACIES SEQUENCES . . . . . 41
FACIES MODELS . . . . . 43
ORIGIN OF "CYCLES" . . . . . 47

CHAPTER 3 - CRYPTALGAL STRUCTURES

INTRODUCTION . . . . . 52
LAMINATED STRUCTURES . . . . . 53
Stromatolites . . . . . 53
Hemispheroidal stromatolites . . . . . 53
Columnar stromatolites . . . . . 59
Aberrant forms . . . . . 59
Discussion . . . . . 61
Cryptalgal laminites . . . . . 66
Oncolites . . . . . 68

Page

UNLAMINATED STRUCTURES . . . . . 69
Thrombolites . . . . . 69
Thrombolite morphology . . . . . 69
Thrombolite mounds . . . . . 73
Thrombolite-metazoan mounds . . . . . 76
Discussion . . . . . 77
MOUND COMPLEXES . . . . . 84
Introduction . . . . . 84
Vertical cryptalgal associations . . . . . 84
Green Head bioherm complex . . . . . 87
Hare Bay bioherm complex . . . . . 97
PALEOECOLOGY OF BIOHERMS . . . . . 98
CRYPTALGAL MICROSTRUCTURE . . . . . 104
Introduction . . . . . 104
Microstructural types . . . . . 105
Massive . . . . . 105
Vermiform . . . . . 107
Tubiform . . . . . 107
Cavernous . . . . . 108
Peloidal . . . . . 108
Spongy . . . . . 108
Cancellous . . . . . 112
Distribution of microstructures . . . . . 112
ALGAE . . . . . 116
Renalcis . . . . . 116
Girvanella . . . . . 121
SUMMARY . . . . . 126
Morphology and structure . . . . . 126
Blue-green algal communities . . . . . 129

CHAPTER 4 - DIAGENESIS
INTRODUCTION . . . . . 133
CALCITE . . . . . 133
Cementation . . . . . 133
Introduction . . . . . 133
Radial bladed . . . . . 133
Spar . . . . . 134
Neomorphism . . . . . 137
Introduction . . . . . 137
Spherulitic spar . . . . . 137
Microspar . . . . . 138
Pseudospar . . . . . 139
OOLITES . . . . . 141
Introduction . . . . . 141
Radial . . . . . 141
Concentric . . . . . 142
Combination . . . . . 142
Discussion . . . . . 144
DOLOMITE . . . . . 147
Introduction . . . . . 147
Syngenetic dolomite . . . . . 147
Diagenetic dolomite . . . . . 147
Epigenetic dolomite . . . . . 154
CHERT . . . . . 160
Introduction . . . . . 160

Page

Cryptoquartz . . . . . 161
Microquartz . . . . . 161
Limpid megaquartz . . . . . 163
Flamboyant megaquartz . . . . . 164
Lutecite . . . . . 164
Quartzine . . . . . 164
Chalcedony . . . . . 166
Discussion . . . . . 168
AUTHIGENIC SILICATES . . . . . 171
CRUSTIFICATION . . . . . 175
PARAGENESIS . . . . . 178

CHAPTER 5 - ST. GEORGE-TABLE HEAD CONTACT
INTRODUCTION . . . . . 181
TABLE POINT . . . . . 181
AGUATHUNA . . . . . 186
OTHER LOCALITIES . . . . . 191
DISCUSSION . . . . . 193

CHAPTER 6 - CONCLUSIONS . . . . . 195

REFERENCES . . . . . 198

APPENDICES - MEASURED STRATIGRAPHIC SECTIONS . . . . . 208
A. ISTHMUS BAY . . . . . 209
B. NORTHEAST GRAVELS . . . . . 227
C. AGUATHUNA QUARRY . . . . . 230
D. PORT AU CHOIX . . . . . 233
E. EDDIES COVE WEST . . . . . 238
F. BOAT HARBOUR . . . . . 247

# LIST OF TABLES

Table | Page

1. Stratigraphic nomenclature, Great Northern Peninsula . . . .
2. Stratigraphic nomenclature, Port au Port Peninsula . . . . .
3. Lithological characteristics of lithotopes . . . . . .
4. Distribution of cryptalgal microstructures . . . . . .

# LIST OF FIGURES


| Figure | | Page |
|---|---|---|
| 1. | Map of western Newfoundland | 2 |
| 2. | Lithotopes A, C, and D | 15 |
| 3. | Lithotopes D and E, and channel | 20 |
| 4. | Evaporites | 26 |
| 5. | Hardground and paleokarst horizons | 29 |
| 6. | Outcrop sketch of potholes | 30 |
| 7. | Outcrop sketch of paleokarst collapse breccia | 33 |
| 8. | Regional correlation of the Isthmus Bay Formation | 37 |
| 9. | Correlation of the Aguathuna Formation across the Gravels | 40 |
| 10. | Plots of vertical distribution of lithotopes | 42 |
| 11. | Matrices of the abundance of lithotope contacts | 44 |
| 12. | Lithotope sequences | 45 |
| 13. | Hypothetical island facies maps | 48 |
| 14. | Hypothetical patterns of progradation and regradation | 50 |
| 15. | Types of stacked hemispheroidal stromatolites | 55 |
| 16. | Hemispheroidal stromatolites | 56 |
| 17. | Sequence of development of eroded cryptalgal structures | 57 |
| 18. | Hemispheroidal and columnar stromatolites | 58 |
| 19. | Columnar stromatolites | 60 |
| 20. | Aberrant columnar stromatolites | 62 |
| 21. | Cryptalgal laminites and oncolites | 67 |
| 22. | Thrombolite tracings | 70 |
| 23. | Thrombolites | 71 |
| 24. | Thrombolites | 72 |
| 25. | Thrombolite mounds | 74 |
| 26. | Outcrop plan of linear thrombolite mounds | 75 |
| 27. | Archaeoscyphiid sponges | 78 |
| 28. | Tracings of thrombolite-metazoan mounds | 79 |
| 29. | Vertical changes in cryptalgal structure morphology | 82 |
| 30. | Columnar sections of three vertical cryptalgal associations | 85 |
| 31. | Outcrop sketch of Green Head bioherm complex | 89 |
| 32. | Thrombolite-*Lichenaria*-*Renalcis* boundstone | 90 |
| 33. | Serial sections of thrombolite-*Lichenaria*-*Renalcis* boundstone | 91 |
| 34. | Tracings of Green Head bioherm boundstones | 93 |
| 35. | Green Head bioherm complex | 94 |
| 36. | Reconstruction of living thrombolite mounds | 102 |
| 37. | Reconstruction of living Green Head bioherm | 103 |
| 38. | Sketch of seven microstructural types | 106 |
| 39. | Microborings and cryptalgal microstructure | 109 |
| 40. | Cryptalgal microstructure | 110 |
| 41. | Cryptalgal microstructure | 111 |
| 42. | Cryptalgal microstructure | 113 |
| 43. | *Renalcis* | 117 |
| 44. | *Renalcis* | 118 |
| 45. | *Girvanella* | 122 |
| 46. | Sketches of the six modes of occurrence of *Girvanella* | 123 |
| 47. | Cryptalgal morphologram of structure type and tidal height | 127 |

48. Zonation of cryptalgal structures . . . . . 128
49. Calcite cement and neomorphic spar . . . . . 136
50. Neomorphic calcite . . . . . 140
51. Ooids . . . . . 143
52. Diagenetic dolomitization . . . . . 149
53. Compaction effects . . . . . 152
54. Epigenetic dolomitization . . . . . 156
55. Epigenetic dolomite . . . . . 157
56. Chert . . . . . 162
57. Chert . . . . . 165
58. Chert . . . . . 167
59. Authigenic silicates . . . . . 172
60. Sketch of colloform Pb-Zn veins . . . . . 176
61. Paragenetic sequence of diagenetic events . . . . . 179
62. Outcrop sketch of St. George-Table Head contact, Table Point . . . . . 183
63. St. George-Table Head contact, Table Point . . . . . 184
64. Outcrop sketch of St. George-Table Head contact, Aguathuna Quarry . . . . . 187
65. St. George-Table Head contact, Aguathuna Quarry . . . . 189
66. Sequence of formation of silcrete, top of St. George . 192

(In reference to actual stratigraphic units, the following abbreviations are used in figure captions to refer to the measured section: IB = Isthmus Bay; NEG = Northeast Gravels; AQ = Aguathuna Quarry; PAC = Port au Choix; ECW = Eddies Cove West; BH = Boat Harbour.)

# CHAPTER 1 - INTRODUCTION

## PURPOSE

The Lower Cambrian to Middle Ordovician carbonate rocks of western Newfoundland represent the shallow-water deposits of a largely equatorial continental shelf that rimmed the Lower Paleozoic Proto-Atlantic Iapetus Ocean. The continental shelf extended from New Mexico to Newfoundland, and beyond to the British Isles, Greenland and Spitsbergen. A coeval epeiric sea spread into the continental interior of North America which was also bound in the west by a continental margin of similar depositional characteristics.

Limestones and dolostones of the Lower Ordovician St. George Group are very well exposed at many places along the coast of western Newfoundland, from Port au Port Peninsula in the south to Hare Bay and Boat Harbour in the north (Fig. 1). In general, these strata are much less deformed than equivalent rocks in the Appalachians to the south in the United States. The first stratigraphic framework for western Newfoundland was established in 1934 by Schuchert and Dunbar. Since then, the Lower Ordovician sediments have received only cursory attention in mapping studies, until the investigations of Lévesque (1977) and Knight (1977b, 1978). The paleontology of the St. George was treated in Billings' (1865) classic monograph, and later studies permit regional biostratigraphic correlation. The sedimentology of the St. George has received a broad treatment in Lévesque (1977). Reconnaissance diagenetic studies were undertaken by Smit (1971), Swett and Smit (1972), and Collins and Smith (1975).

The purpose of this study is: (1) to interpret, in detail,

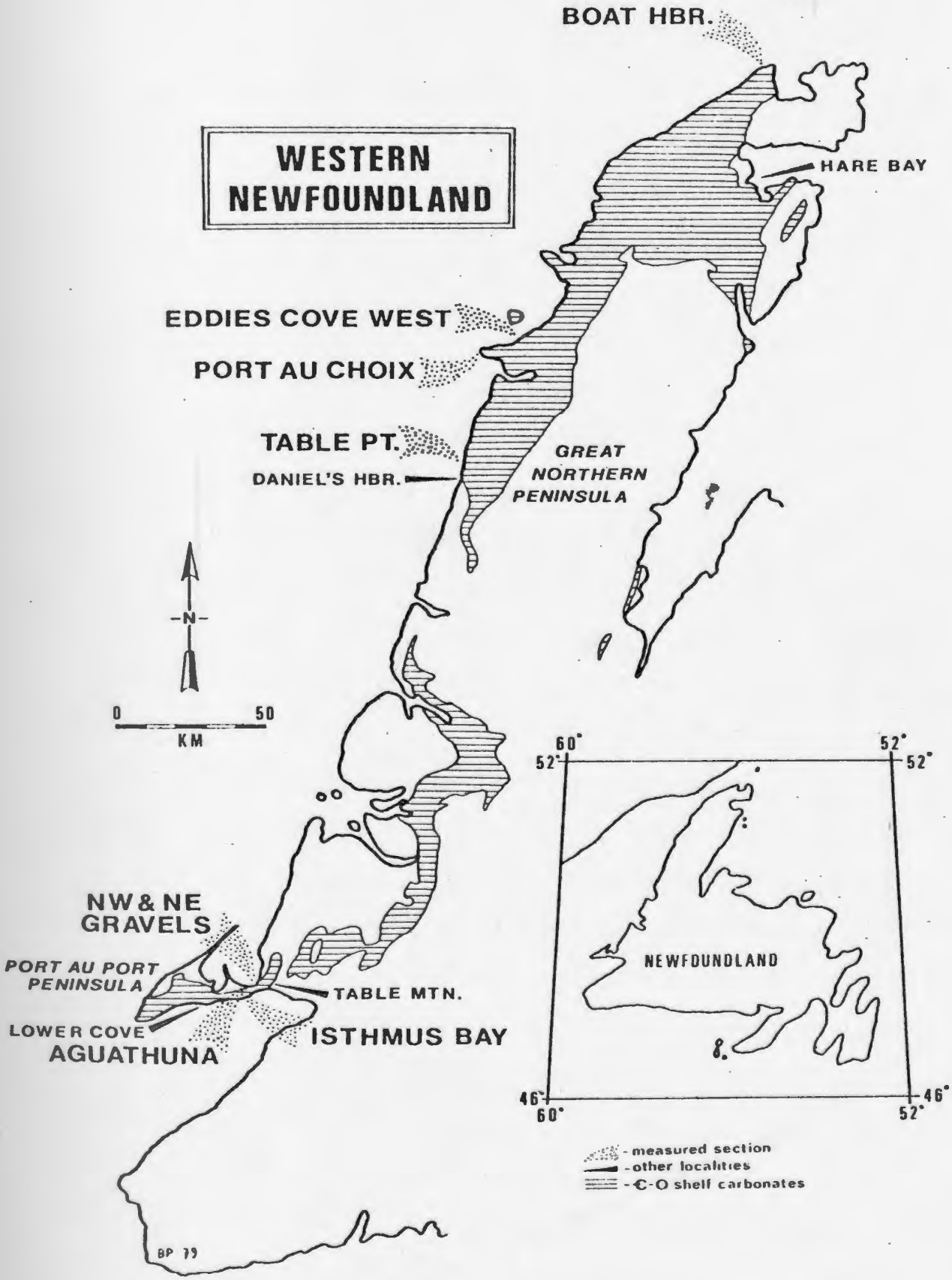


Figure 1: Map of western Newfoundland showing location of sections measured and localities examined in this study.

the sedimentary environments and record the vertical and lateral relations between them, (2) to describe the different types of cryptalgal and biohermal structures, (3) to document the character and timing of the diagenetic processes involved in lithogenesis, and (4) to characterize the nature of the unconformity separating the St. George and overlying Table Head Groups.

## METHODS

Stratigraphic sections were measured in seven areas along the coast of western Newfoundland (Fig. 1): Boat Harbour, Eddies Cove West, Port au Choix, Table Point, Isthmus Bay and northwest of the Gravels, northeast of the Gravels, and Aguathuna Quarry. In addition, strata were examined for comparative purposes in Hare Bay, Table Mountain, Daniel's Harbour, and Lower Cove on Port au Port Peninsula. Sections were measured with a range pole to the nearest 0.1 metre. Covered intervals were either measured with the range pole, or estimated using paced distances and bed geometry when necessary.

Stratigraphic subdivisions were made in the field on the basis of lithologic character, including rock type (limestone or dolostone), depositional texture (mudstone, wackestone, packstone, grainstone, and boundstone), and sedimentary structures. Particular attention was paid to contacts between units, where not obscured by stylolitization. Over 800 samples were collected. Fossil specimens were also collected and keyed into stratigraphic sections for biostratigraphic purposes. In the laboratory, rock samples were slabbed, ground with carborundum grit, and etched with dilute hydrochloric acid. Acetate peels were made

from nearly all samples, and thin sections prepared from selected samples for further petrographic study. Most thin sections were stained with alizarin red-S and potassium ferricyanide. In total, about 450 thin sections and approximently 800 peels were examined in this study.

## REGIONAL SETTING AND STRATIGRAPHY

The island of Newfoundland is the northern termination of the Appalachian orogen. The island has been divided into four tectono-stratigraphic zones by Williams (1979): the Avalon, Gander, Dunnage, and Humber Zones. The Humber Zone, in which this study is located, represents the deposits of the Lower Paleozoic contintental margin in eastern North America (Williams and Stevens, 1974). Widespread shallow-water carbonate deposition on the margin began in Middle Cambrian time, and continued with occasional interruptions until Middle Ordovician time. Slope and basin deposits, coeval with the shelf sediments, are exposed as allochthonous slices in various places in western Newfoundland. The platform foundered in Middle Ordovician time, and was covered by siliciclastic sediments derived from advancing allochthons of oceanic crust to the east (Stevens, 1970).

The earliest stratigraphical work in western Newfoundland was done by James Richardson (Logan, 1863) who presented the first subdivision of the rocks including those now known as the St. George Group. They were measured in the Port au Choix and Eddies Cove West area, and separated into divisions D,E,F,G,H,I, K,L,M, and N of the Lower Silurian Quebec Group (Table 1). Schuchert and Dunbar (1934), in their study of the stratigraphy

of western Newfoundland, proposed the name St. George series for the Lower Ordocician shallow-water carbonate rocks. The strata exposed from March Point to northwest of the Gravels on Port au Port Peninsula were designated the type section (Table 2). Due to lack of fossil data, included in the St. George series were Richardson's divisions D and E on the Great Northern Peninsula, and rocks on the Port au Port Peninsula now known to be Upper Cambrian in age. They determined that the St. George series overlay the Cambrian March Point series on Port au Port Peninsula, but the lower contact on the Great Northern Peninsula was not observed. The St. George series was overlain unconformably in all places studied by the Middle Ordovician Table Head series (divisions K,L,M, and N of Richardson). Sullivan (1940) questioned the type section along the southern shore of Port au Port Peninsula, pointing out the faulted nature of the whole coast. He also believed the St. George was in fault contact with the underlying Petit Jardin Formation, the latter name proposed by Lochman (1938) after splitting the March Point series. Johnson (1949) discounted the faulted nature of the contact, but noted the barrenness of the section between Cambrian and Ordovician fossil occurrences. Walthier (1949) re-examined the type section and considerably shortened it by placing the lower part into the Petit Jardin Formation.

Limestones and dolostones of Lower Ordovician age were recognized in other parts of western Newfoundland. Cooper (1937) mapped the Hare Bay area and subdivided Lower Ordovician carbonate rocks into the Southern Arm Limestone and the Brent Island Limestone. Betz (1939) mapped the Canada Bay area, and placed Lower Ordovician carbonate rocks into the Chimney Arm Formation.

Table 1. Stratigraphic nomenclature, Great Northern Peninsula

| Logan (1863) | | | Schuchert and Dunbar (1934) | | Whittington and Kindle (1969) | | Kluyver (1975) | | Knight (1977) | | Lévesque (1977) | | James et al. (in prep.) | |
|---|---|---|---|---|---|---|---|---|---|---|---|---|---|---|
| LOWER SILURIAN | Quebec Group | K | MID. ORD. | Table Head Series | | Table Head Group | | Table Head Group | | Table Head Group | | Table Head Form. | | Table Head Group |
| | | I | LOWER ORDOVICIAN | St. George Series | LOWER ORDOVICIAN | St. George Form. | St. George Group | Port au Choix Form. | St. George Group | Siliceous Dolomite Fm. | St. George Formation | Upper Cyclic Mbr. | St. George Group | Aguathuna Form. |
| | | H | | | | | | Catoche Form. | | "Diagenetic Carbonates" | | Middle Limestone Member | | Catoche Form. |
| | | G | | | | | | Barbace Point Form. | | Laignet Pt.Mbr. | | | | |
| | | F | | | | | | | | Catoche Fm. | | | | |
| | | E | | | | | | | | (un-named) | | Lower Cyclic Member | | Isthmus Bay Form. |
| | | D | | | CAMBRIAN | | | | | Watts Bight Form | | | | |
| | | C | CAMBRIAN | | | | | | | Unfortunate Cove Form. | | | Port au Port Group | Petit Jardin Form. |
| | | | | | | | | | | Dolomite Form. | | | | |

Table 2. Stratigraphic nomenclature, Port au Port Peninsula

| Schuchert and Dunbar (1934) | | Lochman (1938) | Whittington and Kindle (1969) | | Besaw (1972) | | Lévesque (1977) | | James et al. (in prep.) | |
|---|---|---|---|---|---|---|---|---|---|---|
| MID. ORD. | Table Head Series | | | Table Head Form. | | Table Head Group | | Table Head Form. | | Table Head Group |
| LOWER ORDOVICIAN | St. George Form. | | LOWER ORDOVICIAN | St. George Form. | St. George Group | Port au Port Unit | St. George Formation | Upper Cyclic Member | St. George Group | Aguathuna Form. |
| | | | | | | White Hills Unit | | | | |
| | | | | | | Pine Tree Unit | | Middle Limestone Member | | Catoche Form. |
| | | | | | | Pigeon Head Unit | | | | |
| | | | | | | Lower Cove Unit | | Lower Cyclic Member | | Isthmus Bay Form. |
| CAMBRIAN | March Point Series | Petit Jardin Form. | CAMBRIAN | Petit Jardin Form. | | | | Petit Jardin Form. | PortauPort Gp. | Petit Jardin Form. |

Cambrian and Ordovician rocks were studied in Bonne Bay by Troelsen (1947) who subdivided the St. George Group into five numbered units, with the contact drawn arbitrarily above the last Cambrian fossiliferous horizon. Troelsen (1947) also suggested that the lower St. George Group may be partially Upper Cambrian in age, because of the large barren interval between horizons containing fossils of the two periods. In the Humber Gorge, Lilly (1961) subdivided the St. George Group into the Hughes Brook and Corner Brook Formations, overlying the Reluctant Head Formation of Cambrian age. Various reconnaissance studies by Oxley (1953), Nelson (1955), Woodward (1957) Riley (1962), Cumming (1968), Tuke (1968), and Smit (1971) considered the St. George Group but did not alter the stratigraphy.

Kindle and Whittington (1965) and Whittington and Kindle (1966) discovered Cambrian trilobites in rocks of the Port au Port and Great Northern Peninsulas previously placed in the St. George Group, and later presented a revised stratigraphic summary (Whittington and Kindle, 1969), pointing out that the St. George Formation was best seen at the eastern end of Port au Port Peninsula.

A number of recent investigators have further subdivided the St. George Group. Besaw (1972) separated the St. George Group into five lithological units which he felt were mappable throughout the Port au Port Peninsula and adjacent mainland Newfoundland. In ascending order, they were the Lower Cove unit, Pigeon Head unit, Pine Tree unit, White Hills unit, and Port au Port unit. The Lower Cove unit was not measured in its entirety, and is now known to include strata of Cambrian age.

Further north, Kluyver (1975) subdivided the portion of the St. George Group exposed at Port au Choix, erecting the Barbace Point Formation, Catoche Formation and Port au Choix Formation, corresponding roughly to Richardson's units G,H, and I respectively. Collins and Smith (1975) employed the informal lithologic names "lower limestone", "dark grey dolomite", and "cyclic dolomite" for correlating drill cores in the Daniel's Harbour area.

In the course of stratigraphical work on the Great Northern Peninsula, Knight (1977a,b; 1978) modified Kluyver's (1975) subdivisions and informally proposed new ones. They are, in ascending order, the Unfortunate Cove Formation, probably spanning the Cambro-Ordovician boundary, Watts Bight Formation and an overlying un-named unit, both approximately equivalent to the Barbace Point Formation, Catoche Formation with the Laignet Point Member at the top, "Diagenetic Carbonates", and Siliceous Dolomite Formation, the latter two equivalent to the Port au Choix Formation. Lévesque (1977) studied the St. George Group in the Port au Port and Port au Choix areas, and reduced it to formational status with three members, the lower cyclic, middle limestone, and upper cyclic members. This three-fold subdivision coped with the problem of local lateral diagenetic changes to coarse epigenetic dolostones, misunderstood by previous investigators. James _et al_. (in prep.) have restored the St. George to group status with three formations, in ascending order the Isthmus Bay Formation, Catoche Formation, and Aguathuna Formation.

# CHAPTER 2 - SEDIMENTOLOGY

## INTRODUCTION

Rocks of the St. George Group have been shown by Lévesque (1977) to be broadly divisible into two different types: (1) shallow-water "cyclic" sequences in the lower and upper parts, and (2) subtidal shelf lithologies in the middle part, corresponding to the three formations of James *et al.* (in prep.), Isthmus Bay, Catoche, and Aguathuna Formations. In this study, detailed lithologic description of most exposed St. George strata in western Newfoundland has been grouped to produce seven lithotopes, which are interpreted to be the deposits of seven distinct shallow-marine peritidal paleoenvironments or facies (Table 3). In addition, secondary lithologic features such as ooids, hardgrounds, evaporites, and subaerial exposure horizons are described. The lithologies are typical for the Lower Paleozoic continental shelf and epeiric sea sediments preserved in North America. Despite the lack of siliciclastics, these Lower Paleozoic rocks show many sedimentary features in common with siliciclastic peritidal sediments. Similar interpretations have been arrived at by previous workers, based on the evidence preserved in the rocks, augmented by the accumulated experience of numerous studies of tropical shallow-marine carbonate environments carried out in the last twenty years. The repetition of lithotopes does not produce ideal cycles, and facies sequences are constructed instead on the basis of the relative abundance of vertical contacts. Using Walther's Law, island sedimentary models are suggested to account for the deposition of the different parts of the St. George.

Table 3. Summary of lithological characteristics of lithotopes

| Lithotope | Facies | Lithological Characteristics | Inter-relationships |
|---|---|---|---|
| A | supratidal | cryptalgal lamination, common mudcracks, frequent doming to low-relief hemispheroidal stromatolites | vertically with C, laterally to D and E |
| B | intertidal stromatolite | hemispheroidal stromatolites, stacked and laterally-linked | vertically with A, flanked by and laterally to D |
| C | bioturbated intertidal | bioturbated, unfossiliferous, thinly bedded dolostone | vertically with D |
| D | intertidal flat | thinly bedded grainstone and mudstone, sporadic burrowing (Chondrites and U-shaped spreite-burrows), bedding types: current-laminated, parallel, lenticular, wavy, flaser, nodular, scour and fill structures | laterally to A and B, vertically with C |
| E | intertidal shelf | thin- to medium-interbedded grainstone, mudstone and wackestone, frequently burrowed, common ripples | laterally to A |
| F | subtidal shoal | thrombolite mounds, fossiliferous, flanking grainstones | laterally to G |
| G | subtidal shelf | thickly interbedded wackestone and mudstone, burrowed, common grainstone channels, lenses, and beds, fossiliferous | laterally to F |

# LITHOLOGIES

## Lithotope A

Description - These rocks are composed of uniform but sometimes discontinuous millimetre-sized laminae of mudstone and finely peloidal grainstone, with a primary fenestral fabric that is microscopic. Lamination is frequently wavy, sometimes doming to low-relief laterally-linked hemispheroidal (LLH) stromatolites. In rare cases, layers of laminae are buckled into small tepee structures, and torn up into intraclasts (Figs. 2A, 2B), especially at the base of overlying lithotopes. Discontinuous beds, up to several centimetres thick, of intraclastic and peloidal grainstone are frequently intercalated. This lithotope is usually affected by dolomitization, producing alternating laminae of finely crystalline dolostone and limestone, or finely crystalline dolostone with laminae outlined by crystal size differences and colour. Mudcracks are common but deep prism cracks are rare (Fig. 2C).

Lithotope A is found only in the Isthmus Bay and Aguathuna Formations, and ranges in thickness from 0.1 to 1.5 metres. In the Isthmus Bay Formation at Boat Harbour, a unit of this lithotope changes laterally to lithotope D (intertidal flat facies) over a distance of 100 metres.

Interpretation - Arguments for the environmental interpretation of this common lithology have been frequently put forward (e.g.: Aitken, 1967), and it is termed cryptalgal laminites (algalaminites), formed by the trapping and binding of sediment by blue-green algal mats. This is evidenced by uniformity of laminations, their buckling and doming, and fenestral fabric. These algal

mats are interpreted, on the basis of many modern examples (e.g.: The Persian Gulf [Kendall and Skipwith, 1968] and the Bahamas [Hardie, 1977]), to have formed on supratidal (and probably uppermost intertidal) flats as indicated in the rocks by mudcracks and tepee structures. Discontinuous grainstone beds are storm deposits. The intraclasts and peloids comprising these beds originated in other areas of the tidal flat and offshore. The paucity of bioclasts reflects considerable distance from subtidal areas, long residence time and possible micritization of subtidal sediment on the flats before final deposition.

## Lithotope B

Description - This lithotope consists of domal stromatolites in various combinations of laterally-linked hemispheroidal (LLH) shape. Stromatolites have low relief, diameters ranging from less than 0.2 to 2 metres, and are internally well-laminated, with the laminae often wavy or defining laterally-linked hemispheroids. Beds between stromatolites and immediately over- and underlying them are lithotope D and frequently contain mudcracks, are rarely burrowed, and rarely contain fossils. Stromatolites are frequently formed by the doming of cryptalgal laminites.

Lithotope B is found in the lower part of the Isthmus Bay Formation and the Aguathuna Formation. Units are generally less than 0.3 metres thick, and commonly pass laterally to lithotope D (intertidal flat facies). The stromatolites are considered in further detail in Chapter 3.

Interpretation - These stromatolites are interpreted to have grown in the intertidal zone, in areas protected from strongly erosive tidal currents, as evidenced by associated mud-cracks, lateral transition to lithotope D, rarity of fossils and burrows, and vertically associated cryptalgal laminites (lithotope A). The well-laminated internal fabric indicates episodic but regular addition of sediment.

## Lithotope C

Description - This lithotope consists of extensively burrowed to completely burrow-mottled and churned, thinly bedded (when preserved), unfossiliferous, usually medium-crystalline dolostone (Fig. 2D). Burrows are uncompacted, and dolomitization is of the diagenetic type (see Chapter 4).

This lithotope is somewhat uncommon and occurs only in the Isthmus Bay and Aguathuna Formations. It occurs usually in relatively thick units, from 0.5 to 5.5 metres. Gradation into lithotope D (intertidal flat facies) occurs frequently, and is marked by an increase in the amount

FIGURE 2

LITHOTOPES A, C, AND D

A. Vertically oriented slab of cryptalgal laminite with upper layers peeled back and overlain by grainstone. Scale in cm; Catoche Fm.; IB-262.

B. Vertically oriented slab of dolomitized brecciated cryptalgal laminite overlying grainstone containing large and curled intraclasts of cryptalgal laminite. Scale in cm; Isthmus Bay Fm.; IB-209.

C. Vertical view of dolomitized cryptalgal laminite cut by desiccation cracks and deeper prism cracks. Lens cap 6 cm across; Isthmus Bay Fm.; IB-153.

D. Vertically oriented slab of dolomitized lithotope C showing almost totally burrowed thin bedding. Scale in cm, Isthmus Bay Fm.; IB-98.

E. Vertically oriented slab of dolomitized lithotope D showing parallel bedding, scour and fill lenses, and burrowed beds. At bottom centre are vertical spreite burrows (Diplocraterion). Scale in cm; Isthmus Bay Fm.; IB-141.

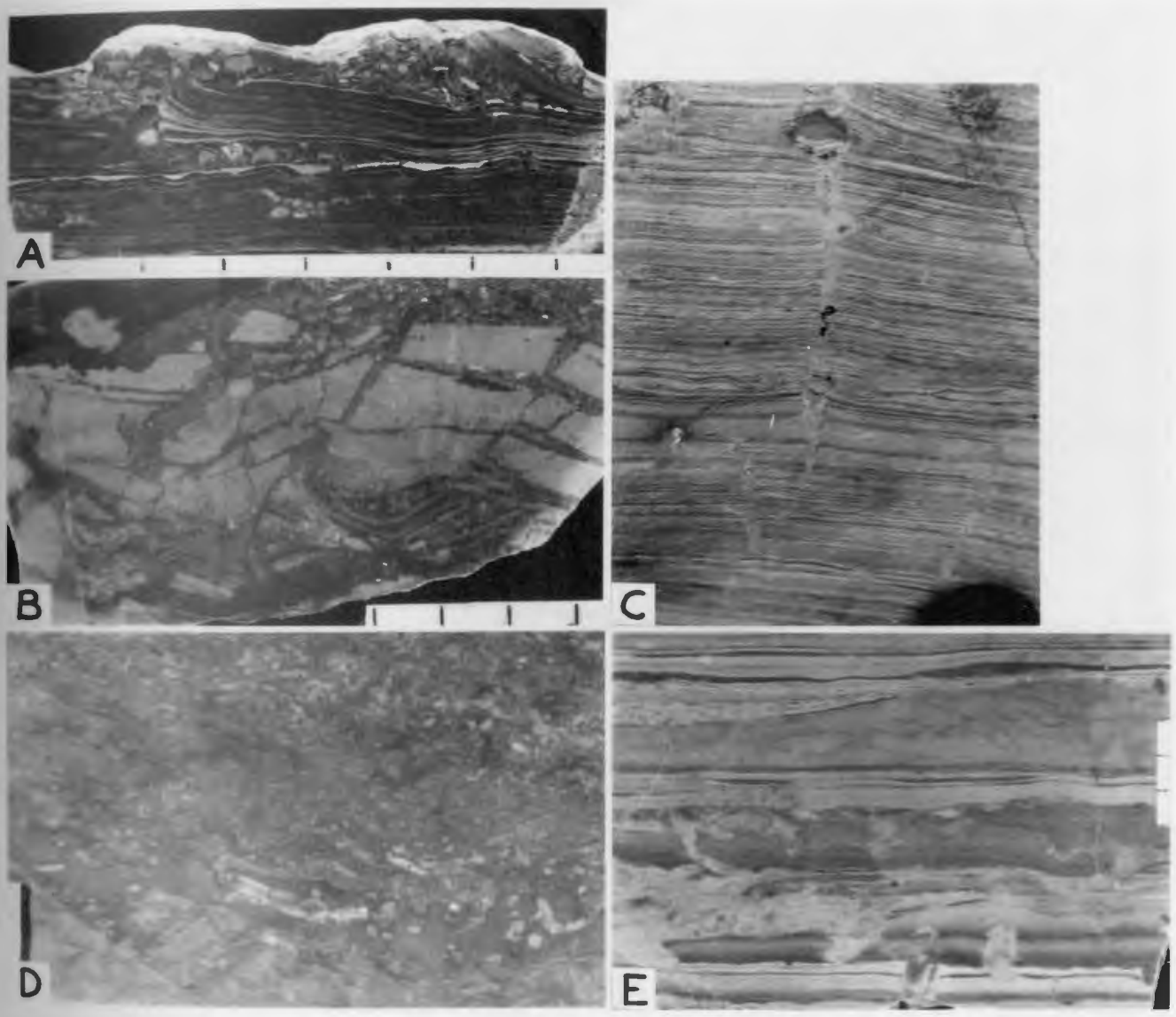
A
B
C
D
E

of bioturbation. When lithotope C is vertically juxtaposed with lithotope H (subtidal shelf facies), the two lithotopes are distinctively different.

Interpretation - This lithotope is the most difficult to interpret because dolomitization obscures components. The burrow-mottled nature indicates frequent submergence, but the units are too thick to have been deposited in ponds on intertidal flats. The rarity of fossils suggests some distance from subtidal areas, which is also suggested by the distinctiveness of the two lithotopes when vertically juxtaposed. The gradation in degree of bioturbation from lithotope D also suggests intertidal deposition. It is interpreted that this lithotope was deposited on intertidal flats in areas protected from erosion by tidal currents, where there was intermittent sedimentation with nearly pervasive bioturbation. The relative thickness suggests that this depositonal locality was a sediment trap, less prone to rapid shifting.

## Lithotope D

Description - Rocks of this lithotope are variable but common features are thin bedding (less than 5 centimetres thick), common dolomitization often giving rise to interbedded peloidal grainstone, mudstone, and dolostone, and bedding types that include current lamination, parallel, wavy, lenticular, and, rarely, flaser bedding (Figs 3A, 3B). Partial diagenetic dolomitization of soft-sediment compacted limestone beds has resulted in nodular bedding (Fig. 3A). Grainstones are sometimes graded, cross-laminated, herring-bone cross-laminated, and may be intraclastic, rarely oolitic

or bioclastic. Fossils are rare, but large planispiral gastropods and lingulid brachiopods do occur. Stacked hemispheroidal stromatolites, mudcracks, U-shaped vertical burrows (Fig. 2E), and, less commonly, horizontal burrows (Chondrites) occur in scattered beds. Corrosion surfaces occur infrequently.

Units of this lithotope range in thickness from 0.2 to about 3 metres and are not traceable laterally between neighbouring sections. At Boat Harbour, one unit passes laterally to lithotope A (supratidal facies) over a distance of 100 metres. Stromatolites of lithotope B are flanked by lithotope D (Fig. 3B). Lithotopes D and C (bioturbated intertidal facies) intergrade with each other in the degree of burrow-mottling.

Interpretation - This lithotope is interpreted to have been deposited in the intertidal zone because of: (1) the thin bedding indicating episodic deposition by bed-load and suspension transport, (2) the suite of sedimentary structures and bedding types which is typical of intertidal sediments, (3) mudcracks, (4) rare non-diverse indigenous fauna of gastropods and lingulids, (5) sporadic nature of bioturbation, with dominance of U-shaped and Chondrites burrows, and (6) lateral transition to lithotope A. This lithotope is similar to modern sediments of both carbonate and siliciclastic tidal flats, and is similar to other ancient examples from Lower Paleozoic shelves (e.g.: Matter, 1967). The similarity with modern siliciclastic tidal deposits is probably due to the high volume of sediment that was generated on the western

continental shelf during the Lower Ordovician. The variable nature of the lithologies grouped in this lithotope is due to variability in current strength and direction, grain size of sediment, degree of bioturbation, and frequency of storms.

## Lithotope E

Description - This lithotope is characterized by laterally continous interbedded thin-to medium-bedded (beds less than 10 centimetres thick) burrowed wackestone, mudstone, and cross-laminated grainstone beds with dolomitic partings (Fig. 3C, 3D). Herringbone cross-lamination and mudcracks (Fig. 3E) are occasionally present. Horizontal *Chondrites* and U-shaped burrows are common, often penetrating ripple tops during or after deposition of overlying beds, but pervasive bioturbation is rare. Grainstones are usually peloidal, fossiliferous, intraclastic, and in rare cases oolitic. Small, thrombolite mounds, less than 0.1 metre in diameter, occur in scattered beds.

This lithotope is most common in the upper part of the Isthmus Bay and lower part of the Catoche Formation. Units tend to be thick, up to about 50 metres on Port au Port Peninsula. Lateral gradation to lithotope A (supratidal facies) has been observed at Boat Harbour.

Interpretation - This lithotope is interpreted to have been deposited in the intertidal environment because: (1) periodic subaerial exposure and desiccation are indicated by mud-cracks, (2) herringbone cross-lamination suggests reversing tidal currents, (3) vertical U-shaped and *Chondrites* burrows

are a common intertidal association, (4) lack of pervasive bioturbation suggests unfavourable conditions such as tidal exposure, and (5) lateral gradation to supratidal cryptalgal laminite. The fossiliferous nature of the grainstone beds suggest nearness to subtidal areas. Most beds are probably the result of storm transport as the thickness suggests episodic movement of large volumes of sediment. Dolomitic partings are probably dolomitized mudstone from normal tidal deposition. The lack of bedding types of lithotope D (intertidal flat facies), such as lenticular bedding, suggests a different intertidal depositional setting which is interpreted to have been a more open and continuous intertidal shoreline exposed to subtidal sediment sources.

Lithotope F

Description - Mound structures between 0.4 metres and up to 2 metres in both diameter and thickness are found abundantly in the St. George Group. These structures often coalesce to form banks and are usually flanked by cross-laminated grainstone that grades laterally to lithotope H (subtidal shelf facies). Both mounds and flanking beds are highly fossiliferous, containing gastropods, rostroconchs, cephalopods, trilobites, pelmatozoan debris, corals, sponges, and sometimes brachiopods. The mounds are made up of digitate, clotted thrombolites (unlaminated stromatolites) with burrowed wackestone between.

Interpretation - These mound structures are cryptalgal and are identical with thrombolite mounds described by Aitken (1967) from rocks equivalent in age to the St. George in

FIGURE 3

LITHOTOPES D AND E AND CHANNEL

A. Vertical view of lithotope D, showing lenticular and nodular bedding of light-coloured limestone (originally peloidal calcarenite) in dark-coloured dolostone (originally mud). Lens cap 6 cm across; Isthmus Bay Fm.; IB-93.

B. Vertical view of dolomitized lithotope D, Showing Lenticular bedding and scour and fill structures, with 10 cm thick stromatolites (S) in upper right. Isthmus Bay Fm.; IB-203.

C. Bedding plane view of lithotope E, showing straight-crested ripples. Isthmus Bay Fm.; ECW-95.

D. Vertical view of lithotope E, showing interbedded grainstones of variable coarseness, some burrowed. Lens cap 6 cm across; Catoche Fm.; IB-268.

E. Bedding plane view of lithotope E, showing mudcracked ripples. Isthmus Bay Fm.; PAC-30.

F. Field sketch of vertical view of a portion of grainstone channel fill, showing imbricated intraclasts, graded beds, and scour surfaces. Catoche Fm.; PAC-41.

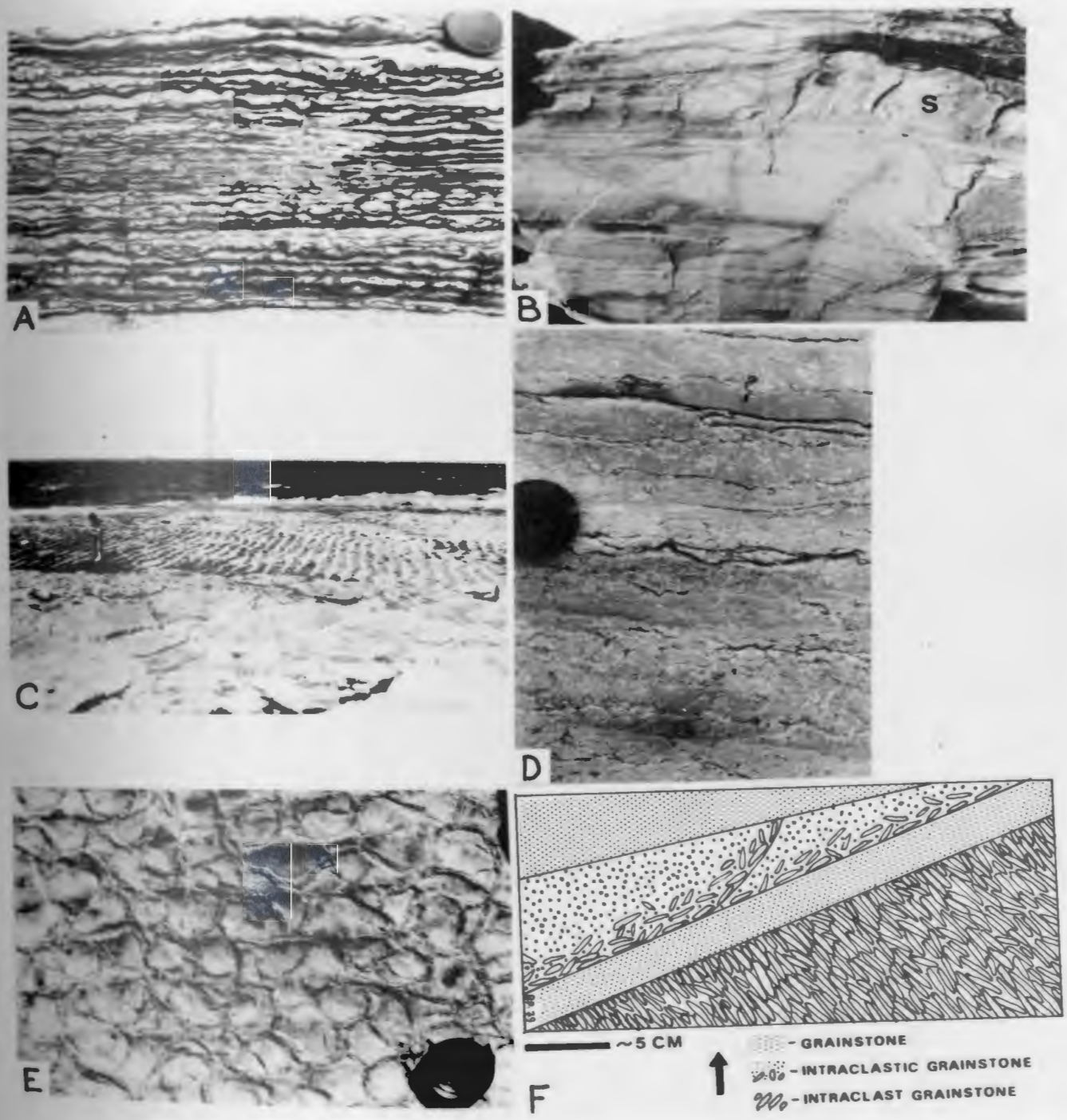
A
B
S
C
D
E
F
~5 CM
- GRAINSTONE
- INTRACLASTIC GRAINSTONE
- INTRACLAST GRAINSTONE

the Canadian Rocky Mountains. They are interpreted to have grown in agitated shoal conditions in the subtidal zone because of their fossiliferous nature and associated grainstone. They are somewhat similar to modern colloform mat structures forming in the subtidal zone of parts of Shark Bay, Western Australia (Logan et al., 1974). These cryptalgal structures are discussed further in Chapter 3.

Lithotope G

Description - This lithotope consists of burrowed fossiliferous wackestone, with beds of burrowed mudstone and scattered beds, lenses and narrow linear channels less than 0.1 metre thick of peloidal, intraclastic, bioclastic, and cross-laminated grainstone commonly interbedded in the Catoche Formation. Bedding is thick, but difficult to recognize on account of the stylolitization. Burrows are usually outlined by diagenetic dolomite. In the Catoche Formation, continuous units of this lithotope are many metres thick, and broken only by scattered thin units of nodular-bedded lithotope D (inter-tidal flat facies) or horizons of thrombolitic mounds of Lithotope F (subtidal shoal facies). Units of lithotope G in the Isthmus Bay and Aguathuna Formation are thinner, less than 2 metres thick, vertically associated with inter- and supratidal lithotopes and often contain hardgrounds, small thrombolitic mounds, and less mudstone.

Interpretation - These rocks are interpreted as having been deposited in the subtidal zone, under fully marine conditions, as has been previously suggested by Lévesque (1977) and James et al. (in prep.). An open subtidal environment is

indicated by: (1) widespread nature and thickness of the lithotopes, (2) lack of evidence for subaerial exposure, (3) lack of common "cyclic" shallowing units of other lithotopes in the Catoche Formation, (4) lateral gradation to lithotope F (subtidal shoal facies), (5) ubiquitous bioturbation, and (6) abundant fossils. The thinness of this lithotope in the Isthmus Bay and Aguathuna Formations and occurrence in vertical association with intertidal and supratidal facies suggests that subtidal conditions in those formations were short-lived and less open. In the Catoche Formation this lithology was probably deposited as mudbanks of slight relief that supported a zoned benthos, with winnowed calcarenites between, possibly similar to mudbanks in south Florida which have organism community zonations (e.g.: Turmel and Swanson, 1969). Some grainstone beds were likely deposited by major storms as single events.

## SECONDARY LITHOLOGICAL FEATURES

### Channels

Throughout the entire St. George Group measured in western Newfoundland, only one example of a major grainstone-filled channel was found. At the base of the Catoche Formation, on both the north and south sides of Barbace Cove, Port au Choix Peninsula, 1.9 metres of grainstone grade laterally to lithotope E (intertidal shelf facies). By reconstruction, the contact is linear, trending NE/SW, slightly oblique to the sea-cliff, and the unit is at least tens of metres wide and at least 700 metres in length. In vertical

order, the sequence consists of: (1) 0.4 metre of herringbone cross-bedded intraclast and intraclastic grainstone, (2) 0.3 metre of thinly bedded mudstone, grainstone, and dolostone with scour and fill structures and scattered U-shaped burrows (lithotope D), (3) 0.8 metre of herringbone cross-bedded intraclast and intraclastic grainstone, (4) 0.2 metre of burrow-mottled mudstone, and (5) 0.2 metre of herringbone cross-bedded intraclastic grainstone. The intraclasts are both mudstone and grainstone, sometimes fossiliferous, flat and rounded, and commonly imbricated (Fig. 3F). Many cross-beds have scoured bases, and many are normally graded with large intraclasts at the bases. The sequence is overlain by lithotope G (subtidal shelf facies).

Although only one margin of this lithotope is exposed, it is likely a narrow linear channel because herringbone cross-stratification indicates reversing current directions, unlikely to occur in a sand bank or shoal. The channel was intermittently the site of strong current activity, giving rise to steeply dipping beds exhibiting grading and imbricated pebbles. During more quiescent periods, bioturbated mudstone and rocks similar to lithotope D were deposited. It is difficult to estimate the amount of compaction of laterally equivalent lithotope G, but undeformed burrows suggest that there was little and that the channel was not very deep. This contrasts with deep modern subtidal channels (e.g.: Davies, 1970a) cut into seagrass-stabilized sediment. This may indicate that the Lower Ordovician subtidal sea bottom was not cohesively bound by algae or rooted organisms (even though seagrass only

evolved at the end of the Mesozoic (Brasier, 1975).

## Ooids

Ooids, coated grains and oolitic units are present in the St. George, though are comparatively rare in comparison with Cambrian rocks of western Newfoundland (Lévesque, 1977). Oolite beds are less than 0.2 metre thick, usually cross-laminated often with rippled tops, and occur within lithotopes A, D, and E, that is, within intertidal and supratidal facies. Those occurring within the supratidal facies are frequently silicified.

Oolite shoals of large proportions, such as those of the Bahama Banks, did not develop probably because hydrodynamic conditions on the Lower Ordovician continental shelf were unfavourable. Using Shark Bay and the Persian Gulf as better analogues, it is suggested that local, thin patches of oolites formed in scattered areas marginal to or on tidal flats, around promontories, in agitated bays, or at the mouths of small tidal channels. Many of the oolite beds appear to have been deposited as single events onto flats, probably by storms, short distances from their place of generation.

## Evaporites

Evaporite minerals are entirely replaced by other minerals, except for microscopic vestiges. All evidence indicates that evaporite precipitation was very minor and local in its occurrence in the St. George. Collapse breccias occur only at one horizon and may have been caused by dissolution of underlying evaporite beds. Three groupings of replaced evaporites are described: (1) dolomitized laths,

(2) dolomitized nodules, and (3) silicified anhydrite.

Dolomitized laths - In intertidal lenticular bedded dolostones (lithotope D) in the Isthmus Bay Formation at Eddies Cove West, scattered lenticular beds contain dolomite rosettes interpreted to be dolomitized evaporite laths (Fig. 4A). The rosettes are parallel to bedding, average about 3 centimetres in diameter, and are composed of radiating needle-and lath-shaped aggregates of coarse dolomite, up to 2 centimetres in length and several millimetres in width. The evaporite mineral, probably anhydrite, grew locally in lenses of sediment during periods of extreme desiccation on a tidal flat. The lenses of grainstone may have been sealed by mud drapes that prevented groundwater replenishment.

Dolomitized nodules - In the Aguathuna Formation at Aguathuna Quarry is a unit of cryptalgal laminite containing elongate pods, up to 25 centimetres in length and 10 centimetres in width, of fine-grained dolostone (Fig. 4B). With the pods are discontinuous layers and possible mudcrack infillings; the margins of the pods have shrinkage cracks, are irregular and compacted by soft-sediment deformation. Cryptalgal lamination is deformed around the pods. The above characteristics indicate that the pods formed within soft, unlithified sediment, and they are tentatively interpreted to be dolomitized evaporites.

Silicified anhydrite - Silicified evaporites are the most common evidence of evaporites in the St. George. Abundant laths of quartz, 500 microns in length and 30 microns in width occur in mudstones in a subaerial rubble horizon in

FIGURE 4

EVAPORITES

A. Bedding plane view of dolomitized radiating anhydrite laths in a lens of lenticular bedded lithotope D. Scale in cm; Isthmus Bay Fm.; ECW-77.

B. Vertical view of dolostone pods interpreted to be replaced evaporite nodules, showing soft-sediment compacted seams and cryptalgal laminae around the pods. Aguathuna Fm.; AQ-11.

C. Vertically oriented slab of chert nodules replacing enterolithic anhydrite replacing cryptalgal laminite. Scale in cm; Aguathuna Fm.; IB-332.

D. Vertically oriented slab of chert pebble lag in dolostone. The white chert pebbles are replaced evaporite nodules. Scale in cm; Isthmus Bay Fm.; BH-124.

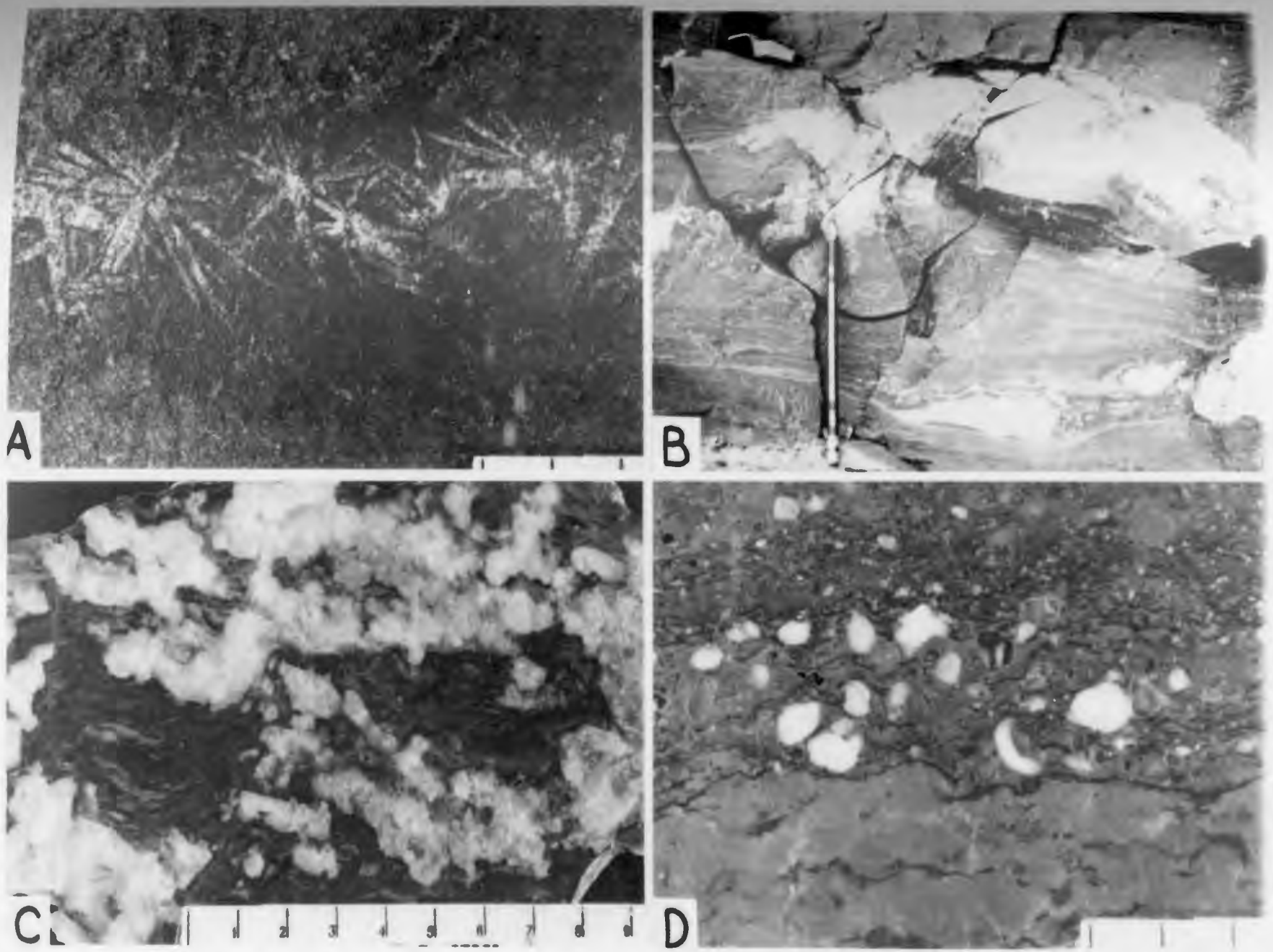
A
B
C
D

the Aguathuna Formation northwest of the Gravels. A horizon of discountinuous chert layers 1 centimetres thick that contain microscopic relic dusty inclusions outlining a primary felted lath texture occurs in the Aguathuna Formation at Table Point. Isoloated chert nodules and beds of coalesced nodules (Figs. 4C, 4D) similar to enterolithic anhydrite occur within cryptalgal laminites in the Aguathuna and the lowermost part of the Isthmus Bay Formations. Algal laminations are deformed around the chert. Examples of all these structures were examined petrographically and contain relics of anhydrite textures. In the upper part of the Isthmus Bay Formation at Boat Harbour is a chert pebble horizon; the pebbles are replaced evaporite nodules and have relic felted texture. Other occurrences of chert nodules and geodes in the St. George cannot be proven to be of an evaporite origin, especially when they replace subtidal limestones unlikely to have been affected by hypersaline waters.

## Hardgrounds

Corrosion surfaces or hardgrounds are found in scattered horizons in the Isthmus Bay and Aguathuna Formations. They are commonly within grainstones of lithotopes D and E (intertidal facies), and on mudstone and wackestone surfaces of lithotope H (subtidal facies) in the Isthmus Bay and Aguathuna Formations. Allochems and cement (synsedimentary radial bladed calcite) are planed off (Fig. 5A), and the surfaces in places are penetrated by microborings. In some grainstone sequences, multiple corrosion surfaces occur together, separated by less than a centimetre of sediment.

Corrosion was by abrasion because the surfaces are not pitted. The rare lithified mudstone and wackestone surfaces probably developed in the subtidal zone in a similar manner to modern hardgrounds such as those of the Persian Gulf (Shinn, 1969) during periods of little sedimentation.

In the middle part of the Isthmus Bay Formation on Port au Port Peninsula is a horizon (Figs. 5B, 6) interpreted to have been a potholed surface somewhat similar to those of modern limestone coasts. The sequence consits of 4 consecutive units or events: (1) 0.1 metre of fenestral cryptalgal laminite erosively overlain by patches of light-coloured cross-laminated peloidal and intraclastic grainstone cemented by synsedimentary radial bladed calcite. The top of the grainstone is a scalloped corrosion surface, (2) initiated on the scalloped grainstone and eroded cryptalgal laminite are thrombolite mounds 0.4 metre thick and up to 0.3 metre in diameter, flanked by dark-coloured peloidal and slightly oolitic grainstone, cemented by bands of synsedimentary radial bladed cement and spar cement, and containing flat-pebble intraclasts and small blocks of the underlying grainstone and cryptalgal laminite. The dark-coloured grainstone is 0.2 metre thick, and its top is a planar corrosion surface that also has planed off parts of the thrombolites, leaving eroded pillars. (3) between the pillars of thrombolite mounds is grainstone that is itself eroded out in most places and replaced by a fourth generation grainstone that is light-coloured, containing synsedimentary marine cement and abundant cryptalgal intraclasts. The light-coloured grainstone involved the most

Figure 5

HARDGROUND AND PALEOKARST HORIZONS

A. Vertically oriented slab showing two corrosion surfaces (hardgrounds) (arrowed) in an intraclastic grainstone sequence. Scale in cm; Isthmus Bay Fm.; IB-84.

B. Outcrop of eroded thrombolite mounds (outlined by black line) interpreted to have been a potholed surface. Photograph corresponds to left half of outcrop sketch Fig. 6. Lens cap (bottom centre) 6 cm across; Isthmus Bay Fm.; IB-133-135.

C. Bedding plane view of rounded solution runnels (Rundkarren). Lens cap 6 cm across; Isthmus Bay Fm.; BH-124.

D. Vertical view of dolomitized collapsed brecciated cryptalgal laminite (see outcrop sketch Fig. 7). Isthmus Bay Fm.; IB-191.

E. Vertical view of subaerial rubble horizon showing angular limestone fragments in shaly matrix. Lens cap 6 cm across; Aguathuna Fm.; NEG-12.

A
B
C
D
E

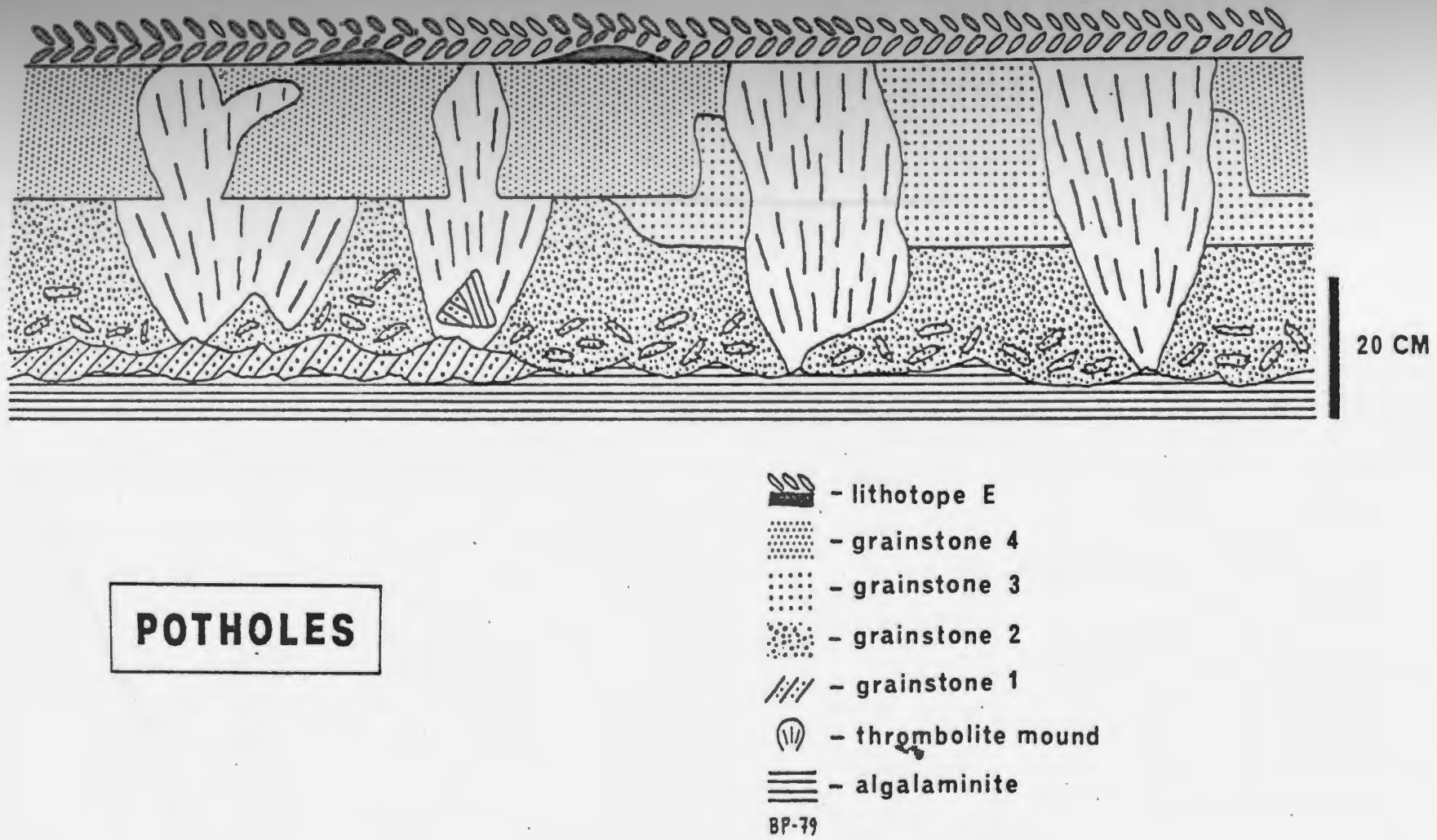


Figure 6: Outcrop sketch of potholed surface eroded into unit of thrombolite mounds, Isthmus Bay Formation, Isthmus Bay. Horizontal scale slightly foreshortened. IB-133-135.

erosion of the thrombolitic pillars. (4) the tops of the thrombolite mounds were planed flat and overlain by rocks of lithotope E as patches of mudstone with burrows extending down into the light-coloured grainstone, overlain by herring-bone cross-laminated intraclastic grainstone. This sequence records several events of potholing and infilling that occurred in the shallow subtidal and intertidal zone. The subtidal thrombolite mounds indurated by algal binding and synsedimentary cementation were most resistant to abrasion. Infilling grainstones were indurated to a lesser degree by bands of early synsedimentary cement and tended to be eroded out. These surfaces are somewhat similar to the scalloped erosion surfaces described by Read and Grover (1977) from Middle Ordovician limestones of Virginia and attributed to solution by meteoric water. However, no evidence of solution is seen here, and abrasion is interpreted to have occurred in the marine environment.

## Paleokarst

There are only a small number of horizons interpreted to record periods of subaerial exposure and karstification in the St. George, other than brecciation of supratidal crypt-algal laminites. Karst processes included solution pitting, collapse brecciation, and formation of subaerial rubble.

Solution Pitting - Near the top of the Isthmus Bay Formation at Boat Harbour is a 0.8 metre thick unit of medium crystalline dolostone containing in the middle a lag of chert pebbles, many of which are replaced anhydrite nodules subsequently

eroded out and redeposited in a dolomitized grainstone. The top of the dolostone unit is sculptured by irregular pits, 5 centimetres deep with steep but smooth walls (Fig. 5C). This surface is similar to Rundkarren, or rounded solution runnels that commonly form on limestone surfaces under a soil cover. There is no evidence of a soil cover above this horizon which is overlain by a thin dolostone seam, and it is uncertain whether the pitting developed on exposed or covered carbonate rock.

Collapse Brecciation - Near the top of the Isthmus Bay Formation on Port au Port Peninsula a 0.8 metre thick unit of thrombolite mounds is eroded into a hummocky surface, with the mounds standing out in relief compared with the grainstone and burrowed wackestone between them. The depressions are filled with a dolomitized intraclastic grainstone, and where the mound bed is missing, the underlying cryptalgal laminite unit is overlain directly by burrow-mottled dolostone. The eroded mound unit and depression-filling is overlain by 0.7 metre of dolomitized cryptalgal laminite that dips gently into the low where the mound unit is missing. In the low, the cryptalgal laminite is fractured and brecciated into angular blocks in a grainstone matrix (Fig. 5D). The cryptalgal laminite is overlain by a thin bed of peloidal and intraclastic grainstone that grades laterally to a 0.3 metre deep channel in the depression, floored by large rounded intraclasts (Fig. 7).

Erosion of the thrombolitic unit took place after at least partial lithification, but it cannot be determined

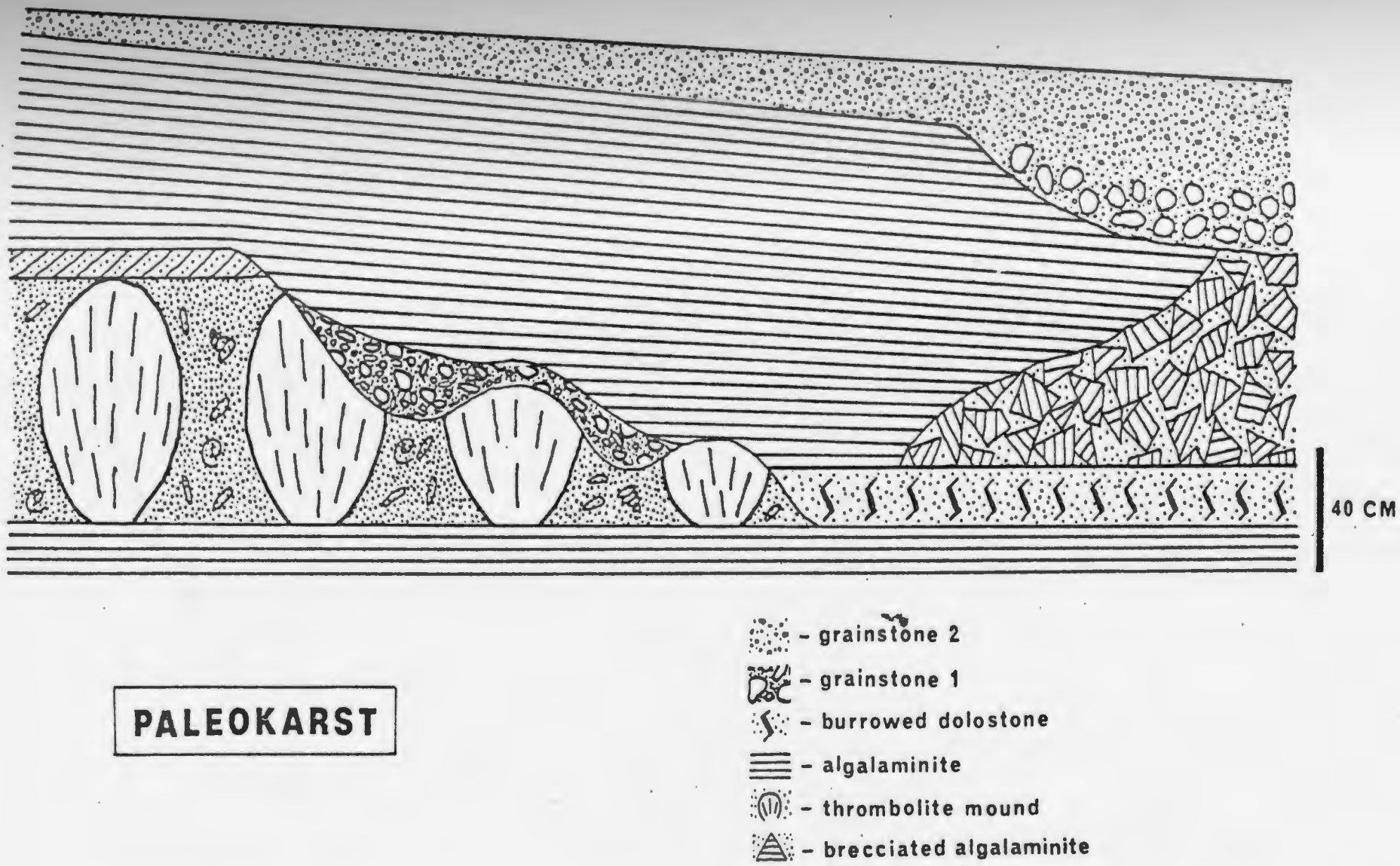


Figure 7: Outcrop sketch of eroded thrombolite mounds overlain by collapse brecciated cryptalgal laminite, Isthmus Bay Formation, Isthmus Bay. Horizontal scale slightly foreshortened. IB-189-192.

whether the hummocky surface was due to subaerial, or intertidal or shallow subtidal erosion. Collapse brecciation of the overlying cryptalgal laminite into the lowest part may have been due to solution of evaporites but this cannot be proven. This sequence of beds is probably correlative with the pitted surface considered above from Boat Harbour, and an intraclastic horizon at Eddies Cove West.

Subaerial rubble - A 0.4 metre thick rubble unit in the Aguathuna Formation crops out on both sides of the Gravels separating Port au Port Peninsula from mainland Newfoundland. The unit is composed of a rubble of angular grainstone and cryptalgal laminated clasts that are mostly tabular, in a shaly (clay-rich) and mudstone matrix (Fig. 5E). Northwest of the Gravels, the rubble passes laterally to buckled mudstone and cryptalgal laminated beds forming tepee structures. There is considerable silicification and chertification, preserving anhydrite nodules and disseminated laths. Northeast of the Gravels, some clasts have in situ fractures containing calcite spar cement and internal sediment of subaerial origin. The depressions on the surface between the tepees are filled with cross-laminated intraclastic grainstone. This horizon is not a solution feature, but it does record subaerial exposure of lithified beds and the beginnings of soil formation, probably caused by a slight lowering of sea level. It may be correlative with a thin conglomeratic horizon containing angular chert fragments in the Aguathuna Formation at Table Point.

## LITHOLOGICAL SUMMARY

The different lithologies and lithologic features described from the St. George are all low energy peritidal deposits. Three basic zones associated with tidal flats are recognized: supratidal, intertidal, and subtidal, which are represented by 7 lithotopes. Lithotopes intergrade with one another in some cases, and separation and interpretation is necessarily somewhat simplistic.

Supratidal rocks are cryptalgal laminated, and may be associated in scattered cases with evaporites and subaerial erosion (karstification). Intertidal rocks are complex and lithologically diverse, depending on the volume of sediment, degree of bioturbation, and wave, current, and storm energy. Three types have been distinguished that suggest three different but coeval depositional settings: extensive intertidal flats open to direct currents and sediment from the open subtidal shelf, smaller and more protected tidal flats deposited under variable conditions of sedimentation, currents strengths and directions, and bioturbation, and further protected tidal flats where bioturbation exceeded sedimentation leaving no preserved sedimentary structures. The subtidal zone is represented by both shoal and quiet-water deposits. Shoaling occurred by growth of thrombolite mounds. Quiet subtidal bottoms were sites of development of a diverse benthic fauna on muddy bioturbated substrates between small channels and areas of winnowed sand.

The tidal interpretations presented here for the St. George lithologies are similar in most cases to lithological interpretations of previous workers such as Matter (1967), Laporte (1967), Walker (1973), and Schwarz (1975), and can be equated in part to numerous ancient siliciclastic tidal sequences (such as examples in Ginsburg, 1975). The peritidal nature of the lithologies indicates that the Lower Ordovician shelf of western Newfoundland, despite its broadness, was not tideless, as suggested for epeiric seas by Shaw (1964), because accumulation of these rocks by processes not dominated by tides and storms superimosed on tides cannot be substantiated.

## REGIONAL CORRELATION

Approximate correlation of the Isthmus Bay Formation from Port au Port Peninsula to the Great Northern Peninsula is possible on the basis of a distinctive subaerial exposure horizon, trilobite biostratigraphy, and first appearances of distinctive fossils such as the early coral Lichenaria and archaeoscyphiid sponges (Fig. 8). Preliminary trilobite collections of D. Boyce (pers. comm., 1979) and R.A. Fortey (in press) suggest that the base of the Catoche Formation is diachronous and slightly older at Boat Harbour than elsewhere. Occurrences of lithotope A (supratidal facies) is marked on each column by horizontal bars, giving an indication of "cyclicity" within each section. The lowermost part of the Isthmus Bay Formation, which may include Upper Cambrian rocks, is "cyclic" both at Boat Harbour and Port au Port. This is followed in both places by subtidal and reefal units.

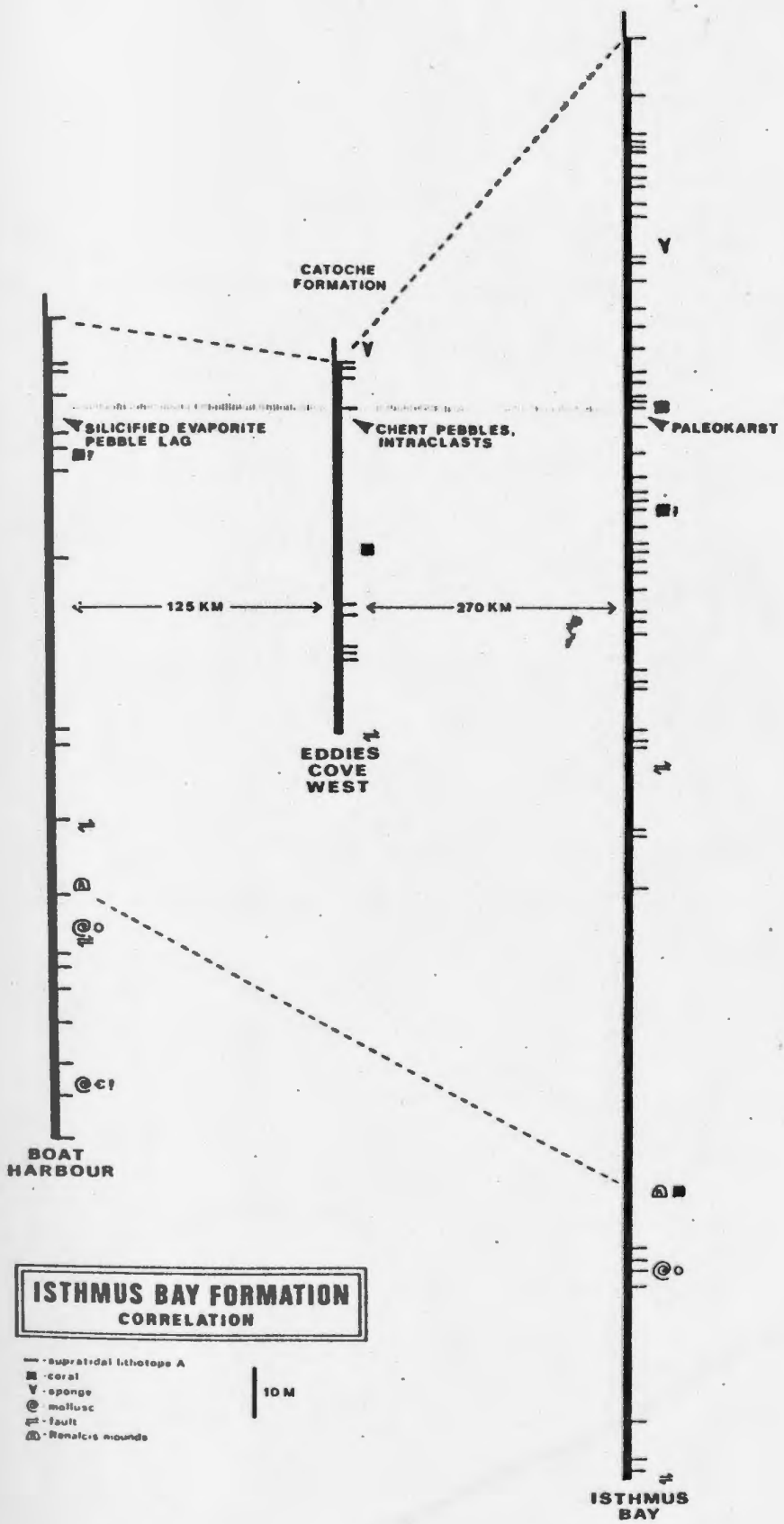


Figure 8: Regional correlation of the Isthmus Bay Formation, western Newfoundland. The sections are hung on a distinct horizon of subaerial exposure that occurs in each and is interpreted to be a time line.

The rest of the Isthmus Bay everywhere is more or less "cyclic". Despite faulting, it is probable that the Isthmus Bay Formation on Port au Port Peninsula is truly thicker than further north.

The Catoche Formation is similar in character in most exposures, being composed of lithotopes F and G (subtidal shoal and shelf facies) with scattered thin units of lithotope B (intertidal flat facies). However, the lower half of the Catoche at Port au Port is composed of lithotope E (intertidal shelf facies), and at Hare Bay the entire formation is lithotope G (subtidal shoal facies). Hare Bay may have been the site of shelf-margin shoaling and reef development during the Catoche time. The Catoche is estimated to be about 135 metres thick in the north, and about 165 metres thick in the south. Thicknesses in Lévesque (1977) of 206 metres at Port au Port and approximately 190 metres at Eddies Cove West are in error because the large covered intervals were overestimated.

The Aguathuna Formation is not exposed at Boat Harbour, but appears to be less than 10 metres thick at Eddies Cove West. It is 75 metres thick at Table Point (Lévesque, 1977), and 55 metres thick northwest of the Gravels on Port au Port Peninsula. The thickness at Hare Bay appears to be about 10 metres (N.P. James, pers. comm., 1978). Besaw (1973) and F. Manns (pers. comm., 1978) noted that the "cyclic" nature of the Aguathuna Formation is not present in the western part of Port au Port Peninsula where it is interbedded limestone and "buff dolomite mudstone" (Besaw, 1973). This may be due to hydrodynamic influences brought about by the configuration

of the shelf margin to the east and south of Port au Port Peninsula: a re-entrant in the shelf margin may have been present.

The three subdivisions of the St. George indicate that the St. George was deposited in one major transgressive-regressive cycle that culminated in subaerial exposure of the continental shelf before deposition of the Table Head Group. This is broadly similar in depositional style to Lower Ordovician rocks elsewhere in the Appalachians such as the Beekmantown Group Maryland (Sando, 1957). The lower Member of the Stonehenge Limestone is similar to the lower, subtidal, part of the Isthmus Bay Formation. The Upper Member and lower Rockdale Run Formation are similar to the upper part of the Isthmus Bay. The Dolomite Member of the Rockdale Run Formation is similar to the Catoche. The Pinesburg Station Dolomite is lithologicaly similar to "cyclic" Aguathuna Formation.

## LATERAL VARIATION

Sections of the Aguathuna Formation measured on both sides of the Gravels connecting Port au Port Peninsula to mainland Newfoundland are two kilometres apart. The two sections can be correlated by means of a rubble horizon of subaerial origin assumed to be common to both (Fig. 9). The rubble horizon in each section is sufficiently distinctive that it probably was not a local exposure horizon, and may even be correlative with a similar horizon at Table Point. As well as this, alternate correlations suggested by lithotopes

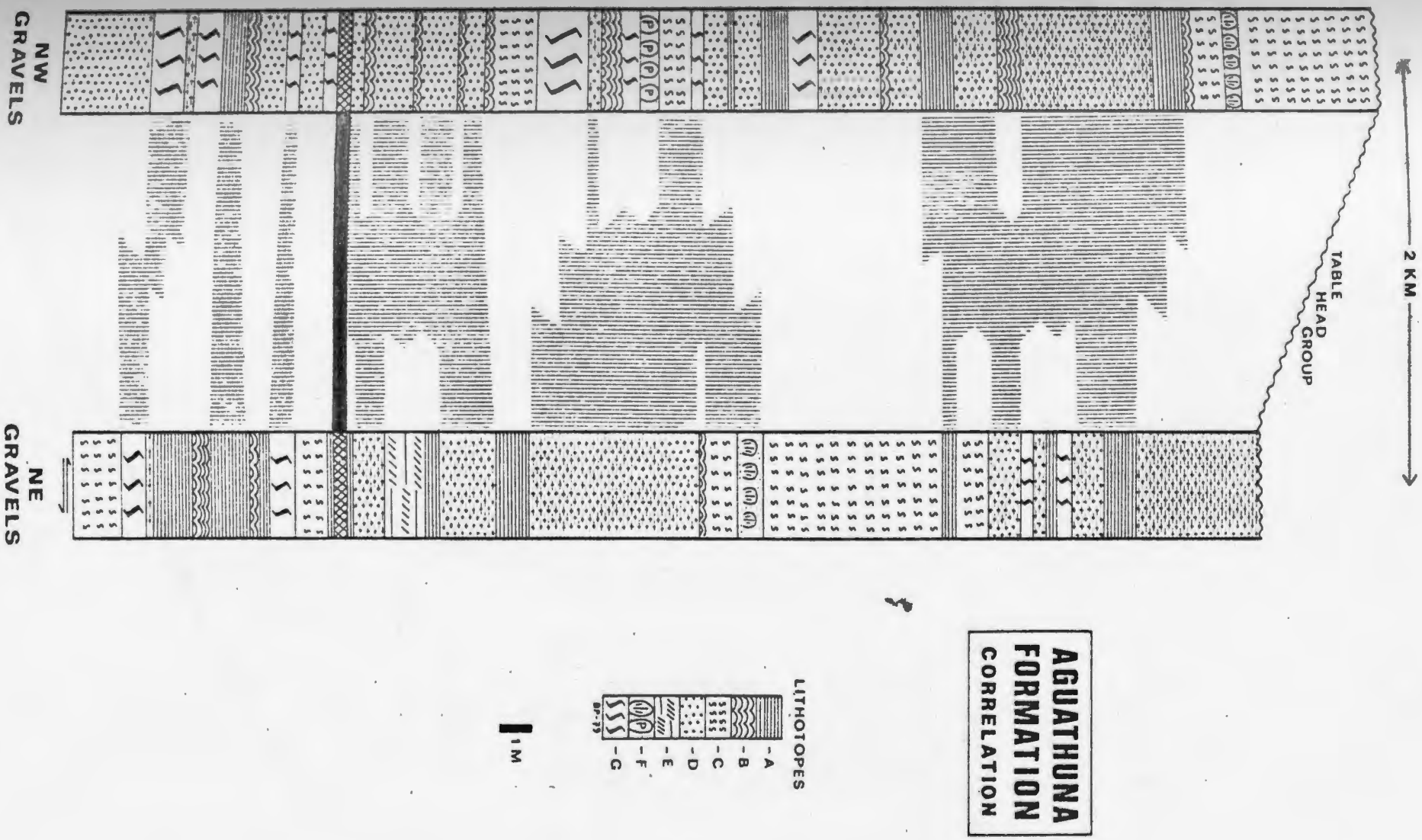


Figure 9: Correlation of lithotopes of the Aguathuna Formation across the Gravels. Toothed correlation is drawn where probable facies shifting occurred. The sections are hung on a subaerial rubble horizon interpreted to be a time line. (P = Pulchrilamina mounds)

that may have been laterally extensive for at least two kilometres are less likely because that imply too great a relief of the St. George - Table Head contact, inconsistent with observed relations elsewhere. Nevertheless, regardless of the way in which the sections are correlated, noticeably few lithotopes are traceable without change across the distance, illustrating that lateral facies transitions occurred over short distances. The two sections have not been differently compacted because some lithotopes can be correlated directly. This permits the use of toothed lines in places to indicate facies shifting. No consistent landward direction is indicated by the pattern of facies changes between the two sections.

## FACIES SEQUENCES

Earlier studies of shallow-water carbonates have shown that vertical sequences can be explained by means of logical idealized shallowing-upward cycles using "end-member" subtidal and supratidal facies as bounding styles of deposition (James, 1977). The vertical distribution of lithotopes (facies) of the Isthmus Bay and Aguathuna Formations was plotted (Fig. 10), and inspection shows that ideal shallowing-upward cycles are rare in the sequence of repeated vertical oscillations. This indicates that there was considerable lateral variation of facies which did not give rise to ideal cycles after progradation and accretion. The style of oscillation of lithotopes differs in various parts of the sections, and based on visual inspection of the plots, the St. George can be divided into a lowermost Isthmus Bay

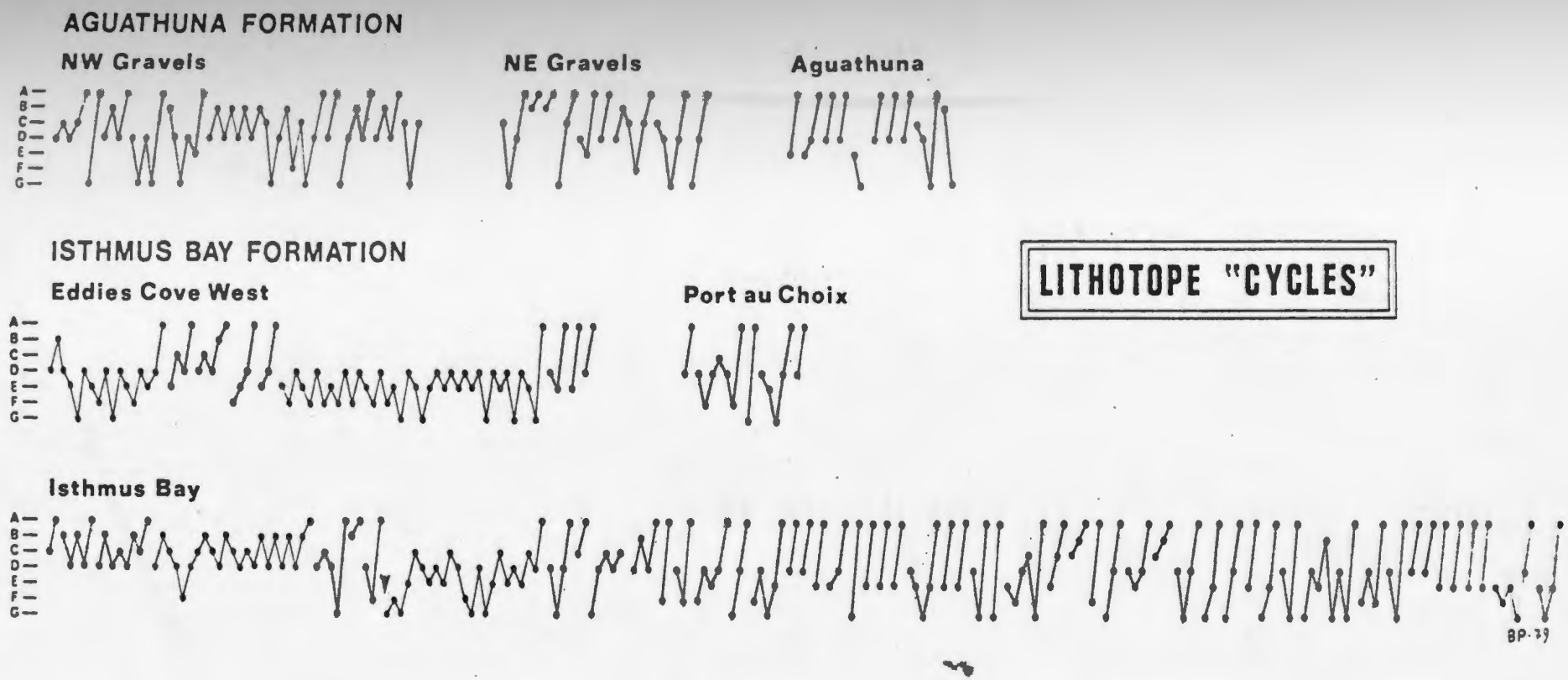


Figure 10: Plots of the distribution of lithotopes for each measured section with the lithotopes arranged vertically, approximating their relative depths: supratidal at the top and subtidal at the bottom. The triangular arrow in the lower Isthmus Bay section marks the level of the first Ordovician fossil.

Formation (west of Green Head, Port au Port Peninsula, that likely includes Upper Cambrian strata), upper Isthmus Bay (beginning east of Green Head, just west of the fault of unknown throw), the (upper) Isthmus Bay in the Eddies Cove West-Port au Choix area, and the Aguathuna Formation. The Isthmus Bay at Boat Harbour is too discontinuous and faulted to be used. The Catoche Formation is simply lithotopes D, E, F, and G in a non-cyclic pattern.

For each subdivision, a matrix was constructed showing the over- and underlying relationships for each lithotope (Fig. 11). The most common vertical contacts were used to construct lithotope sequences that portray the common vertical associations of two or more lithotopes (Fig. 12). The lithotopes drawn to one side are those that occur less commonly in the sequence. The sequences are not single shallowing- or deepening-upward cycles but may contain several supratidal levels. Contacts between lithotopes were found to be of little importance in this approach because all shifts involved changes in degree of bioturbation and bottom scour.

## FACIES MODELS

The rarity of simple shallowing-upward cycles and the complexity of the facies sequences indicates that there was considerable lateral variation of facies. Depositional facies models can be suggested using Walther's Law, because there are no significant breaks in the section, and reworking of underlying facies or lack of deposition due to rapid shifting presents no problem.

**AGUATHUNA FM.**
Port au Port Pen.

| | A | B | C | D | E | F | G |
|---|---|---|---|---|---|---|---|
| A | | 4 | 3 | 14 | 2 | 0 | 3 |
| B | 2 | | 2 | 7 | 0 | 1 | 1 |
| C | 2 | 0 | | 3 | 0 | 1 | 4 |
| D | 14 | 9 | 2 | | 3 | 0 | 5 |
| E | 4 | 0 | 0 | 1 | | 0 | 1 |
| F | 0 | 0 | 2 | 0 | 0 | | 0 |
| G | 3 | 0 | 2 | 8 | 0 | 0 | |

**ISTHMUS BAY FM.**
Great Northern Pen.

| | A | B | C | D | E | F | G |
|---|---|---|---|---|---|---|---|
| A | | 0 | 0 | 6 | 4 | 1 | 1 |
| B | 1 | | 0 | 1 | 0 | 0 | 0 |
| C | 0 | 0 | | 3 | 0 | 0 | 0 |
| D | 8 | 2 | 2 | | 14 | 5 | 3 |
| E | 2 | 0 | 1 | 8 | | 6 | 5 |
| F | 1 | 0 | 0 | 8 | 3 | | 0 |
| G | 1 | 0 | 0 | 5 | 1 | 0 | |

**ISTHMUS BAY FM.**
Port au Port Pen.

| | A | B | C | D | E | F | G |
|---|---|---|---|---|---|---|---|
| A | | 2 | 1 | 4 | 0 | 0 | 0 |
| B | 2 | | 4 | 7 | 0 | 0 | 0 |
| C | 2 | 1 | | 6 | 0 | 0 | 0 |
| D | 2 | 9 | 4 | | 0 | 2 | 1 |
| E | 0 | 0 | 0 | 0 | | 0 | 0 |
| F | 1 | 0 | 0 | 1 | 0 | | 0 |
| G | 1 | 0 | 0 | 0 | 0 | 0 | |

| | A | B | C | D | E | F | G |
|---|---|---|---|---|---|---|---|
| A | | 0 | 3 | 12 | 16 | 5 | 9 |
| B | 2 | | 0 | 1 | 0 | 0 | 1 |
| C | 2 | 2 | | 4 | 1 | 0 | 1 |
| D | 16 | 1 | 2 | | 7 | 3 | 8 |
| E | 15 | 1 | 5 | 5 | | 2 | 3 |
| F | 4 | 0 | 0 | 4 | 1 | | 2 |
| G | 7 | 0 | 0 | 11 | 6 | 1 | |

**LITHOTOPE CONTACTS**

Figure 11: Matrices showing the abundances of contacts between lithotopes. The horizontal and vertical axes are the over- and underlying lithotopes respectively.

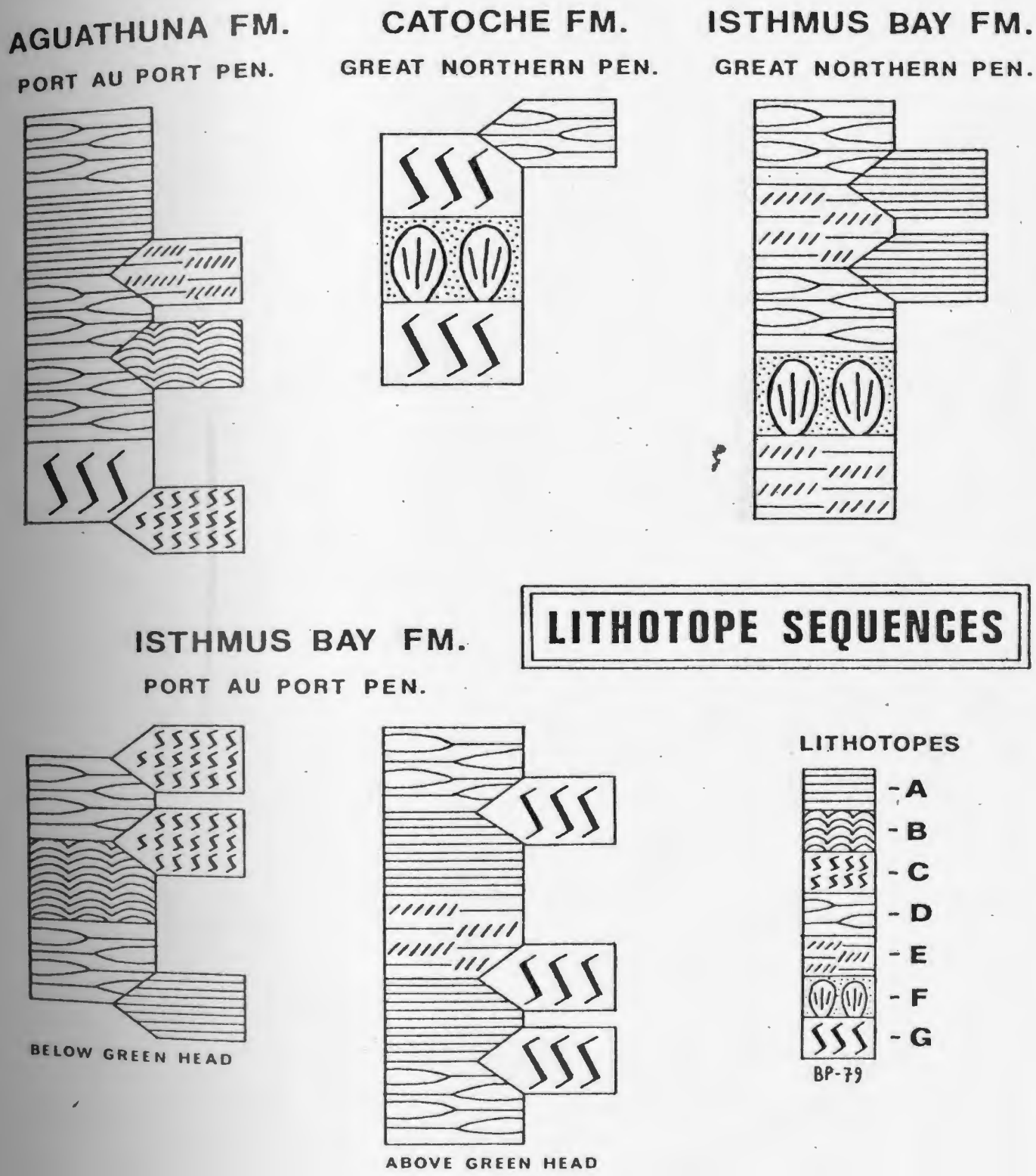


Figure 12: Lithotope sequences constructed from most common under- and overlying relationships. Lithotopes drawn to the side are those that occur less frequently. No thickness implied.

Two basic models of shallow-water carbonate sedimentation on a continental shelf can be considered: a shoreline model and an island model. The shoreline model for the St. George is rejected because extensive land surfaces do no occur in the section, deposition took place at a great distance from crystalline basement (Precambrian Shield), siliciclastics are lacking, and consistent landward directions are not indicated by short distance correlation of the Aguathuna Formation. The continental shelf during Isthmus Bay and Aguathuna times is envisaged as a quilt of low-relief intertidal banks and islands whose continually exposed surfaces were covered by algal mats. Islands probably had dimensions of several to at most 10 kilometres, judging from facies changes observed across the Gravels. The distribution of facies around islands and banks would have varied from place to place, and would have altered as islands and banks accreted. The shapes of islands and banks is unknown, and paleocurrent measurements do not render a consistent orientation. The spacing of islands probably varied, judging from the commonness of lithotope G (subtidal shelf facies) in the section. For instance, the sequences constructed for the lower Isthmus Bay Formation on Port au Port Peninsula and the Isthmus Bay on the Great Northern Peninsula show that lithotope G occurred infrequently, suggesting that there were not extensive subtidal areas between islands and banks and that lateral shifting of facies occurred rapidly preventing accumulation of thick units of lithotope G.

In the lowermost part of the Isthmus Bay Formation, islands and banks were probably small because of the rarity of lithotope E, and may even have been interconnected. The upper Isthmus Bay was more complex and the presence of lithotope E, F, and G and rarity of lithotope C suggest that islands were larger and subtidal areas present between them. Shoaling was more common in subtidal areas on the Great Northern Peninsula. The Catoche Formation consisted of subtidal low-relief mud banks, with periodic accretion to intertidal conditions as evidenced by the thin nodular and dolomitic horizons. Shoals of thrombolite mounds also developed periodically, except to the west in Hare Bay which was entirely a shoal complex. The lower half of the Catoche on Port au Port consists of lithotope E. Islands and banks during Aguathuna time were probably also small but with more extensive subtidal areas between. Simplistic hypothetical facies maps of the islands are suggested on the basis of the lithotope sequences (Fig. 13).

## ORIGIN OF "CYCLES"

The lithotope sequences and thicknesses seen in outcrop are related to a number of factors: (1) bias of the outcrop preserving the paleogeographic site of deposition, (2) rate of sediment accumulation (dependent on hydrodynamic influences on sediment accretion), and (3) rate of sea level rise, or subsidence. Facies shifts are caused by progradation and regradation of environments during subsidence or sea level rise. Sedimentary cycles and lithotope oscillations can be

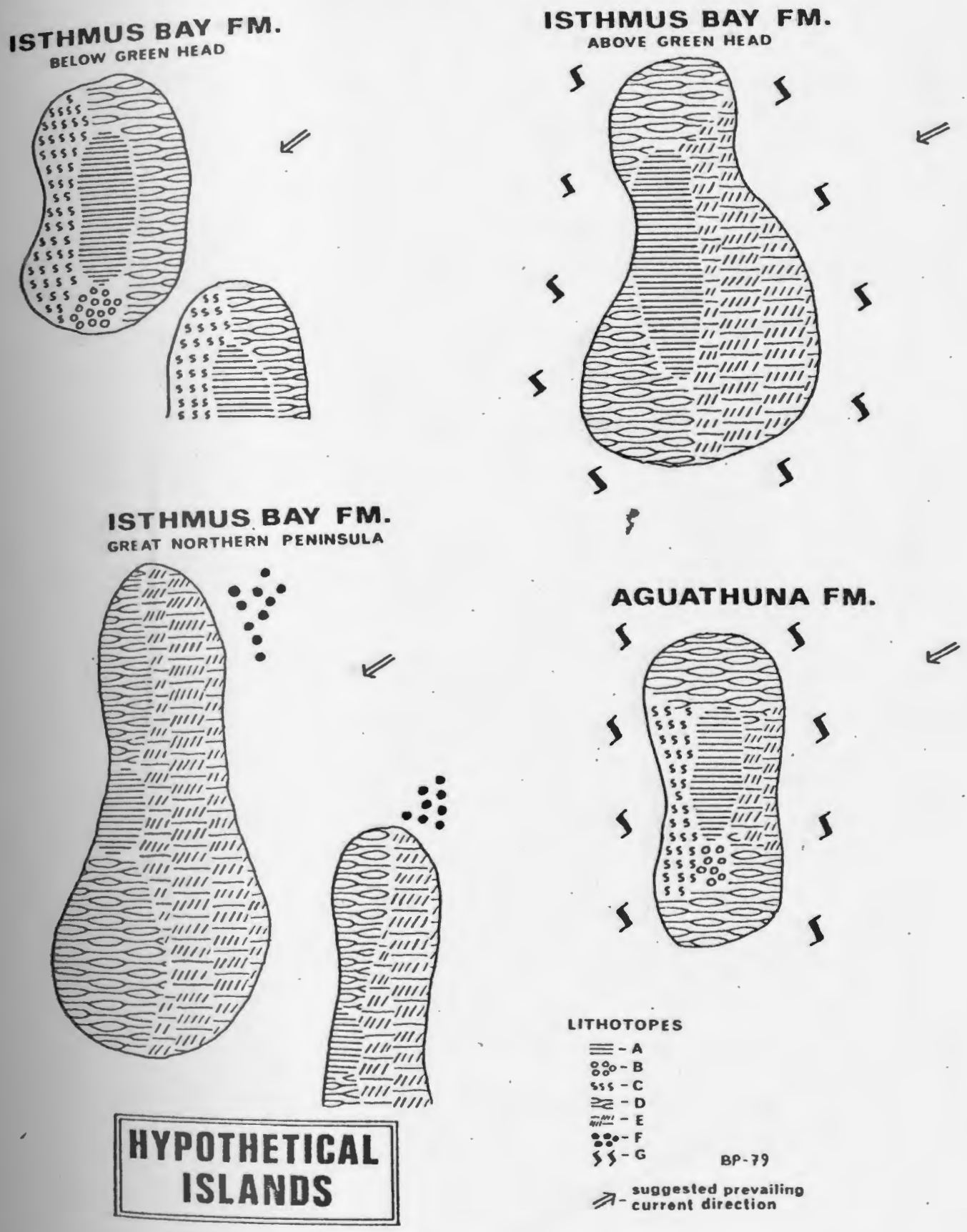


Figure 13: Hypothetical island facies maps drawn on the basis of the lithotope sequences.

produced on a subsiding shelf such as the Lower Ordovician continental shelf, by varying both the subsidence rate and the rate of sediment accumulation. Subsidence rate has a regional effect, but sediment accumulation is a local phenomenon. Five basic hypothetical patterns of sediment progradation and regradation are proposed by considering either subsidence or sedimentation (ie. sediment accumulation) rates, holding one or the other constant (Fig. 14). Actual patterns are more complex because the hypothetical cases deal only in two dimensions, simply sub-, inter-, and supratidal deposits, whereas the St. George has considerable three-dimensional variation. Alternate processes can theoretically explain each pattern: (1) alternating slow and sudden subsidence (with constant sediment supply) or alternating high and zero sedimentation rate (with constant subsidence), (2) alternating rapid and zero subsidence or alternating slow and very high sedimentation, (3) alternating slow and zero subsidence or alternating high and very high sedimentation, (4) alternating rapid and sudden subsidence or alternating slow and zero sedimentation rate, and (5) alternating rapid and slow subsidence or alternating high and slow sedimentation. Situation (1) produces asymmetric cycles and situation (2) produces symmetric cycles. In only situations (2) and (3) can the paleotidal range be measured from the thickness of intertidal units as outlined by Klein (1972). Asymmetric cycles have been called "punctuated aggradational cycles" by Anderson et al. (1978) to imply that they formed in episode of zero subsidence followed by sudden subsidence.

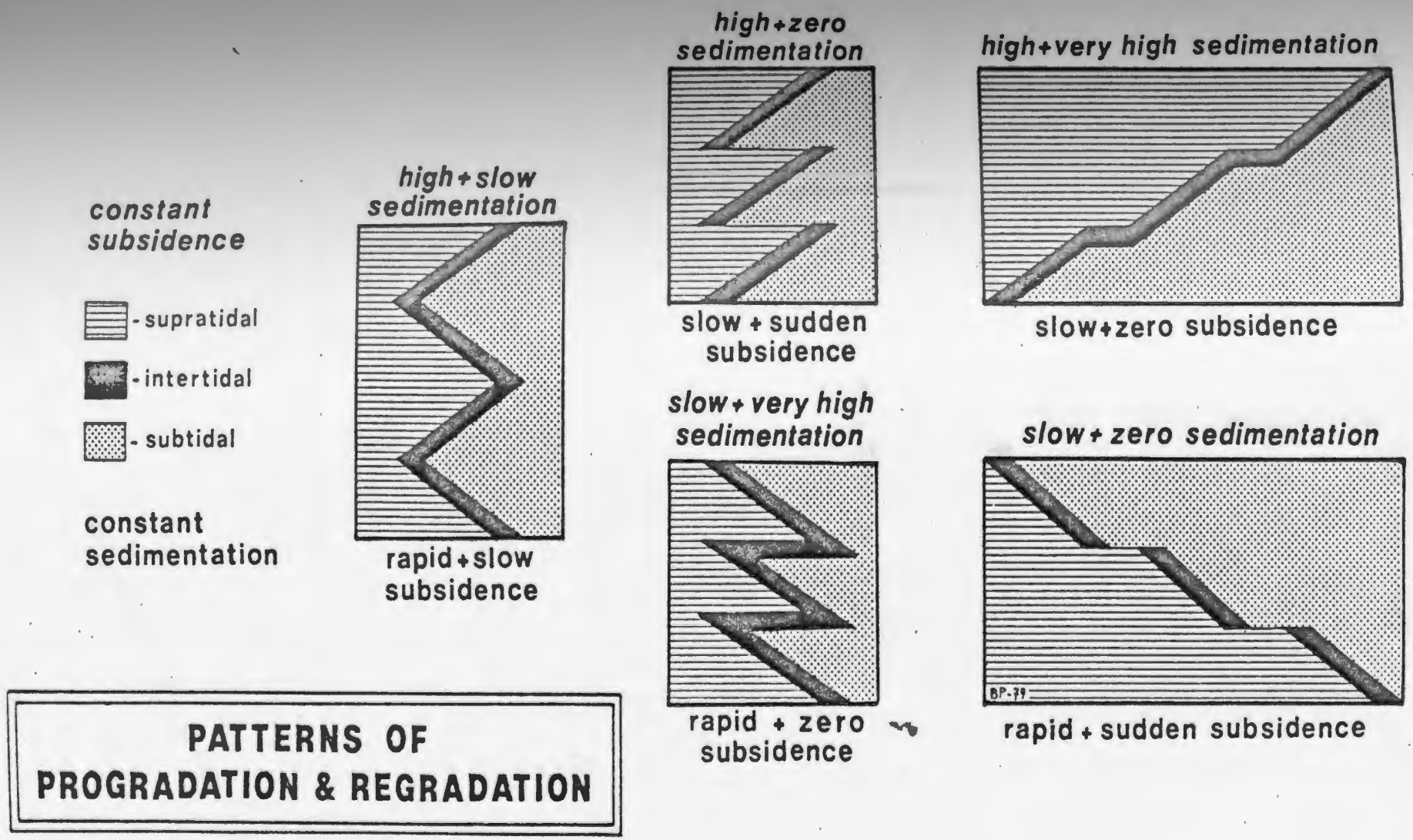


Figure 14: Hypothetical patterns of progradation and regradation produced by varying the subsidence rate and rate of sediment accumulation.

The same type of cycles ("autocycles" of Ginsburg) have been attributed by Mossop (in Kendall, 1978) and Ginsburg ( in Bosellini and Hardie, 1973) to progradation of sediment wedges during continuous subsidence until sediment supply is choked off and hydrodynamic forces shift the focus of sedimentation to another area, and the cycle repeats.

The following observations of the Isthmus Bay and Aguathuna Formations indicate that episodic subsidence does not account for the repetition and oscillation of lithotopes, but rather they formed as a response to local sediment supply on a shelf that was subsiding more or less constantly: (1) ideal sharply-bounded asymmetric cycles are not the rule and (2) shallowing and deepening events are not traceable even over short distances (e.g.: 2 kilometres across the Gravels). Minor fluctuations in subsidence rate would be expected to have occurred, but do not seem to have been enough to produce characteristic cycles traceable over long distances. The Isthmus Bay Formation is thickest in the Port au Port area indicating total subsidence was greater there than on the Great Northern Peninsula. Five subsidence events, however, seem to have affected the St. George on a regional scale: the development of subtidal reef complexes in the lower part of the Isthmus Bay Formation, subaerial exposure in the upper part of the Isthmus Bay, the advent of the Catoche Formation (where subsidence rate increased and subtidal conditions were largely maintained),subaerial exposure in the Aguathuna Formation, and subaerial exposure of the top of the St. George (see Chapter 5).

# CHAPTER 3 - CRYPTALGAL STRUCTURES

## INTRODUCTION

Cryptalgal structures occur abundantly throughout the St. George Group, and range from stromatolites, to thrombolites, to cryptalgal laminites, to oncolites (Aitken, 1967). Cryptalgal structures are divided here into laminated and unlaminated categories, thrombolites comprising the latter. In this chapter, the morphology of each type of structure is documented and related to sedimentological, biological, and diagenetic factors. Cryptalgal microstructures are described and a classification is proposed. The internal structure and framework of a unique Lower Ordovician algal-metazoan reef complex is analyzed in detail. Algal remains associated with cryptalgal structures are also described.

Linnéan nomenclature has been used for stromatolite classification, especially Precambrian forms, but disagreement on the validity of taxonomic subdivision into form-genera and form-species prompted the English language anacronymic classification of shapes of Logan et al. (1964). Aitken (1967) found this scheme partly inadequate and proposed a four-fold classification: cryptalgal laminite (algalaminite), oncolite, stromatolite, and thrombolite. The term "stromatolite" was restricted to fixed bodies with non-planar lamination. Two broad categories of stromatolites are recognized here: hemispheroidal and columnar. Columnar forms are arbitrarily considered to have a high thickness to diameter ratio of simple hemispheroids; columnar stromatolites usually occur together forming stromatolite mounds or bioherms.

Aitken (1967) introduced the term "thrombolite" to refer to mounds in which the unlaminated cryptalgal material possessed a macroscopically clotted fabric, with the clots commonly elongate upwards like columnar stromatolites. Use of the term "thrombolite" to refer to mounds made up of clots is inconsistent when the term "stromatolite" is used to refer to heads or columns that may form mounds. Therefore, "thrombolite" is redefined here: a thrombolite is a cryptalgal structure of variable but usually columnar shape, that may branch and anastomose, that lacks a distinctly laminated microstructure, and that usually occurs in groups forming mounds or bioherms. Structures intermediate between thrombolites and stromatolites occur but are comparatively rare, and Aitken's (1967) "thrombolitic stromatolite" is not used in this study for the sake of simplicity, and an arbitrary separation is made. In some large mounds, however, both types can occur together because conditions controlling fabric varied across the mounds.

## LAMINATED STRUCTURES

### Stromatolites

Hemispheroidal stromatolites - Hemispheroidal stromatolites only occur in the Isthmus Bay and Aguathuna Formations. Laterally-linked hemispheroids (Logan *et al.*, 1964) occur in three styles: (1) broad low-relief domes, 0.5 to 1 metre in diameter and less than 0.5 metre thick, that develop from undulating cryptalgal laminites, (2) hemispheroids up to 0.2 metre in diameter, that occur as discontinuous beds

within intertidal lithologies (lithotope D) (Fig. 16A), and, rarely, (3) hemispheroidal caps on thrombolite mounds. Stacked hemispheroids (Logan et al., 1964), though not ideal geometric structures, can be classed into five shapes (Fig. 15): (1) domes with constant radius and no walls (Fig. 16B), (2) domes with upward-increasing radius and walls, (3) domes with increasing radius and no walls (Fig. 16C), (4) domes with constant radius and walls (Fig. 16B), and (5) domes with internal wavy laminations.

Compound stromatolites are produced when internal wavy laminations can arbitrarily be said to form laterally-linked hemispheroids. Compound stromatolites are larger than simple hemispheroids, with a maximum diameter of 5 metres and plan view ranging from simple elliptical shapes to large lobate mounds (Figs. 16D, 18A). Topographic relief is greater in these than in simple hemispheroids, as shown by tracing individual laminae around the mounds. Internally, they consist of a combination of stacked and laterally-linked hemispheroids of variable diameters, which are themselves often composed of wavy lamination.

Because hemispheroidal stromatolites developed in the intertidal zone, they were sometimes exposed to erosion. A particularly good example of this occurs at the top of the Isthmus Bay Formation at Boat Harbour where stromatolite domes with upward-increasing radius and overhanging walls encrust eroded remnants of thrombolite mounds. The tops of the domes are planed off, and covered by undulating cryptalgal laminite. (Figs. 17, 18B).

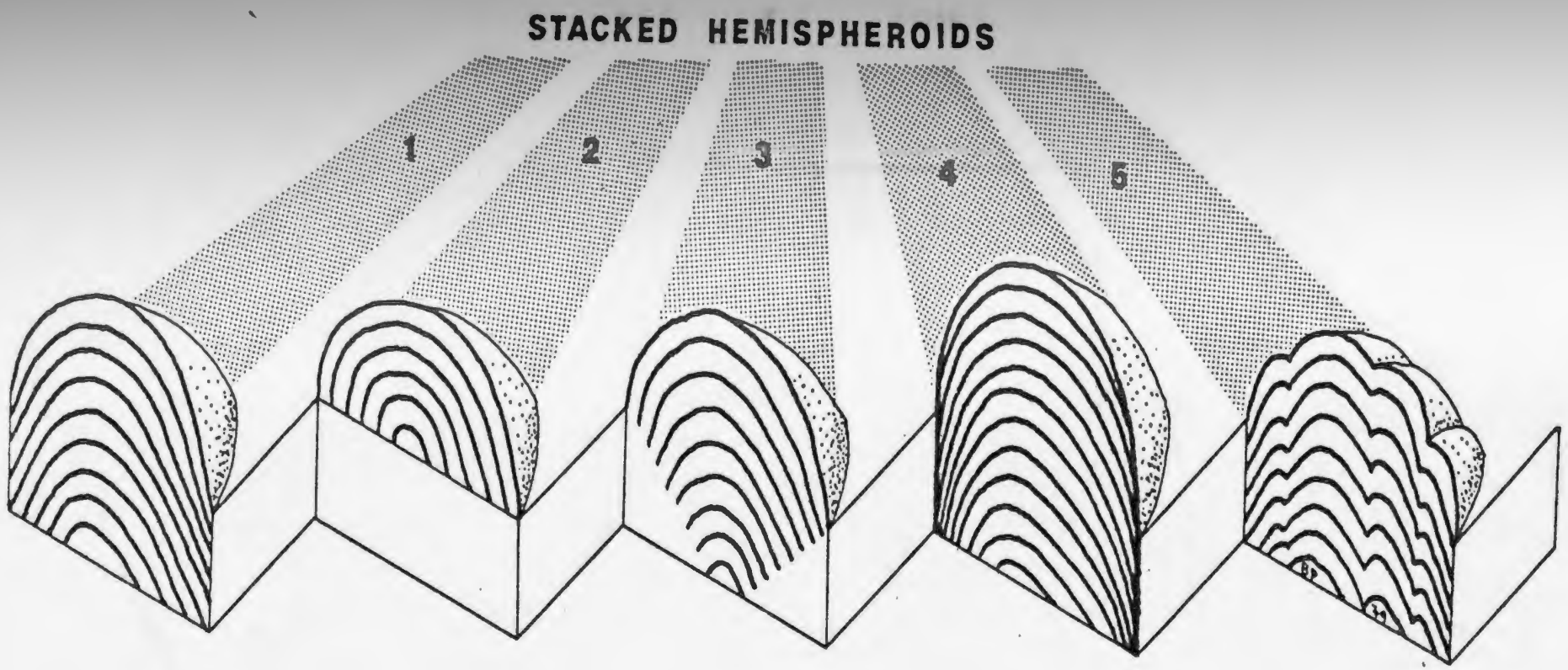


Figure 15: Types of stacked hemispheroidal stromatolites that occur in the St. George. (1 = domes with constant radius and no walls; 2 = domes with increasing radius and walls; 3 = domes with increasing radius and no walls; 4 = domes with constant radius and walls; 5 = domes with internal wavy or compound lamination)

FIGURE 16

HEMISPHEROIDAL STROMATOLITES

A. Bedding plane view of laterally-linked hemispheroidal stromatolites. Lens cap 6 cm across; Isthmus Bay Fm.; IB-115.

B. Vertically oriented slab of cryptalgal laminite doming to laterally-linked hemispheroidal, to stacked hemispheroidal stromatolites (types 1 and 4: constant radius, with and without walls). Scale in cm; Isthmus Bay Fm.; ECW-3.

C. Vertically oriented slab of stacked hemispheroidal stromatolite (type 3: increasing radius, without walls). Scale in cm; Isthmus Bay Fm.; IB-200.

D. Bedding plane view of lobate mound (4 m across) of compound (laterally-linked hemispheroidal) stromatolites. Aguathuna Fm.; NEG-5.

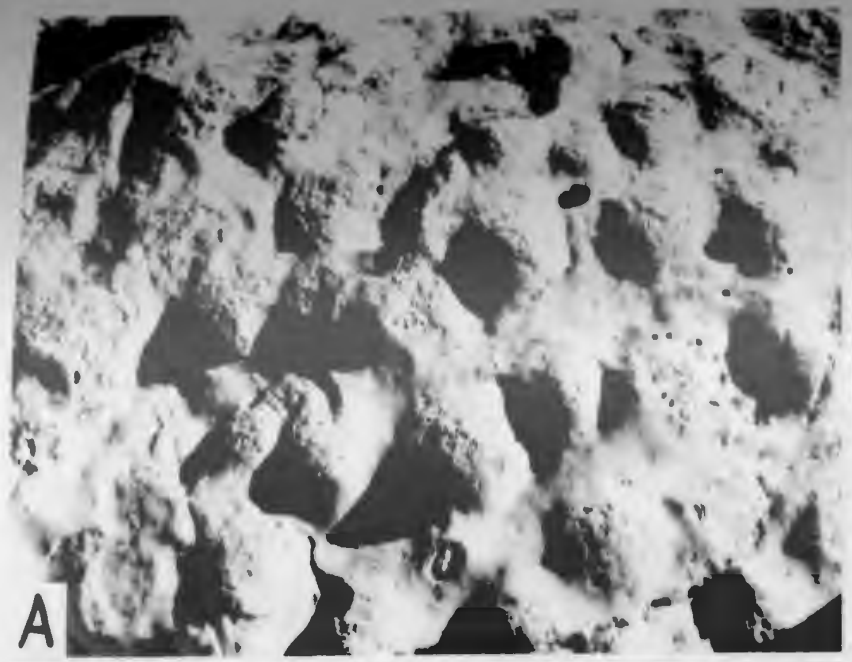
A

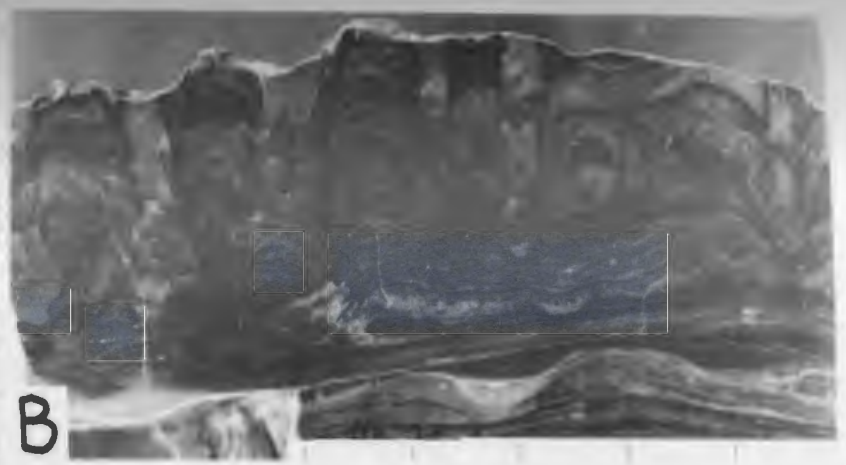
B

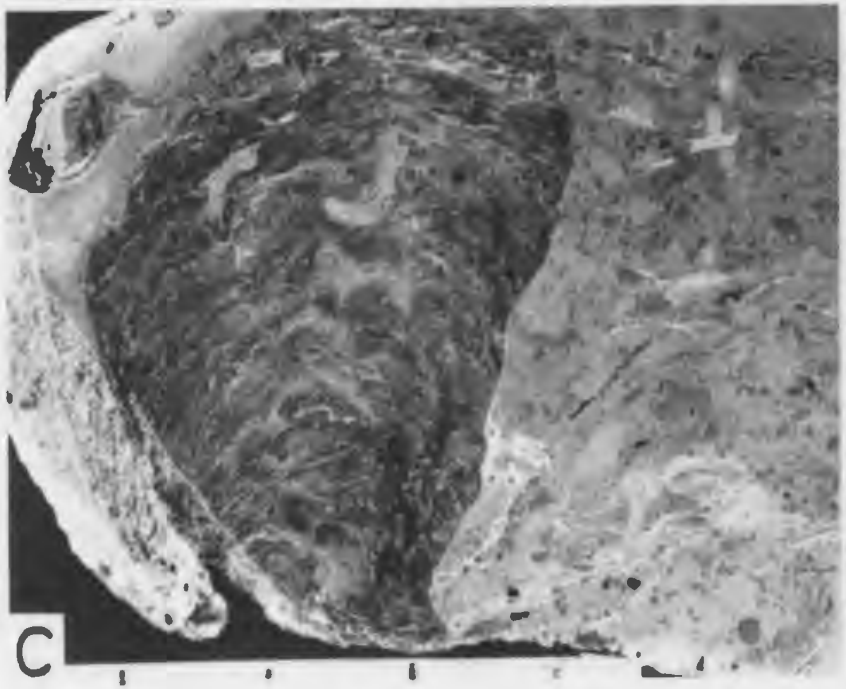
C

D

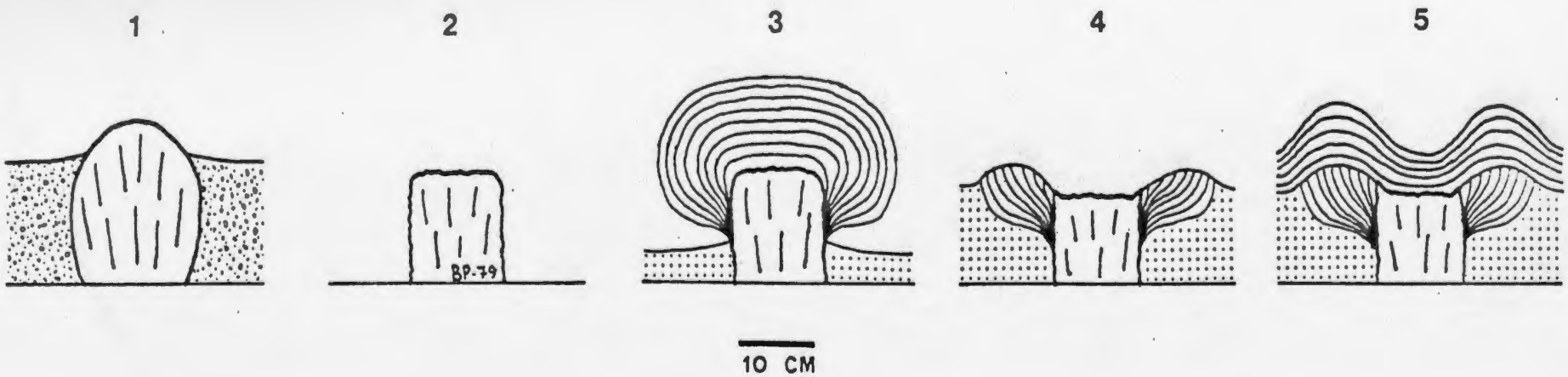


**EROSION OF STROMATOLITES**

Figure 17: Sequence of development of eroded cryptalgal structures, upper Isthmus Bay Formation, Boat Harbour.

FIGURE 18

HEMISPHEROIDAL AND COLUMNAR STROMATOLITES

A. Vertical view of small mound of compound (laterally-linked and stacked hemispheroidal) stromatolites. Lens cap, on left edge of photo, 6 cm across; Aguathuna Fm.; IB-324.

B. Vertical view of eroded 10 cm diameter thrombolite mound encrusted by overhanging stromatolite which is planed off and overlain by laterally-linked hemispheroidal stromatolites. Isthmus Bay Fm.; BH-144.

C. Exhumed circular and coalesced lobate mounds composed of columnar stromatolites (see Fig. 19B). Isthmus Bay Fm.; ECW-41.

D. Vertical view of dolomitized columnar stromatolite mound flanked on the right by intraclastic grainstone. Arrow points to outward inflexion of stromatolite columns. Coin 1.9 cm across, Isthmus Bay Fm.; IB-80.

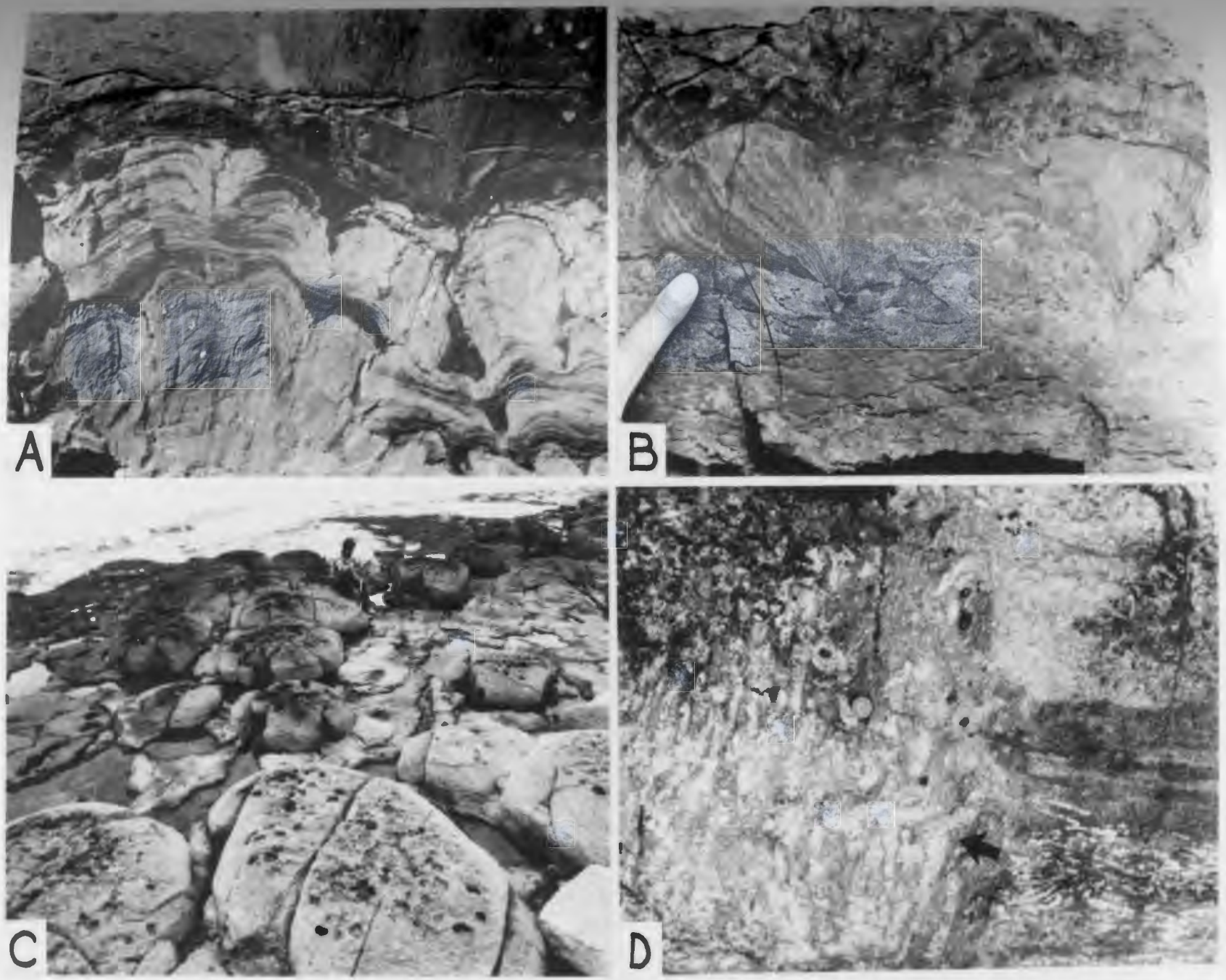
A
B
C
D

Columnar stromatolites - Columnar stromatolites are simple hemispheroids, with a large height to diameter radius that usually branch, in a gymnosoleniform (terminology of Hoffman, 1977) or digitate and slightly dendroid (terminology of Hofmann, 1969) fashion (Fig. 19). The closely spaced columns are convexly laminated, between 1 to 2 centimetres in width, and circular to irregularly lobate in plan. In longitudinal view, columns vary from those with uniform diameters to those with irregular margins and widths. The trend to columns with irregular margins coincides with the trend to less distinct lamination and marks the change to thrombolites.

Columnar stromatolites form mounds up to 1 metre thick and 2 metres in diameter, sometimes coalescing to larger lobate mounds several metres in diameter (Fig. 18C). Exhumed mound upper surfaces are knobby. Sediment between columns is usually mudstone and finely peloidal grainstone, and between mounds is thin-bedded intraclastic and peloidal grainstone that rarely contains fossils or burrows (Fig. 18D). Mounds with forms transitional to thrombolites contain more fossils and burrows. Larger intraclasts are often collected in narrower channels between mounds. Overlying and underlying beds are of the intertidal flat facies (lithotope D).

Aberrant Forms - Stromatolites possessing unusual morphologies not readily categorized in the above subdivisions occur in the Isthmus Bay Formation at three localities. All are columnar in shape, with laminated, nearly vertical walls.

In units spanning the Cambro-Ordovician boundary at Boat Harbour, closely spaced, dolomitized stromatolites 1.2

FIGURE 19

COLUMNAR STROMATOLITES

A. Small branching columnar stromatolites. Scale in cm; Isthmus Bay Fm.; ECW-75.

B. Light-coloured anastomosing columnar stromatolites from large (1 m diameter) mounds (see Fig. 18C). Scale as in A; Isthmus Bay Fm.; ECW-41.

C. Tracing, with simplified lamination, from vertically oriented slab of columnar stromatolites. Isthmus Bay Fm.; IB-118.

D. Tracing, with simplified lamination, from vertically oriented slab of columnar stromatolites. Isthmus Bay Fm.; IB-122.

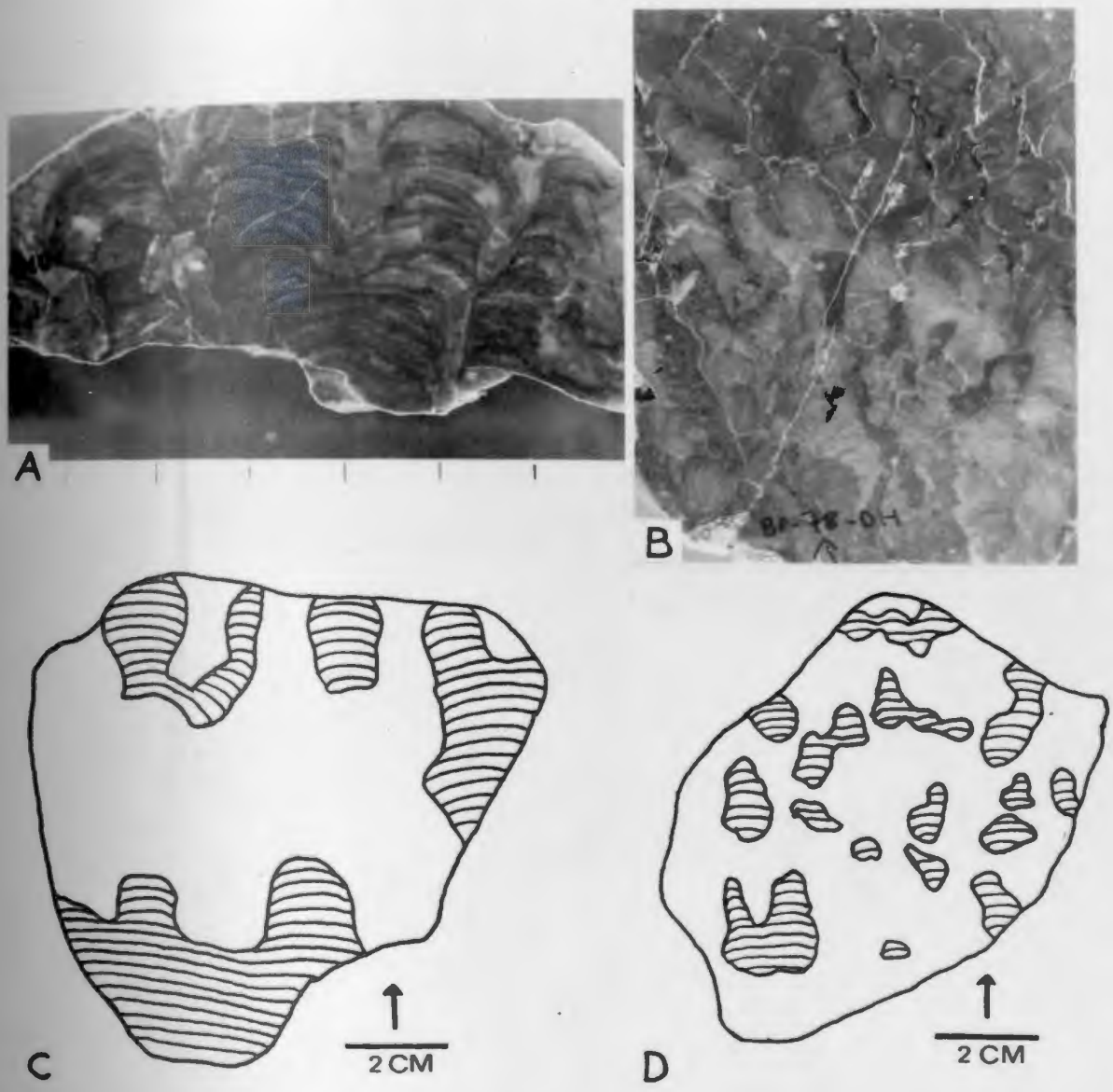
A
B
C
2 CM
D
2 CM

metres high and about 0.4 metre in maximum width have vertically laminated walls and unlaminated axial zones (Fig. 20A). They are not perfect cones and the walls flex inward in stages. They are similar in form to the Precambrian form-genus Conophyton, differing in the nature of the axial zones, or to an unbranching type of the Precambrian form-genus Jacutophyton.

In the lower part of the Isthmus Bay Formation on Port au Port Peninsula, is a unit of unusual columnar stromatolite mounds 1.5 metres in diameter and 0.4 metre thick. At the bases of the mounds are clumps of Conophyton-like conical stromatolites 15 centimetres high and 4 centimetres wide (Fig. 20B). The laminated walls can be termed very acutely inflexed (terminology of Hofmann, 1969) and the axial zones are poorly laminated.

In the Isthmus Bay Formation at Eddies Cove West, aberrant stromatolites form the cores of thrombolite mounds 1.4 metres thick and 1 metre in diameter. The stromatolites have a maximum height of about 0.4 metre. In plan view, they have an interconnecting cerebral pattern of vertically laminated walls up to 4 centimetres thick, that grade to unlaminated (thrombolitic) axial cores of irregular cross-section (Figs. 20C, D). The interstices between walls are filled with mudstone and peloidal grainstone containing burrows. The whole structure has a cerebroid or convoluted boxwork nature, and isolated columns are not formed. Ooids occur in associated grainstones and thrombolites.

Discussion - Stromatolites accrete by the episodic but regular influx of sediment onto predominatly blue-green algal mats,

FIGURE 20

ABERRANT COLUMNAR STROMATOLITES

A. Vertical view of large dolomitized conical stromatolites with inflexed vertically laminated walls and unlaminated axial zones. Pocket knife 9 cm long; Isthmus Bay Fm.; BH-10.

B. Vertically oriented slab of conical stromatolite with thin unlaminated axis. The upper part of the stromatolite has been removed by stylolitization, and it is surrounded by coarse dolomitized grainstone. Scale in cm; Isthmus Bay Fm.; IB-81.

C. Bedding plane view of cerebroid boxwork of dark-coloured stromatolites and light-coloured internal mudstone sediment. Lens cap 6 cm across; Isthmus Bay Fm.; ECW-86.

D. Horizontal and vertical tracing from slab of cerebroid boxwork of C (black=thrombolitic axes; parallel lines=simplified stromatolite lamination; stipled=internal sediment).

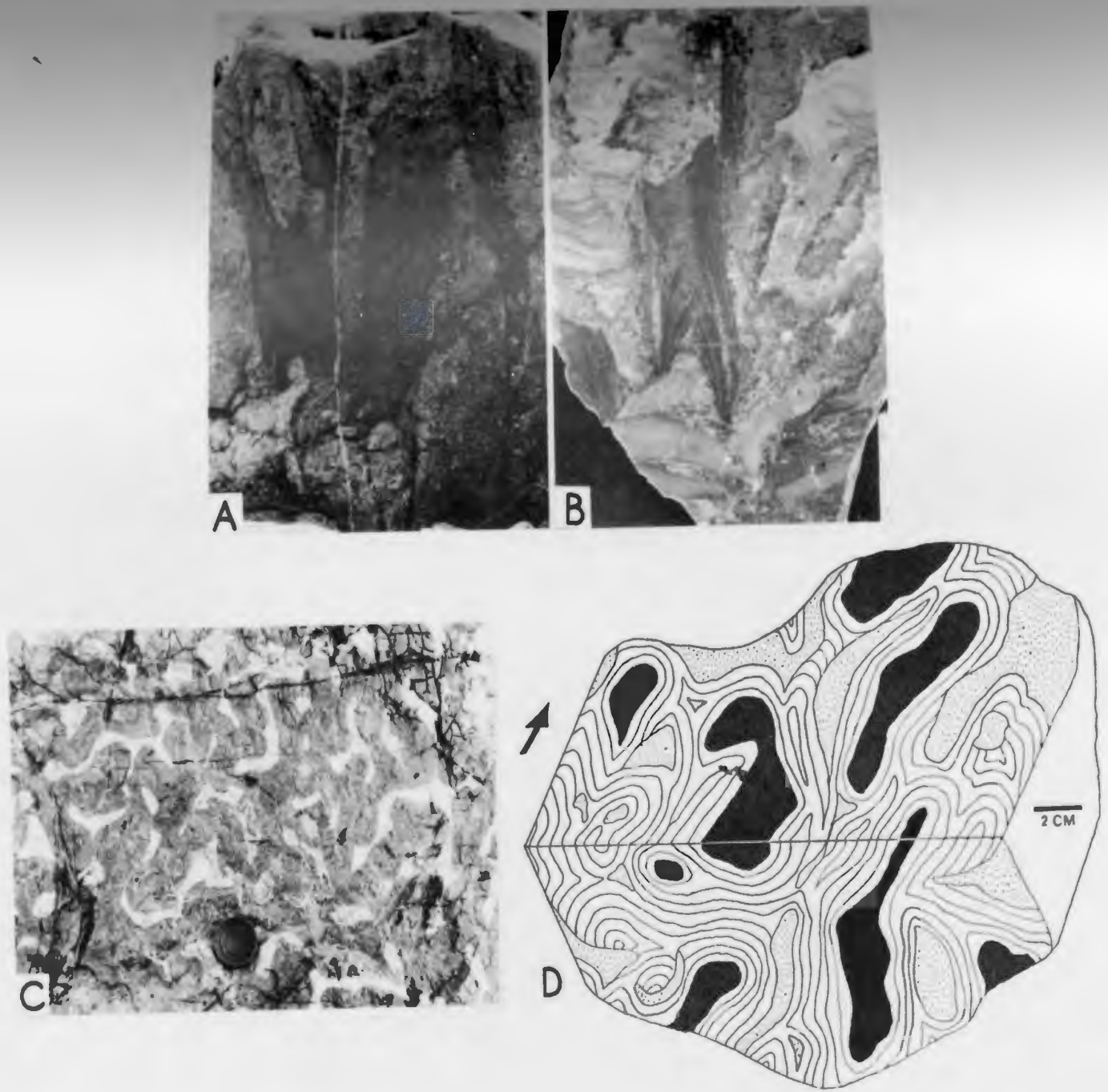
A
B
C
D
2 CM

sedimentary events being preserved as single laminae. Some previous workers have discussed the environmental controls on ancient stromatolite morphology (e.g.: Logan et al, 1964; Aitken, 1967; Horodyski, 1977; Semikhatov et al., 1979), but recently there has been more emphasis on possible influences of the microbial composition of the algal mats (Semikhatov et al., 1979).

Growth of algal mats and eventual formation of stromatolites requires protection from strongly erosive scour. The hemispheroidal stromatolites of the St. George are interpreted to have formed in the intertidal zone because of the associated sediments which possess all the attributes of intertidal deposition, including mudcracks, sporadic burrows, and bedding types. The change upward from cryptalgal laminites (interpreted to be of supratidal or uppermost intertidal origin) to laterally-linked hemispheroids suggests a deepening shift to intertidal conditions and a slight increase in turbulence and resultant scour which would promote the development of domes. Laterally-linked hemispheroids may have in some cases formed in very shallow ephemeral tidal pools as well as on exposed flats.

The morphology of stacked hemispheroids can be explained by varying the sedimentation rate and length of time between periods of sedimentation. The development of stacked hemispheroids with walls suggests that sedimentation rate (on the surrounding substrate) was less than that around hemispheroids without walls because the bases of the former stromatolites are not covered and they had a higher synoptic relief. Increasing radius would suggest longer intervals of time

between sedimentation events which would allow lateral expansion of algal mats during successive quiet spells.

The formation of stromatolites or mounds of laterally-linked and stacked convex lamination is probably related primarily to turbulence and resulting scour which would have promoted doming. Domes would have been maintained by greater sediment accretion on dome crests (Logan et al., 1964). Compound lamination could result also in part from maintenance or enhancement, during growth, of underlying surface irregularities that result from small accumulations of coarser particles in depressions. Larger mounds tended to form probably because of high sedimentation rate onto the mats but with less overall accumulation of unbound detritus in flanking beds.

Columnar stromatolites seem to have developed when hemispheroidal stromatolites grew at a rapid pace because of a high sedimentation rate both on the mat surfaces and around them as the synoptic relief remained more or less constant. Columnar stromatolites are interpreted to have formed in the lower intertidal and probably sometimes shallow subtidal zones, to account for the necessary high sedimentation rate but rarity of burrowing and fossil debris. Isolated mounds probably formed because sediment lodged in the protected areas between the columns, and scour was focussed into intermound areas. Branching and anastomosing likely occurred when mats expanded laterally when unbound detritus accumulated between columns, and when mats were constrained and column inheritance (Hofmann, 1969) interrupted by sediment

accumulation on mat surfaces. Spacing between columns tends to be rather constant, probably because scour was always focussed onto unbound areas between mat surfaces.

Forms similar to the rare, aberrant, near-vertically laminated stromatolites do not appear to have been previously reported from Phanerozoic rocks. The form-genus Conophyton is similar to the aberrant conical forms, except that the latter do not have well-developed crestal zones in the axial area, an essential character of Conophyton (Walter, 1972). The poorly laminated or thrombolitic axial zones probably result from a less even sediment coating, irregular algal growth and sporadic burrowing. This is in contrast to the well-laminated column walls that grew upwards and outwards. The actual height or synoptic relief of these structures above the surrounding sediment was considerable in relation to their diameters. In the cerebroid boxwork structures from Eddies Cove West, open spaces left where the walls did not meet were later filled with mudstone likely during growth of the capping thrombolite mounds. The environmental conditions under which the aberrant structures formed must have been a rare and different combination compared with those that led to growth of more typical stromatolites. The height and lateral growth of the walls indicates low sedimentation rate around the columns and consistently episodic influx of silt-sized peloids carried in suspension, probably in the shallow subtidal zone. The closely spaced columns were probably not affected by strong and directed turbulence and scour and grew not as simple cones but rather as an irregular

boxwork. Conditions favouring the boxwork pattern likely developed in a small protected subtidal lagoon, possibly behind a small oolite barrier.

## Cryptalgal laminites

Description - Cryptalgal laminites are common in the Isthmus Bay and Aguathuna Formations. Units of cryptalgal laminites range in thickness from 0.1 to 1.5 metres.

Cryptalgal laminites are interlaminated mudstone and finely peloidal grainstone, and are commonly dolomitized to finely crystalline ferroan dolostone (Fig. 21A). Laminae are of uniform thickness, are planar to slightly undulating, drape over underlying irregularities, frequently dome upwards forming low-relief hemispheroidal stromatolites, and in rare cases may be buckled upwards forming small tepee structures. Laminae may be laterally discontinuous, and small-scale disconformities are sometimes present. Peloidal and intraclastic grainstone layers are common. The laminae are often broken by mudcracks (Fig. 21B), occasionally by deep prism cracks, and rarely by burrows penetrating from overlying beds (Fig. 21C). Cryptalgal laminites are often brecciated, forming layers of intraclasts which are also transported to other intertidal areas. Contacts with superposed intertidal and subtidal units are usually sharp and underlying cryptalgal laminites may be brecciated into angular blocks.

Interpretation - The above characteristics have been considered criteria indicating a cryptalgal origin for this lithology (e.g.: Aitken 1967), comprising lithotope A in

FIGURE 21

CRYPTALGAL LAMINITES AND ONCOLITES

A. Vertically oriented slab of dolomitized cryptalgal laminite, showing wavy, broken, and grainstone layers. Sediment-floored and spar-filled vugs are epigenetic. Scale in cm; Isthmus Bay Fm.; IB-105.

B. Bedding plane of desiccation cracked cryptalgal laminite. Isthmus Bay Fm.; BH-72.

C. Vertically oriented slab of cryptalgal laminite disrupted by burrows penetrating from above. Many burrows spar-filled (dark-coloured). Isthmus Bay Fm.; IB-247.

D. Vertically oriented slab of oncolites with asymmetric concentric lamination, in intraclastic grainstone and wackestone. Aguathuna Fm.; IB-303.

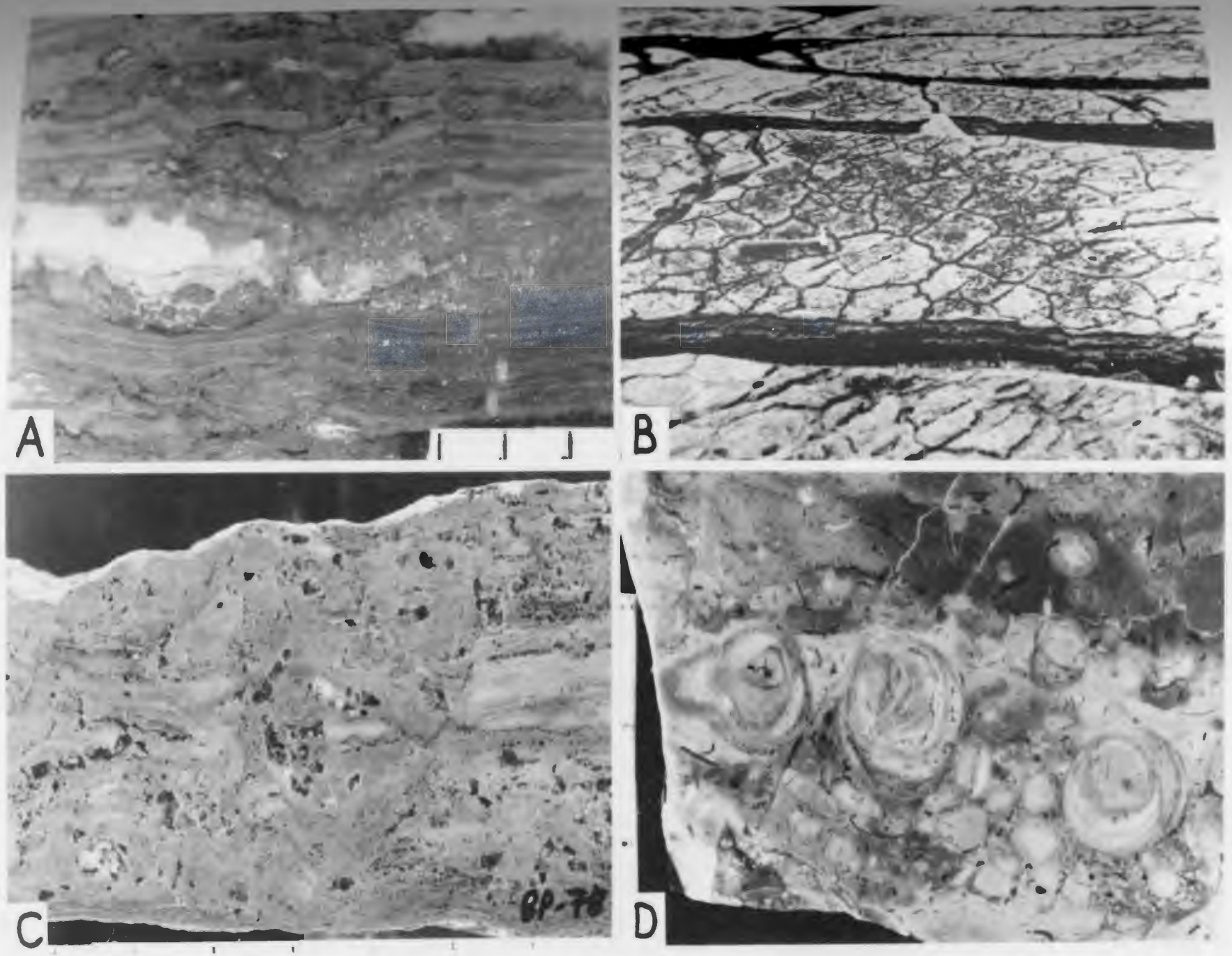
A
B
C
D

Chapter 2. Sediment grains, mud- to sand-sized were carried in suspension onto algal mats where they are bound by algal filaments. The encrusting nature of the algal mats gave rise to the characteristic draping of laminae around underlying irregularites. Storms caused disruption of mats and deposition of grainstone layers. Periods of subaerial exposure produced desiccation cracks, and synsedimentary lithification and expansion caused tepee structures to form (Assereto and Kendall, 1977). The above features indicate formation of these rocks in the uppermost intertidal and supratidal zones of protected areas of tidal flats. During facies shifts, tops of cryptalgal laminated units were often reworked by physical erosion and bioturbation.

## Oncolites

Oncolites are uncommon in the St. George, and are found only in some grainstone beds of the Isthmus Bay and Aguathuna Formations. They range in diameter from about 1 to 5 centimetres and laminae are each approximately 1 millimetre thick. They are characterized by more or less concentric lamination that is asymmetrical about the nuclei, which are intraclasts and fossils, such as gastropods and *Ceratopea* opercula (Fig. 21D). They are interpreted to have formed in agitated intertidal and subtidal environments. Asymmetrical layering suggests periods of stability alternating with periods of rolling.

## UNLAMINATED STRUCTURES

### Thrombolites

Thrombolite Morphology - Individual thrombolites are elongate upwards, but their widths, cross-sections, margins, branching and anastomosing patterns are highly variable (Figs. 22,23), and are related partly to the size of the mounds which they form. Thrombolite columns range in diameter from slightly less than 1 to about 3 centimetres. They branch like columnar stromatolites, in a gymnosoleniform or digitate and slightly dendroid fashion, often radiating outwards as well as upwards (Figs. 22G, 24B). They anastomose more than columnar stromatolites. Cement-filled growth framework cavities occur sporadically. The matrix between columns is fossiliferous and burrowed peloidal wackestone with grainstone areas. In the smallest mounds, less than 0.2 metres in diameter, thrombolites have little vertical elongation (Fig. 24A). In larger mounds, thrombolites anastomose often so much that there is comparatively little matrix (Fig. 22A). The ratio of columns to the volume of the mounds varies widely between mounds of different horizons. In thrombolite mounds larger than about 1 metre in diameter, there is less anastomosing and more vertical elongation (Fig. 22D). When mounds coalesce into extensive banks, thrombolite shape varies considerably and the ratio of columns to mound volume decreases. The irregularity of thrombolite cross-sections, which can range from nearly circular, to irregular, to elongate (Figs. 24C,D), gives an intricate cerebral pattern on weathered bedding planes (Figs. 24E,F) attributed by Smit (1971) to burrow-mottling.

FIGURE 22

THROMBOLITES

Tracings of vertically oriented slabs
(black areas are thrombolites)

A. From a small 0.15 m diameter mudstone-rich mound. Isthmus Bay Fm.; IB-218.

B. The base of a 0.5 m diameter mound; below the dashed line is grainstone upon which the mound developed. See Fig. 23A. Isthmus Bay Fm.; BH-104.

C. Left margin (outlined by dashed line) of 0.3 m diameter mound. Isthmus Bay F.; IB-137.

D. From large 3 m diameter and 2.4 m thick mound. Isthmus Bay Fm.; BH-107.

E. From coalesced 0.6 m thick mounds. See Fig. 23C. Isthmus Bay Fm.; ECW-30.

F. From a 1 m thick bank. See Fig. 23B. Isthmus Bay Fm.; ECW-82.

G. Nearly entire mound (right side outlined by dashed line). Isthmus Bay Fm.; IB-242.

H. Left side of small 0.2 m thick mound. See Fig. 23D. Aguathuna Fm.; IB-340.

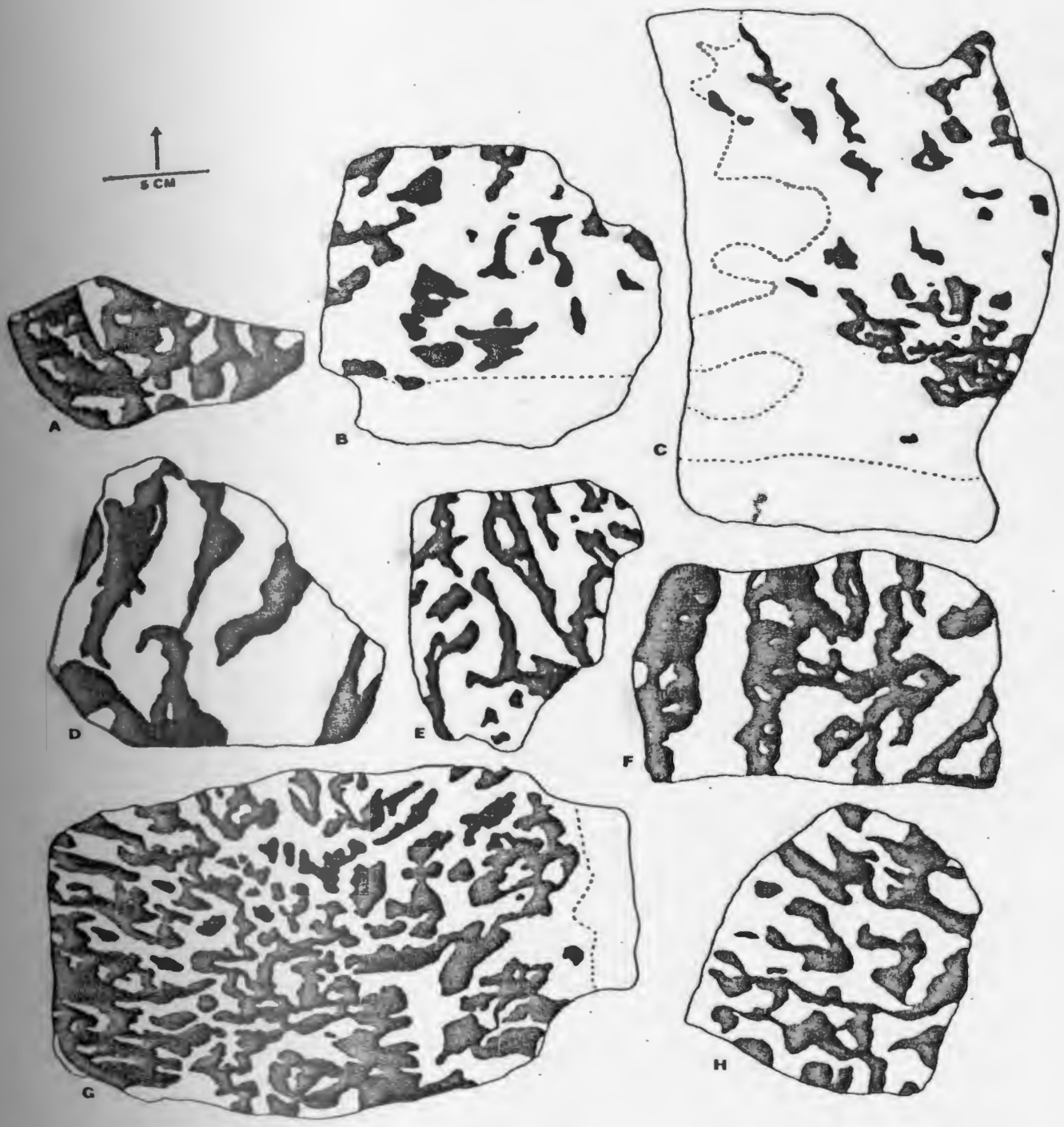
5 CM
A
B
C
D
E
F
G
H

FIGURE 23

THROMBOLITES

Vertically oriented slabs (scale in cm)

A. Corresponds to tracing Fig. 22B. Isthmus Bay Fm.; BH-104.

B. Corresponds to tracing Fig. 22F. Isthmus Bay Fm.; ECW-82.

C. Corresponds to tracing Fig. 22E. Isthmus Bay Fm.; ECW-30.

D. Corresponds to tracing Fig. 22H. Aguathuna Fm.; IB-340.

FIGURE 24

THROMBOLITES

A. Vertically oriented slab of small (10 cm diameter) thrombolite mound showing fossiliferous (trilobitic) wackestone matrix. Patches devoid of fossils are thrombolites. Scale in cm; Catoche Fm.; ECW-112.

B. Vertical view of light-coloured dolomitized columns showing little branching and anastomosing. Lens cap 6 cm across; Isthmus Bay Fm.; BH-47.

C. Bedding plane view of dark-coloured thrombolites approximately circular in cross-sections. Isthmus Bay Fm.; IB-142.

D. Bedding plane view of dark-coloured thrombolites with irregular and interconnecting cross-sections. Catoche Fm.; Lower Cove.

E. Bedding plane view of cerebral weathering pattern of dolomitized thrombolites standing out in relief from matrix. Catoche Fm.; Table Mountain.

F. Bedding plane view of outer edge of a dolomitized thrombolite mound, showing cerebral weathering pattern. Range pole in 20 cm divisions; Isthmus Bay Fm.; BH-107.

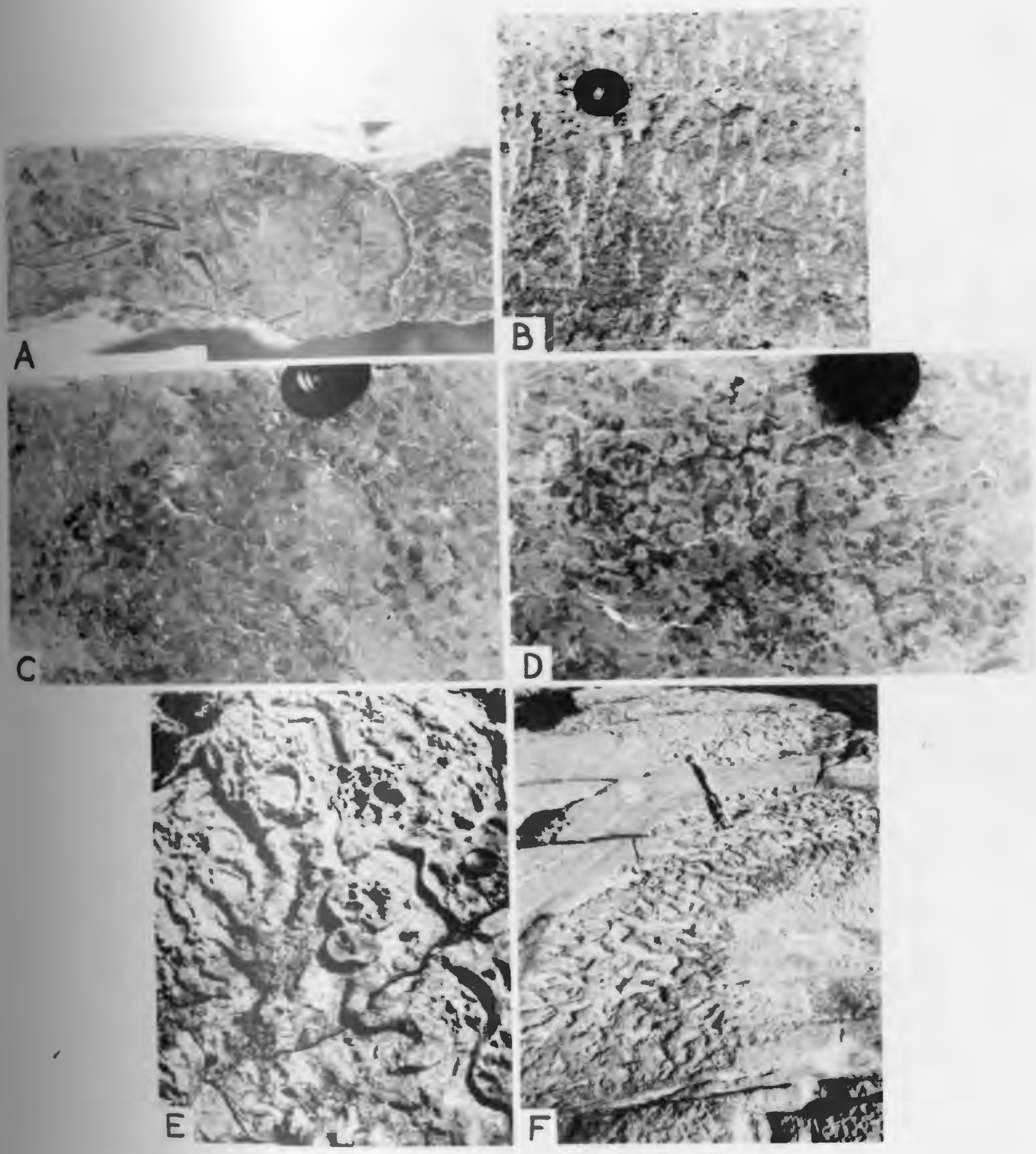
A
B
C
D
E
F

Thrombolite mounds - Thrombolite mounds vary in size and are usually roughly circular in plan. The smallest are about 0.1 metre in diameter and 5 centimetres in thickness, and occur in large numbers on grainstone bedding planes of lithotope E (intertidal shelf facies) in the uppermost part of the Isthmus Bay and lower part of the Catoche Formations (Fig. 25A). Slightly larger mounds, less than 0.4 metre in diameter and 0.2 metre in thickness are common in the Isthmus Bay and Aguathuna Formations of the Port au Port area, but are rare on the Great Northern Peninsula, because of different sedimentological patterns (see Chapter 2). Mounds in the Isthmus Bay and Catoche Formations on the Great Northern Peninsula are commonly larger, ranging in diameter and thickness from 0.5 metre to 1.8 metres, and in one case to 3 metres. They are usually equidimensional to slightly wider than thick but exceptions occur (Fig. 25B). In most cases, individuals in each unit tend to be of the same size.

Mounds are usually closely spaced, less than 1 metre apart, and in the Isthmus Bay and Catoche Formations on the Great Northern Peninsula they often coalesce (Figs. 25C,D), forming small irregular patches, chain-like rows, circular mounds up to 5 metres wide and over 50 metres long (Figs. 25E,26), and large banks that can be over 100 metres in width with grooved margins. At the base of the Catoche Formation on Port au Port Peninsula , extensive banks 2 metres thick were formed by large irregularly shaped mounds that coalesced during upward growth and roofed over grainstone channels.

FIGURE 25

THROMBOLITE MOUNDS

A. Dolomitized small (10 cm diameter) thrombolite mounds. Catoche Fm.; Brent Island, Hare Bay.

B. Vertical cross-section of dolomitized thrombolite mounds with divergent light-coloured thrombolite columns. Isthmus Bay Fm.; BH-17.

C. Bedding plane view of margin of linear thrombolite mound complex showing light-coloured thrombolite mounds with dark-coloured burrowed dolomite-mottled wackestone between. To the left of lens cap (6 cm across) is a horn-shaped archaeoscyphiid sponge. Catoche Fm.; ECW-128.

D. Bedding plane view of coalesced circular thrombolite mounds. Isthmus Bay Fm.; ECW-82.

E. View along the length of linear bank of thrombolite mounds. Person standing to left of bank; Catoche Fm.; ECW-128.

F. Thin section photomicrograph of mound-flanking grainstone composed of cryptalgal fragments. Scale bar 1500 µm; Isthmus Bay Fm.; ECW-86.

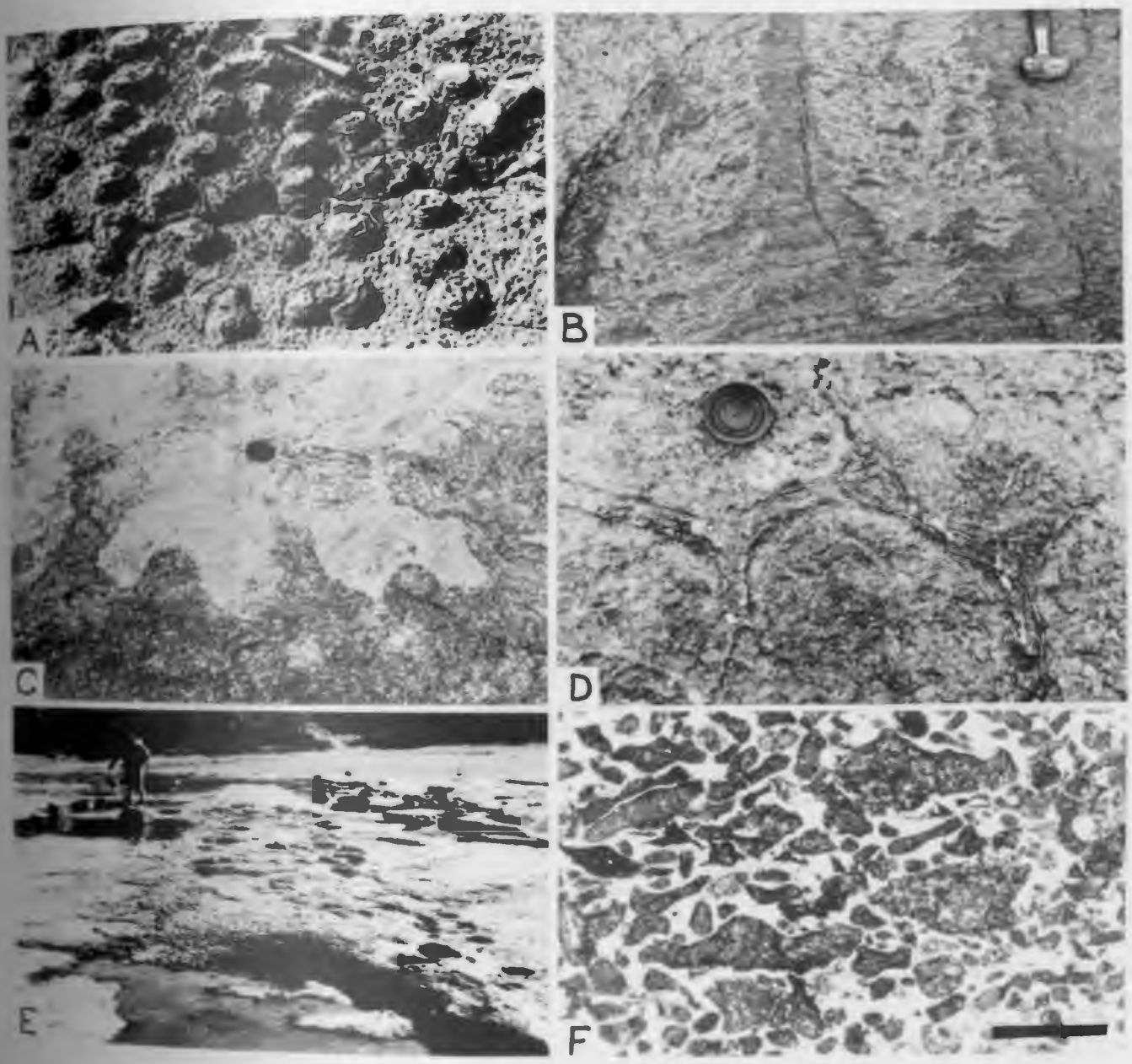
A
B
C
D
E
F

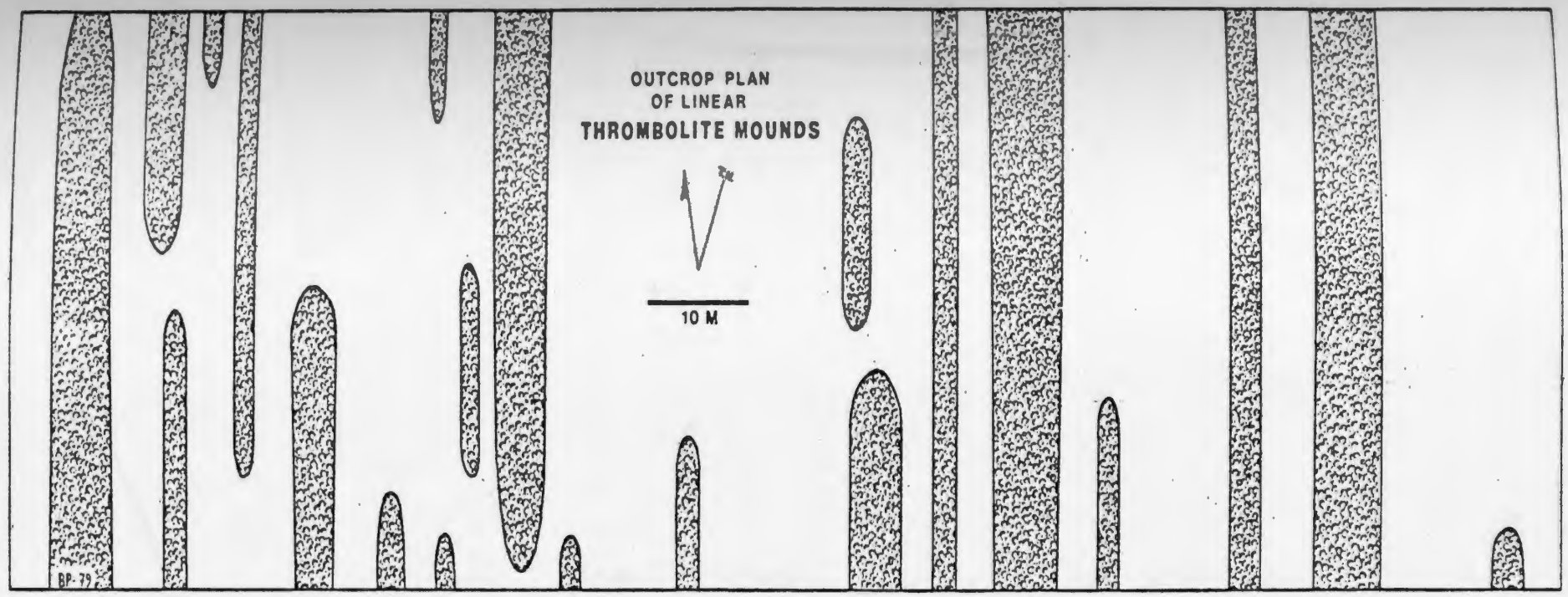


Figure 26: Outcrop plan of linear-shaped coalesced thrombolite mounds 0.4 m thick exposed on a large bedding plane 4 km southwest of Eddies Cove West in Bustard Bay. Catoche Fm.; ECW-128.

In the upper part of the Isthmus Bay Formation on Port au Port, thrombolites forming a bank 0.4 metre thick are abraded by narrow channels, roofed over and flask-shaped in cross-section.

Flanking sediment is unburrowed to sporadically burrowed peloidal, intraclastic, and usually fossiliferous grainstone, that often contains thrombolite fragments (Fig. 25E). Farther from mounds, flanking sediment becomes more burrowed and changes to fossiliferous wackestone (lithotope G). The abundance of fossils, including gastropods, cephalopods, trilobites, rostroconchs, and pelmatozoan debris increases markedly towards and within mounds. Within mounds, rare cases occur where gastropods have been leached and the molds later burrowed. The contacts between mounds and flanking grainstone are sharp, often intertonguing, and sometimes are abraded. Individual mounds are usually rooted in grainstone beds and sometimes in burrowed wackestone beds. In many units, mound bases occur at different levels, and likewise they ceased growth at different levels.

Thrombolite-metazoan mounds - Throughout the St. George there are sporadic occurrences of mounds composed of both thrombolites and sponges or corals. Beginning in the uppermost part of the Isthmus Bay Formation, isolated lithistid sponges of the Archaeoscyphiidae contribute to the structure of thrombolite mounds. These sponges range in shape from shallow wide-mouthed baskets to long narrow horns up to 0.5 metre in length, and are preserved in life position or cast into flanking grainstones (Figs. 27B). Tubular and

stick-shaped sponges occur only as fragments in flanking grainstones and in the matrix of mounds (Fig. 27C). Large sponges never occur in abundance in mounds (Fig. 28E).

The spicular lamellar organism Pulchrilamina Toomey and Ham, 1967 occurs sporadically in a thrombolite bank in the Catoche Formation at Port au Choix and forms isolated 0.6 metre thick heads at one horizon in the Aguathuna Formation on Port au Port Peninsula. Pulchrilamina has an encrusting habit, is largely convex-upward but not without small irregularites and wrinkles, and forms plates less than 5 centimetres in diameter (Fig. 28F). Between successive plates are mudstone and finely peloidal grainstone.

Several horizons of thrombolite mounds in the Isthmus Bay Formation contain significant proportions of in-place corals of the genus Lichenaria (J.E. Sorauf, pers. comm., 1979; identification is tentative in two units). The corals have irregular shapes, with the corallites growing upward and outward, and range in width from 1 to 5 centimetres. In a bank 0.8 metre thick, at Eddies Cove West, corals are concentrated in thrombolite-poor "layers" (Figs. 28C,D). In other cases, both are intergrown (Figs. 28A,B). Large bioherms composed of Lichenaria, Renalcis, and thrombolites at Green Head, Port au Port Peninsula, are treated separately later.

Discussion - Aitken (1967) inferred that thrombolite mounds developed in conditions ranging from the lower intertidal zone to depths of two metres or more, and even at depths greater than 12 metres (Aitken, 1978). In the case of the

FIGURE 27

ARCHAEOSCYPHIID SPONGES

A. Horn-shaped sponge. Lens cap 6 cm across; Catoche Fm.; ECW-128.

B. Basket-shaped sponge. Coin 1.8 cm across; Catoche Fm.; ECW-106.

C. Stick-shaped and tubular sponges. Lens cap 6 cm across; Catoche Fm.; ECW-106.

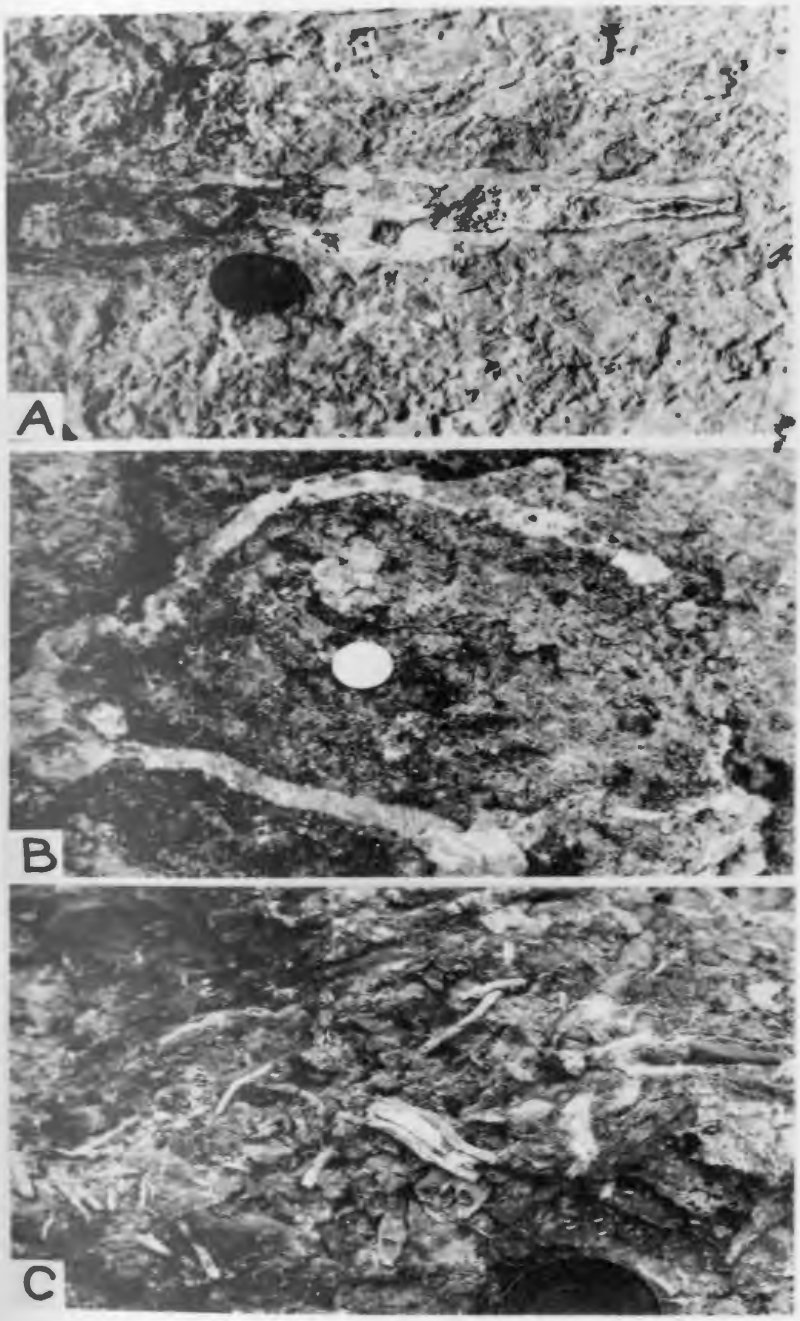
A
B
C

FIGURE 28

THROMBOLITE-METAZOAN MOUNDS

Tracings of vertically oriented slabs

black = thrombolites
stipled = Lichenaria
cross-hatched = sponge
palisade = Pulchrilamina

A. Part of irregular shaped 0.8 m thick mounds composed of thrombolites and Lichenaria corals. The dashed line outlines the edge of the mound. Isthmus Bay F.; IB-190.

B. As in A.

C. Part of coalesced mounds 0.8 m thick composed of thrombolites and Lichenaria; the latter appears to be concentrated in layers. Isthmus Bay Fm.; ECW-53.

D. As in C.

E. Part of coalesced mounds 1.8 m thick containing scattered individuals of archaeoscyphiid sponges. Simplified lamination outlines well-laminated cryptalgal part, showing that in large thrombolite banks conditions varied across them producing areas of distinct lamination. Catoche Fm.; PAC-83.

F. Part of coalesced mounds as in E. with a layer bound by laminar individuals of Pulchrilamina and a single sponge. Catoche Fm.; PAC-83.

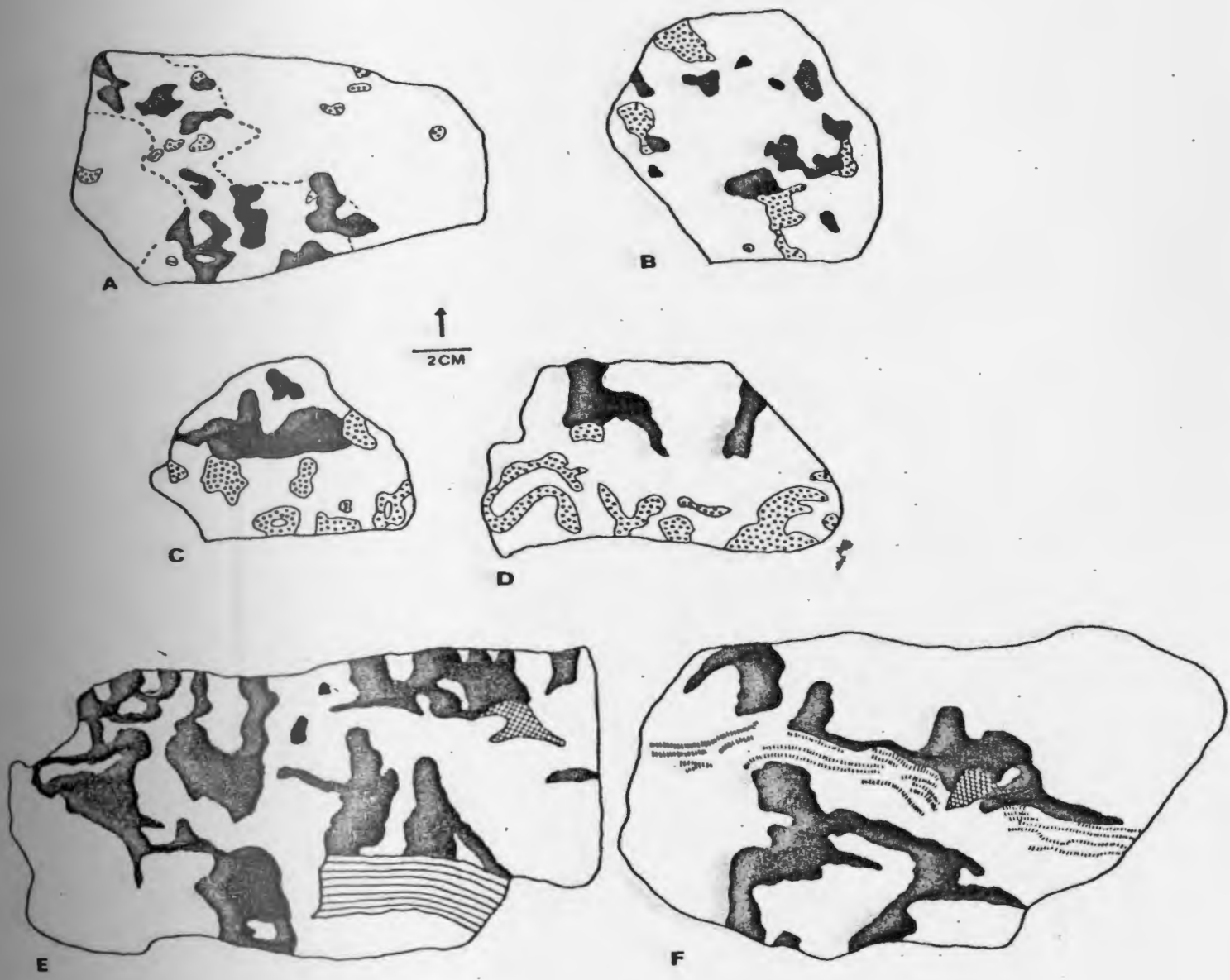
A
B
2CM
C
D
E
F

St. George, it is suggested here that thrombolite mounds formed strictly in the subtidal zone, on the basis of the following evidence: (1) growing surfaces were inhabited by pelmatozoans, gastropods, nautiloids, rostroconchs, sponges, trilobites, corals, and brachiopods, found as whole specimens (except for pelmatozoans) in the mound matrix, (2) the mounds always hosted burrowing organisms, (3) the fossil and bioclastic content of the flanking grainstones falls off markedly with distance from mounds, a situation unlikely to develop in the intertidal zone, (4) burrowing and mud content of flanking beds increases with distance from mounds, which is unlikely to have occurred in the intertidal zone, (5) flanking beds are never mudcracked, and do not show other features normally associated with intertidal flat deposition, and (6) cryptalgal fragments, derived from the mounds, are common only in the flanking grainstones, indicating an <u>in situ</u> source without significant transport, unlikely to occur in intertidal structures. Water depths greater than several metres do not appear likely for thrombolite formation in the St. George, particularly in the Isthmus Bay and Aguathuna Formations where thrombolitic horizons are interposed between intertidal and supratidal lithotopes. In the Catoche Formation, scattered shallowing to intertidal deposition and scattered grainstone beds, channels and lenses which indicate frequent winnowing by bottom turbulence, are evidence of shallow water depths at maximum. Hypersaline conditions, a possible requirement suggested by Aitken (1967) for thrombolite formation,

cannot be substantiated for the St. George. The presence of rare burrowed gastropod molds suggests that extreme tidal lowering of sea level and flushing by fresh meteoric water may have occurred sporadically to account for the dissolution of aragonite in unlithified sediment, also evidence for shallow water formation of thrombolite mounds. Some cases of structures transitional to columnar thrombolites probably formed in the lowest part of the intertidal zone. A sequence of vertical change in type of cryptalgal structure interpreted to be brought about by increasing water depth is illustrated in one unit 15 centimetres thick: cryptalgal laminite at the base becomes wavy and domes to stacked hemi-spheroidal stromatolites which become thrombolite columns in a fossiliferous and burrowed matrix (Fig. 29).

Reconstruction, based on the intertonguing of mound flanks with flanking grainstone indicates that the relief of thrombolite mounds probably did not exceed 0.2 or 0.3 metre above the surrounding sea floor. Hoffman (1976) related the shape of branching stromatolite mounds formed by the colloform mat in Shark Bay to geographic position: at headlands, mounds are circular and commonly coalesce forming banks, and in bights, mounds are elongate and coalesce forming rows. Most of the mounds in the Isthmus Bay and Aguathuna Formations formed near islands, and their circular shape, by analogy with Shark Bay, suggests that they developed near headlands where waves and currents were focussed but of somewhat variable direction. The mounds of the Catoche Formation likely formed on the open shelf because proper islands did not develop, but

FIGURE 29

VERTICAL CHANGES IN CRYPTALGAL STRUCTURE MORPHOLOGY

Vertically oriented slab showing upward change from wavy cryptalgal laminite (A) to laterally-linked hemispheroidal stromatolite (LLH), to stacked hemispheroidal stromatolite (SH), to irregularly shaped thrombolite column (T). The overall cryptalgal sequence is outlined by black line. Scale in cm; Isthmus Bay Fm.; IB-173.

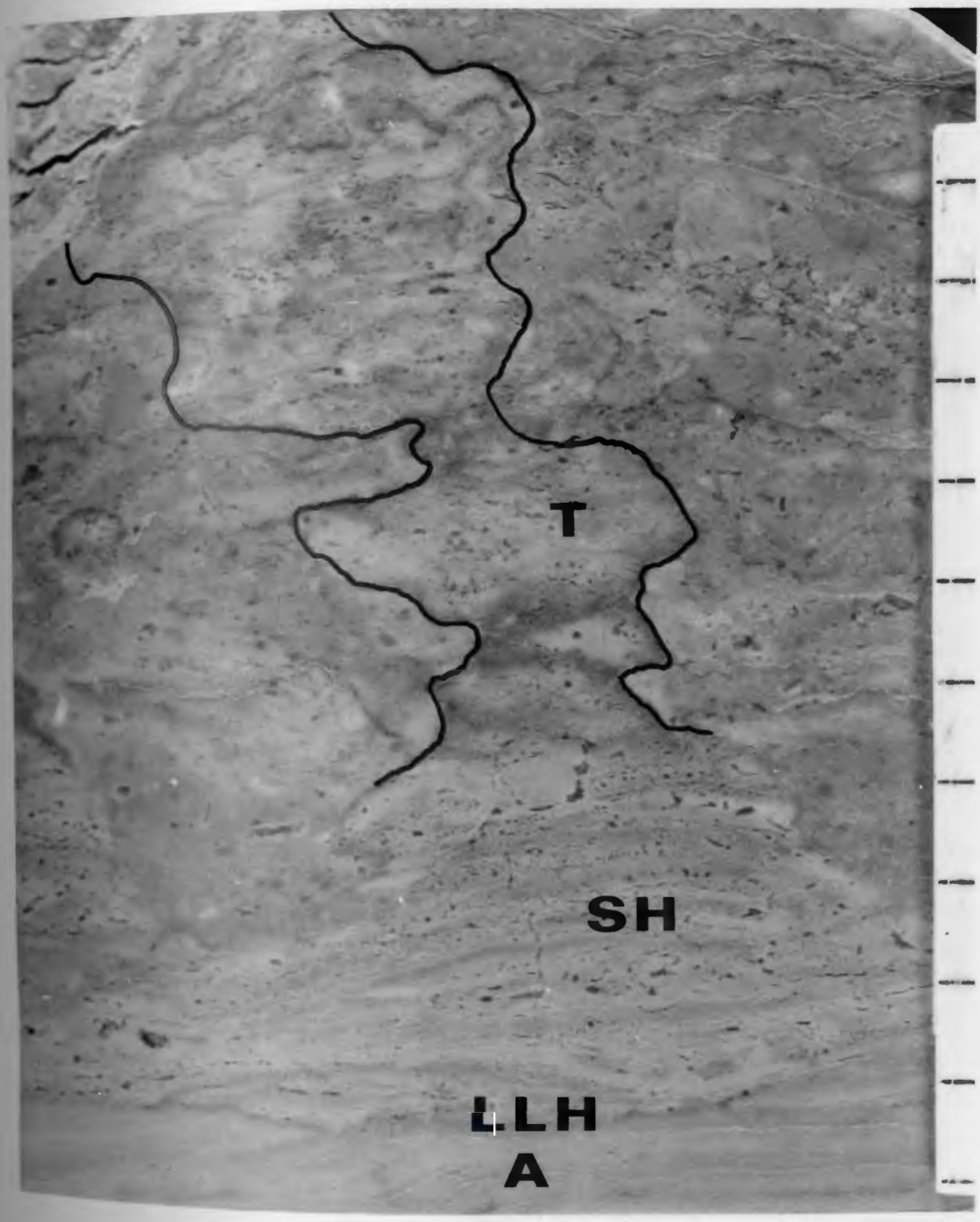
T
SH
LLH
A

the dominant circular shape also suggests focussed but not strongly directed waves and currents. In an exception, the linear mound banks at Eddies Cove West are parallel to grainstone channels in underlying beds, and indicate that energy was funnelled into one direction.

The unlaminated nature of thrombolites probably resulted from a number of factors: (1) irregular distribution of sediment onto algal mat surfaces, (2) variable quantities of sediment in different sedimentation events, (3) irregular time intervals between sediment events, (4) possibly irregular algal (filament?) growth (discussed later), (5) synsedimentary cementation in fenestrae and permineralization of algae (discussed later), and (6) disruption by burrowers. Haphazard non-episodic sedimentation to account for the first three factors is a predictable process in vigorously agitated subtidal areas. The algal mats likely had only slight synoptic relief, and walls are not usually developed, though exhumed and abraded mound flanks have been covered by cryptalgal laminite in several cases.

The large sponges are volumetrically insignificant in their contribution to the framework of mounds. They did assist in the trapping of sediment and were incorporated into the mound structure by thrombolite columns. Tubular and stick-like sponges probably baffled sediment. Encrusting Pulchrilamina was an important mound-builder in Lower Ordovician mounds from west Texas and southern Oklahoma where it occurs in great quantities (Toomey and Ham, 1967; Toomey, 1970). This organism only constructs small mounds

at one level in the Aguathuna Formation. In a few units, large numbers of the primitive coral Lichenaria constructed mounds, in association with thrombolites.

## MOUND COMPLEXES

### Introduction

Whereas most thrombolite and stromatolite mounds are restricted to single horizons, at a number of intervals, however, thicker sequences of cryptalgal structures are encountered. These include: (1) three vertical associations of different types of cryptalgal structures that illustrate the changes in type and morphology brought about by environmental changes, (2) large cryptalgal-metazoan bioherms, and (3) large cryptalgal bioherms occupying a shelf margin or near-shelf margin position.

### Vertical cryptalgal associations

Three vertical sequences in the Isthmus Bay Formation, well exposed at (1) Isthmus Bay, just east of Green Head, Port au Port Peninsula, (2) Isthmus Bay, between Green Head and the Gravels, Port au Port Peninsula, and (3) Eddies Cove West, illustrate vertical changes in cryptalgal structures (Fig. 30).

Sequence (1) - The vertical sequence consists of, in order from base to top: (a) cross-laminated grainstone, (b) 1.5 metre diameter and 0.5 metre thick columnar stromatolite mounds flanked by grainstone, (c) burrowed wackestone, (d) 1.5 metre diameter columnar stromatolite mounds, (e) 1.5 metre diameter mounds composed of aberrant conical

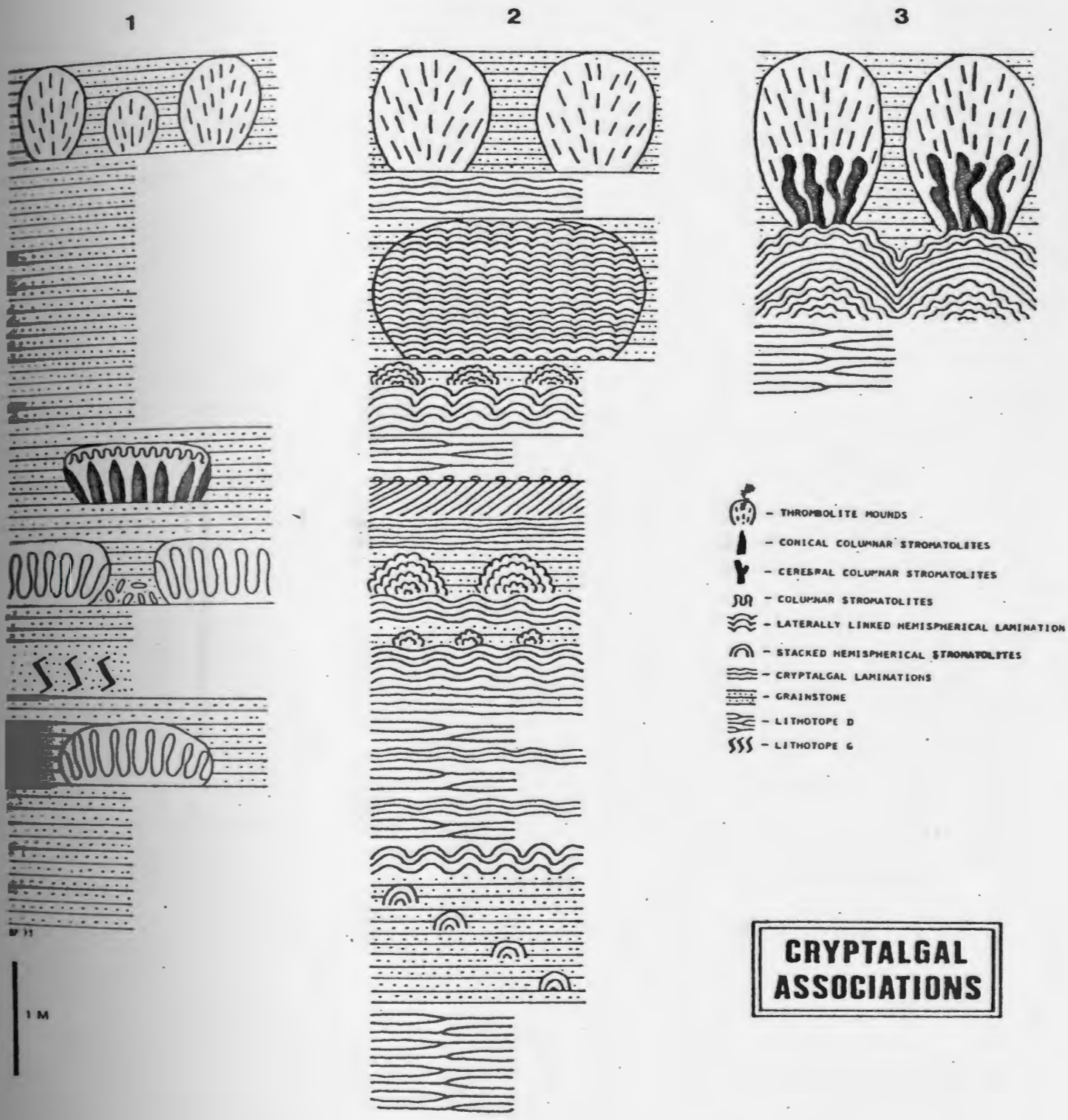


Figure 30: Columnar sections of three vertical cryptalgal associations, Isthmus Bay Fm. (1 = IB-77-83; 2 = IB-114-125; 3 = ECW-85-86)

stromatolites and a capping of columnar stromatolites flanked by intraclastic grainstone, (f) 2.4 metres of thin-bedded cross-laminated well-sorted clean grainstone, and (g) thrombolite mounds up to 0.8 metre thick and 0.4 metre in diameter and flanked by grainstone. The sedimentological history interpreted for this sequence begins with the formation of a shallow subtidal winnowed grainstone shoal, stabilized in places by columnar stromatolite mounds. A short period of quiet subtidal conditions covered this as the shoal migrated before it shifted back again and conical stromatolite mounds developed. The columnar stromatolite caps on these suggest greater sediment influx in the latter part of mound growth. The thick unit of thin-bedded grainstone was likely deposited as a low intertidal and shallow subtidal shoal which deepened slightly and permitted thrombolite growth.

Sequence (2) - The lower part of the sequence is alternating thin-bedded grainstones, wavy cryptalgal laminites, laterally-linked hemispheroidal stromatolites, stacked hemispheroidal stromatolites, and stacked hemispheroids with compound internal lamination. At one level, cryptalgal laminite is buckled and eroded into flat pebbles. Above this series occurs a horizon of large stromatolite mounds, 1.2 metres thick, isolated or coalesced into lobate rows 5 metres long, with internal laterally-linked and stacked hemispheroidal lamination. These are succeeded by wavy cryptalgal laminite and a horizon of large thrombolite mounds 0.8 metre thick and up to 2 metres wide. The lower part of the sequence is interpreted as oscillating supratidal and intertidal flat

environments, stacked hemispheroids forming on flats with more actively shifting sediment than those where laterally-linked and compound types formed. The upper part of the sequence indicates deepening and shoaling, the large compound stromatolites probably in an agitated lower intertidal setting, and the thrombolites in the subtidal zone where sedimentation influx onto the algal mats was not episodic.

Sequence (3) - Large 2.5 metre diameter compound stromatolite mounds are developed on top of a sporadically burrowed lenticular bedded unit of lithotope D. The internal laterally-linked lamination changes upward to cryptalgal laminite of alternating grainstone and mudstone laminae and back to laterally-linked lamination. This forms the substrate for cerebroid boxwork-like mounds of aberrant columnar stromatolites which are capped by thrombolites, forming mounds 1 metre in thickness. The evolution of cryptalgal structures in this mound sequence suggests initial formation in agitated lower intertidal conditions, with an interval of influx of coarse particles. The boxwork-like mounds developed in a protected subtidal environment of low sedimentation that later became open to greater sedimentation, and thrombolites formed.

## Green Head bioherm complex

Description - A unique biohermal sequence 12 metres thick occurs at Green Head, 1 kilometre southwest of the Gravels, Port au Port Peninsula. These are the *Diphragmoceras* beds of Flower (1978), and appear to be equivalent to similar but epigenetically dolomitized biohermal rocks low in the section at Boat Harbour, over 300 kilometres to the north. The complex is represented by two lithotypes, boundstone

and flanking grainstone, that have been variably affected by silicification and epigenetic dolomitization. The vertical sequence is divided into eight units, A to H (Fig. 31).

Unit A is 3 metres thick at the western end of the outcrop and increases to 4 metres at the eastern end. It is composed of thrombolite-Lichenaria-Renalcis boundstone (Figs. 32A, B, C, 31) penetrated in at least two places by 1 metre wide grainstone channels oriented approximately NW/SE. The western flank of the boundstone mass is flanked by sporadically burrowed grainstone. The top of the boundstone mass has a discontinuous capping of small thrombolite mounds, 0.3 to 0.5 metre in diameter. Thrombolites in the boundstone are clots and irregular columns and form irregular "mounds" or clumps of thrombolites and bound wackestone that roof over cavities and tunnels that range from several to more than 20 centimetres wide. The floors and walls of many cavities are coated by light-coloured cryptalgal laminated mudstone that is sporadically disrupted by burrows. Post-cryptalgal laminite cavity fills and the mound matrix are darker in colour, burrowed, and fossiliferous with whole gastropods, nautiloids, rare brachiopods, and pelmatozoan debris. The smaller spaces between thrombolites have less of the coarse fossil material and often exhibit irregular cryptalgal lamination. The margins of some thrombolite "mounds" around grainstone-filled tunnels are scoured. Lichenaria corals are less than 10 centimetres across, are irregular in shape, and have irregular but largely upward and outward corallite growth directions. They usually occur in clumps

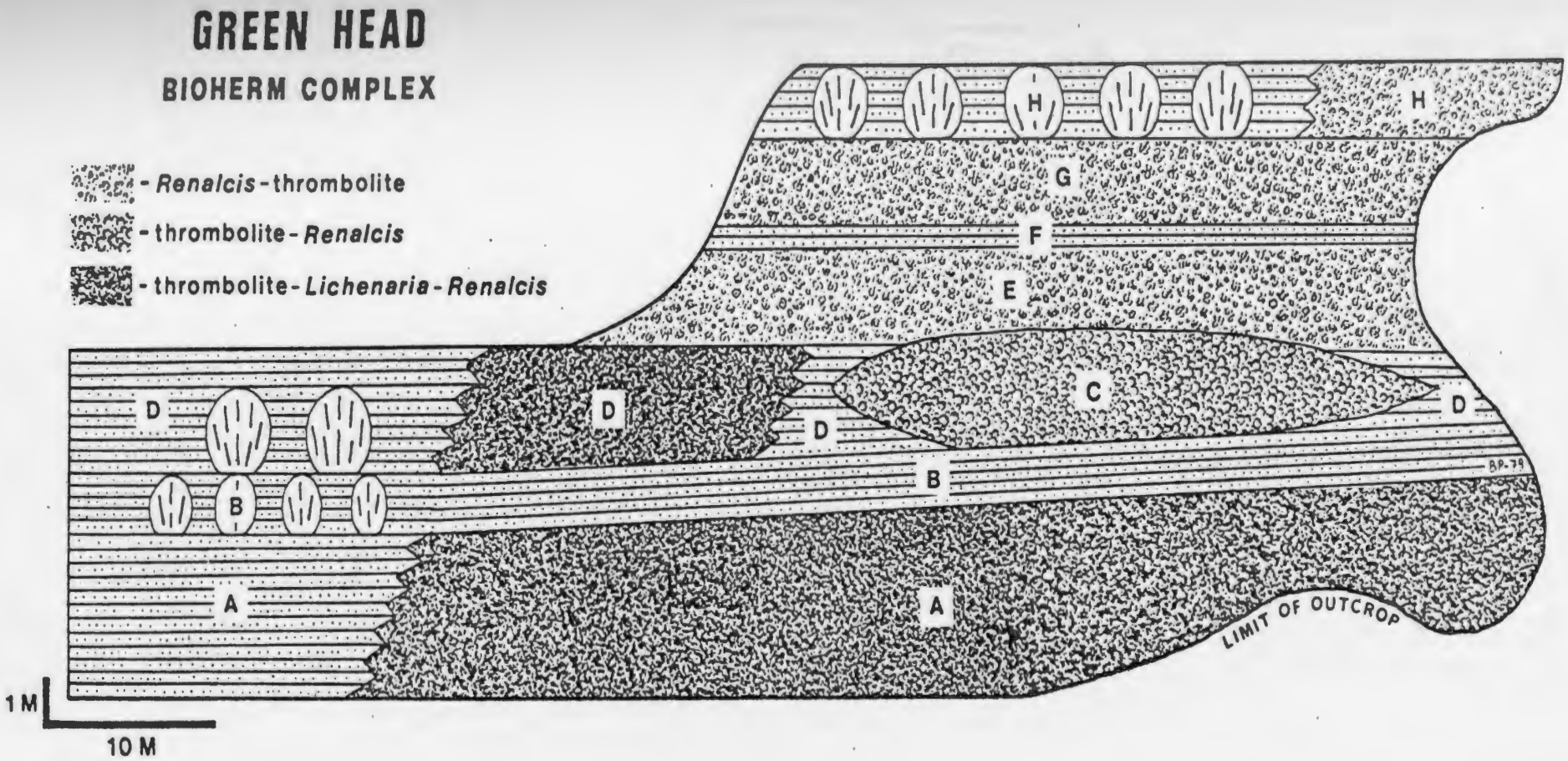


Figure 31: Outcrop sketch of the bioherm complex exposed at Green Head, southwest of the Gravels, Isthmus Bay section, Port au Port Peninsula. Numbers refer to the units described in the text.

FIGURE 32

THROMBOLITE-LICHENARIA-RENALCIS BOUNDSTONE

A. Tracing from vertically oriented slab (black=thrombolites; circles=Lichenaria; stiples=Renalcis; parallel lines=cryptalgal laminated internal sediment; white=matrix sediment). Two thrombolite "mounds" (T) contain cryptalgal laminated cavity fills (A) and mudstone matrix in which gastropod shells have lodged. The thrombolite mounds are bridged by a Renalcis mass (R) with outward and downward growth direction. The sediment in the "tunnels" created by the Renalcis and thrombolite roofs is a burrowed, fossiliferous wackestone (W), the coarse grain content decreasing upwards. The margins of the thrombolite mounds are abrupt and abraded. On the thrombolite mounds and Renalcis roof grew a bridgework of Lichenaria corals (C) around and under which grew drapes of Renalcis (R). Green Head; unit A.

B. Horizontally oriented slab, same as part of tracing 34A. Scale in cm; Green Head; unit D.

C. Vertically oriented slab of thrombolite-Lichenaria boundstone (L) containing drapes of Renalcis, encrusted by a dark-coloured wall of Renalcis (R), and flanked on the right by dark-coloured mudstone followed by wackestone containing nautiloid lodged vertically. Scale in cm; Green Head; unit D.

D. Vertically oriented slab, close-up of left side of C, showing Lichenaria (L), encrusted by a drape of Renalcis (R; white dots) followed by light-coloured internal sediment, and serving as a substrate for a thrombolite column (T) containing light-coloured sediment-filled growth cavities. Scale bar 0.5 cm; Green Head; unit D.

I
C
R
T
A
W
2CM
A

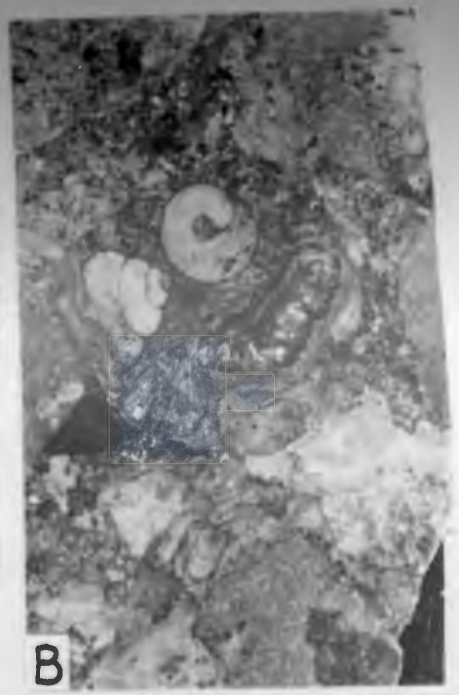
C
B

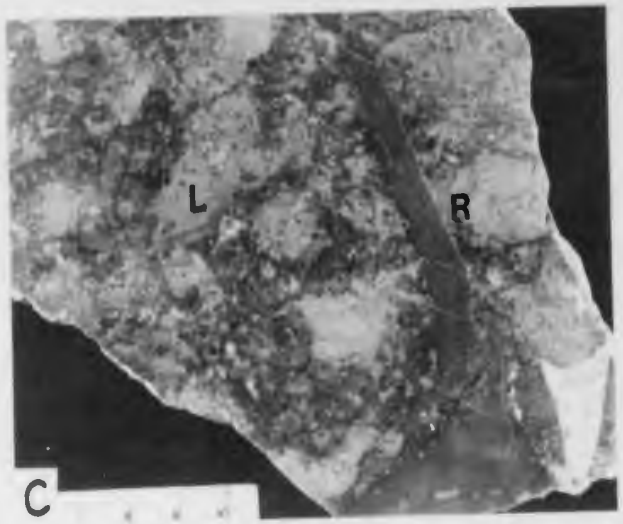
L
R
C

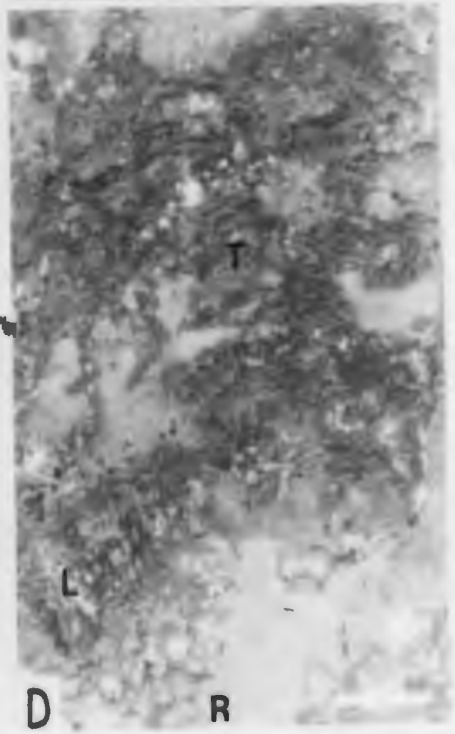
T
L
D
R

FIGURE 33

THROMBOLITE-LICHENARIA-RENALCIS BOUNDSTONE

Vertically oriented tracings of selected serial sections 5 cm apart (black=thrombolites; fine stiples=Lichenaria; coarse stiples=Renalcis; parallel lines=cryptalgal laminated internal sediment; white=internal sediment and matrix). The serial sections (from same block as Fig. 32A) show the change in shape of thrombolite mounds, encrusting Renalcis masses, and Lichenaria clumps. The large white patches are fossiliferous wackestone reef matrix collected in large pockets and tunnels (roofed over in the right side of 4). Smaller white areas between thrombolites and Lichenaria is internal mudstone sediment. Green Head; unit A.

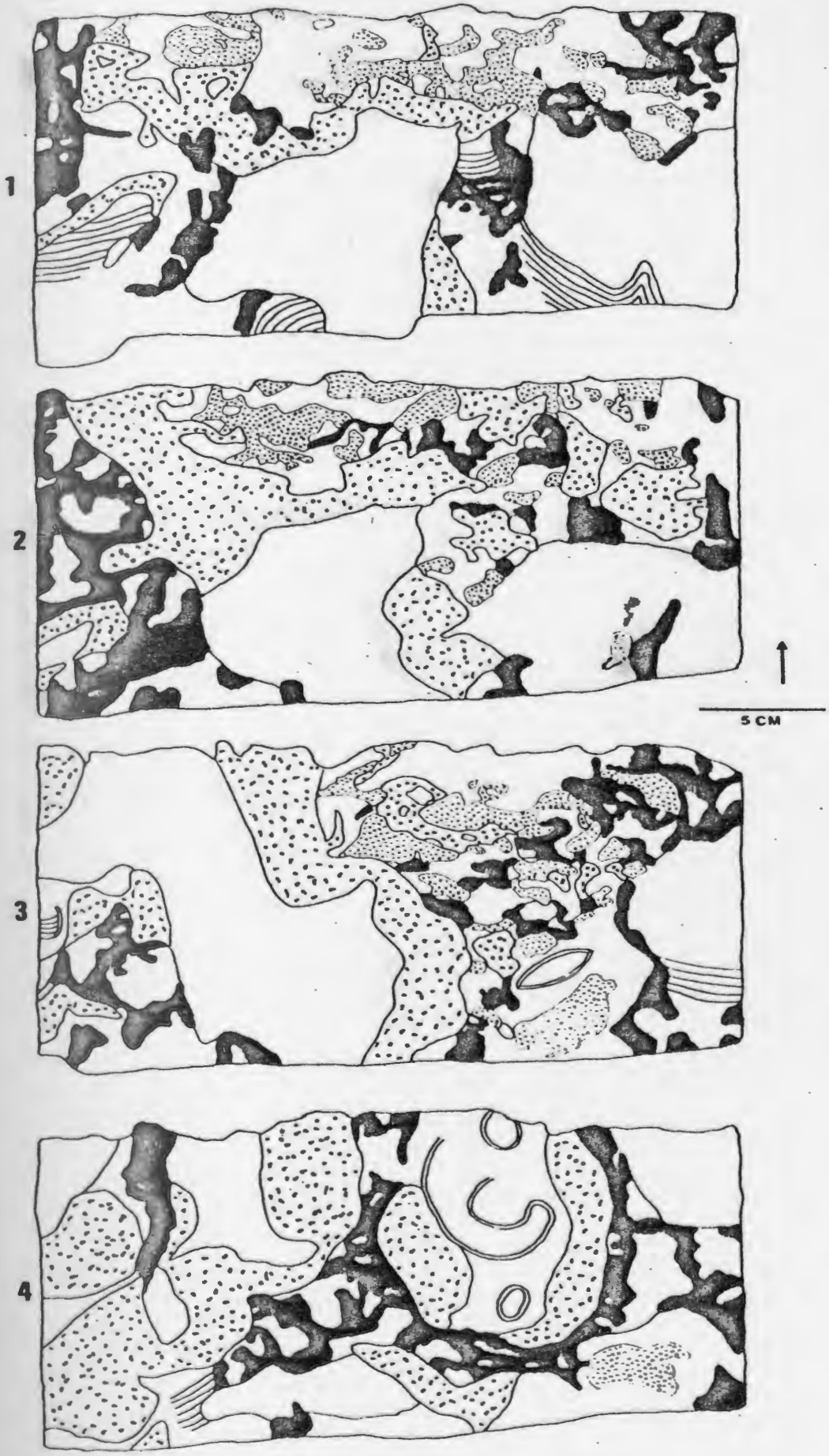
1
2
5 CM
3
4

growing on or against thrombolite "mounds" or on each other, forming irregular bridgeworks. Between the corals, trapped mudstone is irregularly cryptalgal laminated, forming small thrombolite clots. Moss-like Renalcis ('calcareous algae') masses occur as encrusting drapes or manes around but mostly under corals (Fig. 32D), and as encrusting walls on thrombolite "mounds". The individual Renalcis clots or capsules have upward and outward growth directions when encrusting thrombolite "mounds", and when encrusting corals or in thrombolite cavities, downward growth directions as well. Synsedimentary radial bladed cement occurs in all three components.

Unit B is a 1 metre thick grainstone bed that overlies the slightly dipping upper boundstone surface of unit A, the flanks of mound-shaped Unit C, and grades with Unit D. To the western end of the outcrop, off the boundstone mass, it grades to thrombolite mounds.

Unit C is a 2 metre thick mound-shaped unit with an upper surface that weathers with a cerebral or cellular boxwork pattern caused by the differential weathering of partly dolomitized thrombolite-Renalcis boundstone (Fig. 35A). Small thrombolite mounds less than 0.2 metre across which form an irregular interconnecting lobate structure in plan, are surrounded by thick encrustations or walls of Renalcis (Figs. 34B, 35B). The matrix of the thrombolite mounds is burrow-mottled wackestone, in contrast to the grainstone between the Renalcis walls. Whole fossils are uncommon. The base of the unit is not exposed.

Unit D is grainstone that overlies the mound-shaped unit and grades laterally to a 2 metre thick thrombolite-

FIGURE 34

GREEN HEAD BIOHERM COMPLEX

Tracings of horizontally oriented slabs

black = thrombolites
fine stiples = Lichenaria
coarse stiples = Renalcis
parallel lines = cryptalgal laminite

A. Thrombolite-Lichenaria-Renalcis boundstone with gastropods and nautiloids lodged in matrix. See Fig. 32B. Unit D.

B. Thrombolite-Renalcis boundstone showing thrombolite mound with burrowed wackestone matrix on the right, encrusted by a wall of Renalcis, and separated from other mounds by grainstone. See Fig. 35B. Unit C.

C. Thrombolite-Renalcis boundstone showing elongate and coalesced Renalcis heads and subordinate elongate thrombolite columns. See Fig. 35F. Unit G.

D. Thrombolite-Renalcis boundstone showing coalesced Renalcis heads. See Fig. 35D. Unit G.

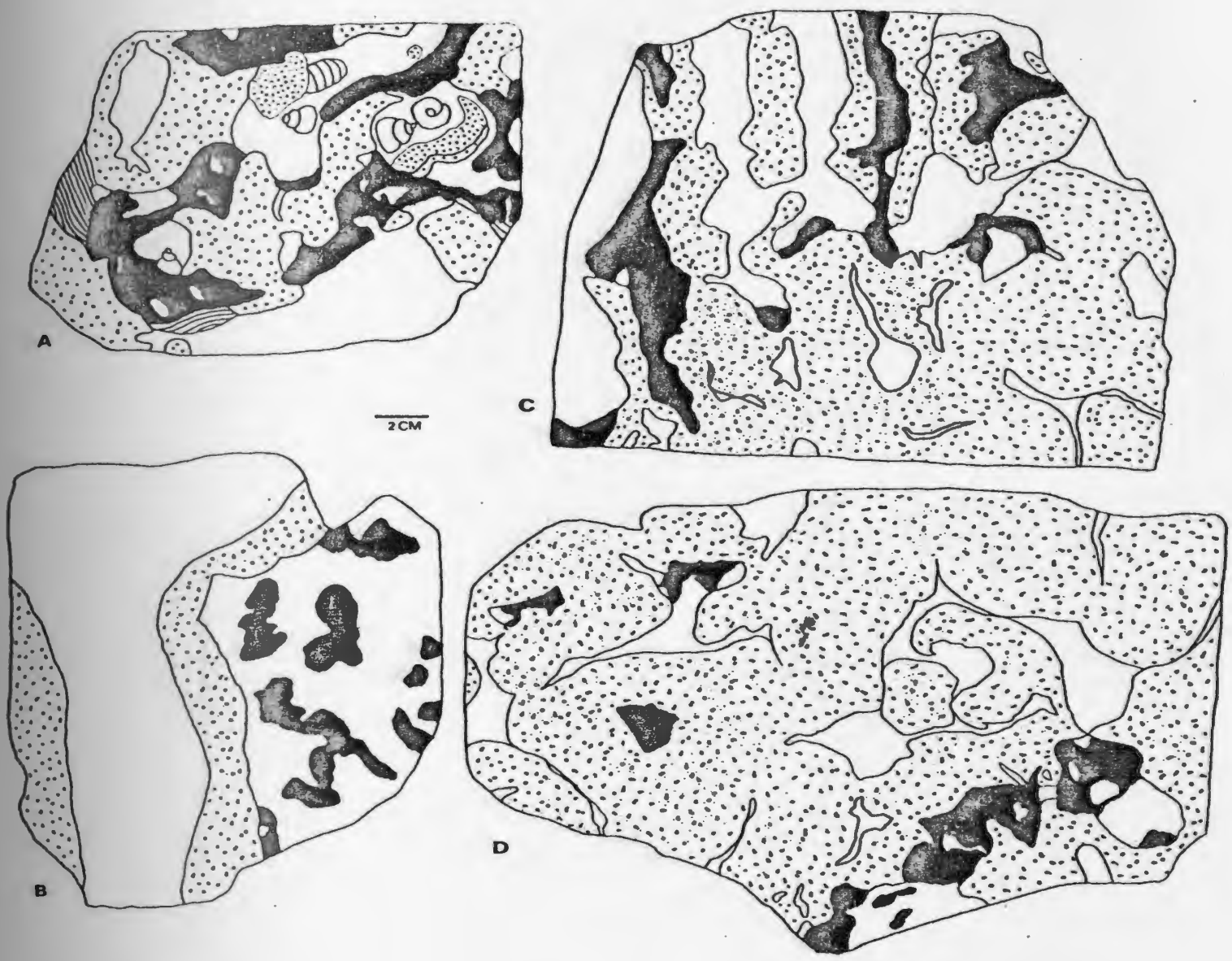
A
C
2 CM
B
D

FIGURE 35

GREEN HEAD BIOHERM COMPLEX

(Isthmus Bay Fm.; IB-57-61)

A. Bedding plane view of mound-shaped unit C, showing cerebral weathering pattern. Dark pitted areas are thrombolite mounds, separated by Renalcis walls and grainstone channels.

B. Horizontally oriented slab of unit C (same as tracing Fig. 34B), showing burrowed thrombolite mound on right, surrounded by a wall of Renalcis, flanked by coarse, fossiliferous grainstone. Scale in cm.

C. Vertically oriented slab of the contact between units F and G, showing Renalcis heads on upper left rooted in coarse, fossiliferous grainstone.

D. Horizontally oriented slab of unit G (same as tracing Fig. 34D); showing free-standing Renalcis heads, scattered thrombolites, and light-coloured burrowed wackestone matrix.

E. Horizontally oriented slab of unit E showing free-standing, coalesced Renalcis heads with burrowed wackestone matrix.

F. Horizontally oriented slab of unit G (same as tracing Fig. 34C), showing elongate Renalcis heads. Scale as in D and E.

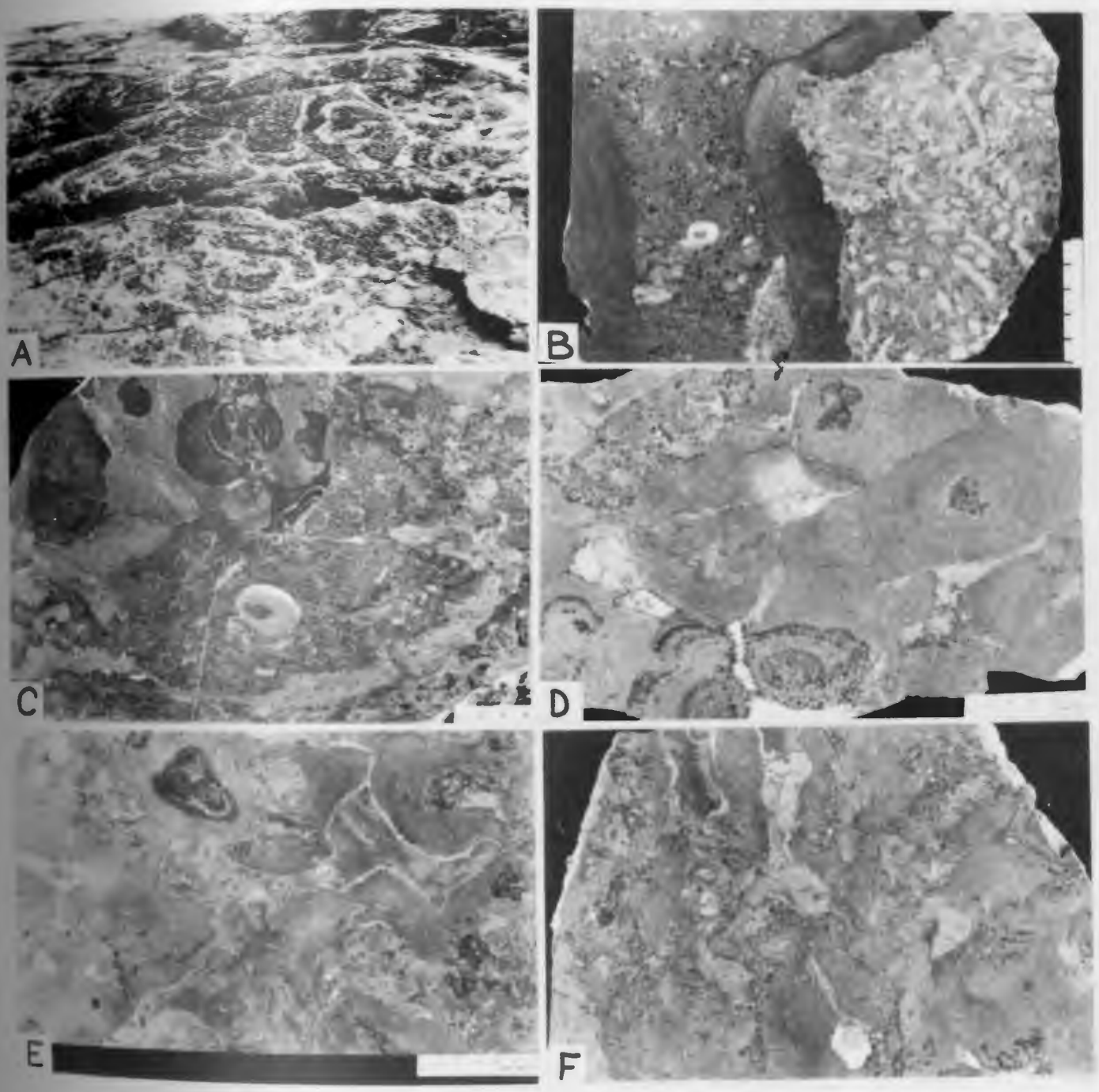
A
B
C
D
E
F

Lichenaria-Renalcis boundstone (Fig. 34A), similar to Unit A, and containing one grainstone channel oriented in the same direction as those of Unit A.

Unit E is a 1.5 metre thick Renalcis boundstone with minor thrombolites. Renalcis formed free-standing masses, ranging from round heads to elongate walls, frequently merging to massive clumps (Figs. 34C, 35D, E, F). Scattered thrombolites are encrusted by Renalcis masses; corals are absent, and growth framework cavities are rare. The matrix is burrowed wackestone but poorer in fossils than the thrombolite-Lichenaria-Renalcis boundstone.

Unit F is a 0.4 metre grainstone unit containing at least one planar corrosion surface (hardground).

Unit G is a 1.5 metre thick boundstone the same as Unit E. Renalcis heads grew on top of unlithified grainstone of unit F which flanks the bases of the heads (Fig. 35C).

Unit H is a 1.5 metre thick dolostone composed of columnar thrombolite mounds and grading laterally to Renalcis boundstone probably similar to Unit E.

Interpretation - The evolution of the bioherm complex shows changes that are likely related to changes in environmental conditions. The maximum thickness and areal dimensions of the bioherm of unit A are unknown, but its growth ceased and it was covered by a grainstone shoal that was stabilized in the less turbulent off-bioherm area by thrombolite mounds. Whether the base of the mound-shaped unit C rests directly on unit A or on the shoal is unknown, but its mound shape, cerebroid structure and fewer associated organisms may have

been caused by variable current directions, greater turbulence, but lesser sediment influx. The overlying boundstone similar to unit A possibly indicates a return to strongly directed turbulence, as evidenced by the grainstone channel. The geometries of the overlying Renalcis-dominated units are also unknown, but the scarcity of thrombolites, rarity of fossils, and lesser volume of matrix sediment may be due to vigorous agitation with comparatively little sediment influx.

Judging by the relation of flanking grainstones, topographic relief of the thrombolite-Lichenaria-Renalcis bioherms was probably not more than 1 metre, though possibly greater in the case of mound-shaped unit C. The presence of channels and cavities with eroded walls suggests that there was active sediment movement within these bioherms. The elongation of free-standing Renalcis masses in the overlying bioherms probably reflects direction of waves, a relationship with turbulence commonly noted, for example, in stromatolites (Hoffman, 1967; Logan et al., 1974) and in the hydrozoan Millepora (Stearn and Riding, 1973).

The encrusting growth habit of Renalcis in units A and D serves to indicate the actual synoptic relief of the bioherm growth surface. Renalcis encrusting the undersides of corals and coral bridgeworks indicate that the spaces below the corals were empty while they were growing. The Renalcis walls on the sides of and under thrombolite "mounds" indicate that, while growing, the thrombolites possessed relief of up to nearly 20 centimetres above the floors of nooks, crannies, and cavities. On the upper growing bioherm surface,

the highest structures were corals because they grew on thrombolite "mounds", but they were only slightly above the living thrombolite-forming blue-green algal mats. Beneath and around open spaces formed by these two framebuilders were drapes, manes, and walls of Renalcis, forming a craggy and knobby surface with a total relief of probably about 20 centimetres, containing abundant hollow cavities. The cryptalgal laminated coatings of many of these cavities indicates that they were well-protected and received only episodic influx of suspended sediment. A small cavity flora and fauna in these bioherms consisted of non-skeletal mat-forming algae, burrowers and Renalcis. Into nooks and crannies between the framebuilders lodged whole gastropod and nautiloid shells which were buried in the fossiliferous wackestone sediment that was then burrowed.

## Hare Bay bioherm complex

Description - Extensive mound complexes, up to 100 metres thick and probably nearly a kilometre in lateral extent, in the Catoche Formation exposed on islands in Hare Bay, have been reported by James and Stevens (1977). They are superimposed mound horizons, similar to smaller banks of other parts of the Catoche Formation, with probable erosion surfaces between many of them, and are incised by channels and flanked by thick units of well-sorted peloidal and bioclastic grainstone beds. Though adversely affected by dolomitization, shearing, and microsparitization, the mounds are composed of thrombolite-Renalcis boundstone, with a burrowed wackestone matrix containing archaeoscyphiid sponges,

gastropods, trilobites, brachiopods, and pelmatozoan debris. They are not composed of sponge boundstones, as suggested by James and Stevens (1977).

Interpretation - The boundstone is similar to other thrombolite mounds, except that masses of Renalcis are common. The actual geometry of the complexes is unknown, but they probably had slightly higher relief off the sea floor than smaller thrombolite banks. The superimposition of mounds indicates that hydrodynamic conditions on the shelf at this place were constant throughout Catoche time. Considerably agitated conditions are suggested by the channels and flank beds and growth of Renalcis (discussed later). It is suggested that these mound complexes occupied a location at or close to the Lower Ordovician continental shelf margin because of the long-term stability of agitated conditions that would have been present there. Development of possible slope Epiphyton boundstones further to the east is suggested by large debris blocks in fore-slope deposits of the Cow Head Group (N.P. James, pers. comm., 1978), but the true nature of the shelf margin is unknown as Hare Bay is the site of the most eastern exposures of the St. George.

## PALEOECOLOGY OF BIOHERMS

Thrombolite mounds and Renalcis- and Lichenaria-bearing bioherms of the St. George can be considered ecologic reefs (Dunham, 1970) because: (1) they possessed topographic relief above the sea floor, (2) they were wave resistant as evidenced from flanking grainstones, (3) they were constructed

by organisms, principally non-skeleton-secreting blue-green algae, (4) they were lithified early, on the sea floor, and (5) they influenced the surrounding environment and were sites of concentrated organism activity.

Reported occurrences of Lower Ordovician reefs are few in number, the Green Head complex being Gasconadian in age (Flower, 1978) and significantly older than previously reported reefs. Mounds in the Fillmore Formation of the Pogonip Group, Utah, described by Pierce (1967) and Church (1974), are Cassinian in age (Hintze, 1973). These mounds are linear in shape, 1 to 1.5 metres thick, 2 to 3 metres wide, and up to 30 metres in length, probably oriented parallel to prevailing currents. They exhibit a vertical succession of a pioneer community consisting of columnar stromatolites developed on an intraclastic grainstone, followed gradually by an increase in abundance of archaeoscypiid sponges, and a climax community of Calathium with lesser amounts of stromatolites and sponges of variable morphology. These mounds resemble thrombolite mounds of the Catoche Formation, except in the latter there is no development of a Calathium dominated community, despite the occurrence of rare Calathium in associated off-reef wackestones. Mounds in the McKelligon Canyon and Kindblade Formations of west Texas and southern Oklahoma respectively, described by Toomey and Ham (1967) and Toomey (1970), are Jeffersonian in age (Whittington, 1968). They attain a maximum thickness of about 20 metres and length of about 60 metres, but most are less than 2 metres thick and long. They are composed

of an assemblage of Calathium, Archaeoscyphia, Pulchrilamina, Renalcis, and columnar stromatolites (Toomey, 1970; Riding and Toomey, 1972), that also seems to exhibit a broad ecological succession. An initial stage ("colonization" of Walker and Alberstadt, 1975) is composed of Calathium and Archaeoscyphia, followed by a "diversification" stage of a more varied community including Pulchrilamina and patches of columnar stromatolites and a final ("domination") stage composed of Pulchrilamina. Renalcis played mostly an encrusting role. The reefs of the St. George differ in the type of framebuilders, and in the more intimate association of cryptalgal structures with attendent Renalcis and Lichenaria. St. George reefs are vertically unzoned, and the vertical change in composition of the successive reef units in the Green Head complex is an ecologic succession controlled by environmental parameters.

The primary framebuilders of St. George reefs were blue-green mat-forming algae, Renalcis-forming algae, Lichenaria, Pulchrilamina, and archaeoscyphiid sponges. The algae occupied a photosynthetic niche, and Lichenaria may have belonged in the low-level suspension feeding or epifaunal carnivorous trophic groups (terminology of Walker and Bambach, 1975), depending on their manner of feeding which is unknown. Pulchrilamina, if an encrusting sponge (as opposed to the hydrozoan interpretation of Toomey and Ham, 1967), occupied a low-level suspension feeding group. Archaeoscyphiid sponges were both high- and low-level suspension feeders, depending on their morphology and size.

Pelmatozoans were also high-level suspension feeders, and the lack of root structures suggests that they may have been motile or rooted in matrix. Brachiopods, uncommon in many reefs, belonged in the low-level suspension feeding trophic group. Cavities were probably encrusted by thin and flocculent blue-green algal mats, protected from erosion and browsing, though sporadiacally burrowed. Irregular cryptalgal laminae in matrix mudstone indicates that flocculent mats of this nature were present on sediment surfaces between the framework components, as they are in modern carbonate environments (Bathurst, 1967). The diverse and abundant gastropod fauna occupied the epifaunal browsing trophic group and probably ate these mats, though with no apparent effect on the thrombolite-forming algal mats. Trilobites, which were also abundant, occupied sediment-water interfacial deposit feeding and, probably as needed, scavenging trophic groups. Cephalopods were nektobenthic sediment-water interfacial carnivores. Rostroconch molluscs probably lived wholly or partially buried within sediment (Pojeta and Runnegar, 1976) and therefore were epifaunal deposit feeders. Infaunal deposit feeding burrowers were ubiquitous. Other soft-bodied metazoans must have been present, but left no preserved burrows or remains. Macroborings such as Trypanites do not occur in the St. George, though they have been reported from older rocks (James et al., 1977). The striking increase in abundance and diversity of the associated fauna in the vicinity of reefs probably reflects not only abundance of food and oxygen supply, as is typical around modern reefs,

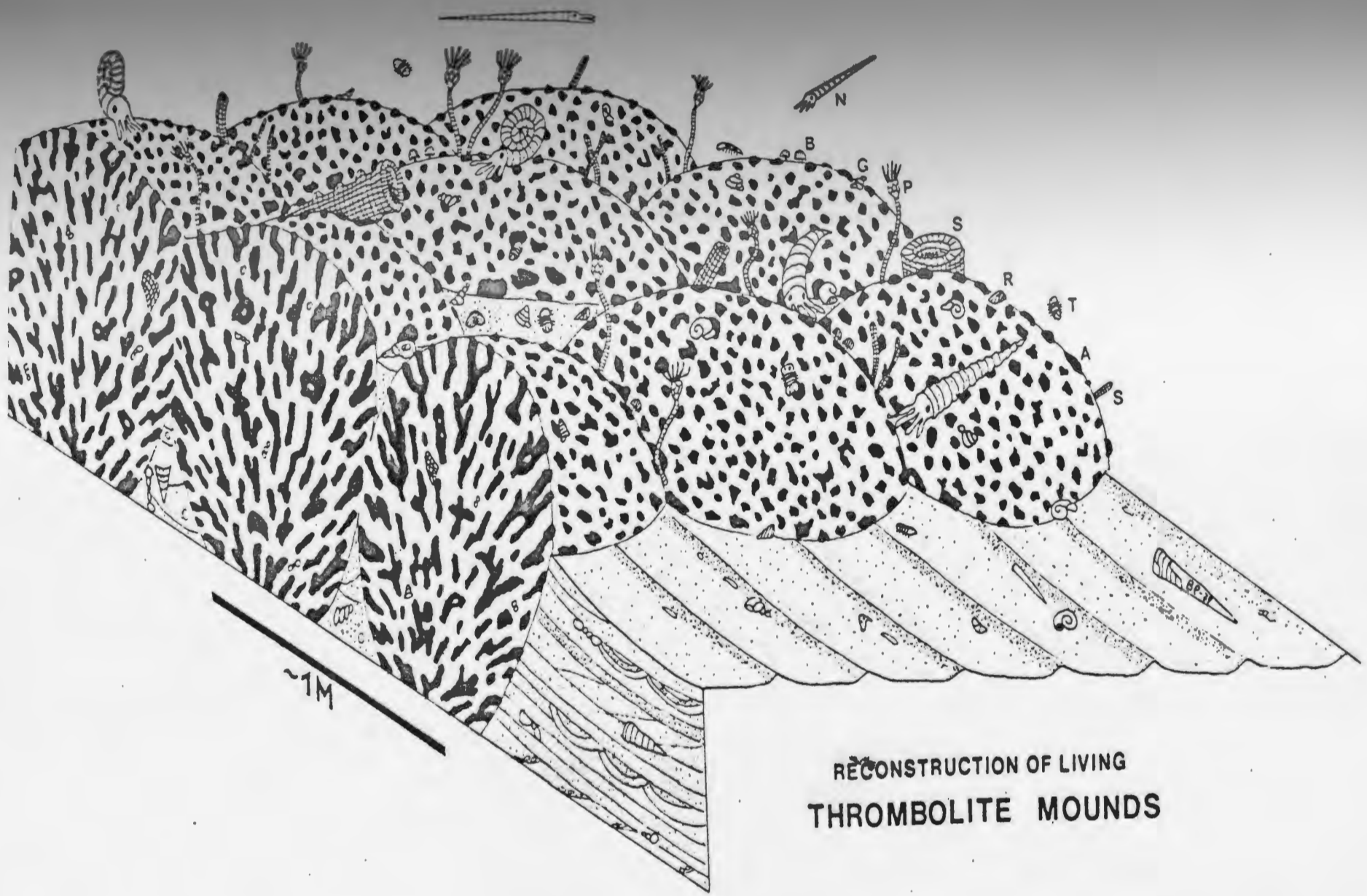


Figure 36; Suggested reconstruction of the living surface of coalesced thrombolite mounds. (Thrombolites and living algal mats (A) are black; S=sponge; T=trilobite; R=rostroconch; P=pelmatozoan; G=gastropod, B=brachiopod; N=nautiloid; no particular species portrayed by the sketched animals).

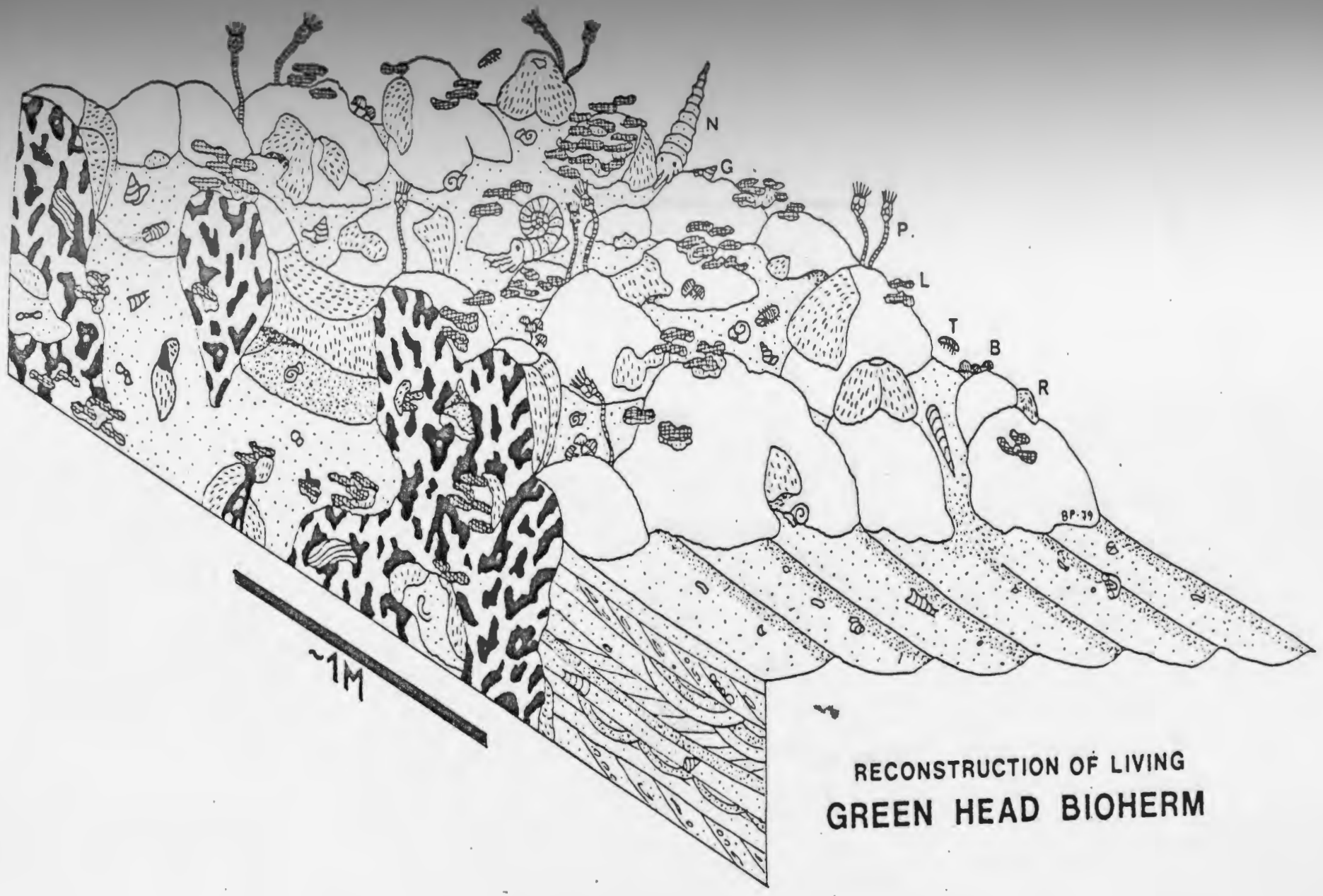


Figure 37: Suggested reconstruction of the living surface of thrombolite-Lichenaria-Renalcis reef. (Thrombolites coloured black but living algal mats not coloured for simplicity--same as Fig. 36; R=Renalcis, also line stiples; B=brachiopod; T=trilobite; L=Lichenaria, also cross-hatched; P=pelmatozoan, G=gastropod; N=nautiloid; no particular species portrayed by the sketched animals).

but also the complexity and rugosity of the substrate presented by the growing framebuilders. Figures 36 and 37 are proposed reconstructions of the living reef surfaces.

## CRYPTALGAL MICROSTRUCTURE

### Introduction

The microstructure of cryptalgal structures was first investigated in detail by Gürich (1906) who erected the protozoan order Spongiostromaceae with the family Spongiostromidae because of the spongy nature of the microstructure. While these taxonomic terms have been since dropped, there has been little detailed study of microstructure until recently now that microstructure is being used in the taxonomy of Precambrian stromatolites (e.g.: Walter, 1972; Bertrand-Sarfati, 1977; Hofmann, 1977). Based on examination of modern stromatolites from the Bahamas, Monty (1977) has documented many of the characteristics of microstructure and how they arise. There are difficulties in their study in ancient rocks because of the presence of variably permineralized algal remains, and alteration by recrystallization, dolomitization, and silicification.

It was found in this study and examination of figured examples in the literature that microstructure frequently varies both within individual cryptalgal structures and between structures in the same unit. Therefore, the study of microstructure must necessarily be focussed on that of each lamina - the sedimentological and biological event - that is, the original stromatoid of Kalkowsky (1908),

regardless of the type of cryptalgal structure (except in the case of thrombolites which are unlaminated).

The microstructure of stromatoids of cryptalgal structures in the St. George is investigated and an open-ended classification of recurring types is proposed that limits observational bias toward outstanding or unusual characters. The classification, which gives clues to the biological composition of mats and sedimentary and environmental conditions, is based on both the nature of particles comprising stromatoids and their arrangement is space (that is, shape of fenestral pores). It does not classify secondary alteration features such as microbored micrite surfaces in thrombolites (Fig. 39 A), neomorphic microspar and spherulitic spar patches (which impart a speckled appearance to thrombolites in reflected light), and dolostone laminae. Stromatoids have apparently not been affected by later compaction, and microstructure is interpreted to be primary.

Seven types are isolated from petrographic study: massive, peloidal, vermiform, tubiform, spongy, cavernous, and cancellous (Fig. 38). Gradation between types is rare.

## Microstructural types

Massive - Stromatoids are composed of micrite with no porosity, are generally uniform and are less than 1 millimetre in thickness. This type of microstructure is produced by the deposition of a single mudstone layer from suspension of storm and tidal generation. It is an oft-illustrated microstructure in the literature, and is especially common in Precambrian forms.

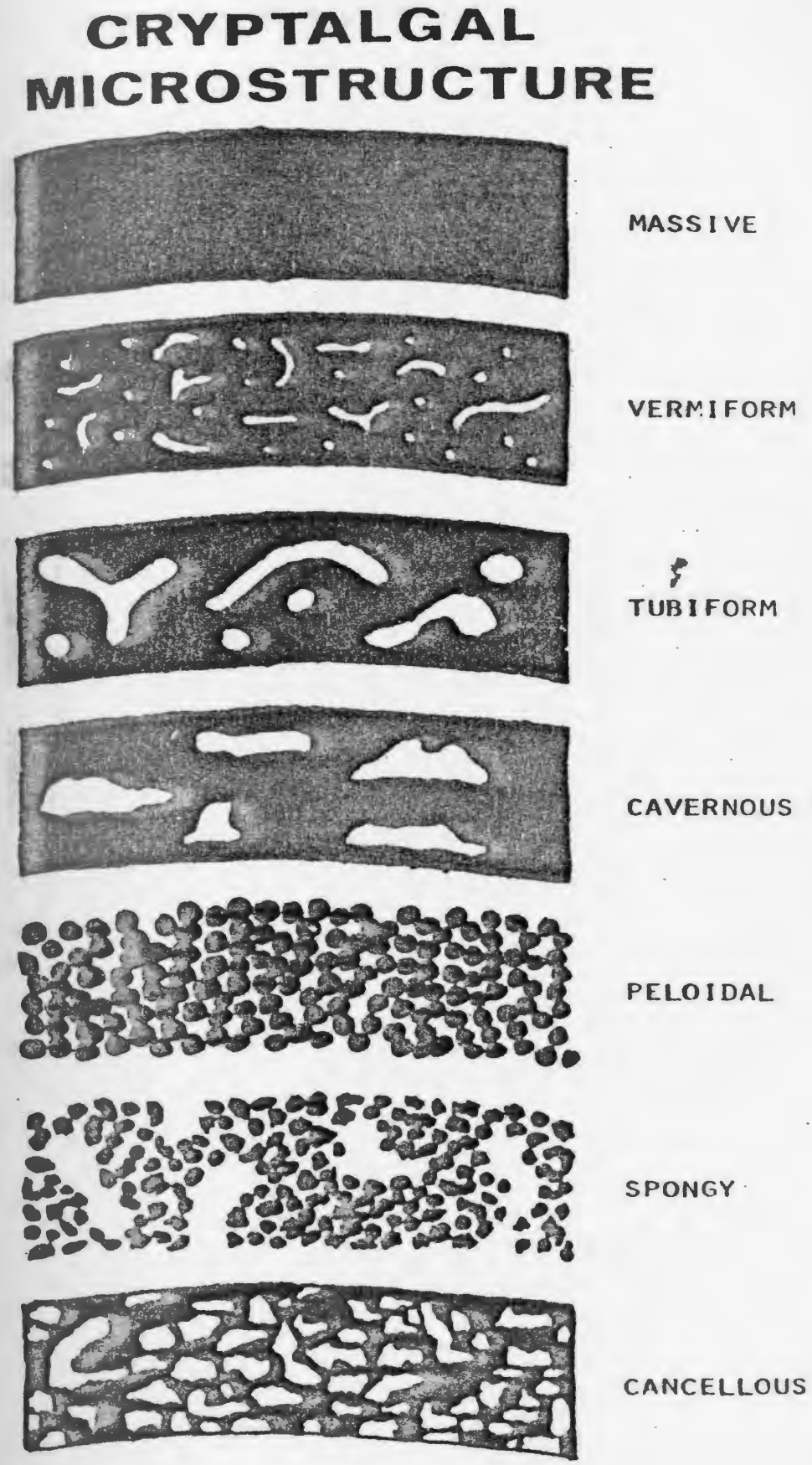


Figure 38: Sketches of seven stromatoids showing the different micro-structural types represented in St. George cryptalgal structures.

Vermiform - Stromatoids with this microstructure are thicker than massive stromatoids, and are composed of micrite that is sometimes vaguely peloidal and possesses abundant small, approximately 100 microns in diameter, branching vermiform tubular fenestrae (Fig. 39B). This structure is not confined to cryptalgal structures but occurs in burrows in mudstone and wackestone, and accordingly it is interpreted to be likely due to compaction and shrinkage of pelleted mud, probably around filament tufts. The "vermiform" microstructure figured by Walter (plate 1, 1972) would be considered peloidal to spongy here.

Tubiform - Stromatoids are thicker than the above, and characteristically have fenestrae the shape of large, approximately greater than 250 microns in diameter, often branched tubes that are oriented in a vertical to subhorizontal direction (Figs. 40A,B,C). The stromatoids are composed of micrite and the tubes sometimes contain internal sediment. In some examples, a gradation between tubiform and spongy types occurs as the sediment changes to distinct peloids. The large diameter of the tubes suggests that they might be molds of filament bundles, but may also be partly related to gas formation or bridging of pores by filaments, altered by sediment shrinkage due to dewatering. Monty (Fig. 14, 1977) figured this type of microstructure as a phalanx of vertical tubes and suggested that the micrite around them was precipitated *in situ*. This seems unlikely because the diameter of the tubes is probably too large to be single filaments, and there is too

much micrite for it to be simply due to the calcification of filaments.

Cavernous - Stromatoids of this type are characterized by large, irregular fenestrae, often with ragged boundaries and connected to smaller fenestral and interpraticle pores (Fig. 39C). Sediment ranges from mud- to sand-sized. It can grade with peloidal microstructure. The irregular nature of the fenestrae is primary, and undoubtedly caused by bridging of large voids by algal filaments or decay of filament tufts, as predicted by Monty (fig. 18, 1977).

Peloidal - Stromatoids are composed of small peloids with interpraticle porosity, without significant development of larger fenestrae except laminoid fenestrae between successive stromatoids (Fig. 39D). Stromatoids tend to be thin, less than 1 millimetre thick. Synsedimentary radial bladed cement is often present, as is internal sediment between the peloids. Gradation is found between peloidal and spongy microstructures as interparticle pores become larger and irregular. Peloidal microstructure is the result of trapping of primary silt- and sand-sized peloids.

Spongy - Spongy microstructure is composed of small peloids with interparticle pores and irregular but generally small fenestrae between (Figs. 40D, 41A). Lamination or individual stromatoids is not present in thrombolites, and in these structures the entire column is spongy. Pores are lined with or filled by synsedimentary radial bladed cement. Gradation between peloidal and tubiform microstructures occurs occasionally, depending on whether the structure is

FIGURE 39

MICROBORINGS AND CRYPTALGAL MICROSTRUCTURE

A. Thrombolite layer corroded by spar-filled algal microborings. Peel; scale bar 150 µm; Isthmus Bay Fm.; ECW-98.

B. Vermiform microstructure in two stromatoids, in hemispheroidal stromatolite. Peel; scale bar 100 µm; Isthmus Bay Fm.; IB-138.

C. Cavernous microstructure in several stromatoids. Peel; scale bar 1500 µm; Aguathuna Fm.; IB-286.

D. Peloidal microstructure with elongate fenestrae, in cryptalgal laminite. Thin section; scale bar 1500 µm; Isthmus Bay Fm.; IB-134.

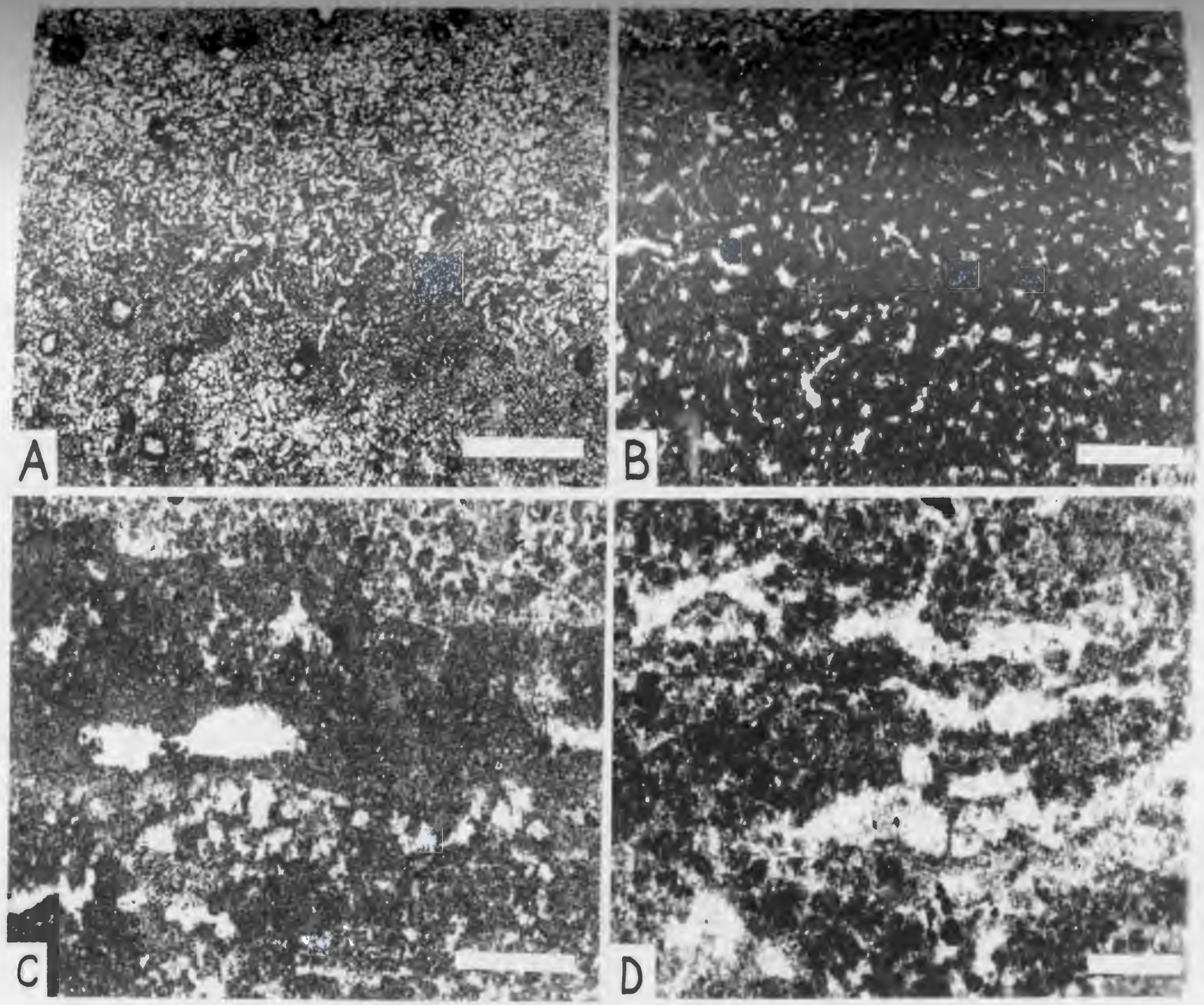
A
B
C
D

FIGURE 40

CRYPTALGAL MICROSTRUCTURE

Photomicrographs

A. Tubiform microstructure showing vertically oriented tubes, in hemispheroidal stromatolite. Peel; scale bar 100 µm; Isthmus Bay Fm.; ECW-86.

B. Tubiform microstructure with internal sediment in tubes, in thrombolite. Thin section; scale bar 1000 µm; Isthmus Bay Fm.; IB-125.

C. Tubiform microstructure with internal sediment, in thrombolite. Thin section; scale bar 1000 µm; Isthmus Bay Fm.; ECW-48.

D. Spongy microstructure with fenestrae lined with radial bladed cement, in thrombolite. Thin section; scale bar 500 µm; Isthmus Bay Fm.; IB-192.

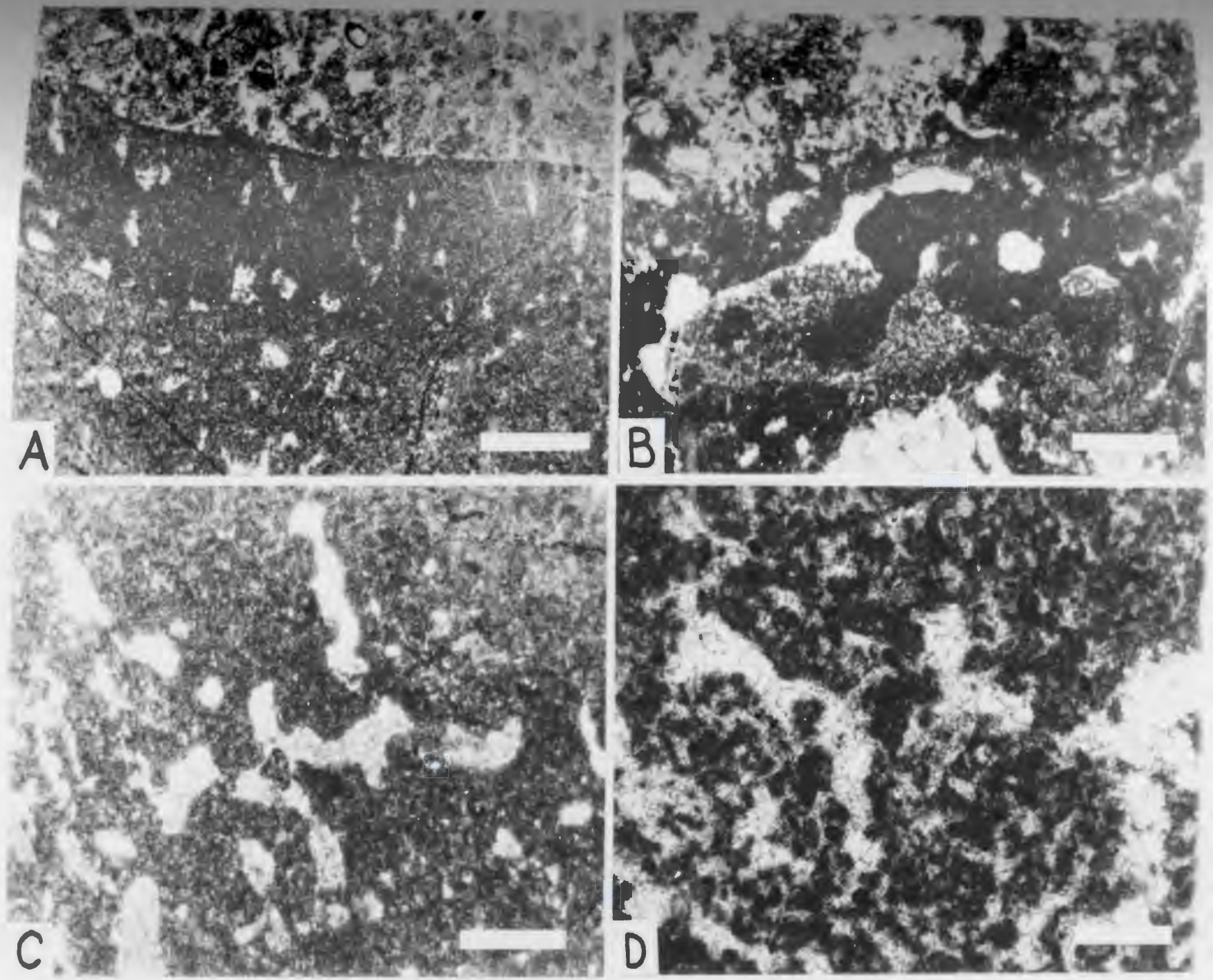
A
B
C
D

FIGURE 41

CRYPTALGAL MICROSTRUCTURE

Photomicrographs

A. Spongy microstructure with bound gastropod shell, in thrombolite. Thin section; scale bar 1500 μm; Isthmus Bay Fm.; IB-229.

B. Cancellous microstructure showing micrite lattice-work, in thin subtidal thrombolite layer. Thin section; scale bar 300 μm; Aguathuna Fm.; IB-303.

C. Cancellous microstructure showing calcified algal filament. Fenestra and filament coated by radial bladed cement, in thrombolite. Thin section; scale bar 150 μm; Isthmus Bay Fm.; IB-192.

D. Alternating massive and vermiform microstructure in hemispheroidal stromatolite. Peel; scale bar 1500 μm; Isthmus Bay Fm.; IB-123.

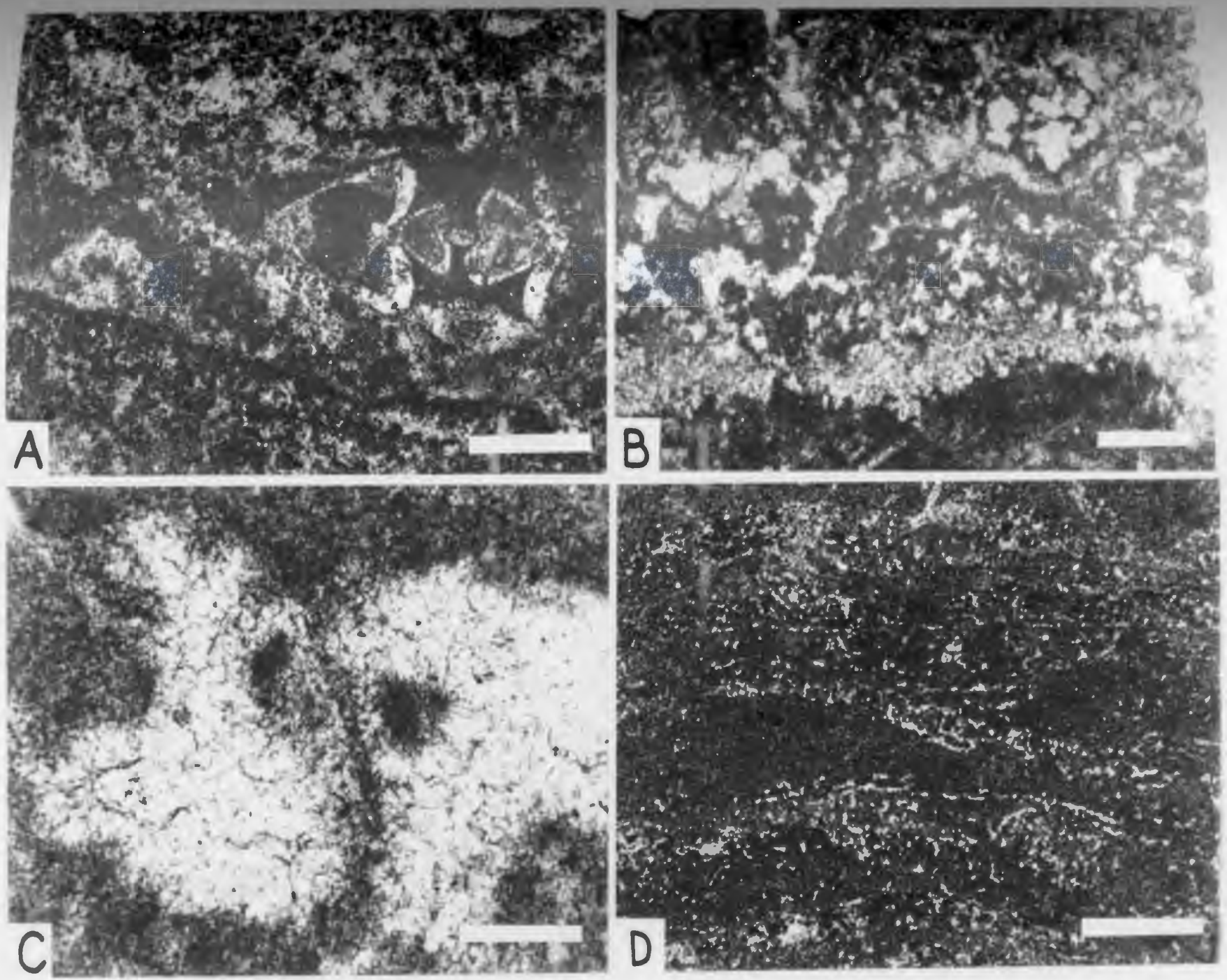
A
B
C
D

mud- or sand-rich. Peloidal stromatoids sometimes pass into unlaminated spongy microstructure on the flank of stacked hemispheriods. Spongy microstructure resulted from the irregularly timed and irregularly distributed addition of sediment, usually in the form of peloids, in the subtidal zone. The microstructure of Proterozic stromatolites illustrated by Cloud et al. (1974) would be classed as spongy, making their interpretation of the sediment-filled tubes between columns as fluid escape tubes most unlikely.

Cancellous - This cellular microstructure is characterized by small but somewhat elongate upwards fenestrae forming a retiform or alveolar lattice of micrite walls (Fig. 41B). This micrite is denser than other micrite in stromatoids, and in some cases the walls are micritic rinds about filaments (Fig. 41C). This rare microstructure is the result of micrite precipitation on mat filaments, creating a porous tufa-like stromatoid. This process of cementation has been described from many modern cryptalgal structures (Pratt, 1979).

## Distribution of microstructures

Table 4 shows the relative abundance of microstructures in the various cryptalgal structures in the St. George (oncolites are left out due to their scarcity). Microstructures usually occur in combination within individual cryptalgal structures (Figs. 41D, 42A,B,C,D), sometimes separated by laminoid fenestrae, except in thrombolites which are usually composed entirely of spongy microstructure. Cryptalgal laminites are, when undolomitized, usually composed of alternating massive and peloidal types. The massive stromatoids in some cases may be deposited during the same

FIGURE 42

CRYPTALGAL MICROSTRUCTURE

A. Massive and peloidal microstructure, in hemispheroidal stromatolite. Peel; scale bar 1000 µm; Isthmus Bay Fm.; ECW-75.

B. Massive and peloidal microstructure, in hemispheroidal stromatolite. Thin section; scale bar 1500 µm; Isthmus Bay Fm.; IB-81.

C. Cavernous and vermiform microstructure together in same stromatoid, in thrombolite. Thin section, scale bar 1500 µm; Isthmus Bay Fm.; BH-116.

D. Tubiform and vermiform microstructure, in thrombolite. Thin section; scale bar 1500 µm; Isthmus Bay Fm.; IB-178.

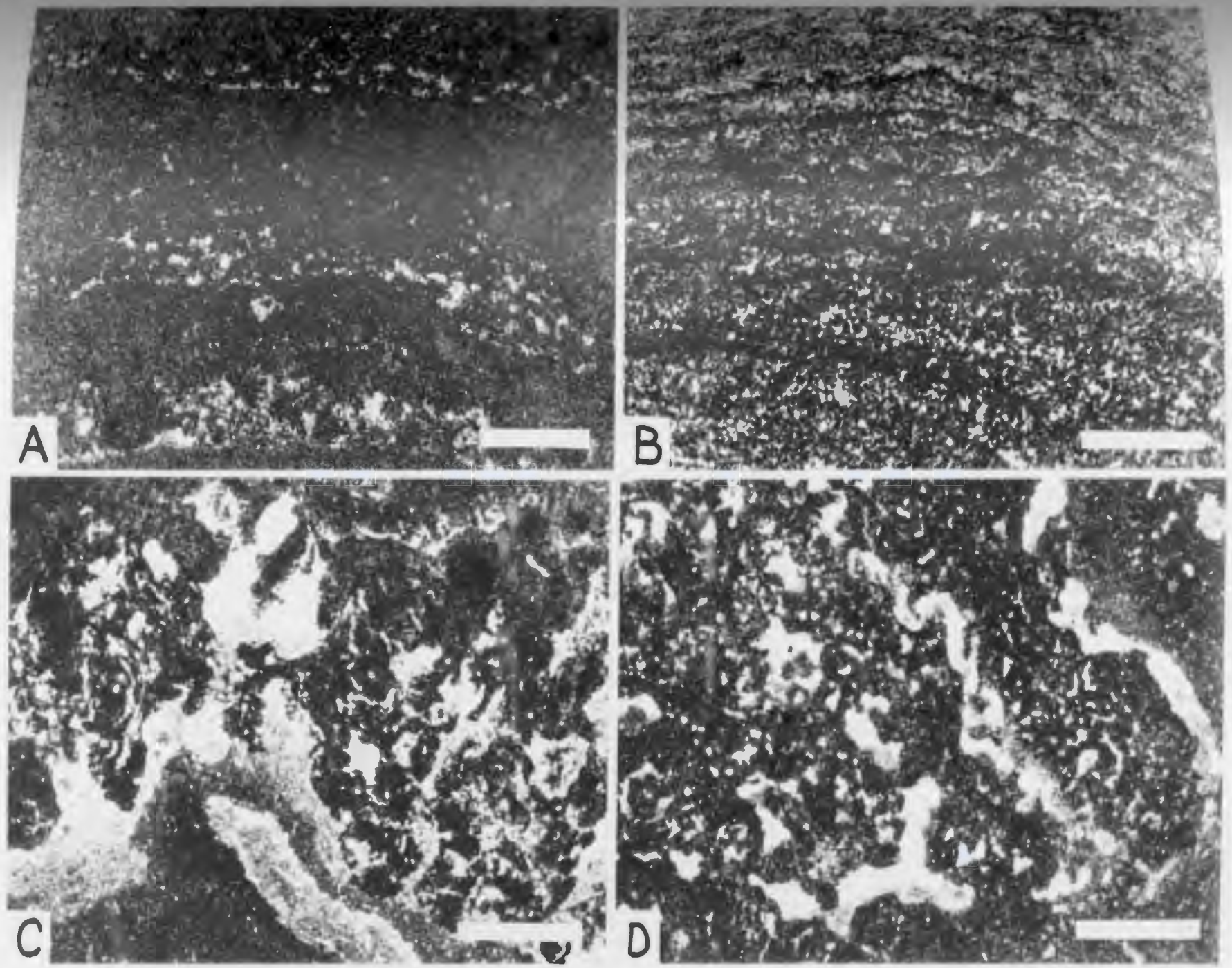
A
B
C
D

| | CRYPTALGAL LAMINITE | HEMISPHEROIDAL STROMATOLITE | COLUMNAR STROMATOLITE | THROMBOLITE |
|---|---|---|---|---|
| MASSIVE | X | P | X | |
| VERMIFORM | | X | | P |
| TUBIFORM | | X | | P |
| CAVERNOUS | P | X | | |
| PELOIDAL | X | X | | |
| SPONGY | | | X | X |
| CANCELLOUS | | | | R |

**Microstructure distribution**

X- TYPICAL
P- PRESENT
R- RARE

Table 4. Distribution of microstructures in cryptalgal structures

event as the underlying peloidal stromatoids. Hemispheroidal stromatolites are more variable, with alternations of massive, peloidal, vermiform, and cavernous types, or alternations of vermiform and tubiform types. Columnar stromatolites have alternating spongy and massive types, the latter sometimes burrowed. Mud-rich thrombolites often have tubiform and vermiform microstructure in the same stromatoid.

The alternation of microstructures was caused by changing sedimentological conditions and biological characters and features of the algal mats (discussed later). The simple alternation in cryptalgal laminites reflects great distance from the subtidal zone where sedimentary particles originate, and addition during storms and high tides only. Thrombolites usually have a single type of microstructure, spongy, because sedimentological conditions are stable in the subtidal zone where they grew. Columnar stromatolites, interpreted to have formed in the low intertidal zone, show the effect of oscillating conditions characterizing the intertidal zone: spongy and massive stromatoids deposited by suspension during alternating agitated and quieter periods. Hemispheroidal stromatolites have the most variability in microstructure reflecting variability of size of sediment that is deposited, timing related to tidal cycles and storms, and mat surface textures (which may also be related to biological composition of mats).

## ALGAE

### Renalcis

Description - Renalcis Vologdin, 1932 is a problematical Paleozoic micrite-walled chambered microfossil (Wray, 1977). It is quite variable in shape and may include a number of synonymous forms (Riding and Wray, 1972). Renalcis is a very important component of many Lower Paleozoic reefs, from the Cambrian to Devonian (Wray, 1971; Riding and Toomey, 1972; James and Kobluk, 1978).

In the St. George, masses of Renalcis occur in the bioherm complexes at Green Head and in Hare Bay, and individual Renalcis occur within thrombolite mounds at two horizons in the upper part of the Isthmus Bay Formation on Port au Port Peninsula (Fig. 43A) and in cryptalgal intraclasts in the Catoche Formation. In the Green Head bioherm complexes, Renalcis masses are free-standing and coalescing heads (Fig. 43B), encrusting walls on thrombolite mounds, and encrusting manes and drapes around corals. In rare cases Renalcis is found within thrombolites. The matrix between Renalcis individuals is micrite (mudstone) with fenestrae filled with synsedimentary radial bladed cement. In reflected light, Renalcis is tan-coloured in a dark-coloured mudstone matrix; in thin section, it is composed of micrite that is finer grained and darker than matrix mudstone and cryptalgal material. The shapes of Renalcis and similar forms are variable, and four basic categories are distinguised, with only the first properly assignable to the genus Renalcis: (1) 'typical' chambered form where successive lunate chambers

FIGURE 43

RENALCIS

A. Vertically oriented slab of light-coloured curtain of Renalcis (R) hanging into a sediment-floored cavity within a thrombolite mound. Scale bar 1 cm; Isthmus Bay Fm.; IB-232.

B. Horizontally oriented slab of the outer margins ~~of~~ two coalesced heads of light-coloured Renalcis in a dark-coloured micrite matrix. Scale in cm; Green Head bioherm complex, Isthmus Bay Fm.

C. Thin section photomicrograph of Renalcis, oriented upside down, showing lunate chambers increasing in size in the direction of growth. Scale bar 300 µm. Green Head bioherm complex, Isthmus Bay Fm.

D. Thin section photomicrograph of arborescent grape-like "Renalcis", oriented upwards. Scale bar 300 µm; Green Head bioherm complex, Isthmus Bay Fm.

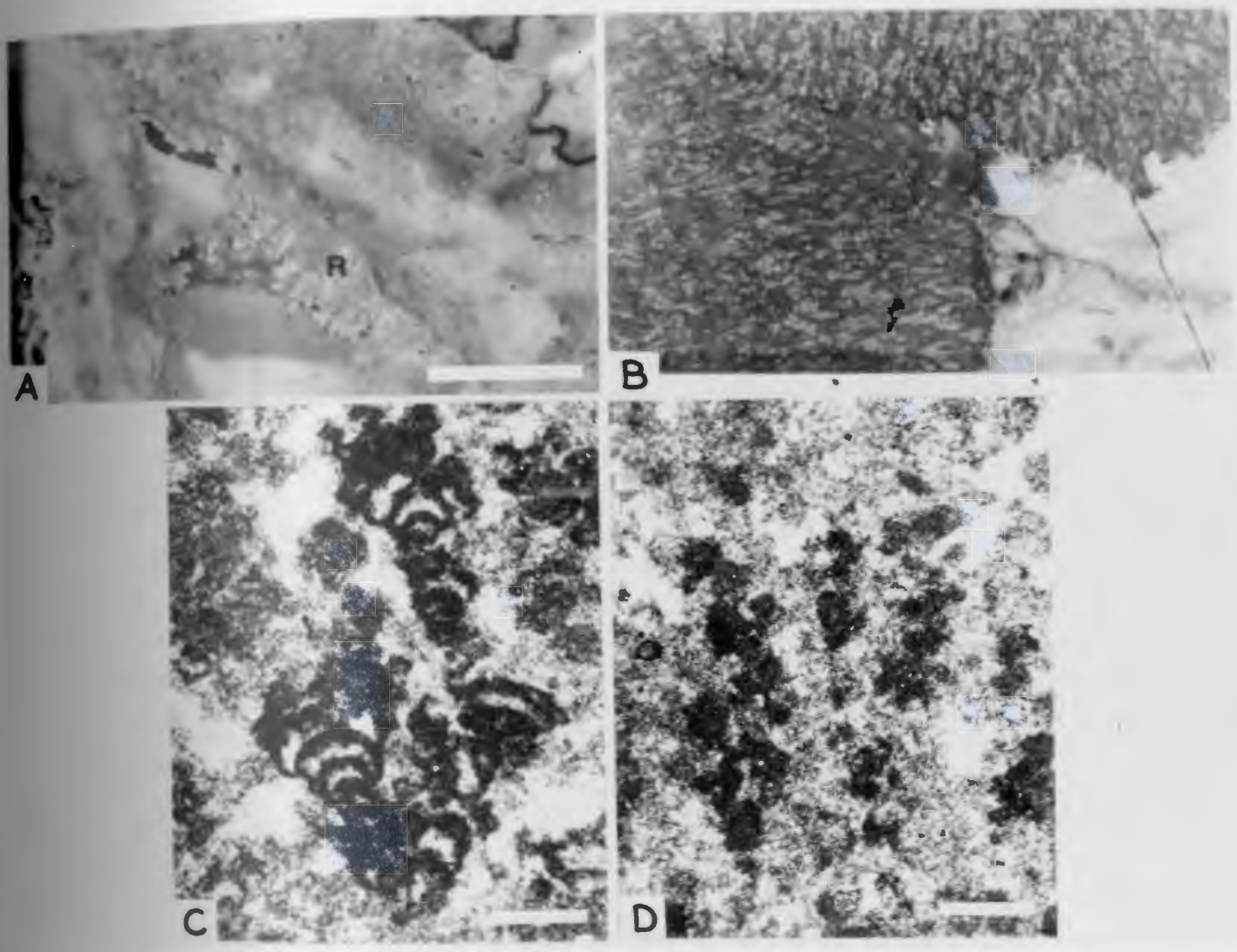
R
A
B
C
D

FIGURE 44

RENALCIS

Thin section photomicrographs

A. Grape-like clotted and chambered "Renalcis". Scale bar 300 µm; Green Head bioherm complex; Isthmus Bay Fm.

B. Grape-like clotted and chambered "Renalcis" with unusual elongate, winding spar-filled chamber, growing into cavity in thrombolite mound. Scale bar 500 µm; Isthmus Bay Fm.; IB-234.

C. Cellular chambered "Renalcis". Scale bar 300 µm; Catoche Fm.; Table Mountain.

D. Shrub-like "Renalcis", showing short diverging branches. Scale bar 300 µm; Green Head bioherm complex; Isthmus Bay Fm.

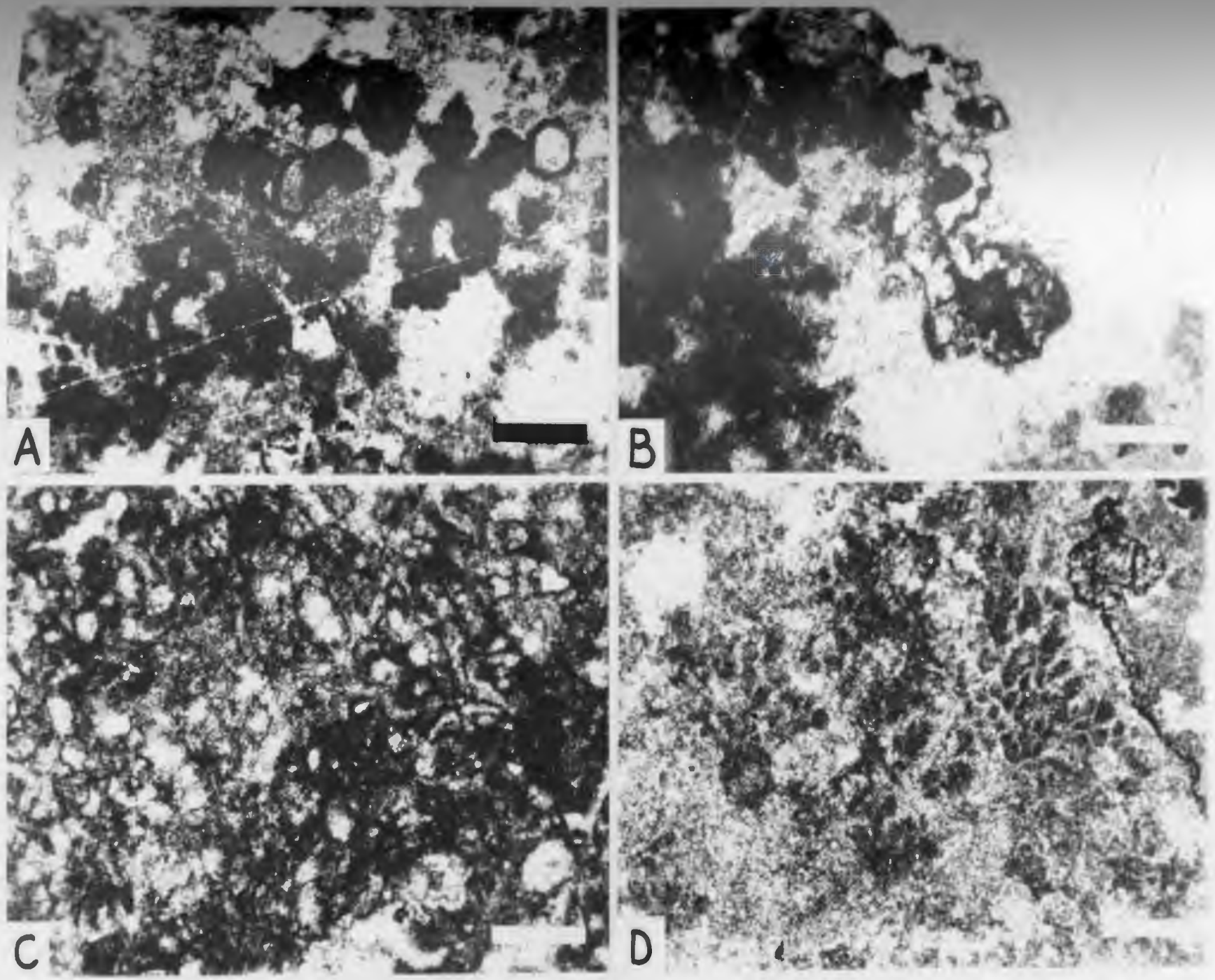
A
B
C
D

of varying size build simple to complex botryoidal aggregates, sometimes producing "microstromatolites" when the diameter of the chambers increases in the direction of growth (Fig. 43C), (in many cases , aggregates are composed of both the chambered and grape-like clotted form (Figs. 44A,B), (2) irregularly shaped chambers sometimes forming clumps of irregular cells (Fig. 44C), (3) grape-like masses of small, occasionally hollow clots that are arranged in an arborescent fashion (Fig. 43D), (4) shrub-like aggregates of short narrow micrite branches which in cross-section appear as clusters of peloids (Fig. 44D). Elongate chambered forms and irregular clots are commonest when the growth vectors are downward or sideways, such as when expanding into cavities. Arborescent clots are commonest in free-standing heads where growth vectors are upwards and divergent. Shrub-like forms are rare and have upward growth direction. The irregularly cellular chambered form occurs within thrombolites. All Renalcis chambers are filled with synsedimentary radial bladed cement.

Interpretation - Renalcis has been variously interpreted, recently as a foraminifer (Riding and Brasier, 1975) and as permineralized clumps of coccoid blue-green algae (Hofmann, 1975; Brasier, 1977). It is difficult to envision a forminiferal origin due to the high variability of shape and the colonial fashion forming large masses. Hofmann (1975) presented a mechanism for the formation of Renalcis whereby the dark walls and light-coloured chambers resulted from pigment gradients within gelatinous colonies of non-

calcareous chroococcalean algae. The larger calcite crystal size of the "chambers" was thought to be due to inhibition of crystallization in the pigmented marginal "walls". Observation from the St. George shows that chambers are always filled with synsedimentary cement crystals which radiate from the walls, and therefore the chambers were primary voids. Accordingly, Hofmann's (1975) algal interpretation is modified: it is suggested here that Renalcis is a diagenetic taxon formed by calcite permineralization (calcification) of the blue-green algae. Clotted shapes were formed by permineralization of smaller clumps or more complete permineralization of the sheath and contents. Successive clumps of cells grew on hard permineralized substrates. Permineralization was calcitic, and not aragonitic, because all primary aragonite fossils in the St. George were selectively leached, and Renalcis never shows signs of this.

It is not clear whether permineralization affected every algal clump that grew, or whether many cells grew, died, and rotted away before biogeochemical conditions were just right to promote calcification. Based on the fact that coccoid blue-green algae have a rapid growth rate, but that Renalcis did not grow faster that thrombolite columns which probably did not accrete rapidly (that is, not even 1 millimetre per year estimated for colloform mat mounds in Shark Bay by Logan et al. [1974]), permineralization was probably only an occasional event of living and/or dead cells, probably during conditions of extremely

vigorous agitation and oxygenation, which are known to promote cementation in modern reefs (James et al., 1976).

It is also not clear why these coccoid cells became calcified and other, probably filamentous, types that constitute thrombolite-forming mats did not. This is likely due to specific organic composition of the sheaths which are variable in modern algae (Chapman and Chapman, 1973).

The microfossil Epiphyton Bornemann, 1886, which is composed of dendritic micrite branches, occurs in resedimented boulders of Lower Ordovician age in the Cow Head Group (N.P. James, pers. comm., 1978) but not in the St. George Group. It is proposed here that this form is also a diagenetic taxon formed by permineralization of coccoid blue-green algae, based on the occurrence of shrub-like Renalcis which appears to be a form transitional to true Epiphyton.

## Girvanella

Description - The algal genus Girvanella Nicholson and Etheridge, 1878 is a well known microfossil consisting of flexuous tubes of uniform diameter with walls composed of micritic calcite crystals (Fig. 45A). It is relatively common in the St. George (Fig. 46), occurring mostly in burrowed fossiliferous wackestone of lithotope G (subtidal shelf facies), twisted or entwined into clumps or 'snowballed' where the tubes are concentrically arranged (Fig. 45B), with a mudstone matrix. In some grainstone pockets in lithotope G, Girvanella occurs as rounded intraclasts (Fig. 45C) whose frequently micritized boundaries cut the

FIGURE 45

GIRVANELLA

Thin section photomicrographs

A. Girvanella tubes, cross- and longitudinal sections. Scale bar 100 µm; Aguathuna Fm.; NE Gravels.

B. "Snowballed" Girvanella tubes with micrite matrix, in subtidal biomicrite. Scale bar 300 µm; Catoche Fm.; PAC-38.

C. Intraclast of Girvanella tubes with micrite matrix in biosparite. Scale bar 150 µm; Catoche Fm.; PAC-38.

D. Girvanella tubes forming lamina in stromatolite. Scale bar 300 µm; Aguathuna Fm.; NE Gravels.

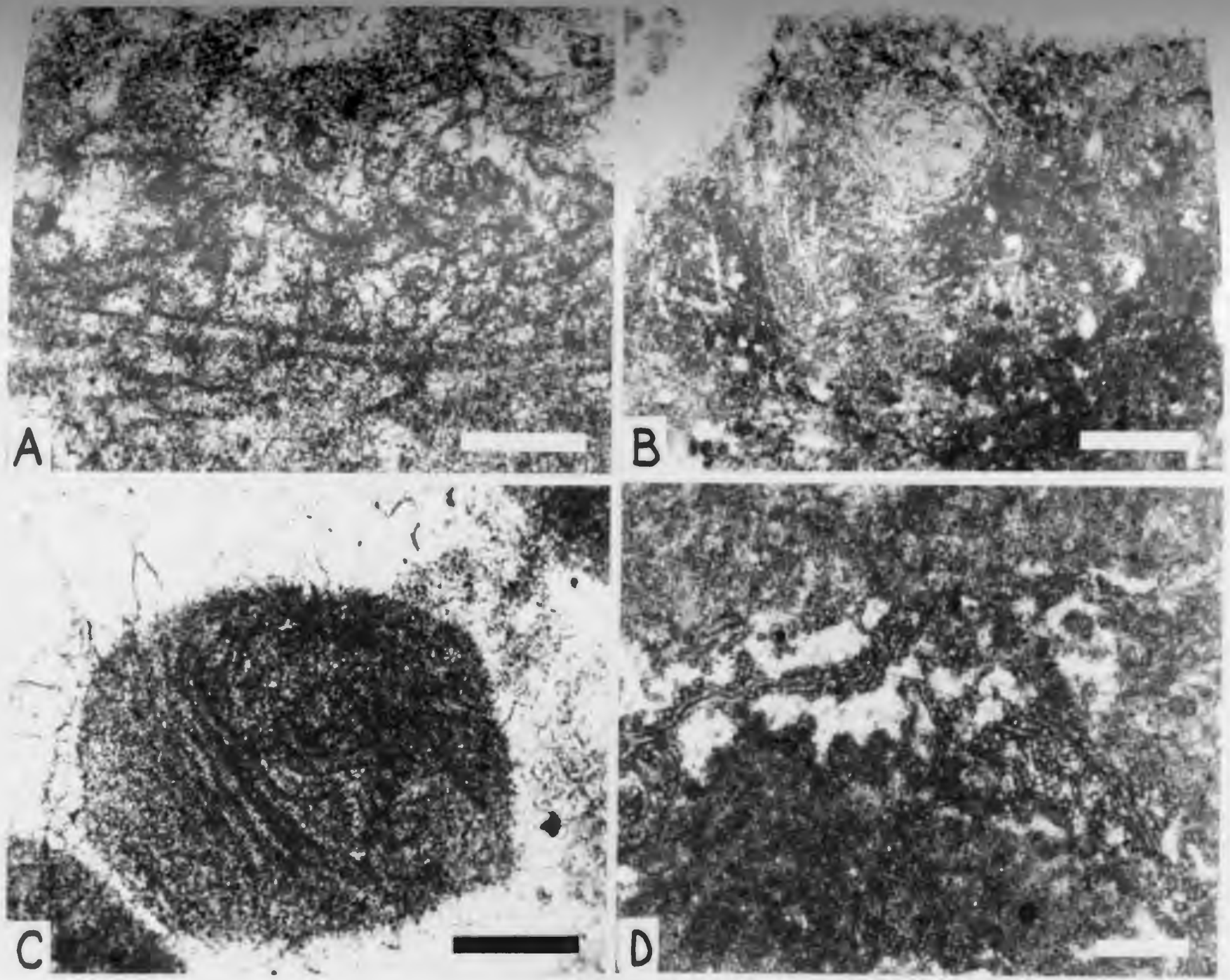
A
B
C
D

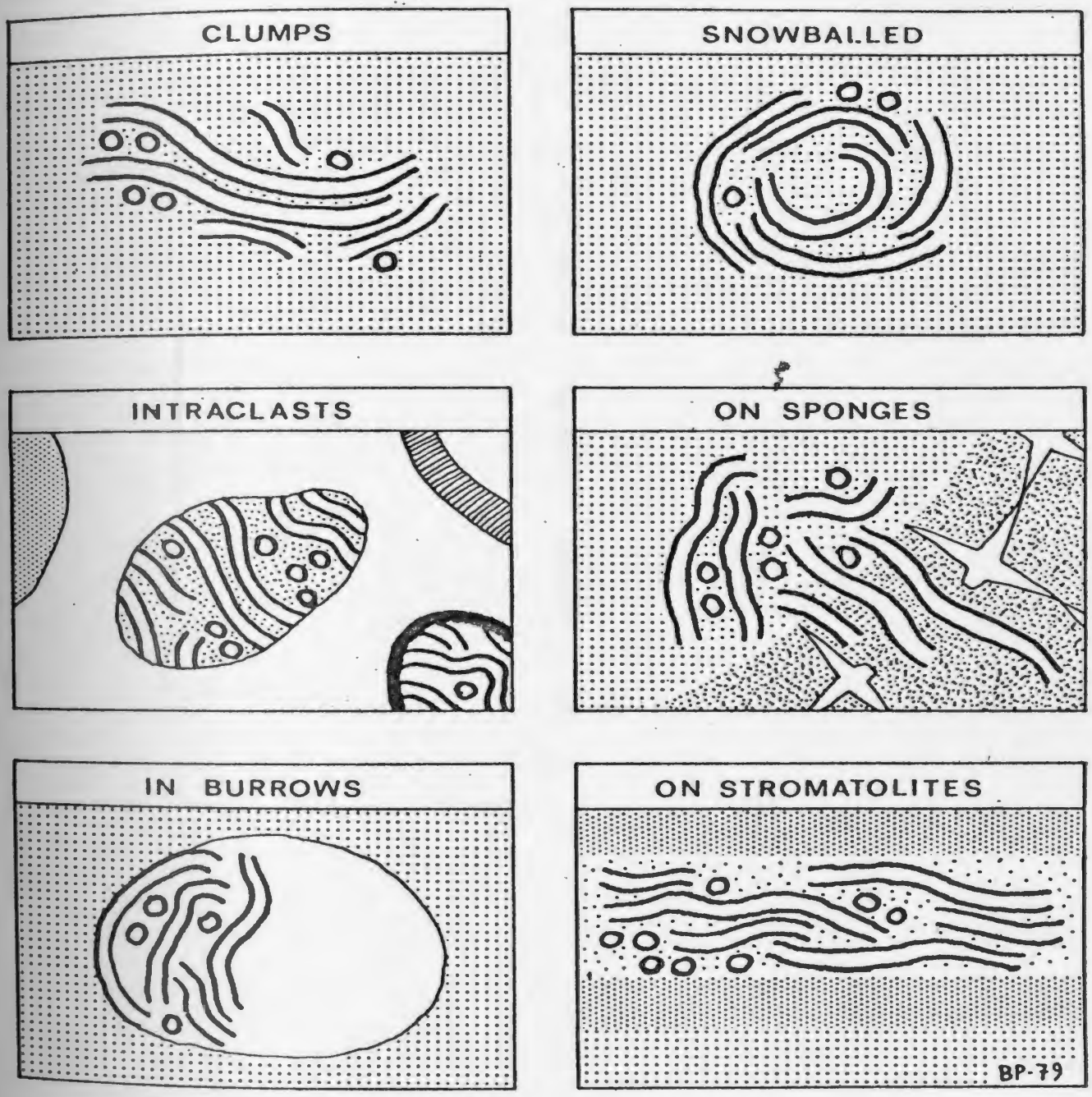


Figure 46: Simplified sketches of the six modes of occurrence of *Girvanella* as observed in thin sections of the St. George.

tubes which are embedded in both mudstone and sparry calcite. Girvanella is also found loosely encrusting the walls of now spar-filled burrows; the tubes do not show evidence of having been packed into the burrows by bioturbating organisms. A wart of Girvanella was found encrusting and penetrating the interior wall of a squat horn-shaped archaeoscyphiid sponge. Girvanella has been commonly reported as forming laminae of stromatolites (e.g.: Ahr, 1971; his illustrations show what are better interpreted as vertically oriented fenestrae rather than spar-walled tubes), but in the approximately 250 thin sections and peels of cryptalgal structures of the St. George, only one sample was found where Girvanella occurs in this way. It forms a discontinuous and loose layer with intercalated entrapped peloids and micrite (Fig. 45D). As pointed out by Riding (1975), Girvanella is not a boring as held by Klement and Toomey (1967) and Toomey and Lemone (1977, their "totally bored intraclast" of figure 2G is interpreted as an intraclast of spar-cemented Girvanella tubes with a micrite envelope), and microborings attributable to algae, which are common in the St. George, are not considered here.

Interpretation - A number of authors (e.g.: Kobluk and Risk, 1977; Riding, 1977) have argued convincingly on the basis of modern analogues that Girvanella is a diagenetic taxon resulting from calcification on the outside, and possibly within, blue-green algal filament sheaths. The growth forms found in the St. George Group indicate that, at least in the Lower Ordovician, the blue-green alga that became Girvanella on calcification was only an encruster of sediment or stable

skeletal substrates. It grew as loose entwined or tangled tufts, even within burrows (possibly subsisting as a heterotroph?), and could be swept off while still soft and uncalcified, and rolled about, as shown by the "snowballed" filaments. The single occurrence within an intertidal stromatolite indicates that stromatolite surfaces could occasionally be suitable substrates, probably only if the mat-forming algae were temporarily killed.

Calcification was synsedimentary as indicated by the intraclasts of Girvanella tubes, and occurred on the sea floor before burial, as indicated by the lack of mud matrix in some of these intraclasts. Calcification took place under normal marine conditions as suggested by the character of the limestone matrix. The "snowballed" tubes were torn up and rolled about before calcification as calcified tubes were probably not sufficiently flexible. Burial and infiltration of mud after calcification accounts for the micrite matrix between most Girvanella tubes. While the soft filaments may have been considerably grazed and browsed by organisms, snowballed filaments indicate that uncalcified filaments existed on the sea floor for enough time to be rolled about. Calcification, a passive diagenetic process related to the biogeochemistry of secretions or breakdown products, probably did not occur every time the Girvanella-forming blue-green algal filaments grew, otherwise Girvanella would be expected to be more abundant as modern filamentous blue-green algae have a rapid growth rate. It follows therefore that the calcification process must have only occurred

in uneaten dead filaments, when biogeochemical conditions associated with rotting favoured calcification.

Girvanella is never found in higher energy grainstones likely because of the fragile nature of the calcified filaments which would not have survived transport. The apparent preference of the Girvanella filaments for subtidal areas is probably real, otherwise more of it should have been discovered in the intertidal facies as the calcite cementing regime is the same as the subtidal or even enhnaced because of possible fresh water influence. The modern analogues described by Riding (1977) from fresh water pools, Hardie (1977) from fresh water stromatolite marshes, and Kobluk and Risk (1977) as calcified epilithic boring algae do not serve as adequate analogues for Girvanella growth occurrences in the St. George.

## SUMMARY

### Morphology and Structure

Laminated and unlaminated cryptalgal structures are abundant and of diverse shapes and internal structures. Shape, lamination, and stromatoid microstrucure are related to environmental factors such as degree and episodicity of sedimentation, length of time between events, total sediment influx, sediment size, scour, synsedimentary cementation, and algal mat surface textures (Figs. 47, 48). A classification scheme has been proposed for stromatoid microstructures that can be expanded to include types not recognized in the St. George.

Thrombolite mounds in the St. George are special in

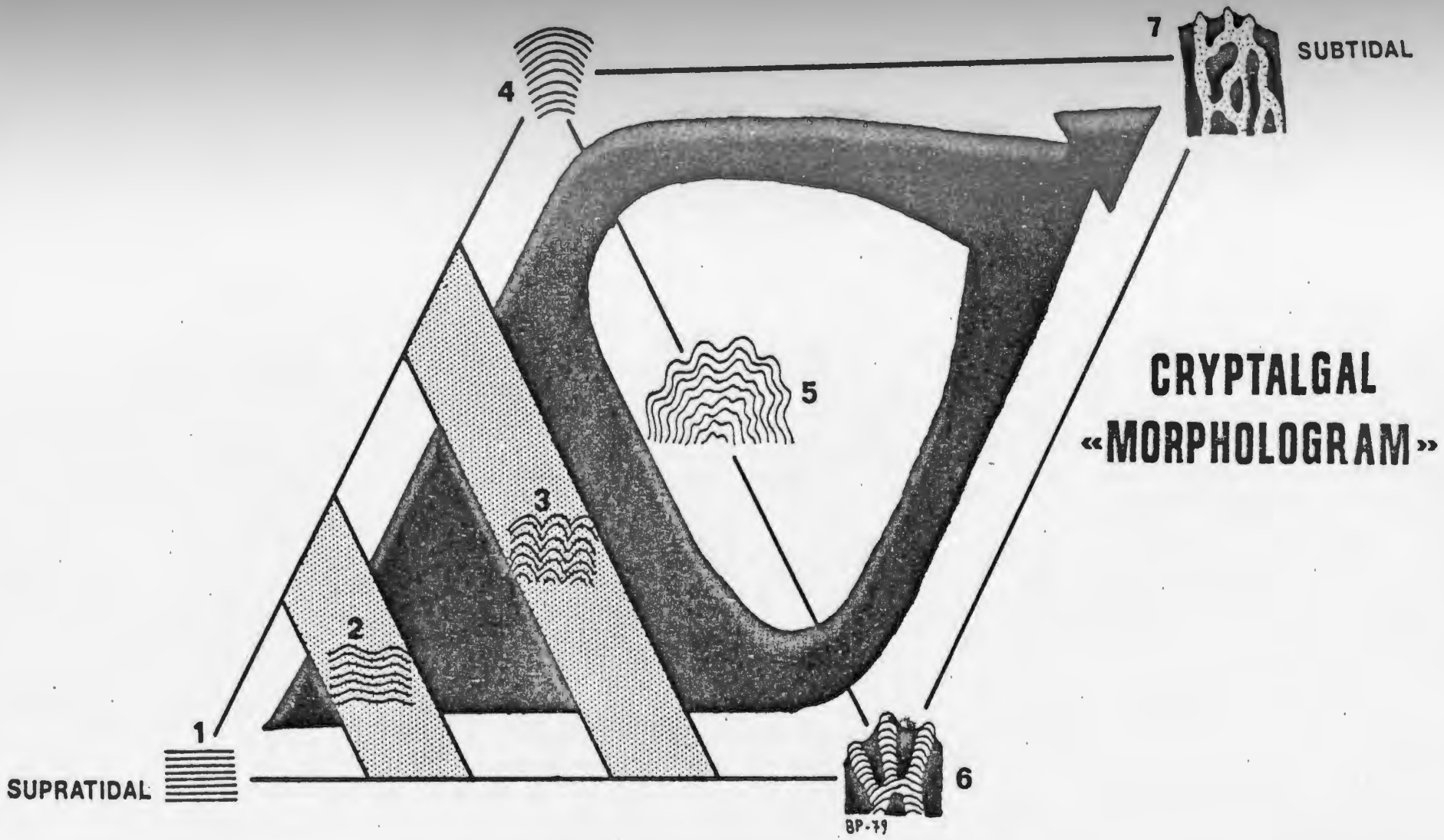


Figure 47: Cryptalgal "morphologram" relating cryptalgal structure types to eachother with supratidal cryptalgal laminite (1) on the left and subtidal thrombolites (7) on the right. Structures between are intertidal wavy cryptalgal laminite (2), laterally-linked hemispheroidal stromatolites (3), stacked hemispheroidal stromatolites (4), compound stromatolites (5), and columnar stromatolites (6). The parallelogram lines show the paths of morphological transitions; the black area shows the path of transition from supratidal to subtidal forms and shows that compound stromatolites do not grade with thrombolites.

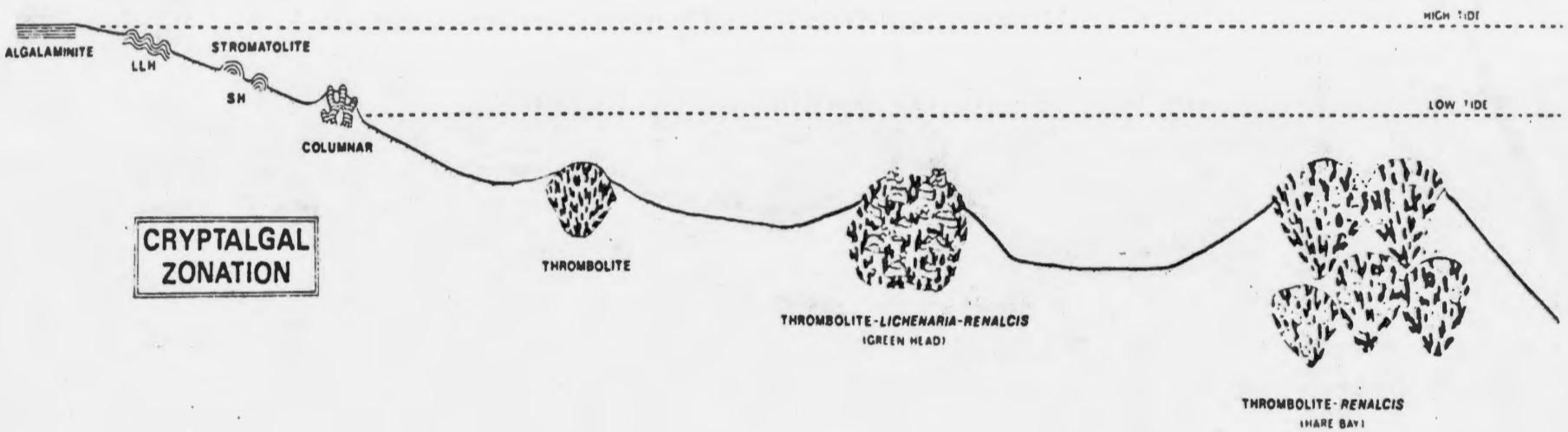


Figure 48: Zonation of cryptalgal structures with depth, on a hypothetical shelf profile.

that in places they have framework elements that include Renalcis (calcified blue-green coccoid algae), the ancestral coral Lichenaria, and sponges. Thrombolite mounds are in fact well-developed reefs, lower in diversity than most younger reefs, but supporting a benthos that occupied all the major niches and represented all trophic feeding groups. The presence of abundant gastropod grazers suggests that they played little or no role in restricting Phanerozoic stromatolites, and other factors are deemed more important (Pratt, in prep.).

## Blue-green algal communities

On the basis of fossil evidence, microstructures, and comparison with modern analogues, some speculations can be made as to the nature of the distribution and types of Lower Ordovician blue-green algae. The taxonomy of living blue-green algae (Cyanobacteria, Cyanophyta) is in an unsatisfactory state (Brock, 1977, among others) due to uncertainty of the affinity of the whole group and the validity of taxonomic distinction on the basis of morphology. It is therefore essential that taxonomy of fossil blue-greens be cautious, especially in the case of diagenetic taxa strongly affected by environmental factors. In fact, most of the species of Epiphyton, Girvanella etc. are likely invalid because they are based on characters of doubtful biological distinctiveness. The taxonomy of diagenetic taxa should be considered in the same way as stromatolites and trace fossils, that is, regarded as form-genera and form-species.

Coccoid blue-green algae probably favoured the vigorous

subtidal conditions of biohermal areas, as their calcified remains never occur in stromatolites or other deposits. Upon calcification, these cells formed Renalcis, Epiphyton, and many intermediate forms related to growth habit and environmental parameters.

Spar-filled tubes made by boring algae are common, on hardground surfaces, on some thrombolite stromatoids, and within allochems, and are similar to examples described by Klement and Toomey (1967) and Toomey and Lemone (1977). Only one type of microboring can be distinguished, though some micrite envelopes around allochems may also be due to other boring algal types.

A loose flocculent algal mat, probably filamentous, must have covered much of the subtidal sea bottom, occupying a sediment-stabilizing role just as it does in modern environments (Bathurst, 1967), to provide food for the abundant grazers. It is probable that the same algal type was present in the reef cavities at Green Head and formed cryptalgal laminated sediment on the walls and floors because of protection from erosion and grazing. Also living on the subtidal sea bottom were loose tangles and tufts of filamentous blue-green algae that calcified on death to produce Girvanella. This alga was probably abundant but was fragile and liable to mechanical breakdown. That Girvanella calcified and the flocculent filaments did not is probably related to differing composition of the sheaths, a feature noted in modern blue-green (Chapman and Chapman, 1973).

In modern environments, algal mats are usually poly-

specific and are composed of communities of different types, though one type is often dominant (e.g.: Neumann et al., 1970; Logan et al., 1974: Gebelein, 1974; Monty, 1977). Golubić (1977) reviewed the environmental effect on biological composition of mats; species diversity is low in harsh environments and increases in the subtidal. The algal communities that formed St. George cryptalgal structures can only be guessed on the basis of stromatoid microstructure, even though it is partly related to environmental parameters, such as desiccation. In subtidal structures, cancellous microstructure appears to have been produced by prostrate filamentous forms that frequently calcified. Spongy microstructure is very consistent in character, suggesting that the mat community was stable. The elongate fenestrae may have been produced by filamentous forms, though modern microstructures somewhat similar, produced by the colloform mat in Shark Bay, are constructed by coccoid algae (Logan et al., 1974). The variability in microstructure in intertidal stromatolites probably reflects in part true differences in the algal composition of mats, a commonly noted character of modern intertidal mats, such as those in Shark Bay. Cavernous and tubiform microstructures were probably formed by tufts or "cords" of robust filaments, possibly of the same type but forming different surface textures. Vermiform microstructure was likely formed by a finely filamentous type; branching of the fenestrae may be "false" and not from branching filaments. Peloidal and massive microstructures provide no clues as to the original mat composition, except

that the lack of fenestrae suggests small algal cells. Not every microstructural type necessarily was produced by the same community because environmental parameters might outweigh any biological role. The speculations involved in trying to guess the biological nature of algal mats from ancient deposits are very tentative when permineralized remains are not found. Caution is stressed, especially in dealing with Precambrian forms; for example peloidal microstructure ("vermiform" of Walter, 1972) in late Precambrian stromatolites is attributed by Gebelein (1977) to trapping by eukaryotic algae, but this is regarded here as extremely doubtful.

# CHAPTER 4 - DIAGENESIS

## INTRODUCTION

The rocks of the St. George Group were examined petrographically to determine the different stages of diagenesis involved in their lithogenesis. The rocks are petrographically similar to other carbonates of Lower Paleozoic age deposited in shallow water, and show diagenetic stages that include silicate authigenesis, chertification, calcite cementation and neomorphism, dolomitization, minor evaporite precipitation, and economic zinc mineralization. Petrographic aspects of the St. George have only been studied in a reconnaissance fashion by Smit (1971) and Swett and Smit (1972). This chapter outlines the types of diagenetic features, their interrelationships, and their sequence of formation. Special attention is given to ooid formation and dolomitization.

## CALCITE

### Cementation

Introduction - Calcite cement is found mainly in primary fenestrae, interparticle and intraparticle pores, in moldic pores after molluscs, and in fractures. Two types of cement are distinguished in the St. George: radial bladed cement and spar cement.

Radial bladed - This cement is composed of bladed crystals 25-100 microns in length and 5-10 microns in width, and is cream-coloured in thin section. Radial bladed cement is non-ferroan, non-luminescing, and always occurs as a first stage

isopachous fringe, commonly preserved in chert nodules. This cement is found in interparticle pores on grainstone intraclasts, hardgrounds, intertidal grainstones, in fenestrae of thrombolites (Fig. 49A), in sediment-floored cavities in boundstones, and in chanbers of Renalcis, corals and gastropods.

This cement is interpreted as synsedimentary marine cement for the following reasons: (1) isopachous nature of fringe indicating fluid-filled pores, (2) occurrence and localization in hardgrounds and thrombolites, (3) occurrence in intraclasts within grainstones otherwise cemented by spar cement, (4) occurrence in fossils cementing internal sediment that defy final geopetal relationships, (5) occurrence as bands within grainstones otherwise cemented by spar cement, and (6) it is the only cement type that is cut by synsedimentary erosion. It is interpreted to have been originally calcite as opposed to aragonite because all fossils presumed to have been originally aragonite, such as gastropods, are always leached. Radial bladed cement seems to have undergone slight syntaxial overgrowth during spar cementation, as evidenced by: (1) radial bladed fringes are followed by relatively large spar cement crystals, rather than the normal sequence of crystal size increase into the pore, (2) the blades are not perfectly isopachous, and sharp boundaries between fringes and spar mosaics are not present, (3) the cream colour of the radial bladed cement does not extend to the tips of the blades.

Spar - Spar cement is typically equant calcite crystals, 10-20 microns in size on pore edges, and increasing in size

towards pore centres to maximum of several hundred microns (Fig. 49B). It is non-luminescing, may be slightly ferroan in the last stage of pore-filling, and is commonly in optical continuity with pelmatozoan, trilobite, and brachiopod substrates, forming elongate crystals when syntaxial on the latter two fossil types (Fig. 49C). The cement is normally inclusion-free, except in one case where they outlined prismatic crystals 500 microns in length and 100 microns in width that later merged into an equant mosaic. Early stages of terminated spar crystals are sometimes preserved in chert. Spar cement is found in interparticle pores, mollusc molds, shrinkage cracks, tectonic fractures (Fig. 49D), and burrows. The micrite matrix is commonly compacted around spar-filled burrows. Tectonic fractures are filled either by large spar crystals, or by palisades of narrow rectangular crystals. Large prismatic crystals several millimetres in length are rare but fill primary cavities in the Green Head reef complex, large solution vugs associated with epigenetic dolomitization, and fractures within a subaerial rubble from the Aguathuna Formation. In fractured clasts from the rubble, crystals contain numerous bands of inclusions (Fig. 49E), and growth was interrupted by internal sediment.

Spar cement is interpreted to be a burial cementation stage because: (1) it occurs later than radial bladed cement, (2) it is a cement habit unknown as a synsedimentary marine cement, (3) it is not facies specific, (4) it fills fossil molds, (5) it fills tectonic fractures that were not surface features. Cementation began soon after burial because

FIGURE 49

CALCITE CEMENT AND NEOMORPHIC SPAR

Photomicrographs

A. Radial bladed cement followed by blocky spar cement in a fenestra of a thrombolite. Peel; scale bar 150 µm; Isthmus Bay Fm.; ECW-82.

B. Spar cement mosaic in interparticle pores. Peel; scale bar 150 µm; Aguathuna Formation; IB-287.

C. Elongate spar cement syntaxial on ?ooid. Peel; scale bar 150 µm; Isthmus Bay Fm.; BH-123.

D. Two tectonic fractures, the first cemented by a palisade of rectangular spar crystals, the second cemented by blocky spar. Scale bar 300 µm; Isthmus Bay Fm.; ECW-9.

E. Subaerial fracture filled by prismatic spar with inclusion-rich growth bands and an internal sediment layer. Peel; Scale bar 500 µm; Aguathuna Fm.; NEG-12.

F. Coalesced spherules of spherulitic neomorphic spar replacing thrombolite column. Scale bar 150 µm; Isthmus Bay Fm.; ECW-86.

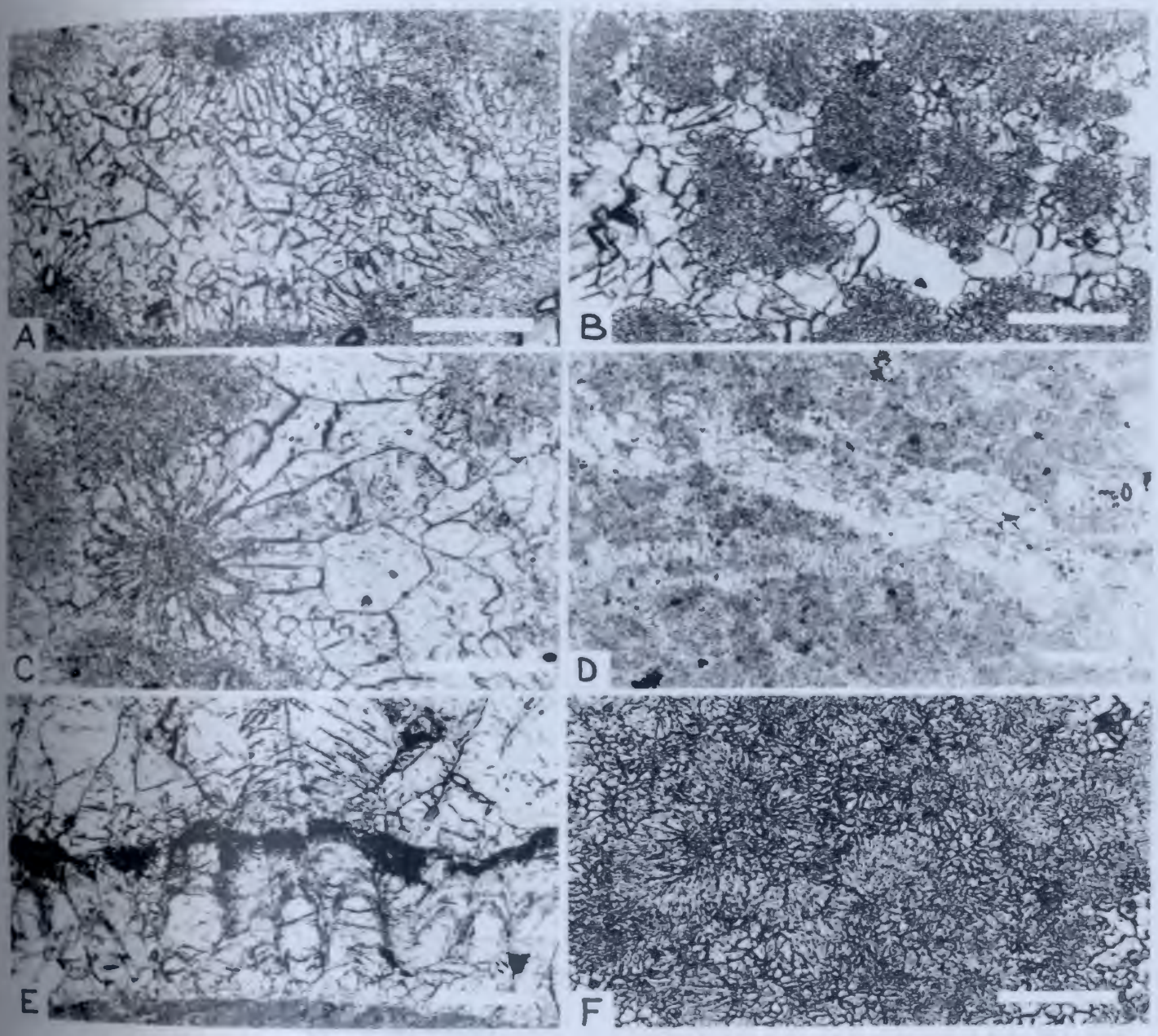
A
B
C
D
E
F

it cements upside-down geopetal ooids, the initial stages are preserved in cherts, and burrows are not compacted whereas the micritic matrix usually is. This implies that leaching of aragonite fossils occurred soon after burial, which is evidenced in rare cases where the molds have been penetrated by burrowers. Spar cementation occurred under phreatic conditions, but it is not certain whether meteoric waters always played a role. However, spar cement in the Catoche Formation suggests that a meteoric influence is not indicated because subaerial exposure in this formation was limited to scattered horizons of intertidal beds. The spar palisades that fill some tectonic fractures indicate cementation while fracturing occurred. The spar filling subaerial fractures in the Aguathuna Formation is interpreted to have been influenced by meteoric conditions because of internal sediment interrupting crystal growth.

## Neomorphism

Introduction - In the St. George, three different neomorphic fabrics that replace calcite grains, matrix, and cement have been recognized: (1) spherulitic spar, (2) microspar, and (3) pseudospar.

Spherulitic spar - This calcite occurs as isolated, roughly circular spherulitic patches 100-150 microns in diameter, which coalesce to form botryoidal masses. Individual spherulites, cream-coloured in plane light, are composed of calcite needles 50-75 microns in length and 5-7 microns in width, that radiate from a central point (Fig. 49F). They are neomorphic because: (1) they replace only micritic clasts and thrombolites,

(2) replacement is not always complete and spherulite boundaries do not coincide with clast and thrombolite boundaries, (3) botryoidal masses are large but are never cut by synsedimentary erosion. It never exhibits pore-lining cement fabrics. They are never in contact with cements, though have replaced radial bladed cement of thrombolite fenestrae. They are replaced by chert and dolomite, embayed by microspar, and sutured by stylolites.

Spherulitic spar appears to be reported here for the first time. It formed early during burial because it is replaced by chert.

Microspar - This calcite is composed of equant interlocking, but not sutured, crystals 4-30 microns across (Folk, 1965), averaging 10-15 microns. It occurs around burrows, as large irregular patches in wackestone and mudstone (Fig. 50A), and as internal sediment within burrows and other cavities. Most of the original micrite in the St. George at Hare Bay is now present as microspar. Trilobite fragments are occasionally partly altered to microspar (Fig. 50B). Microspar is neomorphic because it: (1) replaces originally calcitic material, (2) always replaces micrite except when replacing trilobite fragments, (3) is never in primary contact with cement, (4) is never cut by synsedimentary erosion. Replacement occurred after chertification, before dolomitization but also after dolomitization at Hare Bay, and before stylolitization.

Microspar was shown by Folk (1965) to be product of aggrading recrystallization of micrite. This is true for

the St. George, but it also replaces originally fibrous trilobite fragments, and is a product in such cases of grain diminuition. It occurred during burial after chertification but before dolomitization and therefore likely concurrently with later stages of spar cementation.

Pseudospar - This neomorphic calcite is larger than microspar (Folk, 1965). It occurs as large patches replacing bioclasts, micrite and cement in grainstones (Fig. 50C), and along stylolites (Fig. 50E). One example was found of radial pseudospar, similar to the stellate mass of "radial-fibrous" spar figured by Bathurst (fig. 332, 1971), that replaced micrite (Fig. 50F). Unaltered micrite grades to microspar, equant pseudospar, and large radial calcite blades several millimetres in length. Pseudospar also is never seen in primary contact with cement, cut by syn-sedimentary erosion, nor as transported clasts. It occurred after chertification, before dolomitization, but also after dolomitization at Hare Bay.

Pseudospar was shown by Folk (1965) to also be a product of aggrading recrystallization, which is true also for the St. George. Its occurrence after chertification and before dolomitization suggests that, like microspar, it may have been concurrent with later stages of spar cementation. Formation on stylolites suggests that burial pressure caused recrystallization.

FIGURE 50

NEOMORPHIC CALCITE

Photomicrographs

A. Microspar sutured by stylolite against unaltered micrite. Peel; scale bar 500 µm; Isthmus Bay Fm.; BH-123.

B. Normally fibrous microstructure of trilobite fragment (between arrows) partly replaced by microspar. Thin section; scale bar 150 µm; Catoche Fm.; Port au Choix.

C. Fossiliferous grainstone replaced by pseudospar. Thin section; scale bar 150 µm; Catoche Fm.; Port au Choix.

D. Micrite replaced by pseudospar around peloids. Peel; scale bar 150 µm; Isthmus Bay Fm.; BH-123.

E. Pseudospar generated during stylolitization. Thin section; scale bar 1500 µm; Aguathuna Formation; 1B-287.

F. Radial pseudospar grading to microspar, to unaltered micrite. Thin section, scale bar 1500 µm; Catoche Fm.; PAC-63.

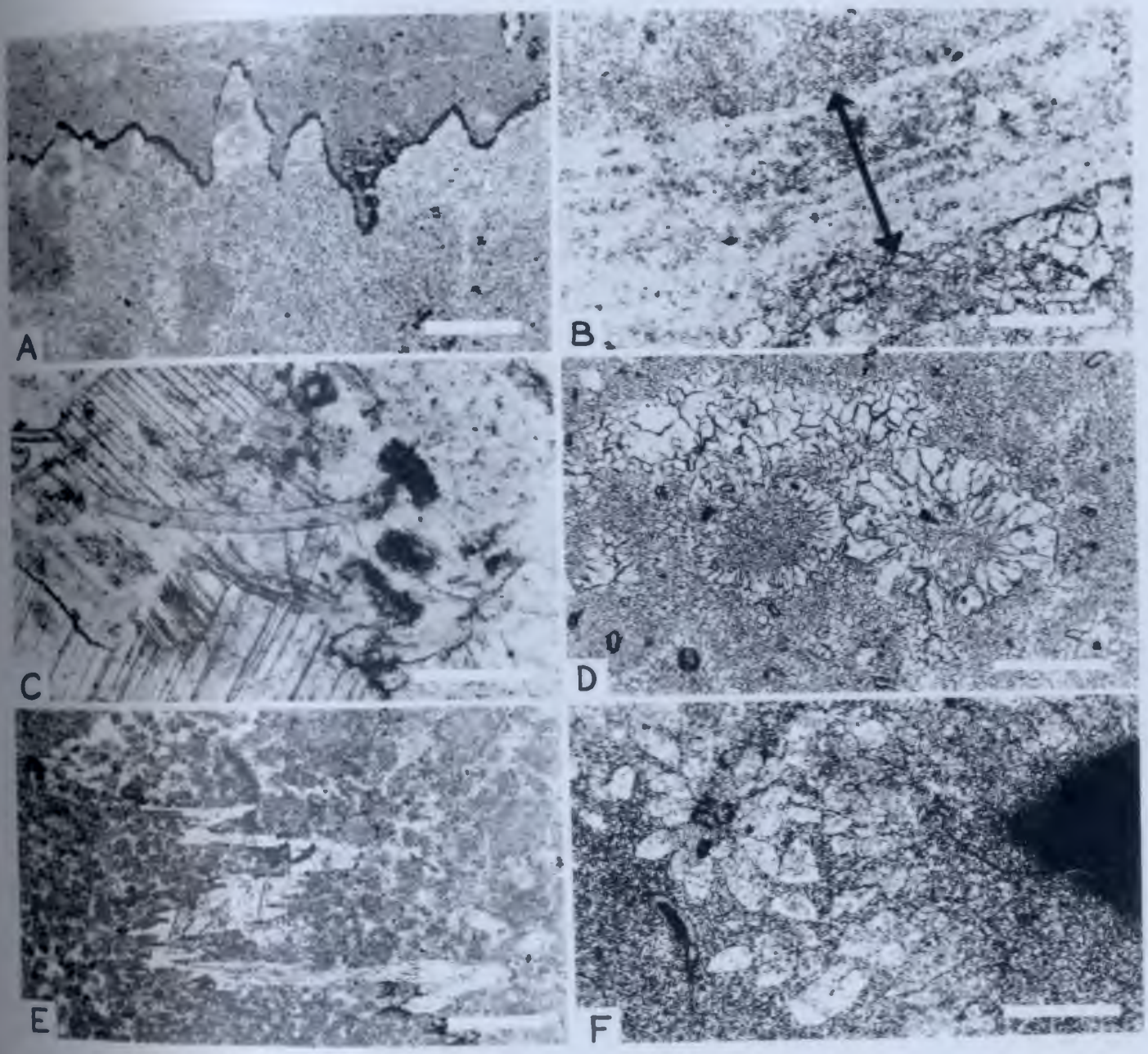
A
B
C
D
E
F

# OOLITES

## Introduction

Oolitic units are rare in the St. George, occurring as scattered particles in fossiliferous grainstones, and with intraclasts in the intertidal and supratidal facies. They are described here because of their well-preserved fabrics that relate to ooid genesis and the diagenesis of the St. George as a whole. Three types of ooids are distinguished on the basis of petrographic character of the cortex: (1) radial, (2) concentric, and (3) combination.

## Radial

Ooids with radial microstructure are the most common and range in diameter from about 0.3 to 0.6 millimetre. Nuclei are usually peloids, rarely fossil fragments. They are composed of radially oriented acicular calcite crystals that usually comprise the entire width of the cortex and are often preserved in chert. Crystals are narrow, wedge-shaped, pointing to the centres, and widen to a width of 5 to 10 microns (Fig.51A).Concentric bands of inclusions sometimes occur and radial bladed cements may be syntaxial with the radial crystals of the ooids. Radial-ooids are cream-coloured in plane light, and in polarized light the characteristic pseudounixial cross is seen which is less well developed when radial crystals are coarse. Inperfections in the radial microstructure occur when: (1) radial crystals sometimes do not radiate from the ooid nucleus (Fig. 51B), (2) large rays of crystals are separated by micritic areas producing a stellate pattern (Fig. 51C),

(3) only segments of the cortex are radial, the rest being concentrically banded (Fig. 51D) or micritic (Fig. 51E).

Concentric

Concentric ooids tend to be larger than radial ones, between 0.5 and 1 millimetre in diameter, and are most commonly found in chert. Concentric laminations are composed of equant micrite, and in chert, equant or slightly radially elongate microquartz, cryptoquartz, and fibrous microquartz, preserving concentric bands of dusty inclusions.

Two horizons containing silicified 'geopetal' ('shrunken' or 'half-moon') ooids and one horizon containing geopetal oolitic intraclasts were found in rocks of the supratidal facies. In the cherts, bands of silicified oomicrite with geopetal ooids (Fig. 51F) and bands of silicified oosparite without alternate with no erosion surface between. In geopetal ooids, cortical layers have been leached, and the nuclei or inner cortical layers and nuclei have dropped to the bottom of the void. The crescentic cavity is filled with chalcedony followed by megaquartz cement. One silicified micrite band contains scattered ooids that have been completely leached and replaced by megaquartz cement (Fig. 51G). In oolitic intraclasts, geopetal ooids give upside-down geopetal directions, and crescentic pores are filled by equant calcite spar cement.

Combination

Ooids having combinations of the above microstructures are in the same size range as concentric ooids, but are uncommon. Radial and concentric cortical layers alternate in

FIGURE 51

OOIDS

Photomicrographs

A. Ooid composed of radial acicular calcite. Peel; scale bar 150 µm; Isthmus Bay Fm.; IB-219.

B. Ooid with isolated and small clusters of acicular calcite replacing micrite. Peel; scale bar 150 µm; Isthmus Bay Fm.; IB-161.

C. Ooid composed of rays of acicular calcite separated by micrite. Peel; scale bar 100 µm; Isthmus Bay Fm.; IB-21.

D. Ooid with right side of concentric cortex replaced by radial calcite. Thin section; scale bar 300 µm; Catoche Fm.; IB-268.

E. Ooid composed of acicular calcite with an unreplaced portion of micrite cortex. Peel; scale bar 150 µm; Isthmus Bay Fm.; ECW-86.

F. Vertically oriented silicified geopetal ooids in oomicrite, with crescentic cavities filled by chalcedony and megaquartz cement. Thin section; scale bar 500 µm; Isthmus Bay Fm.; BH-34.

G. Vertically oriented silicified geopetal ooids in oomicrite with overlying micrite bed containing one ooid completely replaced by megaquartz cement. Thin section; scale bar 500 µm; Isthmus Bay Fm.; BH-34.

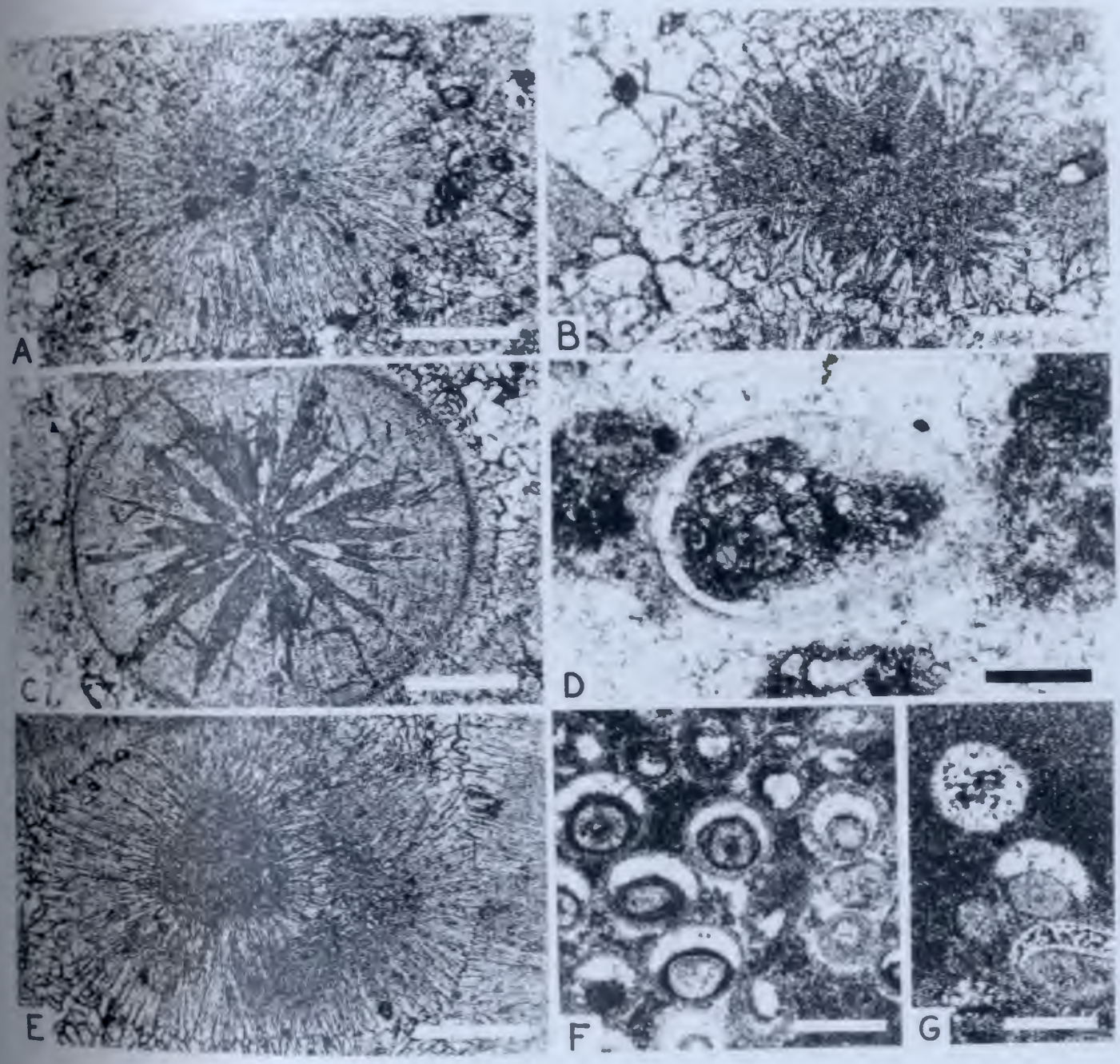
A
B
C
D
E
F
G

these ooids, and intraclasts in the same units can be composed of smaller ooids with the same sequence of inner cortical layers.

## Discussion

The formation of ooids has been the subject of much discussion over the past 100 years (Bathurst, 1971). Both aragonite and high-Mg calcite ooids are now known from the modern marine environment. In using modern ooid analogues to interpret ooids of the St, George, it must be emphasized first that all allochems, principally fossils, that are known or suspected to have been primary aragonite are now dissolved and replaced by cement. St. George ooids are normally never preserved in this way, and therefore were not composed of aragonite. A stage of oomoldic porosity has been seen only once, associated with geopetal ooids. In geopetal ooids, chalcedony and calcite spar cement are void-fillings only, and never replaced pre-existing material. The proposal of Mazzullo (1977) that geopetal ooids resulted from downward recrystallization of the carbonate cortex is untenable for examples in the St. George, and his interpretation of the calcite mosaic in the crescentic areas as neomorphic spar, rather than cement, is suspect. Geopetal ooids formed because some cortical layers were more soluble than others and were selectively leached. Up-side down geopetal ooids in intraclasts indicate that dissolution of cortical layers and initial cementation occurred in subaerially exposed sediment. The restriction of geopetal ooids in oolite units to micritic layers suggests a hydrologic

influence. Residence time of undersaturated rainwater would have been greater in the muddy layers which have lower permeability than grainstone layers, confining leaching of ooids to oomicrites. Certain cortical layers were more susceptible to leaching, but the occurrence of completely dissolved ooids in the micrite layer indicate that, under unusual conditions, entire ooids could not escape complete dissolution. This rules out the possibility that ooids contained both aragonite and calcite layers. Carozzi (1963) argued that geopetal ooids resulted from selective dissolution of evaporitic layers in otherwise calcitic ooids, but this is discounted because of the occurrence of completely leached ooids, unaffected ooids in the same oolitic unit, and lack of evidence for associated evaporites. The suggestion of Folk and Pittman (1971) that evaporites replaced primary calcium carbonate layers prior to dissolution does not adequately explain the presence of unaffected ooids in the same rocks, and the up-side down geopetal ooids in intraclasts, which indicate that St. George ooids were primary calcite, as has been suggested for ancient ooids by Sandberg (1975). Selective leaching would suggests that they were composed of the unstable form, high-Mg calcite, as leaching low-Mg calcite would not be expected. Leaching would have been influenced by the size, surface area, and orientation of crystals, permeability of cortical layers, and probably organic matrix within ooids.

Acicular crystals of radial ooids are interpreted to be neomorphic after concentrically layered calcite because:

(1) they often radiate irregularly from the nucleus, (2) they occur beside unreplaced micritic and concentric cortices, (3) nuclei are often indistinct and penetrated by acicular crystals, and (4) larger stellate rays are separated by micrite which does not embay them. Stellate rays similar to these have been shown to be neomorphic in modern unconsolidated aragonitic Great Salt Lake ooids (Halley, 1977). Marshall and Davies (1975) have illustrated secondary high-Mg calcite radial microstructure that formed in unconsolidated but inactive modern ooids. The orientation of precursor cortical crystals is unknown for St. George ooids, but may have included layers of finely radial crystals like those described by Wilkinson and Landing (1978) and may have exercised some control on neomorphism. Neomorphism probably occurred before or just after early burial because syntaxial spar cement occurs in some oolitic grainstones, but in others it exercised no crystallographic influence on the first stage of calcite spar cement. Preservation in some cherts indicates early formation. The presence of radial crystals in combination ooids, and associated smaller ooids 'fossilized' in the bioclasts during earlier stages of growth, suggests that neomorphism may have occurred syndepositionally, possibly during quiescent periods. Thus, evidence suggests that neomorphism was early and took place in unconsolidated and partly consolidated buried oolitic units.

# DOLOMITE

## Introduction

Dolomite is ubiquitous in the St. George, and dolostones are characteristic of the Isthmus Bay and Aguathuna Formations, occurring locally in the Catoche Formation. Three separate stages of dolomitization are recognized: syngenetic, diagenetic, and epigenetic dolomitization.

## Syngenetic dolomite

Syngenetic or penecontemporaneous dolomite is normally inferred in studies of ancient shallow-water carbonates, on the basis of the occurrence of penecontemporaneous protodolomite in some modern supratidal cryptalgal crusts. Friedman and Sanders (1967) discussed in great detail ancient examples of syngenetic tidal flat dolostones that formed shoreward of marine limestones, but in many of these examples the inference is insufficient and they resemble diagenetic dolostones described in this study. In only one sample in the St. George was evidence of penecontemporaneous dolomite unequivocal. Nearly opaque brown-coloured ferroan microdolomite intraclasts were found silicified in a supratidal grainstone. Rhombs less than 4 microns across were replaced on the clast margins by later larger ferroan diagenetic dolomite rhombs. The small size and pre-chert formation of the dolomite suggests penecontemporaneous precipitation of protodolomite which later, after slight burial in reducing conditions, stabilized to ferroan dolomite.

## Diagenetic dolomite

Description - Dolomite of this type is usually slightly to

strongly ferroan and zoned. Crystal size ranges from 15 to 300 microns, but is commonly 50 to 150 microns across, but averaging 20 microns when replacing cryptalgal laminites. Diagenetic dolomite is found in four intergradational habits that often occur together in the same sample:

(1) as scattered rhombs replacing host grains, neomorphic spar, and chert nodules, including silcrete developed at the St. George-Table Head unconformity.

(2) as scattered rhombs or patches of rhombs located on short clay seams in micritic and pelsparitic limestone (Fig. 52A).

(3) as bands of rhomb masses, with clays and clay seams between crystals, that are laterally continuous wavy layers in supratidal cryptalgal laminites, thin-bedded intertidal rocks, and some subtidal wackestones. These bands also surround spar-filled burrows. Fossil fragments such as trilobite carapaces within bands are sometimes ruptured, and are encased and embayed by dolomite crystals.

(4) as 'beds' and large areas of rhombs and coalesced rhombs replacing limestone, most frequently micrite (Fig. 52B), but also sparite (Figs. 52C,D) and neomorphic spar. Clays and clay seams are present in replaced micrite but not in sparite. Beds of this type at the top of the St. George are brecciated and fragments have been incorporated into basal Table Head limestone. Replaced sparite does not show evidence of compaction (Fig. 52E), but replaced micrite often shows considerable thinning relative to unaltered micrite (Fig. 52F).

Diagenetic dolomitization occurred after chertification

FIGURE 52

DIAGENETIC DOLOMITIZATION

A. Photomicrograph of dolomite rhombs located on dark clay and organic-rich seams of compaction origin, in micrite. Peel; scale bar 500 µm; Catoche Fm.; ECW-118.

B. Photomicrograph of dolostone with remnant micrite nodule with dark clay and organic-rich seams. Peel; scale bar 1500 µm; Isthmus Bay Fm.; IB-127.

C. Vertically oriented slab of uncompacted grainstone layers and lenses partly replaced by light-coloured dolostone. Box outlines view shown in D. Scale in cm; Catoche Fm.; PAC-46.

D. Photomicrograph of close-up of C, showing dark-coloured dolostone partly replacing uncompacted biosparite. Peel; scale bar 1500 µm.

E. Vertically oriented slab of light-coloured dolostone partly replacing grainstone, showing no signs of compaction. Scale in cm; Catoche Fm.; ECW-112.

F. Vertically oriented slab of light-coloured dolostone and dark-coloured fine-grained grainstone, showing pre-dolomitization compaction. Scale in cm; Isthmus Bay Fm.; IB-211.

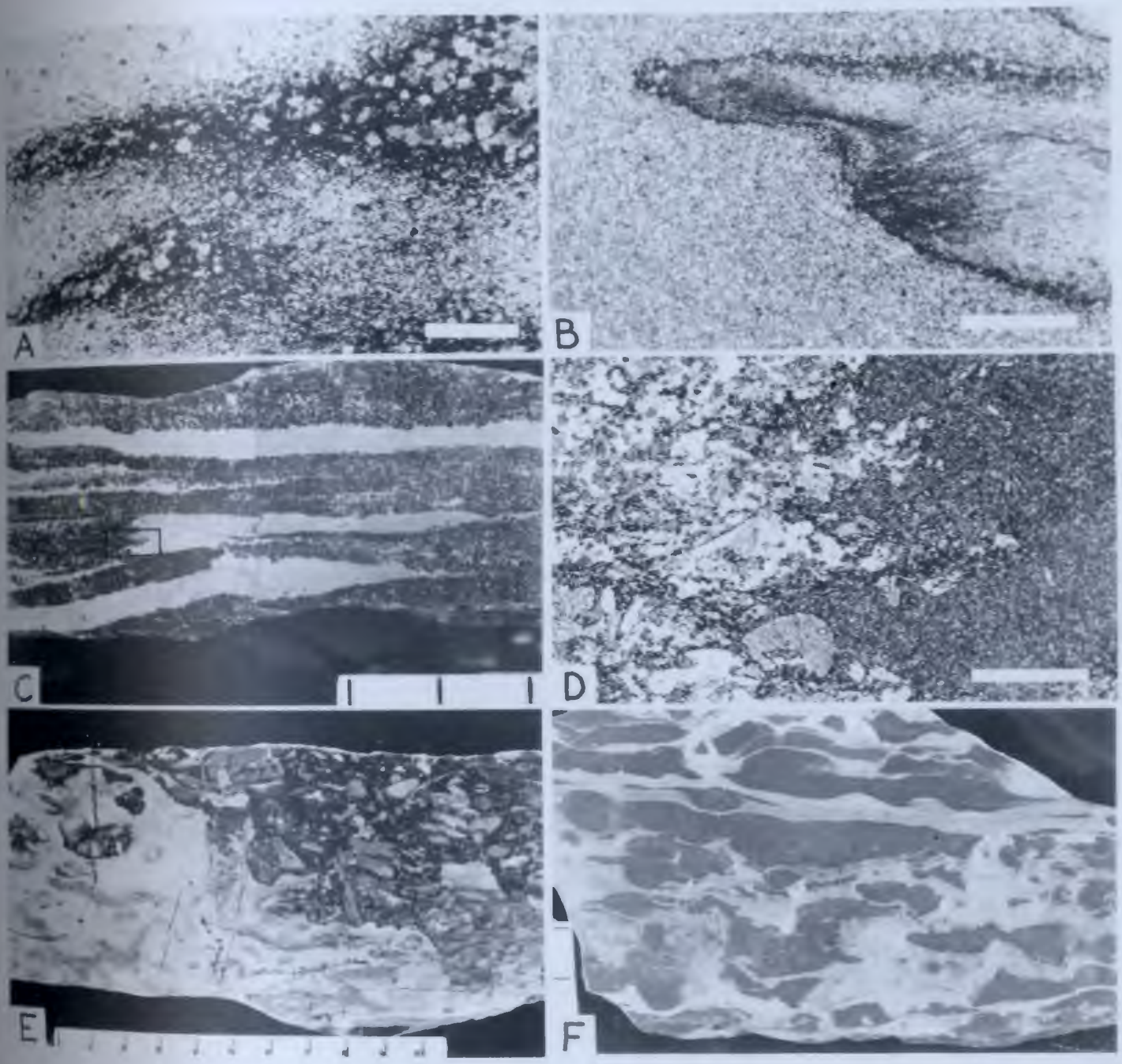
A
B
C
D
E
F

and silicate authigenesis and both before and after neomorphic spar, as evidenced by embayed and calcitized rhombs. Stylolitization occurred after dolomitization because stylolites surround and occur within bands of dolomite, suture rhombs together, and collect isolated rhombs. Epigenetic dolomitization occurred after diagenetic dolomitization and dolostones are redolomitized. Rhombs suffer later overgrowths, but it is difficult to separate the two stages when epigenetic dolomitization is not pervasive and overgrowth only slight.

Interpretation - This type of dolomite formation has been described in detail by Wanless (1979) who termed it "pressure-solution dolomitization". He carefully documented the effects of this dolomitization and the resulting rock fabrics which have often been interpreted in the past as primary sedimentary structures. He attributed this dolomite to precipitation during pressure-solution of original limestone. Evidence cited for this process was the abundance of clay seams containing dolomite, and the volume decrease in dolomitic and dolostone layers as opposed to undolomitized limestone. The effects of pervasive or "non-sutured" pressure-solution are, however, difficult to distinguish from soft-sediment compaction in muddy sediments. Shinn et al. (1977) showed experimentally that compaction of unlithified organic-rich muddy carbonate sediment could be considerable, and wavy seams of organic material were produced.

Several lines of evidence suggest that soft-sediment compaction is the more likely process than pressure solution

to produce volume loss in dolomitic layers: (1) examples of lenticular beds in the intertidal flat facies have been compacted by up to 20 times as shown by folded burrows that were originally vertical (Fig. 53A), (2) Broken fossils in dolomitic bands suggest mechanical compaction rather than pressure-solution (Fig. 53B), and (3) Chert formed during shallow burial has "frozen" early stages of compaction in subtidal wackestones where opaque seams (clays and organics?) occur around uncompressed burrows which were in the initial stages of spar cementation (Fig. 53C). Evidence used by Wanless (1979), such as squashed burrows and mudcracks (Fig. 53D), clay seams, and volume changes in dolostone away from resistant limestone nodules and mud-crack fills, are not unequivocal evidence of pressure-solution because they are more realistically explained by mechanical compaction since these features formed early in the diagenetic history, before complete cementation and sufficient burial for pressure-solution. Neugebauer (1974) observed that pressure-solution in homogeneous chalks occurred only after burial of 300 metres. Burial depths of this order of magnitude for the St. George would indicate that most volume losses, if attributable to pressure-solution, would have occurred after burial by Table Head sediments. This is impossible in the St. George because diagenetic dolomitization occurred before the onset of Table Head sedimentation. Mechanical compaction of unlithified sediment, especially mud and soft peloids, needs much less burial. The inhomogeneous nature of shallow-water carbonate sediments

FIGURE 53

COMPACTION EFFECTS

A. Vertically oriented slab of light-coloured squashed and folded mudstone-filled burrows in dark-coloured dolostone. Burrows were originally vertical Diplocraterion in a lens in lithotope D and suffered pre-dolomitization soft-sediment compaction. Scale in cm; Isthmus Bay Fm.; ECW-75.

B. Vertically oriented thin section photomicrograph of bands of dolomite and clay enclosing a mechanically crushed trilobite fragment. Dolomite in the fracture indicates precipitation after breakage. Suturing along clay-rich stylolite and within dolomitic bands occurred after dolomite precipitation. Scale bar 500 µm; Catoche Fm.; Daniel's Harbour.

C. Thin section photomicrograph of silicified wackestone containing megaquartz-filled burrows surrounded by dark-coloured clay and organic-rich seams, showing that compaction occurred after initial cementation of empty burrows and before silicification. Scale bar 1500 µm; Isthmus Bay Fm.; ECW-86.

D. View slightly oblique to bedding of dolomitized mudcracks that have suffered pre-dolomitization soft-sediment compaction. Lens cap 6 cm across; Aguathuna Fm.; IB-309.

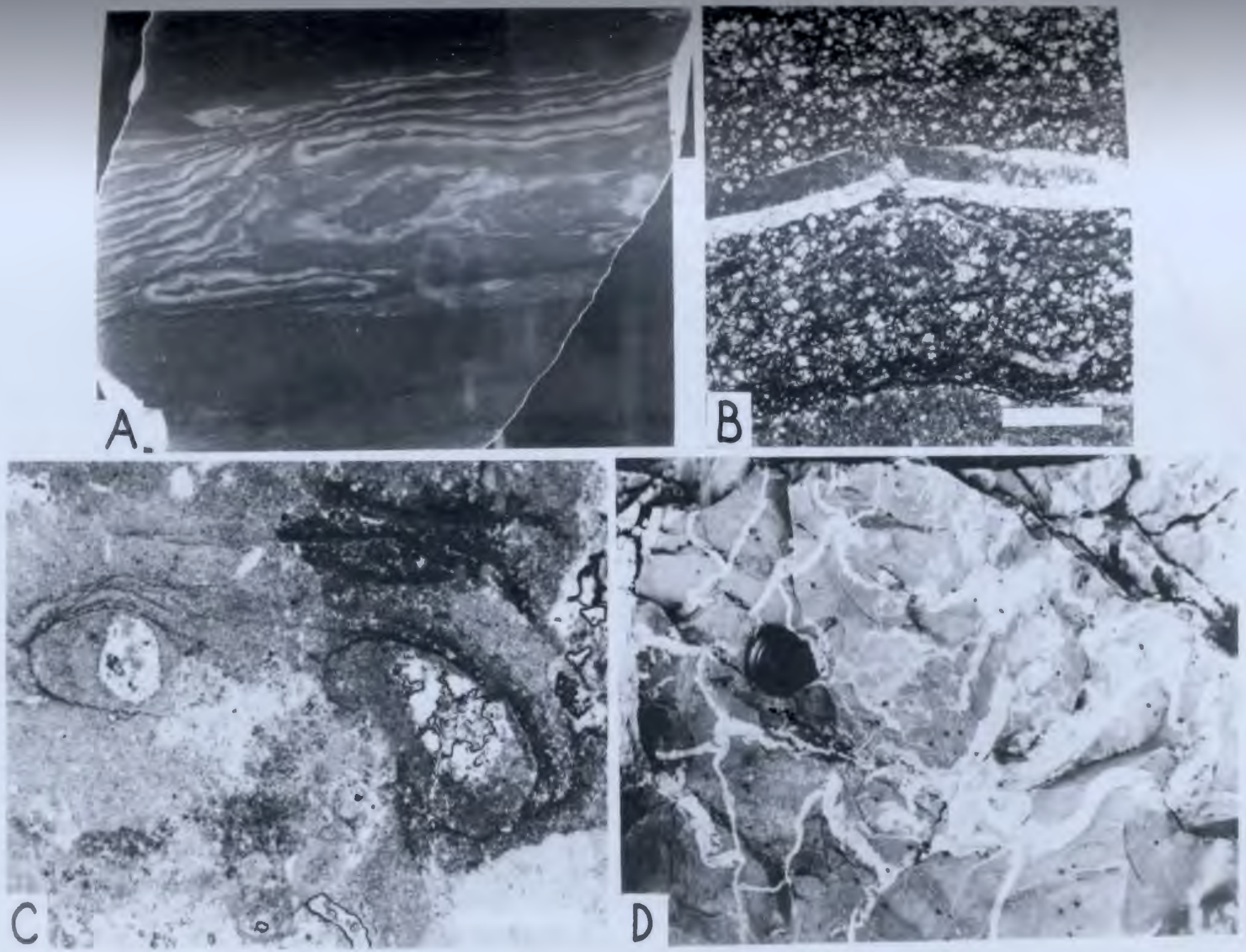
A.
B
C
D

would promote distinct compactional effects under only minimal burial.

Wanless (1979) inferred a causal relationship between dolomite precipitation and volume loss ("non-sutured pressure-solution"), and that they occurred simultaneously. All evidence in the St. George shows that dolomitization occurred after volume loss (by compaction): (1) dolomite precipitated after rupturing of fossils because it embays them and fills the cracks, (2) squashed mudcracked units are completely dolomitized showing that the two processes did not occur together, and (3) clay seam formed before dolomitization because dolomite rhombs overgrow them (as seen in fig. 4 of Wanless, 1979). Any casual relationship is rejected because: (1) dolomite is not found in all clay seams, (2) dolomite bands occur in uncompacted sparites and micrites where no volume loss has occurred, (3) dolomite replaces chert, neomorphic spar, and spar cement, where no compaction has occurred, and (4) dolomite replaced surficial silcrete before subsequent burial.

The mechanism of diagenetic dolomitization is not understood on the basis of petrographic observations alone. Zoning commonly seen in rhombs and size range of crystals suggest precipitation over long periods of time. Kahle (1965) suggested possible roles of clay minerals in dolomitization, and the preference for dolomite to be precipitated on clay seams is evidence for this. Dolomite precipitation in clay-poor limestone might then be due to clay influences in connate waters being felt away from clay-rich sources. Dolostones

are most common in the Isthmus Bay and Aguathuna Formations, possibly because these peritidal rocks were more clay-rich than the subtidal shelf sediments of the Catoche Formation. The greater inhomogeneity of sediment types in the Isthmus Bay and Aguathuna Formations promoted compaction and clay concentration. The model of subsurface dolomitization by a regional epicontinental salinity system as suggested by Harris (1973) for the Lower Paleozoic of eastern North America cannot be substantiated in the St. George. On the other hand, the ubiquity of diagenetic dolomite indicates that connate waters everywhere were able to precipitate dolomite. Preferential dolomite precipitation in primary high-Mg calcite material, such as pelmatozoan ossicles, does not occur, and this criterion suggested by Lohmann and Meyers (1978) and Meyers and Lohmann (1979) does not apply for the St. George.

## Epigenetic dolomite

Description - Epigenetic dolomite occurs as large non-ferroan euhedral to interlocking anhedral crystals, usually greater than 200 microns in diameter. Euhedral rhombs are often zoned with cloudy centres (Fig. 54A), but large interlocking anhedral crystals are clear (Fig. 54B) often with wavy extinction ("baroque" dolomite of Folk and Assereto, 1974) (Fig. 54C). Baroque dolomite fills vugs and is called "white sparry dolomite" when occurring in lithologies called "pseudobreccias". Pore-filling dolomite is occasionally ferroan, for example at Barbace Point. Pseudobreccias are characterized by coarse replacement dolomite with large elongate vugs filled by white sparry dolomite (Figs. 54D, 55A,B). In the Daniel's

Harbour area, 100 metre thick polymictic collapse breccias described by Collins and Smith (1975) grade to collapse-brecciated pseudobreccia, then to psueodbreccia, and finally to normal replaced strata (T. Lane, pers. comm., 1979). Epigenetic dolomite occurs as luminescing (i.e. iron-free) outer zones on diagenetic dolomite rhombs. Preservation of primary structures, such as fossils and ooids, is poor.

Epigenetic dolomitization in the St. George occurs everywhere in western Newfoundland. It is not restricted to the St. George, and underlying Cambrian carbonates as well as the Table Head Group, at its type section at Table Point, are also affected. It occurred after all stages of tectonic fracturing. This is evidenced in thin section because rhombs replace calcite-filled tectonic fractures, and in outcrop, because it is almost always related to earlier structural configurations. Epigenetic dolostones occur as fault-bounded rock bodies, as halos along faults and fractures (Fig. 55C), and as rows of pods several metres in diameter (Fig. 55D), and is always seen to cross-cut primary bedding. Many epigenetic dolostone bodies on the Great Northern Peninsula, including collapse breccias at Daniel's Harbour, are oriented approximately NE/SW and NW/SE, the regional structural lineations.

Epigenetic dolomitization occurred after stylolitization and disrupted the sutures. Collapse breccia clasts have relic stylolites parallel to primary bedding and not to present geopetal directions nor to clast contacts. In scattered pseudobreccias, white sparry dolomite was followed by internal fine-grained dolomite sedimentation, and by large quartz euhedra,

FIGURE 54

EPIGENETIC DOLOMITIZATION

A. Thin section photomicrograph of large cloudy-centred epigenetic dolomite (C) replacing limestone and forming overgrowths on pre-existing diagenetic dolomite (D), producing patches of large and small rhombs. Scale bar 500 µm; Catoche Fm.; PAC-44.

B. Thin section photomicrograph, crossed nicols, of interlocking anhedral epigenetic dolomite mosaic. Scale bar 500 µm; Isthmus Bay Fm.; IB-26.

C. Thin section photomicrograph of cloudy centred replacement dolomite on left passing to cement, on right, of large baroque dolomite showing curved crystal faces. Scale bar 1500 µm; Catoche Fm.; ECW-142.

D. Vertical view of dissolution vug in pseudobreccia, with white sparry dolomite cement and laminated internal dolostone sediment. Lens cap 6 cm across; Isthmus Bay Fm.; BH-37.

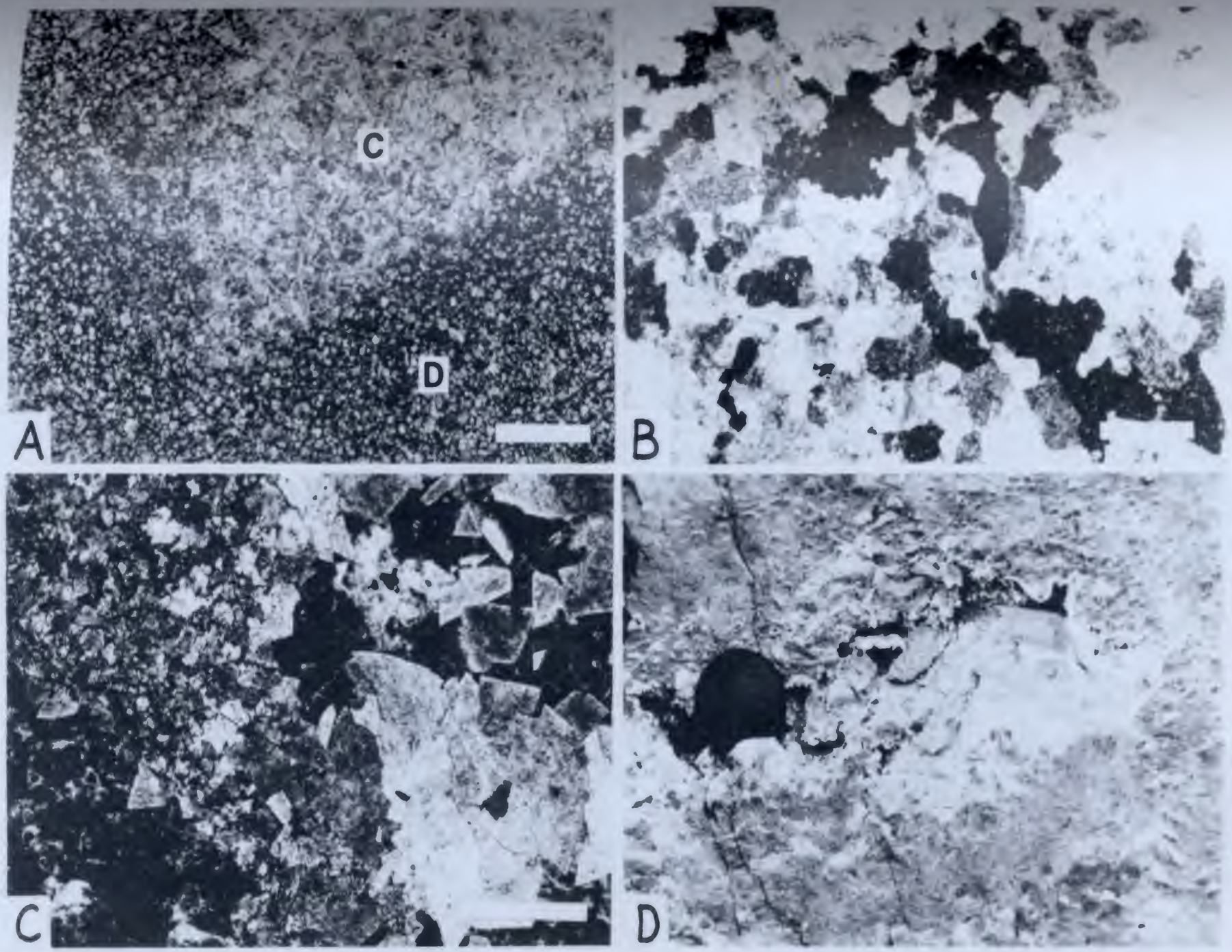
C
D
A
B
C
D

FIGURE 55

EPIGENETIC DOLOMITE

A. Vertically oriented slab of dolostone with small horizontal dissolution vugs filled with white sparry dolomite cement, illustrating the beginning stage of pseudobreccia formation. Scale in cm; Isthmus Bay Fm.; Boat Harbour.

B. Vertically oriented slab of dolostone with pseudobreccia vugs partly filled with white sparry dolomite cement. Scale in cm; Isthmus Bay Fm.; BH-94.

C. Bedding plane view of light-coloured dolostone as a halo along tectonic fracture in limestone. Range pole in 20 cm divisions; Catoche Fm.; PAC-44.

D. Bedding plane view of row of dolostone pods in limestone. Isthmus Bay Fm.; BH-123.

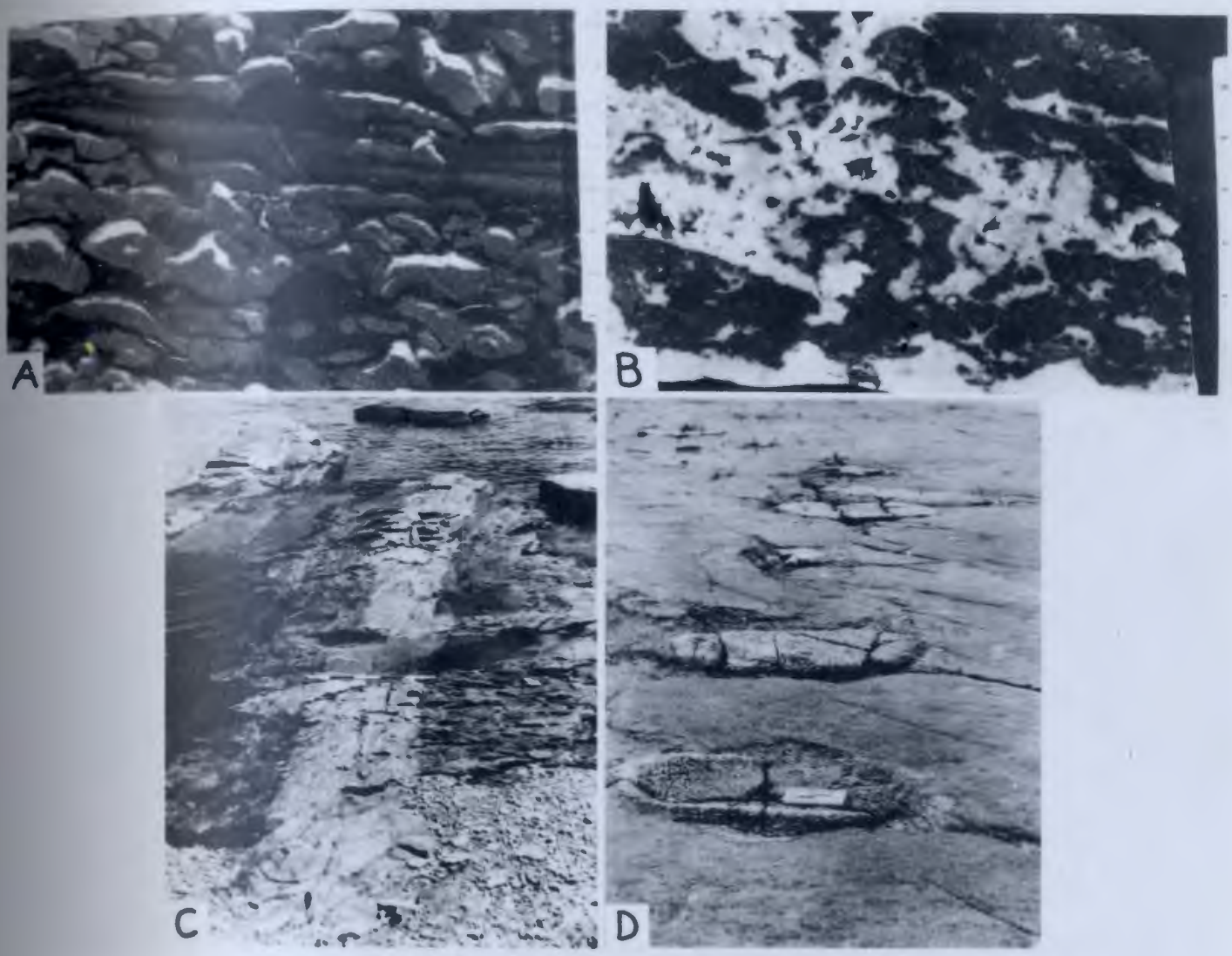
A
B
C
D

up to several centimetres in length. On Port au Port Peninsula, epigenetic dolomitization was followed by calcite spar cement which partially calcitized dolomite rhombs. Sphalerite was a co-precipitate with white sparry dolomite along the St. George-Table Head contact at Daniel's Harbour (Cumming, 1968). Fluorite is a co-precipitate with white sparry dolomite at Daniel's Harbour (T. Lane, pers. comm., 1979) and north of Eddies Cove West. Minor galena occurs in scattered epigenetic dolostones.

Interpretation - Epigenetic dolomitization affected both limestone and diagenetic dolostone in degrees ranging from slight overgrowth on dolomite rhombs to coarsely crystalline pseudobreccia. Replacement often involved considerable dissolution of pre-existing carbonate, and resulted in pseudobreccia and, locally, collapse breccias. The collapse breccias at Daniel's Harbour were attributed by Collins and Smith (1975) to karstification during pre-Table Head exposure of the St. George carbonate shelf. However, the gradation from coarse replacement dolostone to pseudobreccia to brecciated pseudobreccia to collapse breccia does not indicate collapse before pseudobrecciation, as suggested by Collins and Smith (1975), and nor can these features including concomitant dolomitization be explained by normal karst processes as indicated by Collins and Smith (1975). On this basis alone, 100 metres of relief during pre-Table Head exposure determined by Collins and Smith (1975) is rejected. Collapse and internal sedimentation do indicate a strong geopetal influence during dissolution and dolomitization, suggesting fluids were moving rapidly in the

subsurface, rather than as sluggish phreatic pore waters. Whether the hydraulic head was due to a meteoric influence is not known. The absence of geochemical data in this study precludes discussion of the nature of the dolomitizing and mineralizing solutions.

The NW/SE and NE/SW trending structural lineaments of the Great Northern Peninsula are probably due to the Acadian Orogeny which involved regional compression, as opposed to the "thin-skinned" tectonics associated with allochthon emplacement in western Newfoundland during the Taconic Orogeny (Williams and Stevens, 1974). Because epigenetic dolomitization post-dated these tectonic features, it occurred after the Devonian Acadian Orogeny. Dolomitized Table Head Group and disoriented stylolites in collapse breccias support a post-Middle Ordovician age for dolomitization. Localization of the sphalerite ore body and collapse brecciation below the St. George-Table Head unconformity was due to a permeability barrier presented by the contact. It is probable that much or all of western Newfoundland was at one time covered by Middle Paleozoic sediments because it does not seem reasonable to expect that Ordovician sediments and ophiolites that were subaerially exposed in Ordovician times could have survived continual exposure until the present day. Also, Silurian to Mississippian sedimentary rocks are exposed on western Port au Port Peninsula, and crop out on the sea floor to both the west and east of western Newfoundland (Haworth and Sanford, 1976), and it is likely they are the remnants of a onte more continuous cover. Therefore, epigentic dolomitization occurred under an unknown thickness of Middle Paleozoic sediments,

but it is not known whether it occurred during Devonian sedimentation or Mississippian sedimentation. Mississippian evaporitic carbonates on Port au Port Peninsula are not affected by epigenetic dolomitization and may have been the source for dolomitizing and mineralizing brines.

## CHERT

### Introduction

Chert nodules are common in the Isthmus Bay and Aguathuna Formations, and partly silicified limestone occurs throughout. Silicification involved both replacement and cementation, and records the presence of scattered horizons of 'vanished evaporites'. Except for silcrete at the St. George-Table Head contact, post-epigenetic dolomitization quartz euhedra, and spherulitic chalcedony in sphalerite-galena veins, silicification occurred early in the diagenetic history of the St. George. It post-dated formation of authigenic silicates, but occurred before dolomitization and calcite neomorphism which replace chert. Dilation and tectonic fractures in cherts are filled by calcite spar cement. Chert preserves synsedimentary radial bladed calcite cement and initial stages of calcite spar cement that formed during shallow burial (Fig. 56A). Chalcedony fills pores and shell molds before calcite spar cementation. Under an omission surface in the Isthmus Bay Formation, geopetal internal sediment with <u>in situ</u> authigenic K-feldspar overlies and forms inclusions within tips of megaquartz cement (Fig. 56B). A chert pebble lag occurs at a subaerial exposure surface in the upper part of the Isthmus Bay Formation and in the basal

Table Head limestone, indicating relatively early formation under shallow burial.

Cherts are described petrographically, and eight partly intergradational textures are distinguished: cryptoquartz, microquartz, limpid megaquartz, flamboyant megaquartz, lutecite, quartzine, and chalcedony.

## Cryptoquartz

Cryptoquartz is nearly isotropic, tan coloured with minute inclusions in plane light, extremely finely crystalline (less than 4 microns in size), and occurs in stylolites, between dolomite rhombs, and replacing micrite. It is in places gradational with microquartz.

## Microquartz

Microquartz usually occurs as equant anhedral interlocking quartz crystals less than 20 microns in size and replaces micrite (Fig. 56C) and anhydrite laths (Fig. 56D). Slightly elongate microquartz crystals replace concentric ooids, a habit similar to that reported by Choquette (1955). Extinction is often slightly undulose, and gradation to small anhedral megaquartz occurs in interparticle areas. An unusual finely fibrous microquartz with curving length-fast "furry" crystals replaces some concentric ooids (Fig. 56E). Fibres are often parted like hair, and sweep around cortical layers, sometimes becoming tangential to them. Dusty brown inclusions are commonly present and outline precursor fabrics.

Large crystals of calcite replace microquartz by infiltrating, on a minute and petrographically unresolvable scale, between microquartz crystals, causing high birefringence.

FIGURE 56

CHERT

Thin section photomicrographs

A. Megaquartz-replaced radial bladed cement and initial spar cement outlined by inclusions (dark fibres in lower part and dog-toothed terminations, respectively). Scale bar 150 µm; Isthmus Bay Fm.; ECW-86.

B. Megaquartz cement rim overlain by internal sediment, followed by calcite spar cement, in sub-omission surface vugs in cryptoquartz-replaced and partly dolomitized mudstone. Crossed nicols; scale bar 1500 µm; Isthmus Bay Fm.; IB-108.

C. Dark micro- and small megaquartz-replaced radial ooid. Crossed nicols; scale bar 150 µm; Isthmus Bay Fm.; BH-115.

D. Microquartz-replaced felted anhydrite laths with a horizontal fabric, outlined by inclusions. Up is to the right. Scale bar 100 µm; Aguathuna Fm.; Table Point.

E. Ooid cortex replaced by "furry" microquartz. Scale bar 30 µm; Isthmus Bay Fm.; BH-7.

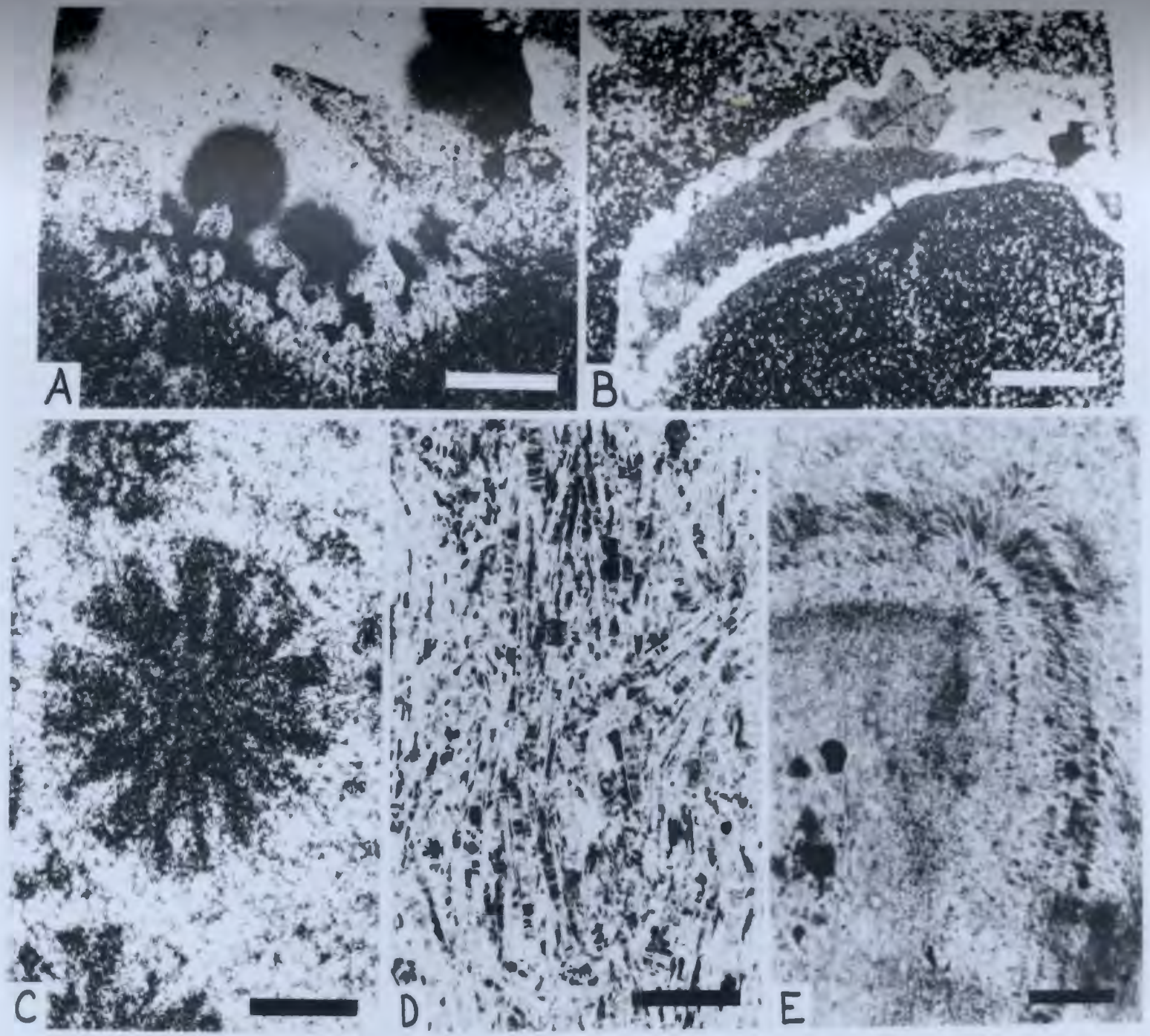
A
B
C
D
E

When the calcite, which does not stain with alizarin red-S, is extinct, microquartz relics are discernible.

Small anhedral megaquartz crystals 30 to 60 microns in diameter with abundant micrite-sized calcite inclusions occur as patches within microquartz. The inclusions are not related to quartz crystal boundaries, and cannot be attributed to incipient calcite replacement.

Limpid Megaquartz

Limpid megaquartz ranges in size from 20 microns to 3000 microns and is anhedral to euhedral, sometimes occurring as elongate terminated euhedra when lining voids. Dusty brown inclusions often outline growth bands of crystal faces (Fig. 57A). Wavy extincion often occurs, especially when crystals are syntaxial on chalcedony and microquartz, and when there is an intergrowth of subcrystals similar to and sometimes grading to flamboyant megaquartz considered below (Fig. 57B). Towards the narrow confines of some voids, euhedral crystals change imperceptibly to smaller elongate crystals with wavy extinction, and finally to coarse quartzine crystals, with growth banding changing similarly from outlining pyramidal terminations to botryoidal.

In silicified grainstones, megaquartz replaces synsedimentary radial bladed and initial calcite spar cements, and fills remaining interparticle pores and other cavities as a cement. Megaquartz replaces anhydrite laths, averaging 30 by 500 microns in size, scattered in a subaerial rubble in the Aguathuna Formation. In cherts, megaquartz fills fractures both after and during microquartz replacement of carbonate. In the former, fracture

boundaries are sharp, and in the latter, boundaries are ragged, do not match, and microquartz grades in size with megaquartz.

Flamboyant megaquartz

Flamboyant megaquartz occurs as masses of large elongate anhedral megaquartz crystals, up to several millimetres in length, that commonly have a coarse radiating habit (Fig. 57C). Crystals interlock forming a patchwork, but crystal boundaries are diffuse and gradation occurs to megaquartz with wavy extiction caused by subcryatal orientations. Small tabular inclusions that are often anhydrite are common.

Flamboyant megaquartz replaces micrite, shell material, and anhydrite. In replaced anhydrite, dusty brown inclusions outline presursor felted anhydrite laths, the number of anhydrite inclusions tends to be greater, they are aligned parallel to the primary alignment of the laths, and quartz crystals tend to be more elongate in the direction of the primary lath alignment.

Lutecite

Lutecite is coarsely fibrous quartz where the slow ray is situated 30° from the c-axis, and commonly shows a chevron extinction pattern. It is rare in the St. George, replacing bioclasts, especially pelmatozoan ossicles and brachipods. It intergrades with megaquartz with wavy extinction.

Quartzine

Quartzine is length-slow, coarsely fibrous quartz or chalcedony. It is not common in the St. George, and is difficult to distinguish from small narrow elongate megaquartz crystals. It occurs as an equant fringing rim replacing

FIGURE 57

CHERT

Photomicrographs, crossed nicols

A. Megaquartz cement with inclusions outlining successive prismatic crystal terminations. Scale bar 300 μm; Isthmus Bay Fm.; IB-39.

B. Large megaquartz crystals containing anhydrite inclusions and becoming flamboyant (fibrous) at the edges. Scale bar 500 μm; Isthmus Bay Fm.; BH-124.

C. Flamboyant megaquartz replacing micrite. Scale bar 500 μm; Aguathuna Fm.; IB-317.

D. Megaquartz becoming fibrous quartzine in the narrowest part of interparticle pore. Scale bar 100 μm; Isthmus Bay Fm.; BH-26.

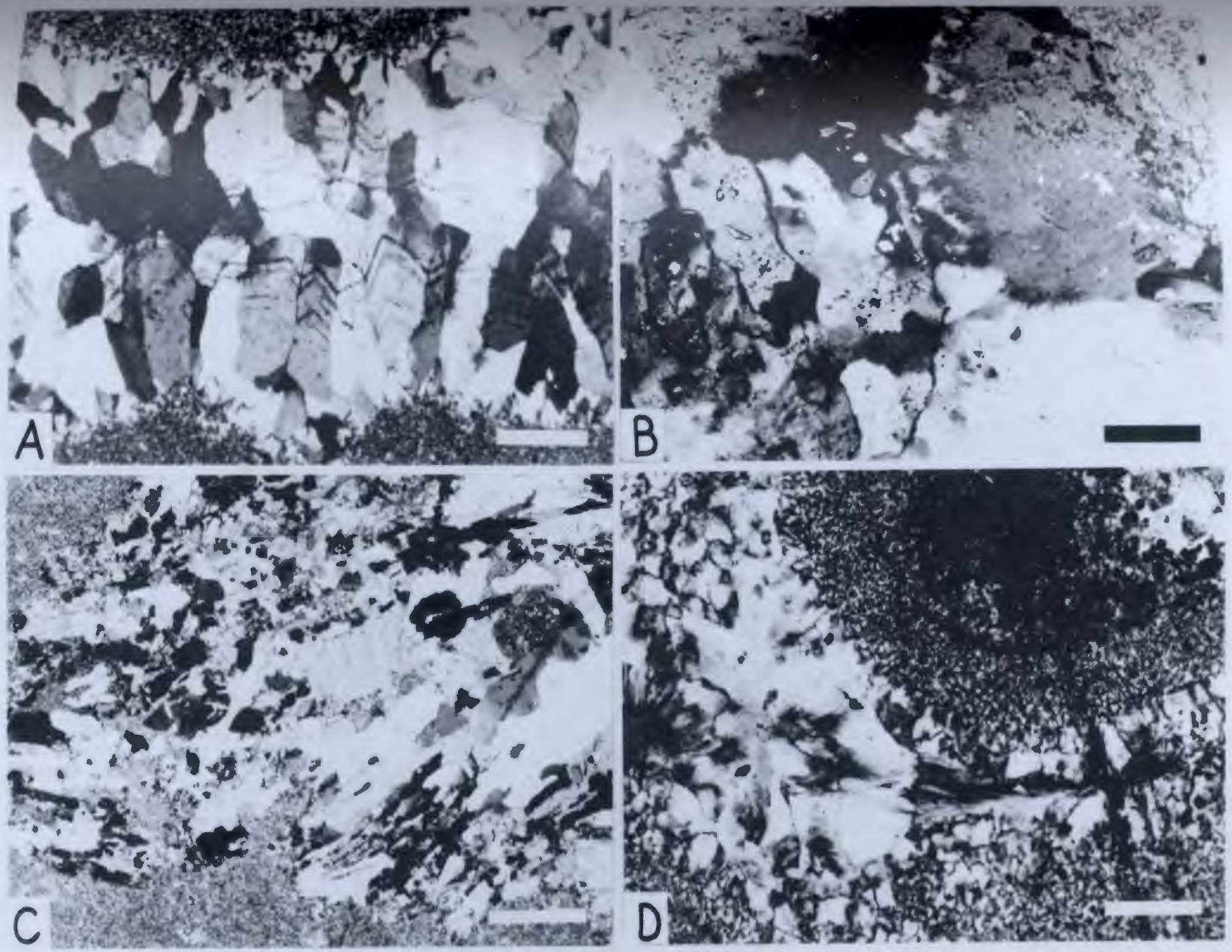
A
B
C
D

synsedimentary radial bladed calcite cement in oolitic grainstones, and replacing the margins of otherwise microquartz-replaced anhydrite layers in the Aguathuna Formation. Palisades of quartzine have been observed replacing trilobite fragments with the same crystal orientation as the primary calcite microstructure (Fig. 58A), but other fragments in the same section are replaced by lutecite. Botryoidal fans of finely fibrous quartzine occur rarely as a cement on top of megaquartz euhedra. One example was observed where quartzine and chalcedony were pore-filling cements in neighbouring pores. Megaquartz with wavy extinction replacing calcite spar cement sometimes passes laterally to finely fibrous curving quartzine (Fig. 57D). Quartzine spherulites have been found twice, replacing anhydrite and calcite spar cement in sphalerite-galena veins (Fig. 58B).

## Chalcedony

Chalcedony is length-fast quartz, that ranges from finely to somewhat coarsely fibrous (Fig. 58C). It occurs as a layered botryoidal pore-filling cement, often brown with dusty inclusions. It fills pores after initial microquartz replacement of allochems and small megaquartz replacement of radial bladed calcite cement in silicified grainstones. It fills gastropod shell molds before initial calcite spar cementation, and the crescent-shaped pores of half-moon ooids. When it occurs, not every pore contains it, but when pores are not completely filled, it is followed by megaquartz. Zebraic chalcedony is characterized by fibre optic axes that twist about the c-axes, but is rare in the St. George, seen once

FIGURE 58

CHERT

Photomicrographs, crossed nicols

A. Palisade of quartzine replacing trilobite fragment. Scale bar 150 µm; Catoche Fm.; ECW-135.

B. Spherulitic quartzine replacing anhydrite. Scale bar 150 µm; Aguathuna Fm.; Table Point.

C. Coarsely fibrous banded chalcedony cement, followed by megaquartz cement. Scale bar 300 µm; Isthmus Bay Fm.; IB-19.

D. Zebraic chalcedony cement. Scale bar 300 µm; Isthmus Bay Fm.; IB-19.

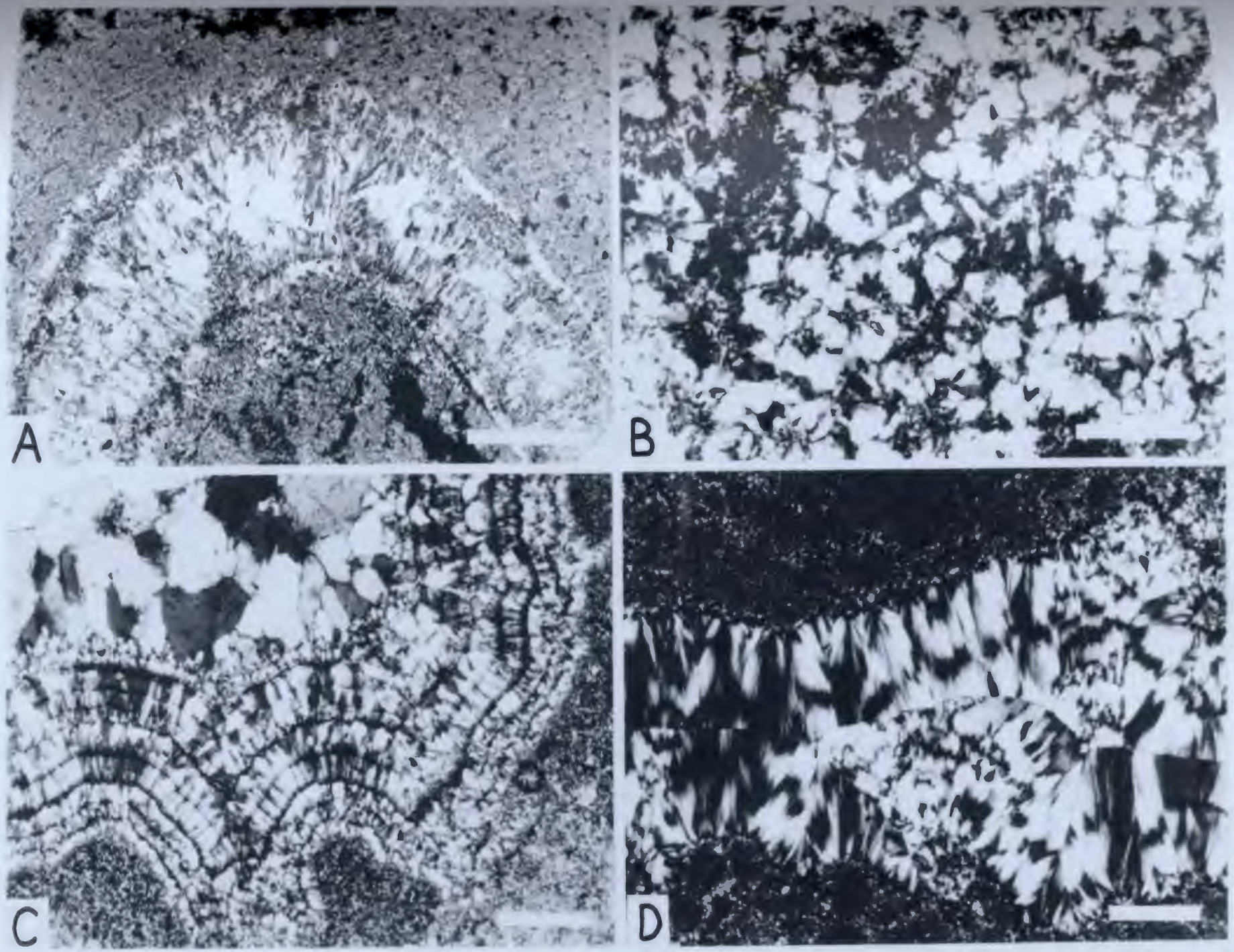
A
B
C
D

as a crust on euhedral megaquartz (Fig. 58D). The deepness of colour banding in chalcedony is variable within the same sample. Chalcedony is normally preferentially replaced by large calcite crystals.

## Discussion

Cryptoquartz replaced fine-grained micrite and is also a styloreactate. Microquartz always replaced micritic calcite and anhydrite, never dolomite. Poor or incomplete replacement resulted in small megaquartz containing micritic calcite inclusions. Limpid megaquartz is both a replacement of calcite and anhydrite, and a cement. Chalcedony is always a cement, the variable colour banding suggesting a local source for impurities. Quartzine and lutecite intergrade with megaquartz with wavy extinction, and replace calcite and, rarely, anhydrite. Finely crystalline quartzine occurs rarely as a cement. Flamboyant megaquartz replaced calcite and anhydrite. The texture of the various replacement quartz types reflects in part the primary nature of the precursor calcite and anhydrite. It may also be related to permeability during silicification, concentration of silicifying solutions, and other unknown factors. Furry microquartz replacing ooid cortices probably developed by elongation of shorter fibres that were replacing finely radial aticular calcite crystals in cortical layers. Bending of the 'fur' was probably caused by spatial competition during growth.

Folk and Pittman (1971) suggested that chalcedony would precipitate rapidly from solutions with a high silica concentration, whereas megaquartz cement would precipitate slowly

from solutions somewhat depleted in dissolved silica. This explanation would indicate that spatial competition during growth would control the elongation of quartz crystals, fibrous being the habit in highly competetive situations due to rapid nucleation and growth, and why chalcedony is followed by megaquartz cement. This would also explain why: (1) chalcedony fibres range from extremely fine needles to coarse blades, (2) large megaquartz crystals grade to narrow megaquartz blades to almost quartzine in small confines of fenestrae, (3) megaquartz changes to quartzine in small parts of interparticle pores, (4) pore-filling quartzine occurs only on megaquartz euhedra, and (5) megaquartz can be flamboyant. Folk and Pittman (1971) pointed out that the differences between quartzine and narrow megaquartz is distinct, but this was not found to be so in this study. It is suggested here that the variability of optic and c-axes and fibrosity relate more to the orientation of calcite and anhydrite precursor fabrics, syntaxial relationships with quartz growth substrates, and competetive crystal growth, than any other particular consistent and diagnostic factor (such as vanished evaporites).

No consistent relationship, as suggested by Folk and Pittman (1971), between silicified evaporites and quartzine was found in the St. George. Indeed, replacement of anhydrite by quartzine palisades and spherulites was observed only once each. Other anhydrite was replaced by microquartz, flamboyant megaquartz, and limpid megaquartz, probably related to the packing density and orientation of the precursor anhydrite laths. The so-called "evaporite syndrome" outlined by Milliken (1979)

does not apply to vanished evaporites in the St. George. The common trait shared by some silicified anhydrite nodules in the St. George and those described by Chowns and Elkins (1974), Siedlecka (1976) and Milliken (1979) is flamboyant megaquartz containing anhydrite inclusions and relic dusty brown inclustions outlining precursor laths. Probable anhydrite inclusions were found also in flamboyant megaquartz replacing calcite. Folk and Pittman (1971) suggested that groundwaters charged with evaporite "effluent" moving in the subsurface could cause quartzine precipitation. This seems unlikely because of the early shallow-burial time of formation of chert, though this may have occurred immediately below the scattered evaporitic horizons that did develop, and below possible slightly hypersaline horizons that may have developed but have left no record. In any case, length slow quartzine is not a reliable indicator of known evaporites in the St. George, and therefore is insufficient evidence of vanished evaporites.

The source for silica cannot be determined. Siliceous sponges were common beginning in the upper part of the Isthmus Bay Formation, and leaching of spicules may have been a source for some chert. Clays in nearshore sediments may have contributed silica. Volcanic tephra is cited later as a possible source for pre-silicification authigenic silicates, and may also have supplied silica for chertification. A biogeneic source from microfossils that have left no other record is also a possibility but cannot be proven.

# AUTHIGENIC SILICATES

## Description

Authigenic feldspars and quartz are common in the St. George, the former more abundantly. Authigenic quartz is recognized by its euhedral, hexagonal in cross-section, doubly terminated, elongate prismatic habit and abundant calcite inclusions concentrated in the centres (Fig. 59A). Crystals range in width from 20 to 200 microns, and in length from 80 to 700 microns. They have no preferred orientation but are well-sorted in that the crystal size is consistent within samples. Detrital cores are not seen petrographically. Authigenic feldspars are euhedral, free from large inclusions, and range in size from 40 to 100 microns (Fig. 59B). Many are zoned, and twinning is common. Orthoclase was recognized by Carlsbad twinning; albite was recognized by polysynthetic twinning; rare crystals of microcline were recognized by cross-hatched twinning (Fig. 59C). The majority of crystals were untwinned and the type of feldspar could not be resolved.

Authigenic feldspar is found abundantly at the base of the Isthmus Bay Formation. Cursory inspection shows it to be present in underlying Cambrian carbonates and overlying Table Head limestones. Authigenic quartz has only been identified in a few units from the lower part of the Isthmus Bay Formation, in rocks of all facies. Authigenic silicates are found in micritic parts of limestones and never in cement. Both can co-exist in the same sample. They are embayed by neomorphic spar and dolomite, are collected by stylolites, and are preserved in chert.

FIGURE 59

AUTHIGENIC SILICATES

Thin section photomicrographs, crossed nicols

A. Large authigenic quartz prism with inclusions in centre. Scale bar 150 µm; Isthmus Bay Fm.; ECW-13.

B. Authigenic feldspars concentrated in stylolite. Scale bar 100 µm; Isthmus Bay Fm.; Port au Choix.

C. Authigenic euhedral microcline with cross-hatched twinning. Scale bar 50 µm; Aguathuna Fm.; NE Gravels.

A

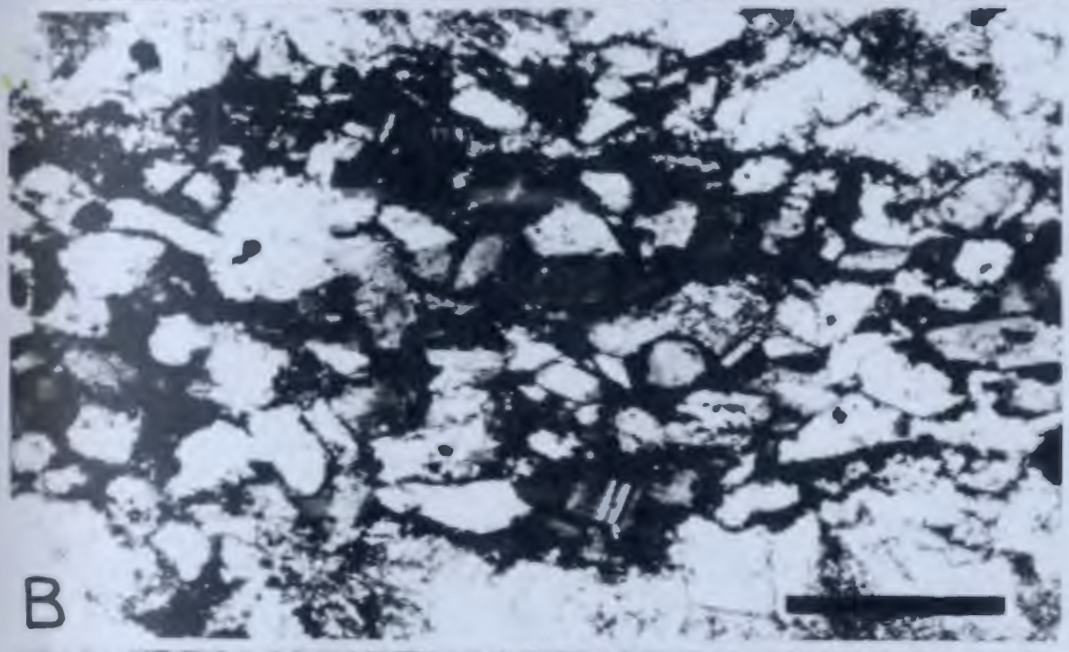
B

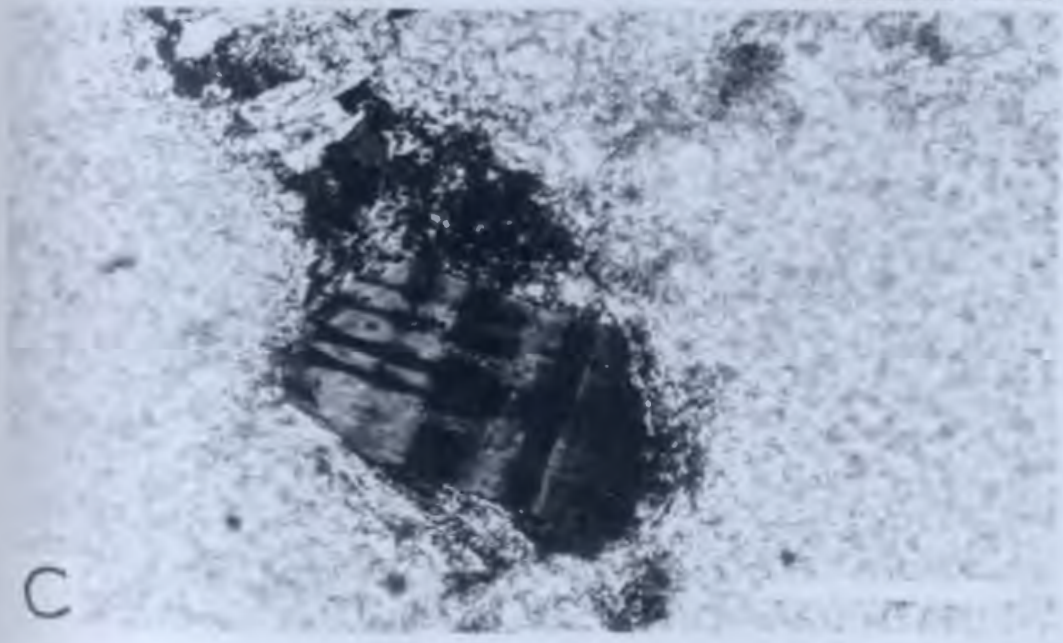
C

## Interpretation

The presence of zoning, calcite inclusions and euhedral shape indicate that these silicates formed *in situ*. The inclusions in authigenic quartz indicate that it formed by replacement of calcite. Feldspar is largely free of inclusions and it is not known whether it replaced calcite or pushed it aside. Kastner (1971), among others, noted carbonate inclusions, suggesting replacement.

The origin of authigenic silicates is still in doubt. Richter (1971) and Schneider (1973) discounted the influence of elevated salinity in the formation of authigenic quartz in Devonian reef complexes. Schneider (1973) suggested a source in groundwaters from nearby landmasses. Richter (1971) suggested that volcanic tephra in the sediment may have been a silica source, but did describe authigenic quartz from evaporite-bearing Triassic rocks where both salinity and volcanism might have been factors. In the St. George, authigenic quartz formed early, before chertification, and therefore required a local source for silica that was remobilized but reprecipitated quickly. Sponge spicules probably did not supply the necessary silica because the earliest ones occur long after the earliest euhedra. Another perhaps planktonic biogenic source would seemingly have resulted in more numerous occurrences. Elevated salinity in pore waters may have played a geochemical role, but this cannot be evaluated as extreme salinity is not indicated by the rocks, and slight hypersalinity cannot be substantiated.

Authigenic feldspars have received more attention with

regard to source (eg.: Baskin, 1956; Swett, 1968; Kastner, 1971; Füchtbauer, 1974; Richter, 1974; Buyce and Friedman, 1975; Kastner and Siever, 1979), and volcanic tephra, detrital feldspar, and illite have all been cited as possible sources. Because detrital cores were not recognized in the St. George, and the great distance from crystalline land (inferred from paleogeography), the only possible detrital source would have been airborn dust. Suchecki et al. (1977) noted a change in clay mineralogy in Lower Ordovician units of the Cow Head Group that could be accounted for by input of detritus coming from volcanic island arcs that developed at that time to the east (Stevens, 1970). The clay mineralogy of the St. George was not investigated in this study, but a volcanic tephra origin is favoured by the rapidity of formation of authigenic feldspar because of the high solubility of glasses. Braun and Friedman (1969) and Mazzullo (1976) suggested that hypersalinity was geochemically important in authigenic feldspar formation. Hypersalinity of subsurface waters could have developed beneath horizons of evaporites. Hypersaline brines are found at least 12 metres below sea level in sediments of the Persian Gulf sabkhas (deGroot, 1973), and scattered similar evaporitic horizons are present in the St. George. However, because authigenic feldspar formed very early during burial, and the ubiquity of its occurrence, even far below any known evaporitic horizons, a hypersaline pore water chemistry is ruled out as more than a possible local factor. Evidence presented by Mazzullo (1976) that cryptalgal laminites studied by him were necessarily deposited in hypersaline conditions is considered

insufficient here. No distinct difference in abundance of authigenic feldspar was seen between cryptalgal laminites and fully marine subtidal limestones of the St. George.

## CRUSTIFICATION

### Description

Colloform sphalerite-galena veins occur in limestones of the St. George at the section northwest of the Gravels, Port au Port Peninsula. Similar veins cutting Upper Mississippian limestones of Port au Port Peninsula were described by Watson(1943). Veins are sinuous, have no preferred orientation, may be crusts between bedding planes, and cross-cut calcite veins of tectonic origin. The margins of the veins erode the host limestone, leaving calcite veins standing out in relief. Five stages of vein-filling occur (Fig. 60):

(1) a first stage of white banded radial columnar calcite crystals (terminology of Kendall and Broughton, 1978) with mostly non-planar crystal boundaries, undulose extinction, curved twins, and minute bands of inclusions outlining successive toothed crystal termination.

(2) a thin and patchily distributed internal sediment that is green coloured, altered to slightly ferroan coarse microspar and finely crystalline pseudospar, and contains scattered 15 micron-sized limpid dolomite euhedra. Replacing parts of the neomorphic spar is spherulitic quartzine; spherules are 60 microns in diameter.

(3) a colloform crust of banded sphalerite containing large cubes of galena up to several millimetres in size.

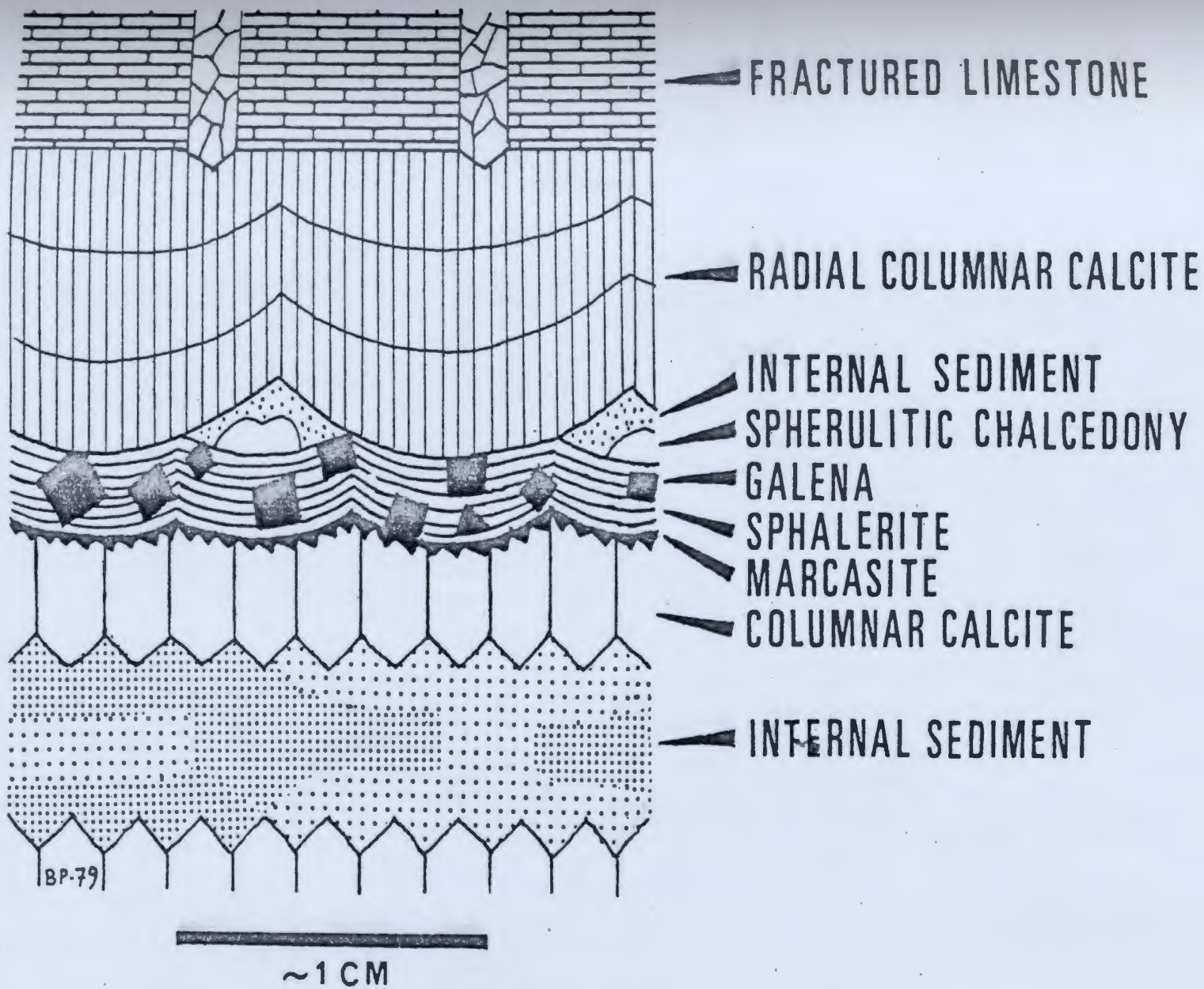


Figure 60: Simplified sketch of components in colloform Pb-Zn veins in St. George limestones, Port au Port Peninsula.

(4) a patchy rind of marcasite

(5) an equant rim of coarse columnar calcite spar

(6) a green and brown colour-banded internal sediment composed of microspar, and containing scattered silt-sized quartz grains and dolomite euhedra.

## Interpretation

The mineralization of the open spaces occurred after the Upper Mississippian Codroy Group limestones were deposited since these are also affected. A phase of dissolution preceeding crustification is indicated by the relief of calcite-filled tectonic fractures; this may be associated with post-Middle Ordovician karstification of the Paleozoic carbonates on Port au Port Peninsula. The first stage in crustification was calcite spar similar because of minute inclusions, curved twins, and non-planar crystal boundaries to speleothem fabrics described by Kendall and Broughton (1978), and similarly interpreted to be primary, rather than replacement of precursor acicular calcite. Bent twins probably were caused by competetive crystal growth. The mineralizing solutions were not acidic because there was no corrosion of the terminated calcite crystals. Quartzine replacement of neomorphic spar after internal micritic sediment was not recognized in the veins described by Watson (1943), and took place after precipitation of colloform sphalerite and galena. The equant calcite cement precipitated on top of the metallic crust suggests phreatic conditions. Banded internal sediments suggest a near-surface origin, the quartz silt possibly originated in the Upper Mississippian sandstones that overly the carbonates of the

Codroy Group. Stratigraphic relationships on Port au Port Peninsula indicate that burial of the Lower Ordovician carbonates by Mississippian rocks must have been less than a hundred metres.

Watson (1943) implied that the source of the mineralizing fluids was igneous, and that they ascended from considerable depths. It appears more likely that they were meteoric in origin on the basis of internal sediments and lack of evidence for igneous activity in western Newfoundland in post-Upper Mississippian time. It seems likely that the high concentration of metals needed to precipitate the crust relatively close to the surface required a localized source enriched in metals. It is suggested here that Pb and Zn were scavenged by meteoric waters from Mississippi Valley type deposits in underlying and neighbouring Lower Paleozoic epigenetic dolostones, that are no longer exposed because of later erosion. If these veins are truly remobilized Mississippi Valley type deposits, then the possibility exists that there are further deposits on Port au Port Peninsula.

## PARAGENESIS

Based on cross-cutting relationships, the sequence of diagenetic events that were involved in the lithogenesis of the St. George can be outlined. Resolution is hindered in some cases, such as the timing of formation of authigenic silicates relative to the formation of botryoidal neomorphic spar, because these two events never cross-cut each other. In the paragenetic sequence (Fig. 61.), silcrete development

## Paragenesis

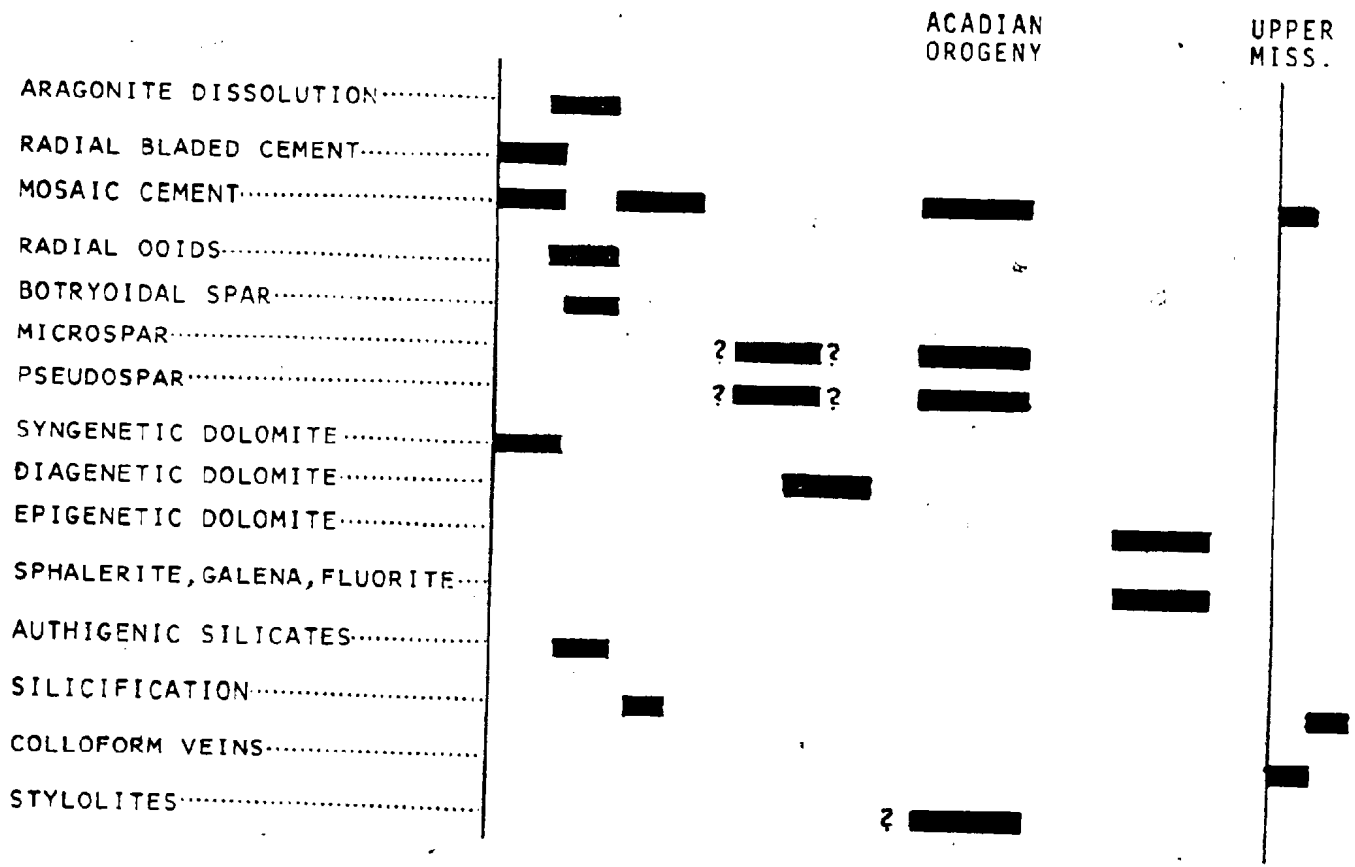


Figure 61: Paragenetic sequence of diagenetic events involved in the lithogenesis of the St. George.

on the St. George-Table Head contact is not entered; the various stages involved in the sphalerite-galena veins on Port au Port Peninsula are considered together.

# CHAPTER 5 - ST. GEORGE-TABLE HEAD CONTACT

## INTRODUCTION

The Lower Ordovician-Middle Ordovician boundary is represented by a time break everywhere in the Appalachians of eastern North America (Twenhofel et al., 1954); this contact is also commonly a disconformity (Rodgers, 1969). The break is present between the St. George and Table Head Groups of western Newfoundland and was first recognized by Schuchert and Dunbar (1934), at Table Point. The hiatus is represented by a polymictic debris flow, Bed 14, in the Cow Head Group of western Newfoundland (Fåhraeus and Nowlan, 1978). Zinc mineralization is located under the contact at Daniel's Harbour. Cumming (1968) and Collins and Smith (1975) have suggested that the contact was a karst surface with as much as 100 metres of relief. Nevertheless, Fåhraeus (1977, his fig. 1) has implied that the St. George and Table Head Groups were facies equivalents of each other, with no break between them.

This contact and the character of the basal Table Head sediments were examined to determine the real nature of the break, at the Table Head type section at Table Point, Port au Choix, Aguathuna, and both northwest and northeast of the Gravels.

## TABLE POINT

Description - The contact is located at the water's edge at the point where sea cliffs increase appreciably in height with the lithological change from dolostone to limestone. The

contact was placed by Schuchert and Dunbar (1934) at the base of the first limestone bed. However, the change from dolostone to limestone is not sharp, and it is obscured by facies changes in the basal Table Head over the 50 metres of exposure (Fig. 62).

Beneath the first limestone bed is a mudcracked cryptalgal laminated bed that buckles seaward to form a small dome several metres wide and 0.4 metre high. Beds below and above the dome are not affected by buckling. This bed is overlain by nodular burrowed limy dolostone, 0.1 to 0.3 metre thick, that contains fossils including the trilobite Bathyurus (identified by R.A. Fortey, [pers. comm., 1978] that is Middle Ordovician in age [Ross, 1970]). Vertical to slightly oblique U-shaped burrows (Diplocraterion) penetrate the flank of the dome and the depression to one side (Figs. 63A,B,C). Chondrites burrow systems reworked the Diplocraterion burrow openings and the top several centimetres of the buckled bed. Overlying the burrowed dolostone unit is fenestral cryptalgal laminite up to 0.1 metre thick. The lower boundary is indistinct as the dolomite content gradually decreases upwards. The upper boundary has been eroded (Fig. 63D), in places completely, during deposition of the overlying unit, linear channel-like pods of black nodular limestone with dolomitic seams that change abruptly laterally to light-coloured burrowed mudstone, totalling 1 metre in thickness (Figs. 63 E, F). Nodules are bioclastic packstone and grainstone (containing fragments of pelmatozoans, brachiopods, bryozoans, ostracodes, gastropods, calcareous algae, and sponges) and dolomitic bands are peloidal mudstone. Succeeding this are thinly bedded grain-

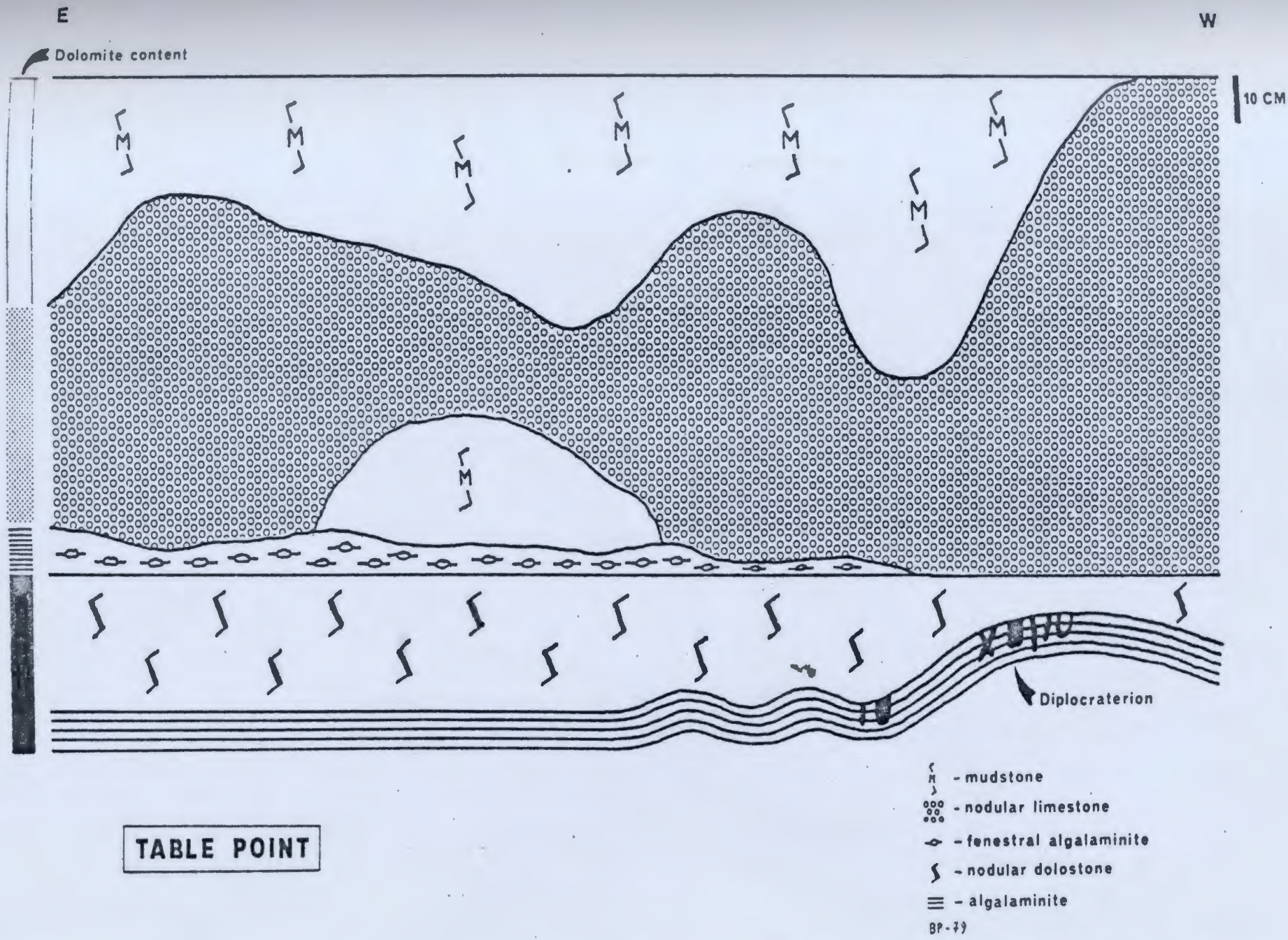


Figure 62: Simplified outcrop sketch of the St. George-Table Head contact exposed at Table Point; The contact is placed lithologically above the burrowed dolostone unit. 50 m of lateral exposure is represented.

FIGURE 63

ST. GEORGE-TABLE HEAD CONTACT, TABLE POINT

A. Gently east-dipping flank of dome of light-coloured dolostone bed penetrated by vertical burrows from overlying dark-coloured Middle Ordovician dolostone, below the St. George-Table Head lithological boundary. Barnacles (white spots) about 1 cm across; Aguathuna Fm.

B. Vertically oriented slab of dome surface with vertical Diplocraterion and Chondrites burrows. The latter are diffuse but many appear as black dots and short bars at the top of the light-coloured dolostone. Scale in cm.

C. View slightly oblique to flank of dome, at its base, of Diplocraterion burrows of varying size (seen as short bars, some dumb-bell-shaped), and branching Chondrites burrows. Edge of tin-opener is 1.8 cm long.

D. Burrowed contact between dark-coloured, basal Table Head nodular limestone and underlying light-coloured Middle Ordovician burrowed dolostone of Aguathuna Fm. Scale in cm.

E. Bedding plane view of channel-shaped pod, 1.5 m wide and at least 20 m long, of dark-coloured nodular limestone. Basal Table Head Group.

F. Vertical view of oblique margin of dark-coloured nodular limestone pod and light-coloured mudstone. Notebook is resting on nodular limestone.

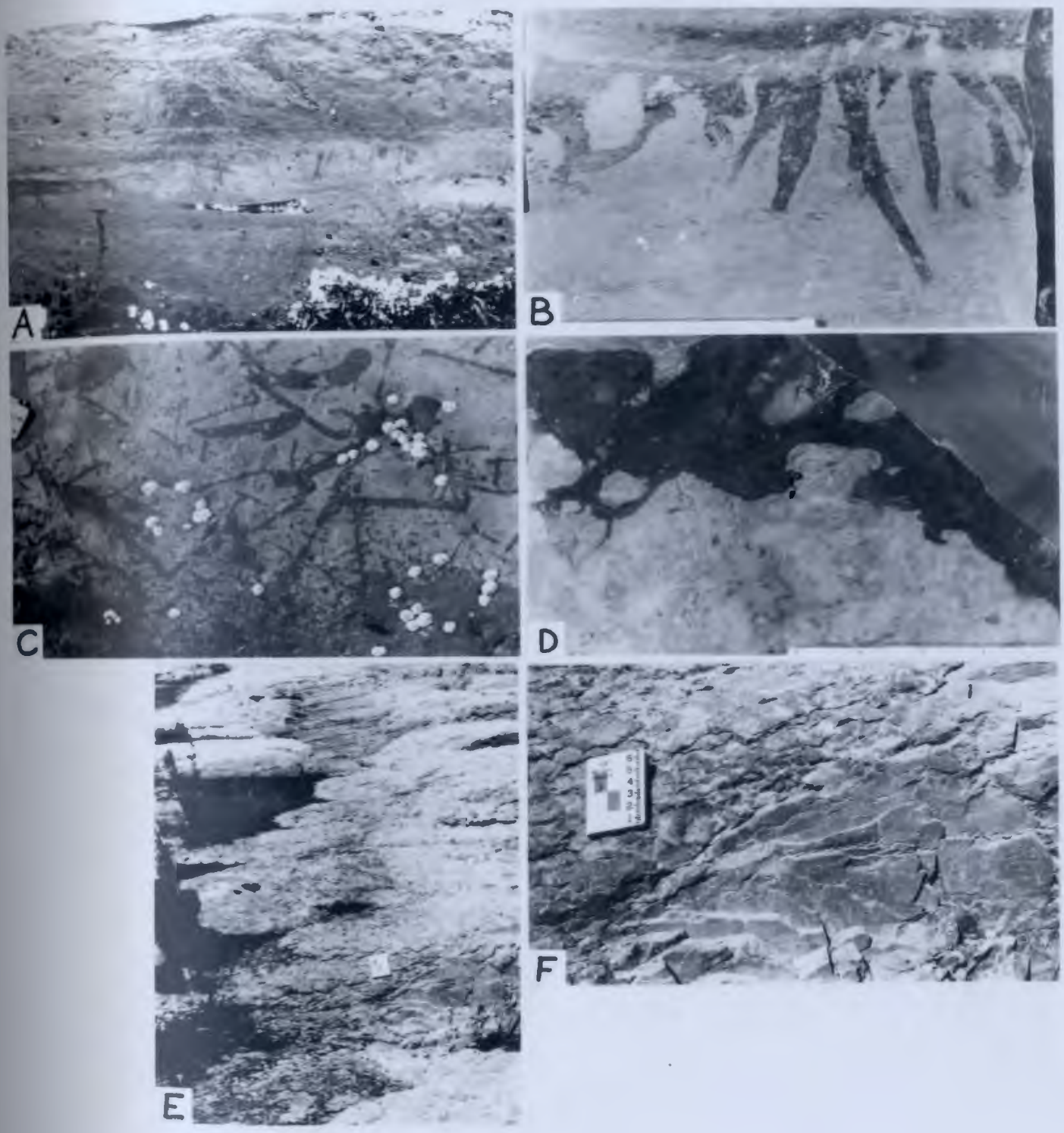
A
B
C
D
E
F

stone, dolostone, and bioturbated mudstone, and the massive dark-coloured mudstone and wackestone of 'typical' Table Head lithology.

Interpretation - The real sedimentary break is the undulating dolostone bed, below the diffuse limestone-dolostone contact. Dolomite is here a secondary diagenetic mineral and is insufficient to separate formations.

The vertical burrows penetrating the St. George are not borings, and indicate that the buckled bed was not lithified, or only so in patches. Lack of compaction around the burrows indicates that the upper surface may have been consolidated, possibly with a chalky texture. The dome is not of tectonic origin because beds above and below are unaffected, and it is interpreted to be a surficial tepee-like structure that developed during subaerial exposure of the cryptalgal laminated sediment. There is no downcutting, indicating that erosion of the St. George was nil at Table Point.

The basal Table Head dolostone is interpreted to have been deposited in the low intertidal zone on the basis of the burrow types. Overlying fenestral cryptalgal laminites were likely deposited in a frequently wetted protected intertidal area. The laterally interfingering pods of dark- and light-coloured limestone indicate a change to considerable sediment accretion and bioturbation. The nodular fabric is a compaction effect on originally interbedded fossiliferous grainstone and packstone and peloidal mudstone. The shape of the pods and the bioclastic and interbedded nature of the dark-coloured limestone suggest that the pods were channels that received

episodic influx of fully marine sediment, developed on a bioturbated intertidal flat. The interfingering indicates that the tidal flat accreted with much lateral shifting of the channels. This was succeeded by thinly bedded tidal flat sediments and subtidal shelf limestones more typical of the remainder of the Table Head.

## AGUATHUNA

Description - The St. George-Table Head unconformity is well-exposed in the quarry 2 kilometres from Aguathuna village. Total relief of the surface has been previously reported to be 10 metres (Cumming, 1968), though much less is apparent now, presumably due to quarrying operations. On the east side of the quarry, the unconformity descends 4 metres into the St. George forming a channel-shaped depression about 50 metres wide. The western flank of the channel rises gradually, with two steps over a distance of about 125 metres from the channel centre (Fig. 64). Table Head sedimentation began in the depression, as a fenestral cryptalgal laminite up to 0.8 metre thick, containing lithoclasts of St. George dolostone and chert. This is overlain with a burrowed and eroded contact by bioturbated light-coloured mudstone that contains ostracodes and is up to 0.7 metre thick in the depression centre. In the deepest part of the depression is a 1 metre wide lens of cross-laminated grainstone containing peloids, ostracodes, and dolostone fragments: the current direction is approximately to the northwest. The light-coloured mudstone is overlain by a unit of dark-coloured nodular lime-

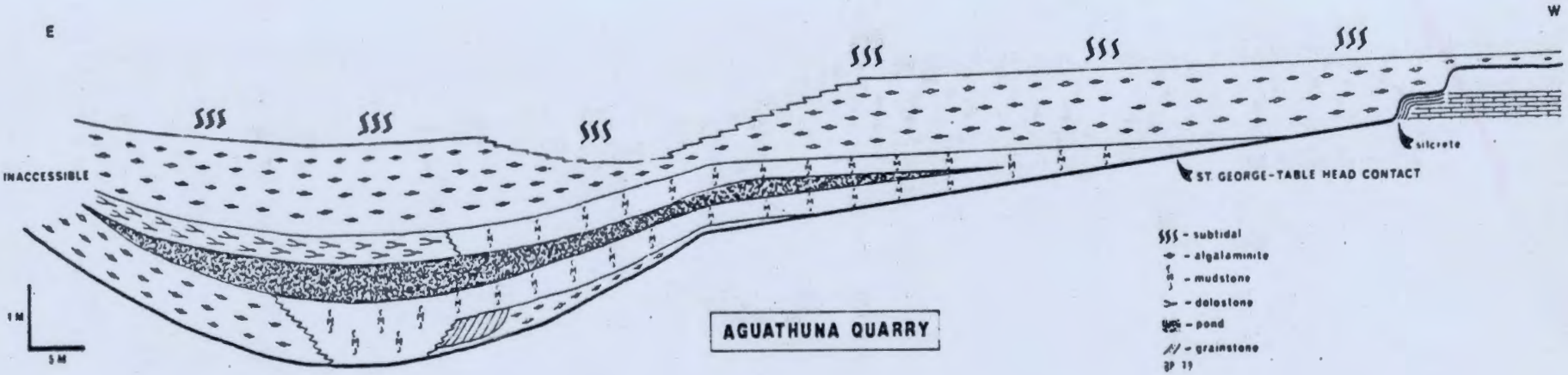


Figure 64: Outcrop sketch of the St. George-Table Head contact exposed on the south wall of Aguathuna Quarry.

stone, up to 0.5 metre thick, that pinches out at the flanks of the depression. This lithology is partly bioturbated dolomitic mudstone and ostracode packstone with scattered cryptalgal laminated layers containing abundant Girvanella-like algal filaments (Fig. 65E ). The filaments are hollow unbranched tubes, 20 to 30 microns in diameter, with nearly opaque organic-rich (imparting a brown stain to acetate peels) micrite walls. The tubes lie horizontally and are not tangled. In the deepest part of the depression, this unit is overlain by thinly and lenticularly bedded dolostone and mudstone (lithotope D) which grades laterally to light-coloured bioturbated mudstone that itself pinches out. Overlying this is up to 1.2 metres of cryptalgal laminated limestone that contains lithoclasts of chert and dolostone and drapes into fractures and crevices and around projections of the underlying Aguathuna Formation (Fig. 65A). This is overlain by dark-coloured burrowed fossiliferous limestone of 'typical' Table Head lithology.

Extensive silicification is present in a limestone bed of the St. George where truncated by the unconformity. At one of the steps in the contact, a banded fabric of silicification is developed in a fossiliferous wackestone bed only at the contact and nowhere else in the beds (Fig. 65B). Silicification does not penetrate into the Table Head. The partly silicified limestone is fractured with infillings of peloidal grainstone of the basal Table Head cryptalgal laminite (Fig. 65C). The uppermost band of chert is composed of microquartz that grades downward to micrite partly replaced

FIGURE 65

ST. GEORGE-TABLE HEAD CONTACT, AGUATHUNA QUARRY

A. Vertically oriented slab of brecciated and eroded dolostone of the Aguathuna Fm. overlain by lithoclastic cryptalgal laminated basal Table Head, western end of quarry. Scale in cm.

B. Vertically oriented slab of banded and fractured silcrete developed in fossiliferous wackestone of the Aguathuna Fm., overlain by basal Table Head grainstone. Scale in cm.

C. Vertically oriented thin section photomicrograph of top of silcrete, showing microquartz (with replacement dolomite rhomb) fractured with infilling of overlying Table Head grainstone. Crossed nicols; scale bar 500 µm.

D. Vertically oriented thin section photomicrograph of silcrete microquartz replaced by dolomite rhomb. Rhomb has been leached out and contains geopetal internal sediment from overlying dark-coloured Table Head sediment, followed by calcite spar cement. Scale bar 100 µm.

E. Vertically oriented thin section photomicrograph of cryptalgal laminated layers in dark-coloured pond sediment of the basal Table Head sequence, showing algal filaments and articulated ostracode valves. Scale bar 500 µm.

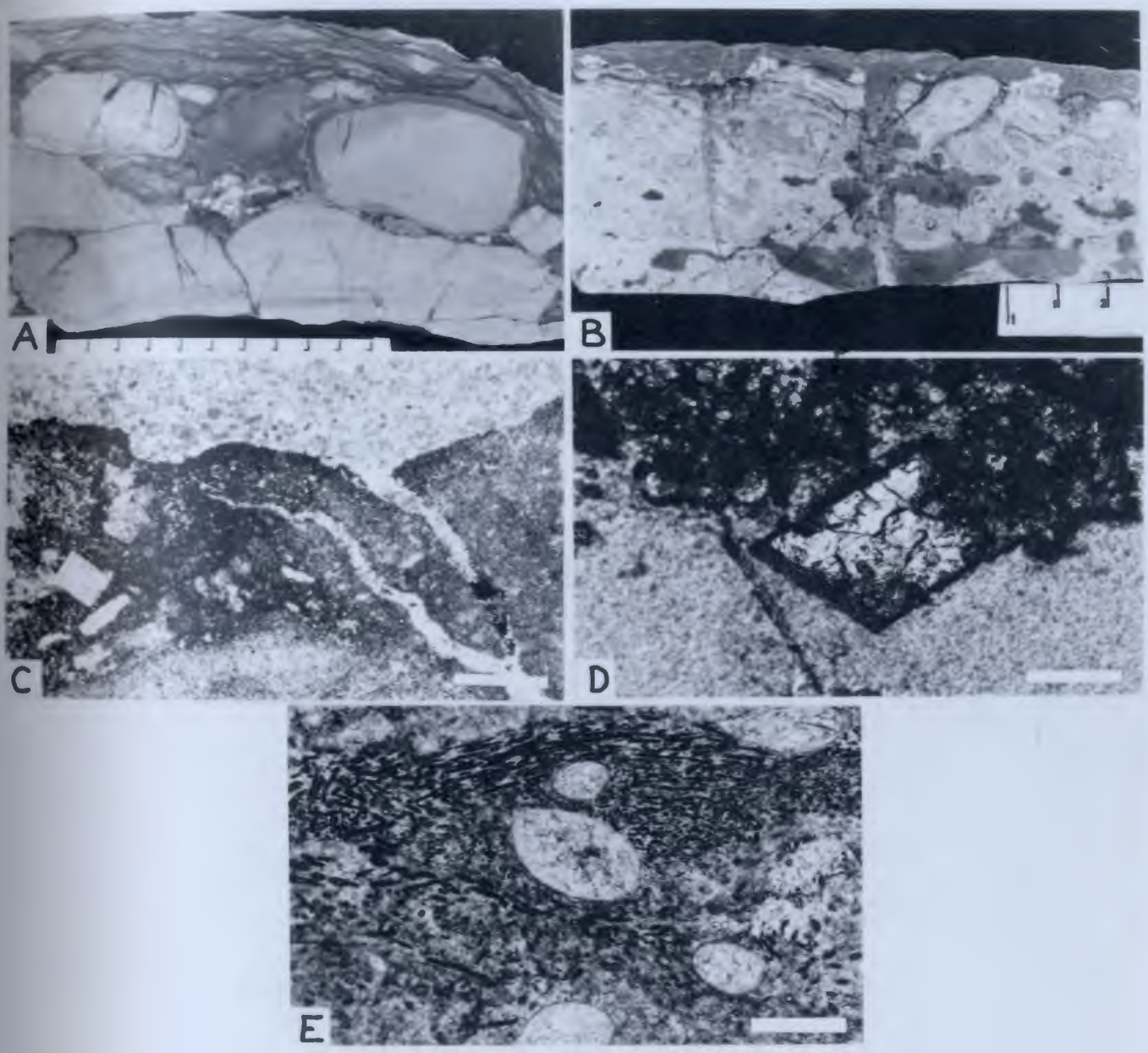
A
B
C
D
E

by cryptoquartz. Successive bands below this are also each marked by a downward decrease in the degree of cryptoquartz silicification. Gastropod molds are filled with megaquartz cement. Dolomite rhombs replace chert and are partly calcitized. At the top of the chert crust, dolomite rhombs have been leached and the crystal molds geopetally filled by micrite and peloids of the basal Table Head (Fig. 65 D).

Interpretation - The contact is interpreted to be a channel at its deepest point, rather than a closed depression, because of the cross-laminated grainstone that is probably a small channel fill. The fenestral cryptalgal laminites are interpreted to have been deposited in frequently wetted protected intertidal areas, and topographically higher cryptalgal laminites containing lithoclasts were probably supratidal. Deepening and an increase in sediment supply gave rise to bioturbated mudstone, interpreted to be an intertidal flat deposit. The dark-coloured limestone in the channel is interpreted to have been deposited in a lagoon or pond of variable salinity with brackish conditions suggested by the ostracode fauna, whose floor was sporadically covered by algal mats. Preservation of algal filaments was probably promoted by the non-marine conditions enhancing calcification. Overlying this, bioturbated intertidal mudstone passed laterally to tidal-bedded sediment in the deeper part of the channel, the site of active sediment movement where currents would have been stronger. The tidal flat complex accreted to the upper intertidal zone because it is overlain by cryptalgal laminites. Subtidal conditions rapidly prograded over the whole complex.

The banded chert crust developed in the limestone bed where truncated by the unconformity is interpreted to be a silcrete developed in lithified limestone while it was subaerially exposed before Table Head sedimentation. It did not form within the St. George before Table Head sedimentation because it is only developed where the contact cuts across the limestone bed. It did not develop after burial by Table Head sediments because post-chertification dolomite rhombs have been leached and geopetally filled by Table Head sediment (Fig. 66).

## OTHER LOCALITIES

Description - At Port au Choix, the contact is poorly exposed in a cliff on the southeast side of Back Arm, 2 kilometres from the town. Epigenetically dolomitized Catoche Formation is overlain by about 6 metres of massive finely crystalline ferroan dolostone that is indistinctly laminated in places. The contact has been placed previously (Lévesque, 1977) at the top of this dolostone, though there is no relief apparent. Successively overlying this is 0.6 metre of mudstone containing ostracodes, 0.4 metre of interbedded cryptalgal laminite and ostracode-rich mudstone, 1.2 metres of ostracode-rich packstone and mudstone, 1.6 metres of interbedded peloidal grainstone and cryptalgal laminite, and finally 'typical' dark-coloured fossiliferous wackestone and mudstone.

The contact is exposed 2 kilometres northeast of the Gravels. Thinly bedded dolostone of lithotope D is overlain successively by 0.15 metre of dolomitic cryptalgal laminite

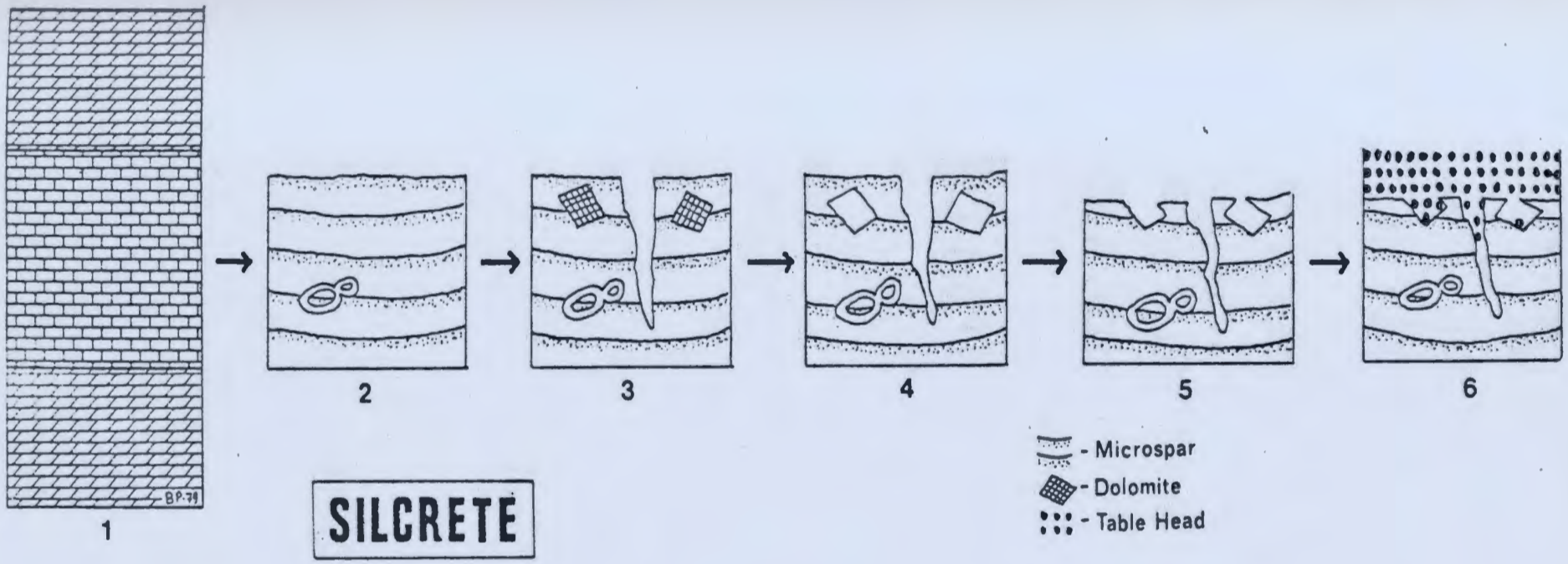


Figure 66: Interpreted sequence of formation of silcrete developed in St. George limestone subaerially exposed before Table Head deposition.

containing chert fragments, 0.2 metre of dark-coloured nodular fossiliferous limestone, 1.2 metre of light-coloured bioturbated mudstone, 1.0 metre of fenestral cryptalgal laminite, and finally 'typical' wackestone with scattered grainstone interbeds. No relief is seen on the contact except for compaction around chert nodules.

The contact is also exposed 1 kilometre northwest of the Gravels. Burrow-mottled dolostone (lithotope C) is successively overlain by 0.8 metre of fenestral cryptalgal laminite that is cut by a small reverse fault, 0.6 metre of mudstone containing scattered fossils, 0.4 metre of dark-coloured wavy- and nodular-bedded fossiliferous wackestone and mudstone, and 'typical' burrowed fossiliferous wackestone with grainstone interbeds. There is no relief on this surface other than compaction around large chert nodules.

Interpretation - The overlying basal Table Head lithologies are all suggestive of a tidal flat complex. The ostracode fauna suggests restricted conditions of salinity, probably brackish.

## DISCUSSION

While a sedimentary and time break is indicated by the St. George-Table Head contact at Table Point and Aguathuna, biostratigraphic studies to date in western Newfoundland are insufficient to estimate the amount of time involved. It appears that the lower Whiterock stage is missing, that is, the *Didymograptus hirundo* graptolite zone (S. Stouge, pers. comm., 1979). The unconformity is interpreted to have been

a time of subaerial exposure because of silcrete development, tepee formation, brecciation and erosion. No strata were removed at Table Point, but at Aguathuna there is at least 4 metres of down-cutting into already lithified and dolomitized St. George beds. The breccias and zinc mineralization at Daniel's Harbour have already been shown (Chapter 4) not to be of pre-Table Head age as suggested by Cumming (1968) and Collins and Smith (1975), and are therefore not evidence of a high relief karst topography.

The shallow-water peritidal lithologies of the Aguathuna Formation indicate that the amount of relative sea-level lowering needed to expose the Lower Ordovician carbonate platform was not much. That erosion seems to have been much greater at Aguathuna than further north suggests that simple sea-level drop may have occurred, but more likely that gentle warping of the shelf caused some areas to be uplifted slightly more than others. The period of subaerial exposure was reflected in the polymictic character of Bed 14 of the Cow Head Group. The warping may have been tectonically generated during the initial stages of closing of Iapetus Ocean (Williams and Stevens, 1974). The Table Head transgression appears to have occurred more or less simultaneously across western Newfoundland, on the basis of conodont data (S. Stouge, pers. comm., 1979). At the base of the Table Head, Bahamas-style tidal flat complexes developed everywhere before rapid progradation of a subtidal shelf sedimentary regime reflecting increased subsidence rate.

# CHAPTER 6 - CONCLUSIONS

The St. George Group was examined at twelve localities in western Newfoundland. Lithologies can be described under seven lithotopes, plus a number of miscellaneous characters, that formed in the peritidal environment. Lithotopes changed abruptly laterally, and short distance facies correlation shows that lateral facies patterns were complex. The St. George varies in character in different geographic areas and in different parts of the section. The vertical oscillation of lithotopes and the abundance of contacts between them in the Isthmus Bay and Aguathuna Formations generate lithotope sequences that suggest that these two formations accumulated on a shelf dotted with low-relief islands and banks that differed in character in different areas and changed with time. The Catoche Formation was dominantly a subtidal mudbank complex, with scattered reef shoals and intertidal banks. Depostion took place under conditions of more or less continuous subsidence that was more rapid in Catoche time. Regional relative lowering of sea level only occurred momentarily near the top of the Isthmus Bay Formation, in the Aguathuna Formation, and at the top of the St. George before the onset of Table Head deposition. On the unconformity between the St. George and Table Head Groups, four metres of relief is seen on Port au Port Peninsula, but none is apparent at Table Point. Silcrete developed in exposed St. George limestone at one place before the whole shelf was inundated by Bahamas-style tidal flat complexes of the basal Table Head.

Cryptalgal structures are abundant in the St. George and include oncolites, cryptalgal laminites, thrombolites, and stro-

matolites of hemispherical, branching columnar, and aberrant conical and "cerebral" morphologies. The type and branching style is related to biological and environmental parameters including scour, sediment size, sedimentation rate, and episodicity of sedimentation. An open ended classification was erected for cryptalgal microstructure which is also related to both environmental and biological and textural characteristics of the algal mats. Thrombolite mounds formed subtidal reefs, often coalescing into large banks, and supported a diverse benthos. In places, framework-building algal mats were aided by sponges, primitive corals, and the calcified blue-green algae Renalcis (shown to be a diagenetic taxon, like the encrusting Girvanella). Unique thrombolite-Lichenaria-Renalcis boundstones of surprising complexity occur low in the Isthmus Bay Formation. These boundstones had irregular growth surfaces with abundant cavities, tunnels, nooks, and crannies. The character of the frameworks and associated benthos show that the subtidal reef community was well developed, though not as diverse compared with later reefs. St. George thrombolitic mounds are a reef type in the middle of the transition from stromatolitic bioherms of the Precambrian and Cambrian, and metazoan bioherms of the later Phanerozoic.

Numerous stages of diagenetic alteration were involved in the lithogenesis of the calcareous sediments of the St. George. On the sea floor, facies specific radial bladed calcite cementation occurred in cryptalgal reefs and formed hardgrounds. During the early stages of burial, compaction occurred in inhomogeneous sediments, aragonitic molluscs were leached, authigenic silicates formed, botryoidal neomorphic spar and silica replaced carbonate

components, and calcite spar began to cement the soft sediment. Ooids, shown to be primary high-Mg calcite, recrystallized to produce a coarse radial microstructure. A finely fibrous fur-like microquartz replaced ooids in some beds. During continued burial, neomorphic spar and diagenetic dolomite replaced limestone. This diagenetic sequence appears typical for Lower Paleozoic shallow-water carbonates of North America. In addition, parts of the St. George suffered slight tectonic deformation during the Acadian Orogeny, and after this epigenetic dolomitization affected many areas, emplacing at least one economic sphalerite deposit.

Much further work remains to be done on the St. George. Paleontological study is still minute compared with the vast numbers of organisms preserved. The Cambro-Ordovician boundary has not been precisely positioned on Port au Port Peninsula. Coupled with taxonomic work, detailed paleoecological study of subtidal units, especially the mudbank complexes of the Catoche Formation, would be very valuable. The St. George is a typical Lower Paleozoic "burrow-mottled" carbonate unit, and deserves ichnological study. Preliminary work suggests that the ichnofauna is similar to that of siliciclastic peritidal rocks, but preservation is different owing to the nature of cementation and dolomitization.

## REFERENCES


Aitken, J.D., 1967; Classification and environmental significance of cryptalgal limestones and dolomites, with illustrations from the Cambrian and Ordovician of southwestern Alberta. J. Sed. Petrol., 37, 1163-1178.

Aitken, J.D., 1978; Revised models for depositional grand cycles, Cambrian of the southern Rocky Mountains, Canada. Bull. Can. Pet. Geol., 26, 515-542.

Anderson, E.J., Goodwin, P.W., and Cameron, B., 1978; Punctuated aggradational cycles (PACS) in Middle Ordovician and Lower Devonian sequences. In Merriam, D.F., ed., New York State Geol. Assoc. Guidebook, 50th Ann. Mtg., Syracuse, 204-220.

Assereto, R.L.A.M., and Kendall, C.G. St.C., 1977; Nature, origin and classification of peritidal tepee structures and related breccias. Sedimentology, 24, 153-210.

Baskin, Y., 1956; A study of authigenic feldspars. Jour. Geol., 64, 132-155.

Bathurst, R.G.C., 1967; Subtidal gelatinous mat, sand stabilizer and food, Great Bahama Bank. Jour. Geol., 75, 736-738.

Bathurst, R.G.C., 1971; Carbonate sediments and their diagenesis. Dev. Sedim. 12, Elsevier, 1-620, Amsterdam.

Bertrand-Sarfati, J., 1977; An attempt to classify Late Precambrian stromatolite microstructures. In Walter, M.R., ed., Stromatolites, Dev. Sedim. 20, Elsevier, 251-259, Amsterdam.

Besaw, D.M., 1972; Limestone evaluation, Port au Port Peninsula. Internal Rept., Min. Dev. Div., Nfld. Dept. Mines Energy.

Besaw, D.M., 1973; Limestone evaluation, Project 4-1, evaluation of deposits in the Port au Port Peninsula area. Internal Rept., Min. Res. Div., Nfld. Dept. Mines Energy.

Betz, F., 1939; Geology and mineral deposits of the Canada Bay area, northern Newfoundland. Geol. Surv. Nfld., Bull. 16, 1-53.

Billings, E., 1865; Palaeozoic fossils, vol. I. Dawson Bros., 1-426, Montreal.

Bornemann, J.G., 1886; Die Versteinerungen des Cambrischen Schichtensystems der Insel Sardinien. Nova acta Ksl. Leop.-Carol. Deutsch Akad. Naturforsch., 51, 1-147.

Bosellini, A. and Hardie, L.A., 1973; Depositional theme of a marginal marine evaporite. Sedimentology, 20, 5-27.

Brasier, M.D., 1977; An early Cambrian chert biota and its implications. Nature, 268, 719-720.

Braun, M. and Friedman, G.M., 1969; Carbonate Lithofacies and environments of the Tribes Hill Formation (Lower Ordovician) of the Mohawk Valley, New York. J. Sed. Petrol., 39, 106-112.

Brock, T.D., 1977; Environmental microbiology of living stromatolites. In Walter, M.R., ed., Stromatolites, Dev. Sedim. 20, Elsevier, 141-148, Amsterdam.

Buyce, M.R. and Friedman, G.M., 1975; Significance of authigenic feldspar in Cambrian-Ordovician carbonate rocks of the Proto-Atlantic shelf in North America. J. Sed. Petrol., 45, 808-821.

Carozzi, A.V., 1963; Half-moon oolites. J. Sed. Petrol., 33, 633-645.

Choquette, P.W., 1955; A petrographic study of the "State College" siliceous oolite. Jour. Geol., 63, 337-347.

Chowns, T.M. and Elkins, J.E., 1974; The origin of quartz geodes and cauliflower cherts through the silicification of anhydrite nodules. J. Sed. Petrol., 44, 885-903.

Church, S.B., 1974; Lower Ordovician patch reefs in western Utah. Brigham Young Univ. Geol. Studies, 21, 41-62.

Cloud, P., Wright, L.A., Williams, E.G., Diehl, P., and Walter, M.R., 1974; Giant stromatolites and associated vertical tubes from the Upper Proterozoic Noonday Dolomite, Death Valley region, eastern California. Geol. Soc. Amer. Bull., 85, 1869-1882.

Collins, J.A. and Smith, L., 1975; Zinc deposits related to diagenesis and intrakarstic sedimentation in the Lower Ordovician St. George Formation, western Newfoundland. Bull. Can. Pet. Geol., 23, 393-427.

Cooper, J.R., 1937; Geology and mineral deposits of the Hare Bay area. Geol. Surv. Nfld., Bull. 9, 1-36.

Cumming, L.M., 1968; St. George-Table Head disconformity and zinc mineralization, western Newfoundland. Can. Inst. Mining Metal. Bull., 721-725.

Dunham, R.J., 1970; Stratigraphic reefs versus ecologic reefs. Amer. Assoc. Pet. Geol. Bull., 54, 1931-1932.

Fåhraeus, L.E., 1977; Isocommunities and correlation of the North American Didymograptus bifidus Zone (Ordovician). Newsl. Stratigr., 6, 85-96.

Fåhraeus, L.E. and Nowlan, G.S., 1978; Franconian (Late Cambrian) to Early Champlainian (Middle Ordovician) conodonts from the Cow Head Group, western Newfoundland. J. Paleont., 52, 444-471.

Flower, R.H., 1978; St. George and Table Head cephalopod zonation in western Newfoundland. Geol. Surv. Can., Pap. 78-1A, 217-224.

Folk, R.L., 1965; Some aspects of recrystallization in ancient limestones. In Pray, L.C. and Murray, R.C., eds., Dolomitization and limestone diagenesis, Soc. Econ. Paleont. Mineral., Spec. Pub. 13, 14-48.

Folk, R.L. and Assereto, R., 1974; Giant aragonite rays and baroque white dolomite in tepee-fillings, Triassic of Lombardy, Italy (abst.). Amer. Assoc. Pet. Geol., Ann. Mtg. Prog., 508.

Folk, R.L. and Pittman, J.S., 1971; Length-slow chalcedony: a new testament for vanished evaporites. J. Sed. Petrol., 41, 1045-1058.

Fortey, R.A., in press; Lower Ordovician trilobites from the Catoche Formation (St. George Group), western Newfoundland. Geol. Surv. Can., Bull.

Friedman, G.M. and Sanders, J.E., 1967; Origin and occurrence of dolostones. In Chilingar, G.V., Bissell, H.J., and Fairbridge, R.W., eds., Carbonate rocks. Origin, occurrence and classification. Dev. Sedim. 9, Elsevier, 267-348, Amsterdam.

Füchtbauer, H., 1974; Sediments and sedimentary rocks 1. Sedim. Petrol. II, E. Schweizerbart'sche. 1-464, Stuttgart.

Gebelein, C.D., 1974; Biologic control of stromatolite microstructure: implications for Precambrian time stratigraphy. Am. J. Sci., 274, 575-598.

Gebelein, C.D., 1977; The effects of the physical, chemical and biological evolution of the earth. In Walter, M.R., ed., Stromatolites, Dev. Sedim. 20, Elsevier, 499-515, Amsterdam.

Ginsburg, R.N., ed., 1975; Tidal deposits. Springer, 1-428, New York.

Golubić, S., 1977; Organisms that build stromatolites. In Walter, M.R., ed., Stromatolites, Dev. Sedim. 20, Elsevier, 113-126, Amsterdam.

de Groot, K., 1973; Geochemistry of tidal flat brines at Umm Said, SE Qatar, Persian Gulf. In Purser, B.H., ed., The Persian Gulf, Springer, 377-394, Heidelberg.

Gürich, G., 1906; Spongiostromides du Viséen de la Province de Namur. Mém. Mus. Roy. Hist. Nat. Belg., 3, 1-55.

Halley, R.B., 1977; Ooid fabric and fracture in the Great Salt Lake and the geologic record. J. Sed. Petrol., 47, 1099-1120.

Hardie, L.A., ed., 1977; Sedimentation on the modern carbonate tidal flats of northwest Andros Island, Bahamas. Johns Hopkins Univ., Studies Geol. 22, 1-202.

Harris, L.D., 1973; Dolomitization model for Upper Cambrian and Lower Ordovician carbonate rocks in the eastern United States. J. Res. U.S. Geol. Surv., 1, 63-78.

Haworth, R.T. and Sanford, B.V., 1976; Paleozoic geology of northeast Gulf of St. Lawrence. Geol. Surv. Can., Pap. 76-1A, 1-6.

Hintze, L.F., 1973; Lower and Middle Ordovician stratigraphic sections in the Ibex area, Millard County, Utah. Brigham Young Univ. Geol. Studies, 20, 3-36.

Hoffman, P., 1967; Algal stromatolites: use in stratigraphic correlation and paleocurrent determination. Science, 157, 1043-1045.

Hoffman, P., 1977; Environmental diversity of Middle Precambrian stromatolites. In Walter, M.R., ed., Stromatolites, Dev. Sedim. 20, Elsevier, 599-611, Amsterdam.

Hofmann, H.J., 1969; Attributes of stromatolites. Geol. Surv. Can., Pap. 69-39, 1-58.

Hofmann, H.J., 1975; Stratiform Precambrian stromatolites, Belcher Islands, Canada: relations between silicified microfossils and microstructure. Am. J. Sci., 275, 1121-1132.

Hofmann, H.J., 1977; On Aphebian stromatolites and Riphean stromatolite stratigraphy. Precamb. Res., 5, 175-205.

Horodyski, R.J., 1977; Environmental influences on columnar stromatolite branching patterns: examples from the Middle Proterozoic Belt Supergroup, Glacier National Park, Montana. J. Paleont., 51, 661-671.

James, N.P., 1977; Facies models 8. Shallowing upward sequences in carbonates. Geosci. Canada, 4, 126-136.

James, N.P. and Kobluk, D.R., 1978; Lower Cambrian patch reefs and associated sediments: southern Labrador, Canada. Sedimentology, 25, 1-35.

James, N.P. and Stevens, R.K., 1976; Large sponge-like reef mounds from the Lower Ordovician of west Newfoundland (abst.). Geol. Soc. Amer., Abst. Prog., 8, 1122.

James, N.P., Kobluk, D.R., and Pemberton, S.G., 1977; The oldest macroborers: Lower Cambrian of Labrador. Science, 197, 980-983.

James, N.P., Ginsburg, R.N., Marszalek, D.S., and Choquette, P.W., 1976; Facies and fabric specificity of early subsea cements in shallow Belize (British Honduras) reefs. J. Sed. Petrol., 46, 523-544.

Johnson, H., 1949; Geology of western Newfoundland (unpub. ms.). Geol. Surv. Nfld.

Kahle, C.F., 1965; Possible roles of clay minerals in the formation of dolomite. J. Sed. Petrol, 35, 448-453.

Kalkowsky, E., 1908; Oolith und Stromatolith im norddeutschen Buntsandstein. Zeitschr. Deutsch. Geol. Ges., 60, 68-125.

Kastner, M., 1971; Authigenic feldspars in carbonate rocks. Am. Mineralogist, 56, 1403-1442.

Kastner, M. and Siever, R., 1979; Low temperature feldspars in sedimentary rocks. Am. J. Sci., 279, 435-479.

Kendall, A.C., 1978; Facies models 11. Continental and supratidal (sabkha) evaporites. Geosci. Canada, 5, 66-78.

Kendall, A.C. and Broughton, P.L., 1978; Origin of fabrics in speleothems composed of columnar calcite crystals. J. Sed. Petrol., 48, 519-538.

Kindle, C.H. and Whittington, H.B., 1975; New Cambrian and Ordovician fossil localities in western Newfoundland. Geol. Soc. Amer. Bull., 76, 683-688.

Klein, G.deV., 1972; Determination of paleotidal range in clastic sedimentary rocks. 24th Int. Geol. Cong., Sec. 6, 397-405.

Klement, K.W. and Toomey, D.F., 1967; Role of the blue-green alga Girvanella in skeletal grain alteration and lime-mud formation in the Lower Ordovician of west Texas. J. Sed. Petrol., 37, 1045-1051.

Kluyver, H.M., 1975; Stratigraphy of the Ordovician St. George Group in the Port-au-Choix area, western Newfoundland. Can. J. Earth Sci., 12, 589-594.

Knight, I., 1977a; The Cambrian-Ordovician platformal rocks of the Northern Peninsula. Min. Dev. Div., Nfld. Dept. Mines Energy, Rept. 77-1, 27-34.

Knight, I., 1977b; Cambro-Ordovician platformal rocks of the Northern Peninsula, Newfoundland. Min. Dev. Div., Nfld. Dept. Mines Energy, Rept. 77-6, 1-27.

Knight, I., 1978; Platformal sediments on the Great Northern Peninsula: stratigraphic studies and geological mapping of the north St. Barbe district. Min. Dev. Div., Nfld. Dept. Mines Energy, Rept. 78-1, 140-150.

Kobluk, D.R. and Risk, M.J., 1977; Micritization and carbonate-grain binding by endolithic algae. Amer. Assoc. Pet. Geol. Bull., 61, 1069-1082.

Laporte, L.F., 1967; Carbonate deposition near mean sea-level and resultant facies mosaic: Manlius Formation (Lower Devonian) of New York State. Amer. Assoc. Pet. Geol. Bull., 51, 73-101.

Lévesque, R.J., 1977; Stratigraphy and sedimentology of Middle Cambrian to Lower Ordovician shallow water carbonate rocks, western Newfoundland. Unpub. MSc thesis, Memorial University of Newfoundland, 1-276.

Lilly, H.D., 1961; Geology of the Goose Arm-Hughes Brook area. Unpub. MSc thesis, Memorial University of Newfoundland, 1-123.

Lochman, C., 1938; Middle and Upper Cambrian faunas from western Newfoundland. J. Paleont., 12, 461-477.

Logan, B.W., Rezak, R., and Ginsburg, R.N., 1964; Classification and environmental significance of algal stromatolites. Jour. Geol., 72, 68-83.

Logan, B.W., Hoffman, P., and Gebelein, C.D., 1974; Algal mats, cryptalgal fabrics, and structures, Hamelin Pool, Western Australia. In Evolution and diagenesis of Quaternary carbonate sequences, Shark Bay, Western Australia, Amer. Assoc. Pet. Geol., Mem. 22, 140-193.

Logan, Sir W.E., 1863; Geology of Canada. Dawson Bros., 1-983, Montreal.

Lohmann, K.C. and Meyers, W.J., 1977; Microdolomite inclusions in cloudy prismatic calcites: a proposed criterion for former high-magnesium calcites. J. Sed. Petrol., 47, 1078-1088.

Marshall, J.F. and Davies, P.J., 1975; High-magnesium calcite ooids from the Great Barrier Reef. J. Sed. Petrol. 45, 285-291.

Matter, A., 1967; Tidal flat deposits in the Ordovician of western Maryland. J. Sed. Petrol., 37, 601-609.

Mazzullo, S.J., 1976; Significance of authigenic K-feldspar in Cambrian-Ordovician carbonate rocks of the Proto-Atlantic Shelf in North America: a discussion. J. Sed. Petrol, 46, 1035-1040.

Mazzullo, S.J., 1977; Shrunken (geopetal) ooids: evidence of origin unrelated to carbonate-evaporite diagenesis. J. Sed. Petrol., 47, 392-397.

Meyers, W.J. and Lohmann, K.C., 1978; Microdolomite-rich syntaxial cements: proposed meteoric-marine mixing zone phreatic cements from Mississippian limestones, New Mexico. J. Sed. Petrol., 48, 475-488.

Milliken, K.L., 1979; The silicified evaporite syndrome-two aspects of silicification history of former evaporite nodules from southern Kentucky and northern Tennessee. J. Sed. Petrol., 49, 245-256.

Monty, C.L.V., 1977; The origin and development of cryptalgal fabrics. In Walter, M.R., ed., Stromatolites, Dev. Sedim. 20, Elsvier, 193-249, Amsterdam.

Nelson, S.J., 1955; Geology of Portland Creek-Port Saunders area, west coast. Nfld. Geol. Surv., Rept. 7, 1-57.

Neugebauer, J., 1974; Some aspects of cementation in chalk. In Hsü, K.J. and Jenkyns, H.C., eds., Pelagic sediments: on land and under the sea, Int. Assoc. Sedimentol., Spec. Pub. 1, 149-176.

Neumann, A.C., Gebelein, C.D., and Scoffin, T.P., 1970; The composition, structure and erodability of subtidal mats, Abaco, Bahamas. J. Sed. Petrol., 40, 274-297.

Nicholson, H.A. and Etheridge, R., 1878; A monograph of the Silurian fossils of the Girvan district in Ayrshire I. Blackwood, 1-135, Edinburgh.

Oxley, P., 1953; Geology of Parsons Pond-St. Paul's area, west coast. Nfld. Geol. Surv., Rept. 5, 1-53.

Pierce, R.W., 1967; Stratigraphy and paleontology of a portion of the Pogonip Group (Opd and Ope), Arrow Canyon Range, Nevada. Unpub. MSc. thesis, University of Illinois (Urbana), 1-122.

Pojeta, J.Jr. and Runnegar, B., 1976; The paleontology of the rostroconch molluscs and the early history of the Phylum Mollusca. U.S. Geol. Surv., Prof. Pap. 968, 1-88.

Pratt, B.R., 1979; Early cementation and lithification in intertidal cryptalgal structures, Boca Jewfish, Bonaire, Netherlands Antilles. J. Sed. Petrol., 49, 379-386.

Read, J.F. and Grover, G.A.Jr., 1977; Scalloped and planar erosion surfaces, Middle Ordovician limestones, Virginia: analogues of Holocene exposed karst or tidal rock platforms. J. Sed. Petrol., 47, 956-972.

Richter, D.K., 1971; Fazies- und Diagenesehinweise durch Einschlüsse in authigenen Quarzen. N. Jb. Geol. Paläont. Mh., 604-622.

Richter, D.K., 1974; Entstehung und Diagenese der devonischen und permotriassischen Dolomite in der Eifel. Contr. Sedim. 2, 1-101.

Riding, R., 1975; Girvanella and other algae as depth indicators. Lethaia, 8, 173-179.

Riding, R., 1977; Calcified Plectonema (blue-green algae), a Recent example of Girvanella from Aldabra Atoll. Palaeont., 20, 33-46.

Riding, R. and Brasier, M., 1975; Earliest calcareous foraminifera. Nature, 257, 208-210.

Riding, R. and Toomey, D.F., 1972; The sedimentological role of Epiphyton and Renalcis in Lower Ordovician mounds, southern Oklahoma. J. Paleont., 46, 509-519.

Riley, G.C., 1962; Stephenville map area, Newfoundland. Geol. Surv. Can., Mem. 323, 1-72.

Rodgers, J., 1970; The tectonics of the Appalachians. Wiley, 1-271, New York.

Ross, R.J.Jr., 1970; Ordovician brachiopods, trilobites, and stratigraphy in eastern and central Nevada. U.S. Geol. Surv., Prof. Pap. 639, 1-103.

Sandberg, P.A., 1975; New interpretations of Great Salt Lake ooids and of ancient non-skeletal carbonate mineralogy. Sedimentology, 22, 497-537.

Sando, W.J., 1957; Beekmantown Group (Lower Ordovician) of Maryland. Geol. Soc. Amer., Mem. 68, 1-161.

Schneider, W., 1973; Einige Beobachtungen zur Diagenese in den devonischen Karbonatkomplexen des ostrheinischen Schiefergebirges unter besonderer Berücksichtigung der Quarzbildung. N. Jb. Geol. Paläont. Mh., 231-257.

Schuchert, C. and Dunbar, C.O., 1934; Stratigraphy of western Newfoundland. Geol. Soc. Amer., Mem. 1, 1-123.

Semikhatov, M.A., Gebelein, C.D., Cloud, P., Awramik, S.M., and Benmore, W.C., 1979; Stromatolite morphogenesis-progress and problems. Can. J. Earth Sci., 16, 992-1015.

Shaw, A.B., 1964; Time in stratigraphy. McGraw-Hill, 1-365, New York.

Shinn, E.A., 1969; Submarine lithification of Holocene carbonate sediments in the Persian Gulf. Sedimentology, 12, 109-144.

Shinn, E.A., Halley, R.B., Hudson, J.H., and Lidz, B.H., 1977; Limestone compaction: an enigma. Geology, 5, 21-24.

Siedlecka, A., 1976; Silicified Precambrian evaporite nodules from northern Norway: a preliminary report. Sedim. Geol., 16, 161-175.

Smit, D.E., 1971; Stratigraphy and sedimentary petrology of the Cambrian and Lower Ordovician shelf sequence of western Newfoundland. Unpub. PhD thesis, University of Iowa, 1-198.

Stearn, C.W. and Riding, R., 1973; Forms of the hydrozoan Millepora on a Recent coral reef. Lethaia, 6, 187-200.

Stevens, R.K., 1970; Cambro-Ordovician flysch sedimentation and tectonics in west Newfoundland and their possible bearing on a Proto-Atlantic Ocean. In Lajoie, J., ed., Flysch sedimentology in North America, Geol. Assoc. Can., Spec. Pap. 7, 165-177.

Suchecki, R.K., Perry, E.A.Jr., and Hubert, J.F., 1977; Clay petrology of Cambro-Ordovician continental margin, Cow Head Klippe, western Newfoundland. Clays Clay Min., 25, 163-170.

Sullivan, J.W., 1940; The geology and mineral resources of the Port-au-Port area, Newfoundland. Unpub. PhD thesis, Yale University, 1-101.

Swett, K., 1968; Authigenic feldspar and cherts resulting from dolomitization of illitic limestones: a hypothesis. J. Sed. Petrol., 38, 128-135.

Swett, K. and Smit, D.E., 1972; Paleogeography and depositional environments of the Cambro-Ordovician shallow-marine facies of the North Atlantic. Geol. Soc. Amer. Bull., 83, 3223-3248.

Toomey, D.F., 1970; An unhurried look at a Lower Ordovician mound horizon, southern Franklin Mountains, west Texas, J. Sed. Petrol., 40, 1318-1334.

Toomey, D.F. and Ham. W.E., 1967; Pulchrilamina, a new mound-building organism from Lower Ordovician rocks of west Texas and southern Oklahoma. J. Paleont., 41, 981-987.

Toomey, D.F. and LeMone, D., 1977; Some Ordovician and Silurian algae from selected areas of the southwestern United States. In Flügel, E., ed., Fossil algae, Springer, 351-359, Berlin.

Troelsen, J.C., 1947; Geology of the Bonne Bay-Trout River area. Unpub. PhD thesis, Yale University, 1-289.

Tuke, M.F., 1968; Autochthonous and allochthonous rocks of the Pistolet Bay area in northernmost Newfoundland. Can. J. Earth Sci., 5, 501-522.

Turmel, R.J. and Swanson, R.G., 1976; The development of Rodriguez Bank, a Holocene mudbank in the Florida reef tract. J. Sed. Petrol., 46, 497-518.

Twenhofel, W.H., et al., 1954; Correlation of the Ordovician formations of North America. Geol. Soc. Amer. Bull., 65, 247-298.

Vologdin, A.G., 1932; The Archaeocyathinae of Siberia 2. Fossils of the Cambrian limestones of Altai Mountains (in Russian). N.K.T.P., State Sci.-Tech. Geol. Expl. Publ. House, 1-106, Moscow-Leningrad.

Walker, K.R., 1973; Stratigraphy and environmental sedimentology of Middle Ordovician Black River Group in the type area- New York State. N.Y. State Mus. Sci. Serv., Bull. 419, 1-43.

Walker, K.R. and Alberstadt, L.P., 1975; Ecological succession as an aspect of structure in fossil communites. Paleobiol., 1, 238-257.

Walker, K.R. and Bambach, R.K., 1974; Feeding by benthic invertebrates: classification and terminology for paleoecological analysis. Lethaia, 7, 67-78.

Walter, M.R., 1972; Stromatolites and the biostratigraphy of the Australian Precambrian and Cambrian. Palaeont. Assoc., Spec. Pap. 11, 1-190.

Walthier, T.N., 1949; Geology and mineral deposits of the area between Corner Brook and Stephenville, western Newfoundland. Nfld. Geol. Surv., Bull. 35, 1-87.

Wanless, H.R., 1979; Limestone response to stress: pressure solution and dolomitization. J. Sed. Petrol., 49, 437-462.

Watson, K.deP., 1943; Colloform sulphide veins of Port au Port Peninsula, Newfoundland. Economic Geology, 38, 621-647.

Whittington, H.B., 1968; Zonation and correlation of Canadian and Early Mowhawkian Series. In Zen, E-an, White, W.S., Hadley, J.B., and Thompson, J.B.Jr., eds., Studies of Appalachian geology: northern and maritime. Wiley, 49-60.

Whittington, H.B. and Kindle, C.H., 1966; Middle Cambrian strata at the Strait of Belle Isle, Newfoundland (abst.). Geol. Soc. Amer., Abst. Prog., 46.

Whittington, H.B. and Kindle, C.H., 1969; Cambrian and Ordovician stratigraphy of western Newfoundland. In Kay, M., ed., North Atlantic geology and continental drift. Amer. Assoc. Pet. Geol., Mem. 12, 655-664.

Wilkinson, B.H. and Landing, E., 1978; "Eggshell diagenesis" and primary radial fabric in calcite ooids. J. Sed. Petrol., 48, 1129-1138.

Williams, H., 1979; Appalachian orogen in Canada. Can. J. Earth Sci., 16, 792-807.

Williams, H. and Stevens, R.K., 1974; The ancient continental margin of eastern North America. In Burke, C.A. and Drake, C.L., eds., The geology of continental margins, Springer, 781-796, Heidelberg.

Woodward, H.H., 1957; Geology of the Port au Choix-Castor River area, Newfoundland. Nfld. Geol. Surv., Rept. 10, 1-44.

Wray, J.L., 1977; Calcareous algae. Elsevier, 1-185, Amsterdam.

# APPENDICES

## MEASURED STRATIGRAPHIC SECTIONS*

*Except for that measured at Table Point because of poor preservation and incompleteness of the section.

# APPENDIX A

## ISTHMUS BAY

This section was measured at the eastern end of Port au Port Peninsula, beginning 1.5 km southwest of the south gravel bar joining the peninsula with mainland Newfoundland, and continuing along the shore to the Gravels. Most of the Catoche Fm. is covered between the two gravel bars, and north of the Gravels the section comprises the Aguathuna Formation

| Unit | Description | Thickness (m) Unit | Total |
|---|---|---|---|
| | **Table Head Group** | | |
| ---- | Continues upward for an unmeasured thickness of wackestone, burrowed, bioclastic, with many grainstone beds | | |
| 6 | Dolostone, recessive | 0.2 | 7.9 |
| 5 | Wackestone, burrowed, gastropods | 2.0 | 7.7 |
| 4 | Wackestone, burrowed | 2.9 | 5.7 |
| 3 | Wackestone, nodular, dark-coloured, fossiliferous | 0.4 | 2.8 |
| 2 | Wackestone, burrowed, light-coloured | 0.4 | 2.8 |
| 1 | Mudstone, cryptalgal laminated, fenestral fabric | 1.8 | 1.8 |
| | Contact sharp and slightly undulating due to compaction around chert nodules | | |
| | **St. George Group** | | |
| | **Aguathuna Formation** | | |
| 341 | Dolostone, thinly bedded, burrowed | 4.2 | 471.3 |
| 340 | Boundstone, thrombolitic, fossiliferous, burrowed, grainstone and wackestone matrix | 0.5 | 467.1 |
| 339 | Dolostone, thinly bedded, burrowed | 1.0 | 466.6 |
| 338 | Boundstone, stacked hemispheroidal stromatolites, dolomitized | 0.2 | 465.6 |
| 337 | Dolostone, cryptalgal laminated, chert nodules | 1.0 | 465.4 |
| 336 | Dolostone, thinly, wavy, and lenticular bedded, scattered bioturbation, chert nodules | 1.2 | 464.4 |
| 335 | Dolostone, thinly, wavy, and lenticular bedded, current laminated, scattered SH stromatolites | 0.6 | 463.2 |

| | | | |
|---|---|---|---|
| 334 | Dolostone, thinly and lenticular bedded, chert nodules | 1.2 | 462.6 |
| 333 | Dolostone, thinly and lenticular bedded, scour and fill structures | 1.2 | 461.4 |
| 332 | Boundstone, wavy cryptalgal laminite to low-relief LLH stromatolites, grades laterally to dolostone, chert nodules | 0.7 | 460.2 |
| 331 | Dolostone, thinly bedded, current laminated | 1.4 | 459.5 |
| 330 | Dolostone, cryptalgal laminated, mudcracked | 1.0 | 458.1 |
| 329 | Dolostone, thinly, wavy, and lenticular bedded, cross-laminated | 1.0 | 457.1 |
| 328 | Boundstone, dolomitized LLH stromatolites, capped by thin cryptalgal laminite, mudcracks, chert nodules | 0.2 | 456.1 |
| 327 | Dolostone, thinly, wavy, and lenticular bedded, current laminated, scour and fill structures | 2.0 | 455.9 |
| | Two normal faults, trending N 15° E, western blocks upthrown a total of 3.5 metres | | |
| 326 | Grainstone, wackestone, mudstone, burrowed, scattered small SH stromatolites, fossiliferous | 1.0 | 453.9 |
| 325 | Mudstone, cryptalgal laminated | 0.8 | 452.9 |
| 324 | Dolostone, thinly and lenticular bedded, intraclastic bed, scattered SH stromatolites up to 0.2 m across | 0.9 | 452.1 |
| 323 | Mudstone, cryptalgal laminated | 0.1 | 451.2 |
| 322 | Dolostone, thinly and lenticular bedded, cross-laminated, chert nodules at top | 1.0 | 451.1 |
| 321 | Grainstone and wackestone, burrowed, fossiliferous | 0.4 | 450.1 |
| 320 | Dolostone, thinly bedded, burrowed | 1.0 | 449.7 |
| 319 | Boundstone, Pulchrilamina mounds, flanked by dolomitized grainstone, grades laterally to thinly bedded dolostone, burrowed, scattered chert nodules, silicified burrows | 0.6 | 448.7 |
| 318 | Dolostone, cross-laminated, burrowed top | 0.6 | 448.1 |
| 317 | Boundstone, LLH stromatolites, low-relief, mudcracked upper surface, scattered chert nodules | 0.6 | 447.5 |
| 316 | Dolostone, thinly, wavy, and lenticular bedded | 0.4 | 446.9 |
| 315 | Grainstone and mudstone, burrowed, fossiliferous, scattered chert nodules | 1.6 | 446.5 |

| | | | |
|---|---|---|---|
| 314 | Dolostone, thinly bedded, burrowed, scattered chert | 1.4 | 446.9 |
| 313 | Boundstone, low-relief LLH stromatolites, chert nodules at top | 0.2 | 445.5 |
| 312 | Grainstone, mudstone, and dolostone, thinly, wavy, and lenticular bedded, cross-laminated, scattered bioturbation, scattered small SH stromatolites and mudcracks, scattered chert nodules | 0.7 | 445.3 |
| 311 | Boundstone, large diameter, low-relief LLH stromatolites | 0.2 | 444.6 |
| 310 | Dolostone, current-laminated, ?cryptalgal laminated | 0.8 | 444.4 |
| 309 | Dolostone, finely crystalline, ferroan, cross-laminated beds, squashed mudcracks, chert nodules at top | 0.4 | 443.6 |
| 308 | Boundstone, LLH stromatolites, low-relief, 0.2 to 0.4 m across, chert nodules at top | 0.2 | 443.2 |
| 307 | Dolostone, current-laminated, ?cryptalgal laminated, scattered chert nodules | 1.3 | 443.0 |
| 306 | Boundstone, low-relief LLH stromatolites and wavy cryptalgal laminites, intraclastic grainstone at base, grades laterally to dolostone | 0.3 | 441.7 |
| 305 | Dolostone, current-laminated, interference ripples, ?crytpalgal laminated; | 0.4 | 441.4 |
| 304 | Mudstone, dolostone, and chert, brecciated rubble and buckled beds, green shale seams, thins to 0.2 m, depressions on upper surface filled with cross-laminated intraclastic grainstone | 0.4 | 441.0 |
| 303 | Grainstone and wackestone, burrowed, fossiliferous, hardgrounds | 0.4 | 440.6 |
| 302 | Dolostone, thinly, wavy, and lenticular beddes | 0.8 | 440.2 |
| 301 | Grainstone and wackestone, burrowed, fossiliferous, small thrombolite mounds of irregular shape, chert nodules at top | 0.4 | 439.4 |
| 300 | Dolostone, thinly, wavy, and lenticular bedded, one burrowed bed | 0.9 | 439.0 |
| 299 | Boundstone, LLH stromatolites, low-relief, wavy cryptalgal laminites, matrix intraclastic grainstone | 0.4 | 438.1 |
| 298 | Dolostone, cryptalgal laminated, mudcracks at base, scattered chert nodules | 0.8 | 437.7 |
| 297 | Mudstone and wackestone, burrowed, scattered dolomitized SH stromatolites, grades laterally to dolostone | 0.8 | 436.9 |

| | | | |
|---|---|---|---|
| 296 | Dolostone, thinly and wavy bedded | 0.3 | 436.1 |
| 295 | Grainstone and wackestone, burrowed, cross-laminated, fossiliferous, two beds of SH stromatolites up to 0.2 m in diameter | 1.1 | 435.8 |
| 294 | Dolostone, thinly, wavy, and lenticular bedded, scour and fill structures, cross-laminated, scattered bioturbation, scattered chert nodules | 2.8 | 434.7 |
| 293 | Dolostone, cryptalgal laminated | 0.6 | 431.9 |
| 292 | Dolostone, thinly, wavy, and lenticular bedded, scour and fill structures, cross-laminated in places, scattered bioturbation | 3.0 | 431.3 |
| 291 | Mudstone, wackestone, grainstone, and dolostone, thinly interbedded, wavy, lenticular and nodular bedded, fossiliferous | 0.5 | 428.3 |
| 290 | Boundstone, LLH stromatolites | 0.2 | 427.8 |
| 289 | Dolostone, thinly, wavy, and lenticular bedded | 0.2 | 247.6 |
| 288 | Dolostone, cryptalgal laminated | 2.2 | 427.4 |
| 287 | Grainstone, thinly bedded, cross-laminated, hardground at top, chert nodules at top, colloform Pb-Zn veins | 0.4 | 425.2 |
| 286 | Dolostone, cryptalgal laminated, mudcracks, intraclastic, chert nodules | 0.7 | 424.8 |
| 285 | Dolostone, burrowed | 0.4 | 424.1 |
| 284 | Dolostone, thinly, wavy, and lenticular bedded, scour and fill structures | 0.4 | 323.7 |
| 283 | Dolostone, burrowed | 0.6 | 323.3 |
| 282 | Dolostone, current- and cryptalgal laminated, burrowed top | 1.2 | 322.7 |
| 281 | Covered | 0.4 | 321.5 |
| 280 | Mudstone, cryptalgal laminated, bioclastic, intraclastic | 0.2 | 321.1 |
| 279 | Covered | 0.6 | 320.9 |
| 278 | Grainstone and wackestone, burrowed, fossiliferous | 0.6 | 320.3 |
| 277 | Mudstone and dolostone, cryptalgal laminated | 0.2 | 319.7 |
| 276 | Covered | 1.0 | 319.5 |

| | | | |
|---|---|---|---|
| 275 | Dolostone, cryptalgal laminated, ?current-laminated | 0.2 | 418.5 |
| 274 | Covered | 0.4 | 418.3 |
| 273 | Grainstone, oolitic, bioclastic | 0.2 | 417.9 |
| 272 | Covered | 0.4 | 417.7 |
| 271 | Mudstone, cryptalgal laminated, grainstone beds | 0.4 | 417.3 |
| 270 | Dolostone, cross-laminated | 0.2 | 416.9 |
| 269 | Grainstone, oolitic | 0.5 | 416.7 |

The base of the Aguathuna Formation is exposed immediately north of the north gravel bar, beside the wooden fish-hut

## Catoche Formation

| | | | |
|---|---|---|---|
| 268 | Grainstone, wackestone, and mudstone, interbedded, thinly in the lower half, cross-laminated, fossiliferous, near top several horizons of large, coalesced thrombolite mounds, dolomitic, poorly exposed between the two gravel bars, thickness estimated | 135.0 | 416.2 |
| 267 | Boundstone, thrombolitic, large, greater than 0.7 m diameter, irregular shaped, intertonguing flanking grainstone | 2.0 | 281.2 |
| 266 | Grainstone and wackestone, burrowed | 0.6 | 279.2 |
| 265 | Grainstone, intraclastic | 0.2 | 278.6 |
| 264 | Mudstone, wackestone, and grainstone, burrowed | 0.8 | 278.4 |
| 263 | Grainstone, thinly bedded, cross-laminated, mudstone interbeds | 1.0 | 276.6 |
| 262 | Mudstone and dolostone, cryptalgal laminated, contact with unit 263 intraclastic and eroded | 0.2 | 275.6 |
| 261 | Grainstone, mudstone, and wackestone, interbedded, burrowed in part, lensoidal grainstone beds, rippled | 5.4 | 275.4 |
| 260 | Mudstone and wackestone, burrowed, thin grainstone interbeds | 1.4 | 270.0 |
| 259 | Wackestone, grainstone, and mudstone, interbedded, burrowed in part, lensoidal grainstone beds, rippled | 3.0 | 268.6 |
| 258 | Mudstone, cryptalgal laminated, intraclastic grainstone beds, mudcracks | 2.0 | 265.6 |
| 257 | Grainstone, intraclastic, bioclastic | 0.2 | 263.6 |

| | | | |
|---|---|---|---|
| 256 | Wackestone, grainstone, and mudstone, interbedded, burrowed, cross-lamination | 3.0 | 263.4 |
| 255 | Grainstone and mudstone, thinly interbedded, intraclastic, scattered horizontal burrows, bioclastic | 1.5 | 260.4 |
| 254 | Boundstone, thrombolitic, small mounds | 0.5 | 258.9 |
| 253 | Grainstone and mudstone, thinly interbedded, scattered burrows | 1.0 | 258.4 |
| 252 | Mudstone, cryptalgal laminated, mudcracked, scattered intraclastic beds, grainstone beds near base | 2.2 | 257.4 |
| 251 | Grainstone and mudstone, rippled, scattered bioturbation | 1.5 | 252.2 |

Isthmus Bay Formation

| | | | |
|---|---|---|---|
| 250 | Dolostone, cryptalgal laminated, gradational with unit 251 | 0.3 | 250.7 |
| 249 | Grainstone, mudstone, and dolostone, thinly interbedded, scattered horizontal burrows | 0.8 | 250.4 |
| 248 | Dolostone, cryptalgal laminated | 0.3 | 249.6 |
| 247 | Grainstone and mudstone, thinly interbedded, bed of low-relief stromatolites, scattered burrows, disrupting cryptalgal laminated bed | 0.7 | 249.3 |
| 246 | Dolostone, cryptalgal laminated, intraclastic beds | 0.3 | 248.6 |
| 245 | Grainstone and mudstone, thinly interbedded, scattered burrows, unfossiliferous | 0.7 | 248.3 |
| 244 | Dolostone, cryptalgal laminated | 1.8 | 247.6 |
| 243 | Grainstone and mudstone, thinly interbedded | 0.5 | 246.6 |
| 242 | Grainstone, scattered thrombolite mounds, up to 0.2 m across, fossiliferous | 0.5 | 246.1 |
| 241 | Dolostone, cryptalgal and current-laminated | 1.2 | 245.6 |
| 240 | Grainstone, intraclastic | 0.4 | 244.4 |
| 239 | Dolostone and mudstone, cryptalgal laminated, scattered intraclastic beds | 1.0 | 244.0 |
| 238 | Grainstone and wackestone, burrowed | 0.4 | 243.0 |
| 237 | Grainstone, intraclastic, bioclastic | 0.4 | 242.6 |

| | | | |
|---|---|---|---|
| 236 | Dolostone, cryptalgal laminated, mudcracks with grainstone infillings, scattered grainstone beds | 0.6 | 242.2 |
| 235 | Grainstone, bioclastic | 0.2 | 241.6 |
| 234 | Boundstone, thrombolitic, irregular shape, up to o.2 m across, flanking grainstone bioclastic, oolitic, cross-laminated | 0.4 | 241.4 |
| 233 | Grainstone and dolostone, thinly interbedded, shrinkage cracks in dolostone, torn forming intraclasts, scattered small SH stromatolites | 0.6 | 241.0 |
| 232 | Boundstone, thrombolitic, sponge sticks, Renalcis in cavity | 0.6 | 240.4 |
| 231 | Dolostone, cryptalgal laminated | 0.4 | 239.8 |
| 230 | Grainstone and wackestone, burrowed | 1.2 | 239.4 |
| 229 | Grainstone and dolostone, thinly interbedded, bioclastic, oolitic, hardground surfaces, horizon of LLH stromatolites, shrinkage cracks, torn into intraclasts | 1.2 | 238.2 |
| 228 | Wackestone and grainstone, burrowed | 1.2 | 237.0 |
| 227 | Grainstone, bioclastic, SH stromatolites | 0.2 | 235.8 |
| 226 | Wackestone and grainstone, interbedded, burrowed in part | 0.7 | 235.6 |
| 225 | Grainstone and dolostone, thinly interbedded, bioclastic, scattered small SH stromatolites | 0.5 | 234.9 |
| 224 | Wackestone and grainstone, burrowed | 0.5 | 234.4 |
| 223 | Dolostone, cryptalgal laminated, mudcracked, intraclastic beds | 0.4 | 233.9 |
| 222 | Grainstone and wackestone, burrowed, small thrombolite mounds, irregular shape | 0.3 | 233.5 |
| 221 | Grainstone, oolitic | 0.4 | 233.2 |
| 220 | Dolostone, cryptalgal laminated, ?current-laminated at base | 0.5 | 232.8 |
| 219 | Grainstone wackestone, and mudstone, thinly interbedded, burrowed in part, bioclastic, oolitic, eroded base | 2.4 | 232.3 |
| 218 | Grainstone and wackestone, burrowed, bioclastic, small thrombolite mounds | 0.8 | 229.9 |
| | Small normal fault, 0.2 m displacement, W side upthrown | | |
| 217 | Dolostone, cryptalgal laminated, current laminated, mudcracks | 0.4 | 229.1 |

| | | | |
|---|---|---|---|
| 216 | Grainstone, bioclastic, burrowed towards top | 1.4 | 228.7 |
| 215 | Grainstone and wackestone, thinly interbedded, burrowed | 0.4 | 227.3 |
| 214 | Grainstone, bioclastic, oolitic | 0.6 | 226.9 |
| 213 | Dolostone, burrowed | 0.3 | 226.3 |
| 212 | Dolostone, cryptalgal laminated, current-laminated, scattered grainstone beds, small SH stromatolites | 0.8 | 226.0 |
| 211 | Dolostone, thinly and wavy bedded, cross-lamination, grainstone lenses, bioclastic | 2.7 | 225.2 |
| 210 | Grainstone and wackestone, burrowed | 0.8 | 222.5 |
| 209 | Dolostone, cryptalgal laminated, cross-laminated grainstone beds, brecciated horizons, top is less dolomitic | 1.0 | 221.7 |
| 208 | Grainstone, thinly bedded, some mudstone interbeds, scattered bioturbation | 0.5 | 220.7 |
| 207 | Grainstone and wackestone, burrowed, some fossils, *Lichenaria*-like metazoan clumps | 2.3 | 220.2 |
| 206 | Dolostone, cryptalgal laminated, mudcracks, grainstone beds and mudcrack infillings | 0.3 | 217.9 |
| 205 | Grainstone, mudstone, and dolostone, thinly interbedded, lenticular and wavy bedding, scour and fill structures, grades laterally to dolostone | 0.3 | 217.6 |
| 204 | Grainstone, mudstone, and wackestone, burrowed, small irregular thrombolite mounds | 1.2 | 217.3 |
| 203 | Dolostone, grainstone, and mudstone, thinly, wavy, and lenticular interbedded, current-lamination, scour and fill structures, several beds of LLH stromatolites | 1.4 | 216.1 |
| 202 | Dolostone, breccia of cryptalgal laminated fragments at base, upwards to grainstone, oolitic and intraclastic, and dolomitized with chert nodules | 0.2 | 214.7 |
| 201 | Dolostone, cryptalgal laminated, top brecciated | 0.4 | 214.5 |
| 200 | Boundstone, small, less than 0.1 m diameter SH stromatolites, beds between bioclastic grainstone | 0.2 | 214.1 |
| 199 | Dolostone, burrowed | 1.2 | 213.9 |
| 198 | Dolostone, cryptalgal laminated | 0.6 | 212.7 |
| 197 | Dolostone, thinly, wavy, and lenticular bedded, current-laminated, chert nodules | 0.4 | 212.1 |
| 196 | Dolostone, burrowed, chert nodules preserving small columnar stromatolite mounds at top | 0.6 | 211.7 |

| | | | |
|---|---|---|---|
| 195 | Dolostone, thinly, wavy, and lenticular bedded, current-laminated, chert nodules at top | 0.8 | 211.1 |
| 194 | Dolostone, cryptalgal laminated, top brecciated | 0.2 | 210.3 |
| 193 | Dolostone, thinly, wavy, and lenticular bedded, scattered small SH stromatolites and bioturbation, chert nodules | 0.4 | 210.1 |
| 192 | Grainstone, thinly bedded, burrowed, small thrombolite mounds, chert nodules, lower contact cuts into unit 191 with a lag of round dolostone intraclasts at base, grades laterally to dolostone | 1.0 | 209.7 |
| 191 | Dolostone, cryptalgal laminated, grades laterally to breccia of large angular blocks | 0.7 | 208.7 |
| 190 | Boundstone, thrombolitic, ?corals, cap of grainstone, eroded into a hummocky surface and completely removed over a distance of 10 m, depressions filled with intraclastic dolostone, where eroded out, unit 189 overlain by burrowed dolostone | 0.8 | 208.0 |
| 189 | Dolostone, cryptalgal laminated, chert nodules | 1.8 | 207.2 |
| 188 | Dolostone, epigenetic, 0.6 m thick stromatolites | 0.6 | 205.4 |
| 187 | Dolostone, thinly bedded, burrowed | 1.4 | 204.8 |
| 186 | Grainstone, intraclastic, chert nodules at top | 0.2 | 203.4 |
| 185 | Dolostone, cryptalgal laminated, mudcracks | 0.2 | 203.2 |
| 184 | Dolostone, burrowed, chert nodules | 2.0 | 203.0 |
| 183 | Grainstone and mudstone, thinly bedded, burrowed, SH stromatolites at base | 1.0 | 201.0 |
| 182 | Dolostone, cryptalgal laminated | 2.0 | 200.0 |
| 181 | Grainstone and wackestone, burrowed, bioclastic | 1.0 | 198.0 |
| 180 | Dolostone, thinly bedded, burrowed | 1.0 | 197.0 |
| 179 | Dolostone, thinly, lenticular, and wavy bedded, current-laminated in places, scour and fill structures | 1.0 | 196.0 |
| 178 | Boundstone, thrombolitic, narrow bulbous heads coalesced towards top roofing over narrow channels, eroded channel margins, top is burrowed wackestone and grainstone | 0.9 | 195.0 |
| 177 | Grainstone and mudstone, thinly interbedded, burrowed | 0.3 | 194.1 |
| 176 | Dolostone, cryptalgal laminated | 1.2 | 193.8 |
| 175 | Grainstone, mudstone, and wackestone, burrowed | 1.4 | 192.6 |

| | | | |
|---|---|---|---|
| 174 | Dolostone, cryptalgal laminated | 0.2 | 191.2 |
| 173 | Grainstone and wackestone, bioclastic, small irregular thrombolite mounds, ?corals, burrowed, oncolitic | 0.4 | 191.0 |
| 172 | Dolostone, thinly and lenticular bedded, scour and fill structures | 0.2 | 190.6 |
| 171 | Dolostone, cryptalgal laminated | 0.4 | 190.4 |
| 170 | Grainstone and mudstone, thinly interbedded, burrowed | 2.0 | 190.0 |
| 169 | Dolostone, cryptalgal laminated, mudcracks | 0.4 | 188.0 |
| 168 | Grainstone, mudstone, and dolostone, thinly interbedded, most beds burrowed, layer with shrinkage cracks | 2.1 | 187.6 |
| 167 | Dolostone, cryptalgal laminated | 1.5 | 185.5 |
| 166 | Grainstone, wackestone, and mudstone, thinly interbedded, burrows, at top small, less than 0.1 m SH stromatolites | 0.5 | 184.0 |
| 165 | Wackestone and grainstone, burrowed | 0.6 | 183.5 |
| 164 | Grainstone and wackestone, thinly bedded, burrowed, hardgrounds? | 0.8 | 182.9 |
| 163 | Dolostone, mudstone, and grainstone, thinly, wavy, and lenticular bedded, scour and fill structures, scattered small, less than 0.1 m diameter SH stromatolites | 1.0 | 182.1 |
| 162 | Dolostone, cryptalgal laminated | 0.3 | 181.1 |
| 161 | Grainstone, mudstone, and wackestone, thinly interbedded, burrowed in part, oolitic bed, chert nodules at top | 0.9 | 180.8 |
| 160 | Dolostone, cryptalgal laminated, mudcracked | 0.8 | 179.9 |
| 159 | Grainstone, mudstone, and wackestone, thinly interbedded, burrowed, ripples, one bed of small SH stromatolites | 0.8 | 179.1 |
| 158 | Mudstone and dolostone, cryptalgal laminated | 0.4 | 178.3 |
| 157 | Grainstone, oolitic at base, small SH stromatolites, omission surface | 0.4 | 177.9 |
| 156 | Mudstone, fenestral, cryptalgal laminated | 0.4 | 177.5 |
| 155 | Dolostone and mudstone, cryptalgal laminated, bed of cryptalgal intraclasts | 2.0 | 177.1 |
| 154 | Grainstone and wackestone, burrowed | 0.5 | 175.1 |
| 153 | Dolostone, cryptalgal laminated, deep prism cracks, mudcracks | 3.0 | 174.6 |

| | | | |
|---|---|---|---|
| 152 | Dolostone, thinly, wavy, and lenticular bedded, scour and fill structures, scattered bioturbation, intraclastic base | 1.0 | 172.6 |
| 151 | Grainstone, wackestone, and mudstone, thinly interbedded, burrowed, gastropods, bed of irregular shape SH stromatolites | 2.3 | 171.6 |
| 150 | Dolostone, cryptalgal laminated and thinly bedded, base scoured and cross-laminated | 0.3 | 169.3 |
| 149 | Grainstone, mudstone, wackestone, and dolostone, thinly interbedded, gastropods, burrows and burrowed | 1.4 | 169.0 |
| 148 | Dolostone, thinly bedded, scattered bioturbation | 0.4 | 167.6 |
| 147 | Grainstone, mudstone, and dolostone, thinly interbedded, wavy and lenticular bedding | 0.2 | 167.2 |
| 146 | Grainstone, cross-laminated, bioclastic, intraclastic | 0.2 | 167.0 |
| 145 | Grainstone, mudstone, and wackestone, thinly interbedded, scattered bioturbation | 0.6 | 166.8 |
| 144 | Dolostone, cryptalgal laminated | 2.0 | 166.2 |
| 143 | Grainstone, wackestone, mudstone, and dolostone, thinly interbedded, nodular in places, scattered bioturbation | 1.6 | 164.2 |
| 142 | Boundstone, thrombolitic, less than 0.5 m diameter mounds, developed on top of hardground which is top of unit 141, top planed and capped by grainstone | 0.2 | 162.6 |
| 141 | Mudstone and grainstone, thinly interbedded, imbricated intraclasts | 0.2 | 162.4 |
| 140 | Dolostone, cryptalgal laminated | 0.5 | 162.2 |
| 139 | Grainstone, wackestone, mudstone, and dolostone, thinly interbedded, burrows and burrowed | 1.4 | 161.7 |
| 138 | Boundstone, SH and LLH stromatolites, burrowed mudstone between | 0.2 | 160.3 |
| 137 | Wackestone and grainstone, burrowed, small thrombolite mounds | 0.5 | 160.1 |
| 136 | Grainstone, dolostone, and mudstone, thinly bedded, scattered bioturbation | 1.6 | 159.6 |
| 135 | Grainstone, imbricated intraclastic, herringbone, base is discontinuous mudstone bed | 0.2 | 158.0 |
| 134 | Boundstone, thrombolitic, mounds up to 0.5 m in diameter, eroded into pillars, grainstone between eroded to superimposed hardgrounds, top planed flat, large intraclasts at base | 0.4 | 157.8 |

| | | | |
|---|---|---|---|
| 133 | Mudstone, cryptalgal laminated, fenestral fabric, upper surface eroded to a cuspate surface | 0.1 | 157.4 |
| 132 | Dolostone, mudstone, and grainstone, cryptalgal laminated, chert nodules | 0.8 | 157.3 |
| 131 | Dolostone, mudstone, and grainstone, thinly interbedded, burrowed in places | 0.4 | 156.5 |
| 130 | Grainstone, bioclastic, burrowed, small irregular shaped thrombolites | 1.4 | 156.1 |
| 129 | Dolostone, cryptalgal laminated, shrinkage cracks | 2.4 | 154.7 |
| 128 | Mudstone, dolostone, and grainstone, thinly interbedded, burrowed in places, cross- and herringbone cross-laminated, bioclastic | 2.7 | 152.3 |
| 127 | Mudstone, dolostone, and grainstone, thinly interbedded, nodular, horizontal burrows | 1.6 | 149.6 |
| 126 | Grainstone and mudstone, thinly interbedded, horizontal burrows, bioclastic | 0.6 | 148.0 |
| 125 | Boundstone, large thrombolite mounds up to 0.8 m thick and 2.0 m wide, grainstone between mounds cross-laminated | 1.0 | 147.4 |
| 124 | Boundstone, wavy cryptalgal laminite to LLH stromatolites, chert | 0.4 | 146.4 |
| 123 | Boundstone, large mounds of compound SH type, 1 to 5 m diameter, infill is grainstone and mudstone, thinly interbedded, mudcracked at top | 1.2 | 146.0 |
| 122 | Boundstone, small columnar stromatolite mounds capped by undulating cryptalgal laminite to LLH stromatolites, rare gastropods | 0.2 | 144.8 |
| 121 | Boundstone, low-relief LLH stromatolites, trilobite bits | 0.4 | 144.6 |
| 120 | Mudstone and dolostone, thinly, wavy, and lenticular interbedded | 0.4 | 144.2 |
| 119 | Mudstone, cryptalgal laminated to low-relief LLH stromatolites, beds at top buckled, upper surface eroded into intraclasts and partly silicified | 0.6 | 143.8 |
| 118 | Boundstone, SH to columnar stromatolites, top burrowed mudstone | 0.4 | 143.2 |
| 117 | Boundstone, wavy cryptalgal laminite to LLH stromatolites | 1.0 | 142.8 |
| 116 | Grainstone, mudstone, and dolostone, thinly interbedded, beds of wavy cryptalgal lamination and LLH stromatolites, mudcracks, oolitic | 1.0 | 141.8 |
| 115 | Grainstone, thinly bedded, bioclastic, oolitic, SH stromatolites, top is LLH stromatolites | 1.4 | 140.8 |

| | | | |
|---|---|---|---|
| 114 | Grainstone and mudstone, thinly, lenticular, wavy and nodular interbedded | 1.0 | 139.4 |
| | Fault, striking approximately N 40° W, western side upthrown, unknown but probably minor displacement | | |
| 113 | Dolostone, thinly bedded, burrowed | 0.8 | 138.4 |
| 112 | Dolostone, thinly bedded, scattered bioturbation | 0.8 | 137.6 |
| 111 | Dolostone, thinly bedded, burrowed, several silicified horizons | 2.0 | 136.8 |
| 110 | Dolostone, thinly and lenticular bedded, scattered bioturbation | 1.6 | 134.8 |
| 109 | Dolostone, burrowed, silicified burrows at top | 2.0 | 133.2 |
| 108 | Dolostone, thinly bedded, burrowed, omission surface with silica-lined vugs | 4.7 | 131.2 |
| 107 | Dolostone, cryptalgal laminated | 0.5 | 126.5 |
| 106 | Dolostone, thinly bedded, burrowed | 0.5 | 126.0 |
| 105 | Dolostone, cryptalgal laminated, mudcracks, scattered intraclastic and cross-laminated beds | 1.0 | 125.5 |
| 104 | Dolostone, thinly bedded, scour and fill structures, scattered burrows | 1.8 | 124.5 |
| 103 | Grainstone, mudstone, and wackestone, thinly interbedded, burrowed, cross-laminated, shallow channels, dolostone at top, bioclastic | 2.7 | 122.7 |
| 102 | Dolostone, thinly bedded, many beds burrowed | 2.3 | 120.0 |
| 101 | Mudstone, grainstone, and dolostone, thinly, wavy, and lenticular interbedded, rippled, nodular, bioturbation near top | 1.2 | 117.7 |
| 100 | Dolostone, cryptalgal laminated, scattered intraclastic and disrupted horizons, low stromatolite domes | 1.9 | 116.5 |
| 99 | Dolostone, thinly bedded, scour and fill structures, scattered bioturbation | 1.2 | 114.6 |
| 98 | Dolostone and grainstone, thinly interbedded, cross-laminated, scour and fill structures, vertical burrows, burrowed beds | 7.2 | 113.4 |
| 97 | Dolostone, thinly bedded, current-laminated, cross-laminated | 0.6 | 106.2 |
| 96 | Dolostone, thinly bedded, burrowed | 0.4 | 105.6 |

| | | | |
|---|---|---|---|
| 95 | Grainstone, mudstone, and wackestone, thinly interbedded, horizontal burrows | 1.6 | 105.2 |
| 94 | Grainstone, intraclastic | 0.1 | 103.6 |
| 93 | Mudstone, grainstone, and dolostone, thinly, lenticular, and nodular interbedded | 0.5 | 103.5 |
| 92 | Grainstone, several hardground surfaces | 0.6 | 103.0 |
| 91 | Dolostone, thinly bedded, lenticular, scattered bioturbation | 1.8 | 102.4 |
| 90 | Mudstone and grainstone, thinly interbedded, ripples, horizontal burrows | 0.6 | 100.6 |
| 89 | Dolostone, thinly bedded, current- and cross-laminated, scattered horizontal burrows | 0.8 | 100.0 |
| 88 | Mudstone and grainstone, thinly and lenticular interbedded, cross-laminated, horizontal burrows | 0.4 | 99.2 |
| 87 | Wackestone, burrowed | 1.0 | 98.8 |
| 86 | Grainstone, thinly bedded, cross-laminated, mudcracks, bioclastic, scattered burrows | 0.4 | 97.8 |
| 85 | Mudstone and grainstone, burrowed | 0.4 | 97.4 |
| 84 | Grainstone, thinly and medium bedded, silicified areas | 0.6 | 97.0 |
| 83 | Boundstone, narrow thrombolite mounds | 0.8 | 96.4 |
| 82 | Grainstone, medium bedded, cross-laminated, hardgrounds | 2.4 | 95.6 |
| 81 | Boundstone, horizons of columnar stromatolite mounds 1 to 1.5 m in diameter and 0.4 m thick, with aberrant conical stromatolites, intraclastic between mounds | 1.4 | 93.2 |
| 80 | Dolostone, dolomitized grainstone | 0.4 | 91.8 |
| 79 | Wackestone, burrowed, nearly dolomitized | 0.4 | 91.4 |
| 78 | Boundstone, columnar stromatolite mounds 1.5 m in diameter and 0.4 m thick, flanked and overlain by grainstone, nearly dolomitized | 1.2 | 91.0 |
| 77 | Dolostone, epigenetic, dolomitized grainstone | 0.8 | 89.8 |
| 76 | Dolostone, thinly and lenticular bedded, scour and fill structures, scattered chert nodules | 0.8 | 89.0 |
| 75 | Dolostone, thinly bedded, burrowed, two dolomitized grainstone beds | 2.8 | 88.2 |

Reverse fault, east side upthrown about 2.2 m

| | | | |
|---|---|---|---|
| 74 | Wackestone, thinly bedded, burrowed | 0.2 | 85.4 |
| 73 | Grainstone, nearly dolomitized | 0.4 | 85.2 |
| 72 | Dolostone, thinly bedded, burrowed | 0.6 | 84.8 |
| 71 | Wackestone, thinly bedded, burrowed | 0.2 | 84.2 |
| 70 | Dolostone, thinly bedded, scattered bioturbation, chert at base, replaces beds | 0.8 | 84.0 |
| 69 | Wackestone, grainstone, and mudstone, thinly interbedded, burrowed, parallel lamination | 1.0 | 83.2 |
| 68 | Dolostone, cross-laminated | 0.6 | 82.2 |
| 67 | Wackestone, burrowed | 0.2 | 81.6 |
| 66 | Grainstone, thinly bedded, cross-laminated | 0.6 | 81.4 |
| 65 | Dolostone, thinly bedded, cross-laminated at top, burrowed | 3.2 | 80.8 |
| 64 | Grainstone and mudstone, thinly interbedded, cross-laminated, scattered bioturbation | 8.0 | 77.6 |
| 63 | Covered | 2.2 | 69.6 |
| 62 | Grainstone and mudstone, thinly interbedded, burrowed, dolomitized in upper | 2.0 | 67.4 |
| 57-61 | Boundstone, the Green Head bioherm complex, see text and Fig. 31 for detailed description | 12.0 | 65.4 |
| 56 | Dolostone, epigenetic, burrowed, remnant pod of wackestone and mudstone, gastropods, chert nodules | 7.6 | 53.4 |
| 55 | Dolostone, cryptalgal laminated to low-relief LLH stromatolites, chert nodules | 0.6 | 45.8 |
| 54 | Dolostone, thinly bedded, current-laminated, scour and fill structures | 0.8 | 45.2 |
| 53 | Dolostone, burrowed | 0.8 | 44.4 |
| 52 | Mudstone, cryptalgal laminated to broad low-relief LLH stromatolites, chert nodules and layers | 0.8 | 43.6 |
| 51 | Boundstone, SH stromatolites grading upward to columnar stromatolites, flanking beds interbedded grainstone and dolostone, laterally to wackestone, burrowed, silicification | 1.0 | 42.8 |
| 50 | Dolostone, thinly bedded, scour and fill structures, base intraclastic grainstone, chert | 0.4 | 41.8 |

| | | | |
|---|---|---|---|
| 49 | Dolostone, cryptalgal laminated, chert | 0.2 | 41.4 |
| 48 | Dolostone and grainstone, thinly interbedded, small columnar stromatolite mounds, chert nodules | 0.2 | 41.2 |
| 47 | Dolostone, cryptalgal laminated, chert | 0.2 | 41.0 |
| 46 | Mudstone, burrowed, chert nodules | 0.8 | 40.8 |
| 45 | Dolostone, thinly bedded, current-laminated | 1.5 | 40.0 |
| 44 | Dolostone, thinly bedded, burrowed | 1.5 | 38.5 |
| 43 | Dolostone, thinly and lenticular bedded, current-laminated | 0.2 | 37.0 |
| 42 | Dolostone, cryptalgal laminated, mudcracks, disrupted laminae | 1.0 | 36.8 |
| 41 | Boundstone, LLH stromatolites, dolomitized, chert | 0.2 | 35.8 |
| 40 | Dolostone, thinly bedded, current-laminated, scattered bioturbation | 1.2 | 35.6 |
| 39 | Dolostone, two horizons of small LLH stromatolites, chert | 0.4 | 34.4 |
| 38 | Dolostone, thinly, wavy, and lenticular bedded, cross-laminated lenses, many burrowed beds, intraclastic base | 5.8 | 34.0 |
| 37 | Boundstone, LLH, SH, and compound stromatolites, flanking beds thinly interbedded mudstone and grainstone, mudcracks | 0.6 | 28.2 |
| 36 | Mudstone and grainstone, thinly interbedded, scour and fill structures | 1.0 | 27.6 |
| 35 | Boundstone, small LLH and SH stromatolites | 0.2 | 26.6 |
| 34 | Grainstone, thinly bedded, cross-laminated, scour and fill structures, dolostone at base | 1.4 | 26.4 |
| 33 | Dolostone, oolitic, cherty | 0.1 | 25.0 |
| 32 | Dolostone, thinly bedded, burrowed | 0.4 | 24.9 |
| 31 | Dolostone, thinly bedded, current-laminated, scattered small SH and LLH stromatolites | 0.5 | 24.5 |
| 30 | Dolostone, thinly bedded, burrowed, dolomitized grainstone at top | 1.0 | 24.1 |
| 29 | Boundstone, SH stromatolites, chert, dolomitized | 0.1 | 23.1 |
| 28 | Dolostone, thinly and lenticular bedded, scour and fill structures | 1.1 | 23.0 |

| | | | |
|---|---|---|---|
| 27 | Dolostone, thinly bedded, burrowed, burrowing decreases upward | 1.0 | 21.9 |
| 26 | Boundstone, SH and compound stromatolites, dolomitized | 0.1 | 20.9 |
| 25 | Dolostone, thinly bedded, burrowed | 1.5 | 20.5 |
| 24 | Dolostone, thinly bedded, 0.2 to 0.3 m thick small columnar stromatolite mounds, scattered bioturbation | 1.5 | 19.3 |
| 23 | Boundstone, SH upward to columnar stromatolite mounds, chert | 1.4 | 17.8 |
| 22 | Dolostone, thinly bedded, current- and cryptalgal laminated | 1.0 | 16.4 |
| 21 | Grainstone, oolitic and intraclastic, rippled, mudcracks at top, chert nodules at top | 0.4 | 15.4 |
| 20 | Dolostone, thinly bedded, burrowed | 2.0 | 15.0 |
| 19 | Boundstone, LLH stromatolites, cherty between domes, dolomitized | 0.4 | 13.0 |
| 18 | Dolostone, thinly bedded, current-laminated | 1.0 | 12.6 |
| 17 | Dolostone, cryptalgal laminated, mudcracks at top | 0.8 | 11.6 |
| 16 | Dolostone, thinly bedded, burrowed | 1.0 | 10.8 |
| 15 | Boundstone, LLH stromatolites, dolomitized | 0.2 | 9.8 |
| 14 | Dolostone, thinly bedded, current-laminated | 1.4 | 9.6 |
| 13 | Dolostone, cross-laminated, mudcracks at top | 0.6 | 8.2 |
| 12 | Dolostone, thinly bedded, burrowed, contact with unit 11 is a burrowed breccia (?omission surface) | 1.4 | 7.6 |
| 11 | Dolostone, thinly bedded, current-laminated | 1.2 | 6.2 |
| 10 | Boundstone, LLH stromatolites | 0.3 | 5.0 |
| 9 | Dolostone, oolitic, cross-laminated | 0.3 | 4.7 |
| 8 | Dolostone, thinly bedded, current-laminated, scattered bioturbation | 1.0 | 4.4 |
| 7 | Dolostone, cryptalgal laminated, small LLH stromatolites, intraclastic | 0.1 | 3.4 |
| 6 | Dolostone, thinly bedded, current-laminated | 0.5 | 3.3 |
| 5 | Boundstone, compound stromatolites | 0.4 | 2.8 |

| | | | |
|---|---|---|---|
| 4 | Dolostone, thinly, wavy, and lenticular bedded | 0.6 | 2.4 |
| 3 | Boundstone, LLH stromatolites, chert nodules and beds, mudcracks at top | 0.2 | 1.8 |
| 2 | Dolostone, cryptalgal laminated | 0.2 | 1.6 |
| 1 | Dolostone, thinly bedded, burrowed | 1.4 | 1.4 |

Fault of unknown throw . This point is approximately 35 m above the last Upper Cambrian trilobites

# APPENDIX B

## NORTHEAST GRAVELS

This section was measured along the shore of mainland Newfoundland, beginning at a fault 1.5 km northeast of the Gravels that separate Port au Port Peninsula from the mainland

| Unit | Description | Thickness (m) Unit | Total |
|---|---|---|---|
| | **Table Head Group** | | |
| ---- | Continues upward for an unmeasured thickness of wackestone, burrowed, bioclastic, with many grainstone interbeds | | |
| 3 | Grainstone, cryptalgal laminated, fenestral, bioclastic | 1.0 | 2.55 |
| 2 | Mudstone, burrowed, dark-coloured, scattered chert nodules at base | 1.4 | 1.55 |
| 1 | Dolostone, limy, cryptalgal laminated, chert lithoclasts | 0.15 | 0.15 |
| | Contact sharp and slightly undulating due to compaction around chert nodules | | |
| | **St. George Group** | | |
| | **Aguathuna Formation** | | |
| 37 | Dolostone, finely crystalline, current-laminated, scour and fill structures, chert nodules at top | 3.4 | 36.9 |
| 36 | Covered | 0.4 | 33.5 |
| 35 | Dolostone, cryptalgal laminatd | 1.0 | 33.1 |
| 34 | Dolostone, current-laminated, scour and fill structures | 1.0 | 32.1 |
| 33 | Dolostone, burrowed, silicified burrows | 0.5 | 31.1 |
| 32 | Dolostone, cryptalgal laminated, doming to LLH stromatolites | 0.3 | 30.6 |
| 31 | Dolostone, current-laminated | 0.4 | 30.3 |
| 30 | Wackestone, burrowed, fossiliferous, 3 hardgrounds, the upper with 5 cm relief, oncolitic grainstone in depressions | 0.4 | 29.9 |
| 29 | Dolostone, current-laminated | 1.0 | 29.5 |
| 28 | Dolostone, burrowed | 1.0 | 28.5 |

| | | | |
|---|---|---|---|
| 27 | Mudstone and dolostone, cryptalgal laminated | 0.4 | 27.5 |
| 26 | Dolostone, thinly bedded, burrowed | 5.6 | 27.1 |
| 25 | Grainstone, dolomite-mottled, rare bioclasts and gastropods | 0.2 | 21.5 |
| 24 | Boundstone, thrombolitic, flanked by grainstone, cross-laminated, bioclastic | 0.4 | 21.3 |
| 23 | Grainstone, burrowed | 0.2 | 20.9 |
| 22 | Dolostone, thinly bedded, burrowed | 1.0 | 20.7 |
| 21 | Boundstone, LLH stromatolites, passes laterally to dolostone, current-laminated, cryptalgal intraclastic | 0.2 | 19.7 |
| 20 | Dolostone, current- and cryptalgal laminated, chert nodules in lower | 5.3 | 19.5 |
| 19 | Dolostone, cryptalgal laminated, intraclatic | 0.4 | 14.2 |
| 18 | Mudstone and grainstone, cryptalgal laminated, intraclastic, chert nodules at top | 0.6 | 13.8 |
| 17 | Dolostone, thinly, wavy, and lenticular bedded, scattered bioturbation | 1.8 | 13.2 |
| 16 | Dolostone, cryptalgal laminated, scattered small SH stromatolites, intraclastic near top | 0.4 | 11.4 |
| 15 | Mudstone and grainstone, thinly interbedded, current-oriented gastropods, bioclastic, mudcracks near top, scattered bioturbation, intraclastic at top with SH stromatolites | 1.3 | 11.0 |
| 14 | Dolostone, current-laminated, scour and fill structures, mudcracks at top | 1.0 | 9.7 |
| 13 | Mudstone and dolostone, cryptalgal laminated, doming to LLH stromatolites | 0.2 | 8.7 |
| 12 | Rubble, angular mudstone, cryptalgal laminated, and stromatolite clasts, up to 0.2 m across, rare pelmatozoan debris, shaly matrix | 0.4 | 8.5 |
| 11 | Mudstone, cryptalgal laminated, doming to LLH stromatolites, chert nodules at top | 0.2 | 8.1 |
| 10 | Dolostone, burrowed | 1.0 | 7.9 |
| 9 | Wackestone, burrowed, fossiliferous | 0.8 | 6.9 |
| 8 | Mudstone and dolostone, cryptalgal laminated | 0.3 | 6.1 |
| 7 | Boundstone, LLH stromatolites | 0.3 | 5.8 |

| | | | |
|---|---|---|---|
| 6 | Mudstone and dolostone, cryptalgal laminated, scattered grainstone beds, bioclastic | 1.2 | 5.5 |
| 5 | Boundstone, large compound LLH stromatolotes | 0.6 | 4.3 |
| 4 | Mudstone, cryptalgal laminated, dolomitic in upper, chert nodules at top | 1.2 | 3.7 |
| 3 | Mudstone and dolostone, thinly interbedded | 0.2 | 2.5 |
| 2 | Wackestone and grainstone, burrowed, fossiliferous | 0.8 | 2.3 |
| 1 | Dolostone, burrowed, chert nodules | 1.5 | 1.5 |

## APPENDIX C

### AGUATHUNA QUARRY

This section was measured in two quarries located 1 km west of the village of Aguathuna, Port au Port Peninsula. The base of the section is in the quarry reached by a gravel road to the south of the paved highway 48. A covered interval separates the two quarries. The contact with the Table Head Group is located along the quarry wall 50 m south of the highway. Beds below the section are faulted.

| Unit | Description | Thickness (m) Unit | Total |
|---|---|---|---|
| | **Table Head Group** | | |
| ---- | The basal few metres show a complicated series of facies changes due to the relief of the unconformity. See Fig. 62 for outcrop sketch and lithological characteristics. | | |
| | Contact sharp, with downcutting 4 m into underlying St. George Group. Lithoclasts of upper beds of St. George Group present in basal Table Head limestones. | | |
| | **St. George Group** | | |
| | **Aguathuna Formation** | | |
| 28 | Wackestone, burrowed, chert replacing burrows (1) | 0.4 | 67.4 |
| 27 | Dolostone, cryptalgal laminated upwards to LLH stromatolites, mudcracked, chert nodules | 0.6 | 67.0 |
| 26 | Wackestone, burrowed, fossiliferous (gastropods, sponge spicules, ostracods), silcrete developed where truncated by unconformity | 0.4 | 66.4 |
| 25 | Dolostone, current laminated, thinly bedded | 1.0 | 66.0 |
| 24 | Dolostone, cryptalgal laminated and current laminated, mudcracks, scattered bioturbation, chert nodules at top | 0.6 | 65.0 |
| 23 | Dolostone, medium crystalline, thinly bedded, burrowed, at its deepest point, the unconformity cuts down 1 m into this unit | 4.8 | 64.4 |
| 22 | Dolostone, finely crystalline, ferroan, cryptalgal laminated, layer of undolomitized tepee structures, intraclastic layer | 3.2 | 59.6 |
| 21 | Dolostone, thinly bedded, lenticular bedded, cross- and current laminated, mudcracks, scattered bioturbation | 3.0 | 56.4 |
| 20 | Dolostone, very fine grained, cryptalgal laminated, mudcracks, brecciated horizons, chert nodules at top | 1.8 | 53.4 |

| | | | |
|---|---|---|---|
| 19 | Dolostone, current laminated, thinly and lenticular bedded, cross-laminated in part | 0.6 | 53.0 |
| 18 | Dolostone and mudstone, cryptalgal laminated, mudcracks in upper part | 1.2 | 52.4 |
| 17 | Dolostone, current and ?cryptalgal laminated, cross-laminated at top, chert laminae | 0.6 | 51.2 |
| 16 | Covered. Exposure is patchy along the gravel road to the southern quarry. Thickness estimate is based on estimated 15° dip and paced distance | ~40.0 | 50.6 |
| 15 | Mudstone and grainstone, burrowed, oolitic lens with thin cryptalgal laminated cap | 1.5 | 10.6 |
| 14 | Dolostone, burrowed, lower contact gradational | 1.4 | 9.1 |
| 13 | Dolostone, cryptalgal laminated | 0.8 | 7.7 |
| 12 | Dolostone, finely crystalline, ferroan, current and ?cryptalgal laminated, mudcracks | 0.4 | 6.9 |
| 11 | Mudstone, cryptalgal laminated, intraclastic, dolostone pods with deformed margins, grades laterally to dolostone | 1.8 | 6.5 |
| 10 | Grainstone and dolostone, thinly interbedded, cryptalgal laminated in part, scattered small SH stromatolites, intraclastic at top | 0.6 | 4.7 |
| 9 | Dolostone, cryptalgal laminated | 0.2 | 4.1 |
| 8 | Grainstone, thinly bedded and current laminated, cross-laminated in places, scattered mudstone beds, oolitic | 0.7 | 3.9 |
| 7 | Dolostone, cryptalgal laminated | 0.2 | 3.2 |
| 6 | Mudstone and grainstone, burrowed | 0.4 | 3.0 |
| 5 | Grainstone, thinly bedded, cross-laminated, intraclastic bed, dolostone seams, very finely peloidal beds | 0.8 | 2.6 |
| 4 | Grainstone, very finely peloidal beds, burrowed | 0.2 | 1.8 |
| 3 | Grainstone, cross-laminated, oolitic | 0.4 | 1.6 |
| 2 | Dolostone, cryptalgal laminated | 0.2 | 1.2 |
| 1' | Mudstone and grainstone, burrowed | 1.0 | 1.0 |

(1) Conodonts collected from this bed: ?*Acodus deltatus* Lindström, *Drepanodus*? *gracilis* (Branson & Mehl), *D. parallelus* Branson & Mehl s.f., *D. toomeyi* Ethington & Clark s.f., *Drepanoistodus* sp., *Oepikodus communis* (Ethington & Clark) and oepikodiform, oistodiform, and gothodiform elements,

"Scolopodus cornutiformis" Branson & Mehl, Scolopodus n.sp., and Ulrichodina sp.; the fauna suggests late Canadian age (G. S. Nowlan, written comm., 1979, report no. 01-GSN-1979).

# APPENDIX D

## PORT AU CHOIX

The section was measured along the western coast of Port au Choix Peninsula, beginning at Barbace Point and continuing to Port au Choix bay. The rocks at Barbace Point are epigenetically dolomitized, and beds below are faulted.

| Unit | Description | Thickness (m) Unit | Total |
|---|---|---|---|
| | **St. George Group** | | |
| | **Catoche Formation** | | |
| | Uppermost beds are covered by water. Beds on the south side of the bay may be Table Head Gp. The St. George-Table Head contact figured by Cumming (1968, his fig.5) is interpreted here as a diagenetic contact between limestone and epigenetic dolostone within the Table Head. | | |
| 91 | Mudstone and wackestone, burrowed, fossiliferous, nearly dolostone at top | 8.8 | 116.1 |
| 90 | Wackestone, burrowed, several grainstone beds, fossiliferous | 2.4 | 107.3 |
| 89 | Mudstone and wackestone, burrowed, mostly dolomitized | 1.2 | 104.9 |
| 88 | Covered | 1.5 | 103.7 |
| 87 | Wackestone and mudstone, burrowed, scattered grainstone beds, six thin interbeds of nodular grainstone and dolostone | 4.9 | 102.2 |
| 86 | Grainstone and dolostone, thinly interbedded and nodular | 0.3 | 97.3 |
| 85 | Wackestone and mudstone, burrowed, common grainstone interbeds | 2.4 | 97.0 |
| 84 | Grainstone and dolostone, thinly interbedded, nodular | 0.4 | 94.6 |
| 83 | Boundstone, thrombolitic, coalesced into banks flanked by grainstone | 1.8 | 94.2 |
| 82 | Wackestone and mudstone, burrowed, common grainstone interbeds | 0.6 | 92.4 |
| 81 | Mudstone, burrowed | 0.4 | 91.8 |
| 80 | Grainstone and mudstone, thinly interbedded and nodular | 0.2 | 91.4 |
| 79 | Mudstone, burrowed | 1.7 | 91.2 |

| | | | |
|---|---|---|---|
| 78 | Wackestone and mudstone, burrowed, scattered grainstone beds | 1.5 | 89.5 |
| 77 | Grainstone and dolostone, thinly interbedded and nodular | 0.4 | 88.0 |
| 76 | Wackestone and mudstone, burrowed, scattered grainstone beds, bed of small thrombolite mounds | 3.6 | 87.6 |
| 75 | Covered | 1.0 | 84.0 |
| 74 | Boundstone, thrombolitic, banks up to 3 m wide, grainstone halos, changes laterally to burrowed wackestone | 0.6 | 83.0 |
| 73 | Wackestone and mudstone, burrowed, scattered grainstone channels | 1.0 | 82.4 |
| 72 | Grainstone and dolostone, thinly interbedded and nodular | 0.8 | 81.4 |
| 71 | Boundstone, thrombolitic, banks up to 2 m wide, grainstone halos, changes laterally to burrowed wackestone | 1.4 | 80.6 |
| 70 | Grainstone and dolostone, thinly interbedded and nodular, grainstone channel, cross-lamination | 0.4 | 79.2 |
| 69 | Wackestone and mudstone, burrowed | 1.4 | 78.8 |
| 68 | Grainstone and dolostone, thinly interbedded and nodular | 0.2 | 77.4 |
| 67 | Wackestone and mudstone, burrowed | 2.8 | 77.2 |
| 66 | Boundstone, thrombolitic, banks with grainstone channels between, changes laterally to burrowed wackestone | 1.0 | 74.4 |
| 65 | Wackestone and mudstone, common grainstone channels with cross-lamination | 2.2 | 73.4 |
| 64 | Wackestone and mudstone, burrowed, scattered grainstone beds | 2.8 | 71.2 |
| 63 | Boundstone, thrombolitic, mounds up to 1 m diameter, capping beds are nodular grainstone and dolostone | 1.2 | 68.4 |
| 62 | Wackestone and mudstone, burrowed, scattered grainstone lenses | 1.8 | 67.2 |
| 61 | Grainstone and dolostone, thinly interbedded and nodular | 0.2 | 65.4 |
| 60 | Wackestone and grainstone, burrowed, small thrombolite mounds at top | 0.5 | 65.2 |
| 59 | Grainstone and dolostone, thinly interbedded and nodular | 0.1 | 64.7 |
| 58 | Wackestone, burrowed | 0.6 | 64.6 |
| 57 | Grainstone and dolostone, thinly interbedded and nodular | 0.2 | 64.0 |

| | | | |
|---|---|---|---|
| 56 | Wackestone, burrowed, fossiliferous grainstone bed with small thrombolite mounds | 0.4 | 63.8 |
| 55 | Wackestone and grainstone, burrowed | 1.8 | 63.4 |
| 54 | Grainstone and dolostone, thinly interbedded and nodular | 0.2 | 61.6 |
| 53 | Wackestone and mudstone, burrowed, scattered grainstone layers and lenses, cross-lamination | 6.2 | 61.4 |
| 52 | Grainstone and dolostone, thinly interbedded and nodular | 0.2 | 55.2 |
| 51 | Wackestone and mudstone, burrowed, scattered grainstone beds, cross-lamination | 3.6 | 55.0 |
| 50 | Mudstone, moderately burrowed, scattered gastropods | 1.0 | 51.4 |
| 49 | Wackestone and mudstone, burrowed, scattered graintone beds | 3.4 | 50.4 |
| 48 | Wackestone and mudstone, burrowed, scattered grainstone beds and lenses, very fossiliferous at top (possibly near thrombolite mounds?) | 1.2 | 47.0 |
| 47 | Grainstone and dolostone, thinly interbedded, lenticular, and nodular | 0.2 | 45.8 |
| 46 | Grainstone and dolostone, thinly interbedded, lenticular, scour and fill structures, bioclastic | 0.8 | 45.6 |
| 45 | Mudstone and wackestone, burrowed, several grainstone beds, thickness is estimated due to faulting, unit is correlated to north side of Barbace Cove where equivalent beds have a minimum thickness of 7 m as the upper beds are eroded; throw of fault unknown | 7.0 | 44.8 |
| 44 | Wackestone, burrowed, frequent grainstone beds, small thrombolite mounds at top, changes laterally to ferroan epigenetic dolostone along fractures | 2.4 | 37.8 |
| 43 | Grainstone, intraclastic, herringbone cross-laminated, bioclastic | 0.2 | 35.4 |
| 42 | Grainstone and wackestone, burrowed | 0.2 | 35.2 |
| 41 | Grainstone and packstone, intraclastic, imbricated, herringbone cross-laminated | 0.8 | 35.0 |
| 40 | Dolostone, grainstone, and mudstone, thinly interbedded, scour and fill structures, scattered burrows | 0.3 | 34.2 |
| 39 | Grainstone, intraclastic, imbricated, herringbone cross-laminated | 0.4 | 33.9 |

Section continued on north side of Barbace Cove. There, units 39 to 43 changes to interbedded grainstone, wackestone, and mudstone; the grainstone sequence reappears further north along the sea cliff

| | | | |
|---|---|---|---|
| 38 | Boundstone, thrombolitic, coalesced into bank, changes laterally to epigenetic dolostone | 0.6 | 33.5 |
| 37 | Wackestone, burrowed | 1.0 | 32.9 |
| | Isthmus Bay Formation | | |
| 36 | Boundstone, small thrombolite mounds | 0.2 | 31.9 |
| 35 | Mudstone and dolostone, cryptalgal laminated, mudcracks, scattered intraclastic grainstone laminae | 1.6 | 31.7 |
| 34 | Mudstone, grainstone, and dolostone, thinly interbedded, lenticular, intraclastic in part | 1.4 | 30.1 |
| 33 | Dolostone, finely crystalline, cryptalgal laminated, mudcracked, bioclastic grainstone bed at top | 0.6 | 28.7 |
| 32 | Mudstone and dolostone, thinly interbedded, scour and fill structures, mudcracks at top | 0.4 | 28.1 |
| 31 | Mudstone, burrowed, scattered grainstone beds | 1.4 | 27.7 |
| 30 | Grainstone, mudstone, and dolostone, thinly interbedded, lenticular, scour and fill structures, scattered bioturbation, intraclastic and bioclastic | 1.2 | 26.3 |
| 29 | Mudstone, wackestone, and grainstone, thinly interbedded, lenticular, burrowed, intraclastic and bioclastic | 1.8 | 25.1 |
| 28 | Grainstone, cross-laminated, intraclastic, bioclastic | 0.2 | 23.3 |
| 27 | Mudstone, grainstone, and dolostone, ferroan, thinly interbedded, lenticular | 0.4 | 23.1 |
| 26 | Grainstone, herringbone cross-laminated, intraclastic and bioclastic | 0.2 | 22.7 |
| 25 | Mudstone, grainstone, and dolostone, thinly interbedded, lenticular | 0.4 | 22.5 |
| 24 | Grainstone, cross-laminated, intraclastic and bioclastic | 0.2 | 22.2 |
| 23 | Mudstone and dolostone, thinly interbedded, scour and fill structures | 0.4 | 21.9 |
| 22 | Dolostone, cryptalgal laminated | 0.6 | 21.5 |
| 21 | Mudstone and grainstone, burrowed, grades laterally to epigenetic dolostone | 0.8 | 20.9 |
| 20 | Dolostone, finely crystalline, cryptalgal laminated, mudcracked | 0.4 | 20.1 |
| 19 | Dolostone, thrombolite mounds 1 m diameter | 0.4 | 19.7 |
| 18 | Dolostone, burrowed | 0.8 | 19.3 |
| 17 | Dolostone, thrombolite mounds, circular to elongate, pseudobrecciated in places | 1.5 | 18.5 |

| | | | |
|---|---|---|---|
| 16 | Dolostone, thinly bedded, lenticular, scour and fill structures, scattered bioturbation | 3.0 | 17.0 |
| 15 | Dolostone, burrowed | 1.0 | 14.0 |
| 14 | Dolostone, thinly bedded, lenticular, scour and fill structures | 0.6 | 13.0 |
| 13 | Dolostone, thrombolite mounds, 1 m diameter | 0.8 | 12.4 |
| 12 | Dolostone, thinly bedded, lenticular, scour and fill structures, scattered bioturbation | 1.8 | 11.6 |
| 11 | Covered | 1.0 | 9.8 |
| 10 | Dolostone, cryptalgal laminated | 0.2 | 8.8 |
| 9 | Dolostone, thinly bedded, lenticular, scattered burrows | 0.4 | 8.6 |
| 8 | Dolostone, dolomitized grainstone, fossiliferous | 0.6 | 8.2 |
| 7 | Covered | 0.5 | 7.6 |
| 6 | Dolostone, burrowed | 0.6 | 7.1 |
| 5 | Dolostone, thinly bedded, lenticular, scour and fill structures | 1.0 | 6.5 |
| 4 | Dolostone, burrowed | 0.5 | 5.5 |
| 3 | Dolostone, thinly bedded, burrowed | 2.0 | 5.0 |
| 2 | Dolostone, thinly bedded, scour and fill structures, fossiliferous | 2.0 | 3.0 |
| 1 | Dolostone, thrombolite mounds 0.2 m diameter | 1.0 | 1.0 |

# APPENDIX E

## EDDIES COVE WEST

The section begins in nearly flat-lying beds at Fish Point, 4 km northeast of Eddies Cove West, where beds are badly faulted and epigenetically dolomitized. Strata continue upwards along the coast southwestward for a horizontal distance of 16 km toward Port au Choix.

| Unit | Description | Thickness (m) Unit | Total |
|---|---|---|---|
| | **Table Head Group** | | |
| ---- | Typical dark-coloured Table Head limestones, burrowed wackestone, mudstone, dolomitic, continues to the top of the cliff for an unmeasured thickness | | |
| 5 | Mudstone and grainstone, thinly interbedded, cryptalgal laminated in part, peloidal | 1.0 | 3.8 |
| 4 | Dolostone, finely crystalline, massive | 0.6 | 2.8 |
| 3 | Mudstone to wackestone, mottled, nodular | 1.2 | 2.2 |
| 2 | Mudstone to wackestone, laminoid fenestral fabric in part, ostracode valves | 0.4 | 1.0 |
| 1 | Mudstone to wackestone, nodular, stylolitic, ostracode valves | 0.6 | 0.6 |
| | Contact sharp with no downcutting visible along several tens of metres of outcrop. | | |
| | **St. George Group** | | |
| | **Aguathuna Formation** | | |
| 143 | Dolostone, finely crystalline, ferroan, massive with laminated parts. | 6.0 | 171.5 |
| | **Catoche Formation** | | |
| 142 | Dolostone, epigenetic, burrowed, scattered dolomitized grainstone beds and lenses, scattered horizons of poorly preserved thrombolite mounds | ~30.0 | 165.5 |
| 141 | Covered in bay | 8.0 | 135.5 |
| 140 | Wackestone and mudstone, burrowed, frequent grainstone beds, channels and lenses, scattered small thrombolite mound horizons, grades laterally to epigenetic dolostone | 5.2 | 127.5 |

| | | | |
|---|---|---|---|
| 139 | Grainstone, mudstone, and dolostone, thinly interbedded and nodular | 1.0 | 122.5 |
| 138 | Wackestone and mudstone, burrowed, frequent grainstone beds and lenses, scattered horizons of small thrombolite mounds | 9.7 | 121.3 |
| 137 | Cover | 0.4 | 111.6 |
| 136 | Wackestone and mudstone, burrowed, frequent grainstone beds and lenses, horizons of small thrombolite mounds, some coalescing into small banks | 1.4 | 111.2 |
| 135 | Wackestone and mudstone, burrowed, grainstone beds, lenses, small thrombolites, chert nodules | 4.4 | 109.8 |
| 134 | Boundstone, thrombolitic, banks up to 1 m by 3 m | 0.6 | 105.4 |
| 133 | Wackestone, mudstone, and grainstone, interbedded, burrowed | 1.0 | 104.4 |
| 132 | Grainstone and dolostone, thinly interbedded, nodular | 0.4 | 103.4 |
| 131 | Boundstone, thrombolitic, coalesced to banks 2 m diameter | 1.2 | 103.0 |
| 130 | Mudstone, wackestone, and grainstone, thinly bedded in upper half, burrowed | 4.0 | 101.8 |
| 129 | Covered | 0.5 | 97.8 |
| 128 | Boundstone, thrombolitic, coalesced to banks up to 5 m wide and 50 m long | 0.4 | 97.3 |
| 127 | Wackestone, burrowed, many linear grainstone channels | 2.0 | 96.9 |
| 126 | Wackestone and mudstone, burrowed | 3.0 | 94.9 |
| 125 | Grainstone and dolostone, thinly interbedded and nodular | 0.2 | 91.9 |
| 124 | Wackestone and mudstone, burrowed, scattered grainstone lenses | 1.6 | 91.7 |
| 123 | Wackestone, mudstone, grainstone, and dolostone, thinly interbedded, nodular, bioclastic, cross-lamination | 1.0 | 90.1 |
| 122 | Mudstone and wackestone, burrowed | 2.2 | 89.1 |
| 121 | Covered | 0.5 | 86.9 |
| 120 | Mudstone and wackestone, burrowed | 1.2 | 86.4 |

| | | | |
|---|---|---|---|
| 119 | Grainstone, mudstone, and dolostone, thinly interbedded and nodular, intraclastic grainstone channels | 0.8 | 85.2 |
| 118 | Grainstone, mudstone, and wackestone, burrowed, cross-lamination, top with herringbone cross-lamination | 2.0 | 84.8 |
| 117 | Grainstone, wackestone, and mudstone, burrowed, cross-laminated channels | 1.6 | 82.8 |
| 116 | Grainstone and dolostone, thinly interbedded, lenticular, herringbone cross-lamination | 0.4 | 81.2 |
| 115 | Mudstone and wackestone, burrowed | 1.6 | 80.8 |
| 114 | Grainstone and wackestone, interbedded, lensoidal, cross-laminated, burrowed, intraclastic | 1.0 | 79.2 |
| 113 | Mudstone, wackestone, and grainstone, interbedded, lensoidal, nodular, burrowed in part | 1.4 | 78.2 |
| 112 | Boundstone, thrombolitic, up to 1 m diameter, grainstone halo | 0.4 | 76.8 |
| 111 | Mudstone, burrowed | 1.0 | 76.4 |
| 110 | Wackestone, packstone, and grainstone, thinly interbedded, cross-laminated | 2.0 | 75.4 |
| 109 | Covered | 0.5 | 73.4 |
| 108 | Wackestone, burrowed | 1.0 | 72.9 |
| 107 | Covered | 0.5 | 71.9 |
| 106 | Boundstone, thrombolitic, up to 1.2 m in diameter, coalescing to form a bank 50 m across, grading off the flank to burrowed wackestone | 1.6 | 71.4 |
| 105 | Grainstone and mudstone, thinly interbedded, burrowed | 0.4 | 69.8 |
| 104 | Mudstone, burrowed, scattered molluscs | 0.2 | 69.4 |

## Isthmus Bay Formation

| | | | |
|---|---|---|---|
| 103 | Mudstone, cryptalgal laminated | 0.2 | 69.2 |
| 102 | Grainstone, cross-laminated and parallel laminated, bioclastic and intraclastic | 0.6 | 69.0 |
| 101 | Mudstone, cryptalgal laminated, petroliferous | 0.6 | 68.4 |
| 100 | Grainstone, intraclastic | 0.1 | 67.8 |
| 99 | Mudstone and wackestone, thinly interbedded, burrowed | 0.3 | 67.7 |

| | | | |
|---|---|---|---|
| 98 | Wackestone and grainstone, burrowed, small thrombolite mounds, graded bedding | 0.1 | 67.4 |
| 97 | Wackestone, mudstone, and dolostone, thinly interbedded, burrowed, intraclastic, bioclastic | 0.4 | 67.3 |
| 96 | Dolostone, cryptalgal laminated, mudcracked | 0.6 | 66.9 |
| 95 | Mudstone, grainstone, and wackestone, thinly interbedded, rippled beds, exhumed scoured surfaces | 1.8 | 66.3 |
| 94 | Grainstone, mudstone, and dolostone, thinly interbedded, lenticular, scour and fill structures, scattered bioturbation increasing upwards | 1.2 | 64.5 |
| 93 | Grainstone, packstone, cross-laminated, bioclastic | 0.4 | 63.3 |
| 92 | Dolostone and mudstone, thinly interbedded, lenticular, scour and fill structures | 0.3 | 62.9 |
| 91 | Grainstone, cross-laminated, intraclastic, bioclastic | 0.4 | 62.6 |
| 90 | Dolostone, grainstone, and mudstone, thinly interbedded, scour and fill structures, mudcracks near top, ripples | 0.5 | 62.2 |
| 89 | Mudstone, cryptalgal laminated, lenses of intraclastic grainstone | 0.4 | 61.7 |
| 88 | Dolostone, cryptalgal laminated, mudcracked, intraclastic, chert nodules | 0.6 | 61.3 |
| 87 | Covered | 2.5 | 60.7 |
| 86 | Boundstone, large 2.5 m diameter and 0.8 m thick LLH compound stromatolites, overlain by 1.4 m thick aberrant columnar stromatolite boxwork overlain by thrombolites, oolitic, chert nodules | 2.2 | 58.2 |
| 85 | Mudstone and grainstone, thinly interbedded, burrows, partly dolomitized | 0.7 | 56.0 |
| 84 | Dolostone, thinly bedded, lenticular bedding, scour and fill structures, scattered SH stromatolites at top | 1.6 | 55.3 |
| 83 | Mudstone, wackestone, and grainstone, burrowed | 0.9 | 53.7 |
| 82 | Boundstone, thrombolitic, 1 m diameter mounds, many coalesced | 1.2 | 52.8 |
| 81 | Boundstone, columnar and SH stromatolites, separated by thinly interbedded grainstone and dolostone, cross-laminated | 0.8 | 51.4 |
| 80 | Dolostone and mudstone, thinly interbedded, lenticular bedding, scour and fill structures, scattered gastropods, vertical burrows | 0.4 | 50.6 |

| | | | |
|---|---|---|---|
| 79 | Dolostone and mudstone, thinly interbedded, lenticular bedding, scour and fill structures, scattered gastropods, Lingula, vertical burrows | 1.4 | 50.2 |
| 78 | Mudstone and wackestone, thinly bedded, burrowed | 0.7 | 48.8 |
| 77 | Dolostone and grainstone, thinly interbedded, lenticular bedding, cross-laminated, scour and fill structures, channelling, vertical burrows, dolomitized anhydrite rosettes | 1.2 | 48.1 |
| 76 | Wackestone and grainstone, burrowed in part, cross-lamination, intraclastic, bioclastic | 0.4 | 46.9 |
| 75 | Boundstone, columnar stromatolite mounds 0.2 m diameter, between mounds is thinly bedded grainstone, mudstone, and dolostone, scour and fill structures | 0.4 | 46.5 |
| 74 | Mudstone and dolostone, thinly bedded, lenticular, scour and fill structures, ripples, scattered bioturbation | 0.2 | 46.1 |
| 73 | Dolostone, burrowed, scattered gastropods | 0.4 | 45.9 |
| 72 | Mudstone and dolostone, thinly interbedded, lenticular, scour and fill structures, scattered bioturbation | 1.0 | 45.5 |
| 71 | Grainstone, mudstone, and dolostone, thinly interbedded, lenticular bedding in places, scour and fill structures, scattered bioturbation, oolitic | 1.0 | 44.5 |
| 70 | Dolostone and mudstone, thinly interbedded, lenticular, scour and fill sturcutres, scattered lenses and beds of burrows, megaquartz vugs | 0.5 | 43.5 |
| 69 | Mudstone and grainstone, thinly interbedded, lenticular, graded, cross-laminated, scour and fill structures, bioclastic, scattered bioturbation | 1.0 | 43.0 |
| 68 | Covered in sandy beach | 1.0 | 42.0 |
| 67 | Wackestone, grainstone, and mudstone, thinly interbedded, scattered cross-lamination, scattered bioturbation | 0.5 | 41.0 |
| 66 | Dolostone and mudstone, thinly interbedded, lenticular bedding, scour and fill structures, scattered burrowed beds and lenses | 0.5 | 40.5 |
| 65 | Grainstone and mudstone, thinly interbedded, ripples | 0.2 | 40.0 |
| 64 | Mudstone, burrowed | 0.2 | 39.8 |
| 63 | Mudstone and grainstone, thinly interbedded, hardground, scattered bioturbation | 0.2 | 39.6 |

| | | | |
|---|---|---|---|
| 62 | Mudstone, wackestone, and dolostone, thinly and lenticular bedded, scour and fill structures, intraclastic | 0.2 | 39.4 |
| 61 | Mudstone and grainstone, thinly bedded, scattered bioturbation, passes laterally under wharf at Eddies Cove West village to epigenetic dolostone | 1.0 | 39.2 |
| 60 | Mudstone, wackestone, grainstone, and dolostone, thinly interbedded, burrowed beds | 2.0 | 38.2 |
| 59 | Boundstone, thrombolitic, up to 0.3 m diameter mounds, between is thinly interbedded grainstone and dolostone | 0.4 | 36.2 |
| 58 | Mudstone and dolostone, thinly interbedded, scattered vertical burrows, scattered small thrombolite mounds | 0.6 | 35.8 |
| 57 | Boundstone, thrombolitic, 0.2 m in diameter | 0.6 | 35.2 |
| 56 | Mudstone, thinly bedded, burrowed | 0.4 | 34.6 |
| 55 | Mudstone, thinly, wavy and lenticular bedded | 0.5 | 34.2 |
| 54 | Mudstone and dolostone, thinly, wavy and lenticular bedded | 0.5 | 33.7 |
| 53 | Boundstone, thrombolitic with Lichenaria, up to 1 m in diameter, coalesced | 0.8 | 33.2 |
| 52 | Dolostone, thinly bedded, current lamination | 0.8 | 32.4 |
| 51 | Boundstone, thrombolitic, dolomitized grainstone between mounds | 0.4 | 31.6 |
| 50 | Boundstone, thrombolitic, 0.2 m diameter, stromatolitic cap forming LLH | 0.4 | 31.2 |
| 49 | Mudstone and wackestone, thinly bedded, burrowed, scattered small thrombolite mounds | 0.6 | 30.8 |
| 48 | Boundstone, thrombolitic, 1 m diameter, thinly bedded dolostone between mounds, scour and fill structures, scattered burrows, dolomite-fluorite-filled vugs and fractures | 0.6 | 30.2 |
| 47 | Grainstone, thinly bedded | 0.2 | 29.6 |
| 46 | Mudstone and dolostone, thinly, lenticular bedded, scour and fill structures, scattered vertical burrows | 2.2 | 29.4 |
| 45 | Wackestone, grainstone, and mudstone, thinly interbedded, bioclastic, scattered bioturbation | 0.3 | 27.2 |
| 44 | Wackestone, burrowed, fossiliferous, scattered small thrombolite mounds | 0.3 | 26.9 |

| | | | |
|---|---|---|---|
| 43 | Mudstone and dolostone, thinly and lenticular bedded, scattered burrows | 1.0 | 26.6 |
| 42 | Dolostone, thinly bedded, lenticular bedding, current lamination, scour and fill structures, dolomite-fluorite vugs * | 0.6 | 25.6 |
| 41 | Boundstone, columnar stromatolite mounds up to 1 m in diameter, coalescing, capped by simple SH stromatolites, flanking grainstone, bioclastic | 1.0 | 25.0 |
| 40 | Grainstone, mudstone, and wackestone, thinly interbedded, vertical burrows in grainstone beds | 0.6 | 24.0 |
| 39 | Dolostone, cryptalgal laminated, inctraclastic | 0.2 | 23.4 |
| 38 | Dolostone, thinly bedded, scour and fill structures | 0.4 | 23.2 |
| 37 | Grainstone and wackestone, thinly interbedded, vertical burrows, fossiliferous with molluscs | 0.8 | 22.8 |
| 36 | Dolostone, cryptalgal laminated, upper 0.4 m brecciated | 1.8 | 22.0 |
| 35 | Mudstone and dolostone, thinly interbedded, lenticular, scour and fill structures, scattered vertical burrows | 0.4 | 20.2 |
| 34 | Grainstone, wackestone, and mudstone, thinly interbedded, cross-lamination, ripples, vertical burrows, gastropods | 1.6 | 19.8 |
| 33 | Grainstone, wackestone, and mudstone, thinly interbedded, scattered 5 cm diameter SH stromatolites, chert | 0.1 | 18.2 |
| 32 | Covered | 1.0 | 18.1 |
| 31 | Grainstone and wackestone, thinly interbedded, burrowed, intraclastic, vertical burrows in grainstone | 0.4 | 17.1 |
| 30 | Boundstone, thrombolitic, coalescing to a bank | 0.6 | 16.7 |
| 29 | Dolostone, cryptalgal laminated, intraclastic | 0.4 | 16.1 |
| 28 | Boundstone, low-relief SH stromatolites, 1 m by several m in diameter, between mounds dolostone, thinly bedded with scour and fill structures | 0.2 | 15.7 |
| 27 | Dolostone and mudstone, thinly interbedded, scour and fill structures | 0.4 | 15.5 |
| 26 | Dolostone and mudstone, thinly interbedded, burrowed | 0.2 | 15.1 |
| 25 | Dolostone, thinly, lenticular bedded, scour and fill structures, scattered small SH stromatolites | 0.3 | 14.9 |
| 24 | Dolostone, cryptalgal laminated, intraclastic | 0.3 | 14.6 |

| | | | |
|---|---|---|---|
| 23 | Dolostone, thinly bedded, scour and fill structure | 0.3 | 14.3 |
| 22 | Dolostone, thinly bedded, burrowed | 0.3 | 14.0 |
| 21 | Mudstone, burrowed, scattered gastropods, silicification of some burrows | 0.4 | 13.7 |
| 20 | Dolostone, cryptalgal laminated, intraclastic near top, possible current lamination | 0.5 | 13.3 |
| 19 | Mudstone and dolostone, thinly bedded, scour and fill structure | 0.2 | 12.8 |
| 18 | Mudstone and dolostone, thinly bedded, burrowed, scattered gastropods | 0.2 | 12.6 |
| 17 | Dolostone, thinly bedded, current laminated, scattered burrows, possible cryptalgal lamination | 1.0 | 12.4 |
| 16 | Boundstone, thrombolitic, 0.3 m diamter, coalesced to small banks, between mounds is dolostone with scour and fill structures | 0.4 | 11.4 |
| 15 | Wackestone, thinly bedded, burrowed, grainstone bed at top | 0.4 | 11.0 |
| 14 | Dolostone, thinly bedded, scour and fill structure, angular intraclasts at base | 0.2 | 10.6 |
| 13 | Grainstone, oolitic, dolomitized in lower part, top is silicified ripples | 0.2 | 10.4 |
| 12 | Mudstone, scattered grainstone beds, burrowed | 0.8 | 10.2 |
| 11 | Wackestone, grainstone, and packestone, thinly interbedded | 0.4 | 9.4 |
| 10 | Covered | 0.5 | 9.0 |
| 9 | Boundstone, thrombolitic, mounds up to 1 m diameter, between is bioclastic grainstone and dolostone, grades laterally to epigenetic dolostone and pseudobreccia, chert nodules | 0.8 | 8.5 |
| 8 | Dolostone, epigenetic, burrowed | 0.4 | 7.7 |
| 7 | Wackestone and packstone, thinly bedded, burrowed, lensoidal grainstone beds, cross-laminated, top is partly dolomitic and nodular | 1.6 | 7.3 |
| 6 | Grainstone, wackestone, and mudstone, thinly interbedded, cross-lamination, scattered burrows | 0.6 | 5.7 |
| 5 | Mudstone and wackestone, thinly bedded, burrowed | 1.4 | 5.1 |

| | | | |
|---|---|---|---|
| 4 | Grainstone, mudstone, and wackestone, thinly interbedded, cross-lamination, intraclastic, scattered gastropods, burrows | 3.6 | 3.7 |
| 3 | Mudstone, wackestone, and grainstone, thinly interbedded and nodular, patches of cryptalgal laminite changing upwards to small SH stromatolites | 1.0 | 1.7 |
| 2 | Boundstone, LLH stromatolites of low relief, up to 2 m diameter | 0.2 | 0.7 |
| 1 | Mudstone and dolostone, thinly interbedded, scour and fill structures, patches of cryptalgal laminite changing upwards to small SN stromatolites, passes laterally to epigenetic dolostone | 0.5 | 0.5 |

* Fluid inclusions in fluorite analyzed by N. Higgins (pers. comm., 1979) are free from particles (inclusions froze at -69°C), implying slow-moving precipitating solution. Salinity average is 17 wt% NaCl, but few NaCl crystals present at room temperature suggest appreciable concentration of other dissolved species. Minimum estimate to keep fluid from boiling indicates very shallow depths of emplacement, a minimum of 20 to 30 m. Temperature range of fluorite formation 120° - 160°.

# APPENDIX F

## BOAT HARBOUR

The section was measured beginning on the northeast side of Lower Cove, 8 km southwest of Boat Harbour. Strata continue northeastward along the sea cliff, broken by Watts Bight and Ope Bay covered areas and small faults southwest of Boat Harbour on Boat Head. The section continues along the coast, with several faulted and covered intervals, to a point 4 km northeast of Boat Harbour at the garbage dump.

| Unit | Description | Thickness (m) Unit | Total |
|---|---|---|---|
| | **St. George Group** | | |
| | **Catoche Formation** | | |
| ---- | Coarsely crystalline epigenetic dolostone continues upward for an unknown thickness until it is faulted out | | |
| 153 | Wackestone and mudstone, burrowed, scattered grainstone lenses with cross-lamination, chert nodules | 4.0 | 167.5 |
| | **Isthmus Bay Formation** | | |
| 152 | Dolostone, cryptalgal laminated | 0.4 | 163.5 |
| 151 | Grainstone, thinly bedded, bioclastic, scattered horizonatal burrows, mudcracks, dolomitic partings | 4.0 | 163.1 |
| 150 | Grainstone and wackestone, burrowed | 2.0 | 159.1 |
| 149 | Grainstone and wackestone, interbedded, some bioturbation | 1.0 | 157.1 |
| 148 | Grainstone, cross-laminated, scattered SH stromatolites | 0.2 | 156.1 |
| 147 | Wackestone, burrowed, common grainstone lenses | 0.6 | 155.9 |
| 146 | Grainstone, cross-laminated, intraclastic, bioclastic, oolitic | 0.2 | 155.3 |
| 145 | Wackestone and grainstone, burrowed | 0.6 | 155.1 |
| 144 | Dolostone, cryptalgal laminated, changes laterally to SH stromatolites over 100 m | 0.2 | 154.5 |
| 143 | Mudstone and dolostone, thinly interbedded, burrowed | 0.4 | 154.3 |
| 142 | Wackestone, burrowed, grainstone bed at top | 0.3 | 153.9 |

| | | | |
|---|---|---|---|
| 141 | Boundstone, thrombolitic, small mounds | 0.3 | 153.6 |
| 140 | Wackestone, burrowed | 0.6 | 153.3 |
| 139 | Grainstone and dolostone, cryptalgal laminated, intraclastic, mudcracked, changes laterally over 100 m to burrowed interbedded wackestone and dolostone | 0.2 | 152.7 |
| 138 | Grainstone, burrowed, fossiliferous, thrombolite mounds up to 0.2 m diameter | 0.2 | 152.5 |
| 137 | Boundstone, thrombolitic, mounds 1 m diameter | 1.2 | 152.3 |
| 136 | Wackestone, burrowed | 0.4 | 151.1 |
| 135 | Grainstone, cross-laminated | 0.2 | 150.7 |
| 134 | Wackestone, burrowed | 0.5 | 150.5 |
| 133 | Grainstone, cross-laminated | 0.2 | 150.0 |
| 132 | Wackestone, burrowed | 0.5 | 149.8 |
| 131 | Grainstone, scattered small SH stromatolites at base, intraclastic at top | 0.2 | 149.3 |
| 130 | Mudstone, burrowed | 0.5 | 149.1 |
| 129 | Mudstone and dolostone, cryptalgal laminated, intraclastic beds | 0.2 | 148.6 |
| 128 | Wackestone, burrowed | 0.2 | 148.4 |
| 127 | Grainstone, cross-laminated, bioclastic | 0.2 | 148.2 |
| 126 | Wackestone and grainstone, burrowed | 0.2 | 148.0 |
| 125 | Dolostone, coarsely crystalline, dolomitized grainstone at base and burrow-mottled in upper | 0.2 | 147.8 |
| 124 | Dolostone, ferroan, lower part mottled, chert pebble lag in middle, top of bed is hummocky with rounded pits and highs | 0.8 | 147.6 |
| 123 | Wackestone and grainstone, burrowed, epigenetic dolostone circular pods 0.2 to 2 m in diameter | 5.6 | 147.6 |
| 122 | Wackestone and grainstone, burrowed, one corrosion surface | 0.6 | 141.2 |
| 121 | Mudstone and dolostone, cryptalgal laminated, scattered intraclasts | 0.4 | 140.6 |
| 120 | Covered | 2.0 | 140.2 |

| | | | |
|---|---|---|---|
| 119 | Mudstone and dolostone, cryptalgal laminated | 0.2 | 138.2 |
| 118 | Boundstone, thrombolitic, small mounds | 0.4 | 138.0 |
| 117 | Boundstone, LLH stromatolites 0.3 m diameter | 0.4 | 137.6 |
| 116 | Boundstone, thrombolitic, isolated mounds | 0.8 | 137.2 |
| 115 | Grainstone. cross-laminated, oolitic, cherty, changes laterally to LLH stromatolites | 0.2 | 136.4 |
| 114 | Boundstone, LLH stromatolites | 0.2 | 136.2 |
| 113 | Mudstone and dolostone, thinly interbedded, scour and fill structures, base stylolitized into unit 112 along lineation which changes to a fault | 0.4 | 136.0 |
| 112 | Wackestone and dolostone, thinly interbedded, burrowed | 1.0 | 135.6 |
| 111 | Mudstone, wavy cryptalgal laminated, doming to low-relief LLH stromatolites, top of unit stylolitized into unit 112 along lineation which becomes a fault | 0.2 | 134.6 |
| 110 | Mudstone and dolostone, thinly interbedded, lenticular, scour and fill structures, bed of low-relief LLH stromatolites | 1.3 | 134.4 |
| 109 | Boundstone, thrombolitic, isolated mounds | 1.0 | 133.1 |
| 108 | Wackestone, burrowed | 0.2 | 132.1 |
| | Fault striking N 50° E, normal with NW beds upthrown about 1 to 1.5 m, pseudobreccia developed along the lineation | | |
| 107 | Boundstone, thrombolitic, large mounds, up to 3 m in diameter, coalescing to banks | 2.4 | 131.9 |
| 106 | Mudstone and dolostone, thinly interbedded, scour and fill structures, small patches of short columnar stromatolites at top | 0.8 | 129.5 |
| 105 | Mudstone, wackestone, and grainstone, interbedded, burrowed | 1.0 | 128.7 |
| 104 | Boundstone, thrombolite mounds 0.5 m across, flanked by wackestone, burrowed | 0.8 | 127.7 |
| 103 | Mudstone and dolostone, thinly interbedded, scour and fill structures, bioturbation in upper part | 0.6 | 126.9 |
| 102 | Wackestone, burrowed | 2.0 | 126.3 |
| 101 | Covered | 5.0 | 124.3 |

| | | | |
|---|---|---|---|
| 100 | Wackestone, burrowed | 1.0 | 119.3 |
| 99 | Covered | 2.0 | 118.3 |
| 98 | Boundstone, thrombolitic, flanked by wackestone, burrowed, grades laterally to epigenetic dolostone and pseudobreccia | 0.8 | 116.3 |
| 97 | Dolostone, cryptalgal laminated, doming at top to low-relief LLH stromatolites | 1.0 | 115.5 |
| 96 | Grainstone and wackestone, interbedded, burrowed beds, grades laterally to epigenetic dolostone and pseudobreccia | 3.5 | 114.5 |
| 95 | Covered, possible fault | 4.0 | 111.0 |
| 94 | Dolostone, epigenetic and pseudobreccia, stromatolitic, faulted | 2.0 | 107.0 |
| 93 | Covered | 3.0 | 105.0 |
| 92 | Wackestone, burrowed, grades laterally to epigenetic dolostone and pseudobreccia | 1.0 | 102.0 |
| 91 | Covered | 4.0 | 101.0 |
| 90 | Grainstone, wackestone, and mudstone, thinly interbedded, lenticular, burrows | 4.6 | 97.0 |
| 89 | Covered | 1.0 | 92.4 |
| 88 | Boundstone, LLH stromatolites, 0.2 m across, chert nodules at top | 0.4 | 91.4 |
| 87 | Grainstone, wackestone, and mudstone, thinly interbedded, scour and fill structures in lower part, burrowed beds | 2.0 | 91.0 |
| 86 | Boundstone, thrombolitic, mounds 1.5 m in diameter, coalescing into banks, flanked by grainstone and wackestone, thinly interbedded | 1.4 | 89.0 |
| 85 | Mudstone and dolostone, thinly interbedded, scour and fill structures | 0.4 | 87.6 |
| 84 | Grainstone, wackestone, and mudstone, thinly interbedded, common burrows | 1.0 | 87.2 |
| 83 | Boundstone, thrombolitic, mounds 1 m in diameter, in places coalescing to banks, flanked by wackestone, mudstone, and grainstone, thinly interbedded | 1.2 | 86.2 |
| 82 | Wackestone, mudstone, thinly interbedded, horizontal burrows | 0.8 | 85.0 |

| | | | |
|---|---|---|---|
| 81 | Boundstone, thrombolitic, mounds 1 m in diameter, coalescing into banks, flanked by mudstone and dolostone, thinly interbedded | 1.4 | 84.2 |
| 80 | Grainstone and wackestone, thinly interbedded, horizontal burrows | 0.6 | 82.8 |
| 79 | Mudstone and dolostone, crytpalgal laminated | 0.4 | 82.2 |
| 78 | Boundstone, SH stromatolites, chert nodules around tops of mounds | 0.2 | 81.8 |
| 77 | Grainstone and packstone, thinly interbedded, thrombolite mounds, 0.5 m in diameter and thickness | 1.0 | 81.6 |
| 76 | Grainstone and wackestone, thinly interbedded, burrows | 1.0 | 80.4 |
| 75 | Covered | 0.5 | 79.4 |
| 74 | Wackestone, burrowed | 0.2 | 78.9 |
| 73 | Covered | 1.0 | 78.7 |
| 72 | Mudstone and dolostone, cryptalgal laminated, large desiccation polygons | 0.4 | 77.7 |
| 71 | Dolostone, burrowed | 1.5 | 77.3 |
| 70 | Dolostone, epigenetic, pseudobreccia, burrowed, gastropods preserved | 0.4 | 75.8 |
| 69 | Mudstone and dolostone, thinly interbedded, scour and fill structures, mudcracks | 0.6 | 75.4 |
| 68 | Dolostone, epigenetic, pseudobreccia | 1.5 | 74.8 |
| 67 | Dolostone, thinly bedded, scour and fill structures, scattered bioturbation | 0.4 | 73.[illegible] |
| 66 | Dolostone, epigenetic, chert nodules at top | 0.5 | 72.9 |
| 65 | Covered in Boat Harbour. Thickness not exposed estimated by Knight (1977b) as 25 m | 5.0 | 72.4 |
| 64 | Dolostone, thinly bedded, scour and fill structures | 0.4 | 67.4 |
| 63 | Dolostone, burrowed | 0.6 | 67.0 |
| 62 | Dolostone, brecciated, brecciated chert fragments, caused by fault striking approximately N 60° E, same fault as seen at unit 44 | 2.0 | 66.4 |
| 61 | Dolostone, burrowed, small thrombolite mounds | 0.8 | 64.4 |
| 60 | Dolostone, cryptalgal laminated, doming to LLH stromatolites | 0.2 | 63.6 |

| | | | |
|---|---|---|---|
| 59 | Dolostone, burrowed | 2.0 | 63.4 |
| 58 | Dolostone, burrowed, scattered thrombolite mounds, 0.1 m across, coalescing into short rows | 2.2 | 61.4 |
| 57 | Dolostone, dolomitized intraclastic grainstone | 0.2 | 59.2 |
| 56 | Dolostone, burrowed, probable thrombolite mounds | 1.5 | 59.0 |
| 55 | Covered | 0.4 | 57.5 |
| 54 | Dolostone, burrowed, scattered thrombolite mounds, possible Renalcis heads | 2.0 | 57.1 |
| 53 | Dolostone, cross-laminated | 0.4 | 55.1 |
| 52 | Dolostone, thrombolite mounds, possible Renalcis heads, small SH stromatolites, burrowed matrix | 1.2 | 54.7 |
| 51 | Dolostone, cross-laminated | 0.2 | 53.5 |
| 50 | Boundstone, thrombolite mounds, probable Renalcis heads forming mounds, fossiliferous, dolomitized grainstone halos around mounds | 5.0 | 53.3 |
| 49 | Dolostone, intraclastic, cryptalgal laminated | 0.1 | 48.3 |
| 48 | Dolostone, burrowed, scattered thrombolite mounds | 2.0 | 48.2 |
| 47 | Dolostone, burrowed, scattered thrombolite mounds 1 m thick and across, dolomitized grainstone channels | 2.2 | 46.2 |
| 46 | Dolostone, burrowed, layer of blocky angular intraclasts from in situ brecciation of underlying bed | 1.0 | 44.0 |
| 45 | Dolostone, omission surface of blocky angular intraclasts from underlying unit | 0.1 | 43.0 |
| 44 | Dolostone, burrowed, base faulted, striking N 63° E | 2.0 | 42.9 |
| | Unit 43 continues northeastward to Ope Bay as a gently dipping pavement at the top of the sea cliff with little appreciable gain in thickness. Section is resumed at Boat Head; probably strata are removed by faulting in Ope Bay | | |
| 43 | Dolostone, burrowed, scattered thrombolite mounds | 1.0 | 40.9 |
| 42 | Dolostone, burrowed | 2.0 | 39.9 |
| 41 | Dolostone, wavy cryptalgal laminated, doming to low-relief LLH stromatolites | 0.2 | 37.9 |
| 40 | Dolostone, burrowed | 2.4 | 37.7 |

| | | | |
|---|---|---|---|
| 39 | Dolostone, wavy cryptalgal laminated, doming to low-relief LLH stromatolites, chert nodules | 0.2 | 35.3 |
| 38 | Dolostone, burrowed | 1.6 | 35.1 |
| 37 | Dolostone, thinly bedded, scour and fill structures | 0.8 | 33.5 |
| 36 | Dolostone, burrowed, pseudobreccia vugs with internal dolostone sediment | 1.0 | 32.7 |
| 35 | Dolostone, thinly bedded, cryptalgal lamination, scour and fill structures | 0.2 | 31.7 |
| 34 | Dolostone, thinly bedded, oolitic, chert beds and nodules | 0.2 | 31.5 |
| 33 | Dolostone, burrowed | 2.4 | 21.3 |
| 32 | Dolostone, thinly bedded, scour and fill structures | 0.5 | 26.9 |
| 31 | Dolostone, burrowed | 0.6 | 26.4 |
| 30 | Dolostone, thinly bedded, scour and fill structures | 0.5 | 25.8 |
| 29 | Dolostone, burrowed | 0.6 | 25.3 |
| 28 | Dolostone, thinly bedded, scour and fill structures, scattered bioturbation, cherty bed | 1.6 | 24.7 |
| 27 | Dolostone, cryptalgal laminated | 0.4 | 23.1 |
| 26 | Dolostone, cryptalgal laminated, intraclastic, low-relief LLH stromatolites, intraclastic, oolitic | 0.2 | 22.7 |
| 25 | Dolostone, thinly bedded, scour and fill structures, scattered bioturbation | 1.2 | 22.5 |
| 24 | Covered | 3.0 | 21.3 |
| 23 | Dolostone, thrombolite mounds, 0.4 m thick, capped by SH stromatolites | 2.5 | 19.3 |
| 22 | Dolostone, thinly bedded, scour and fill structures, current laminated, scattered bioturbation, white sparry dolomite vugs containing large quartz crystals | 1.3 | 16.8 |
| 21 | Dolostone, cryptalgal laminated | 0.8 | 15.5 |
| 20 | Covered | 1.0 | 14.7 |
| 19 | Dolostone, scattered thrombolite mounds, chert nodules | 0.7 | 13.7 |
| 18 | Dolostone, possible omission surface of angular fragments derived from unit 17 | 0.1 | 13.0 |

| | | | |
|---|---|---|---|
| 17 | Dolostone, scattered thrombolite mounds 0.7 m thick and 0.3 m wide | 0.7 | 12.9 |
| 16 | Dolostone, cryptalgal laminated, intraclasts, badly preserved gastropods | 0.1 | 12.1 |
| 15 | Dolostone, scattered thrombolite mounds | 1.1 | 12.0 |
| 14 | Dolostone, possible omission surface of angular fragments derived from unit 13 | 0.2 | 10.9 |
| 13 | Dolostone, thinly bedded, scour and fill structures | 0.6 | 10.7 |
| 12 | Dolostone, cryptalgal laminated, mudcracks | 0.6 | 10.1 |
| 11 | Covered | 5.0 | 9.5 |
| 10 | Dolostone, tall aberrant vertically laminated columnar stromatolites, with unlaminated cores | 1.2 | 4.5 |
| 9 | Dolostone, thinly bedded, intraclastic | 0.2 | 3.3 |
| 8 | Covered | 1.0 | 3.1 |
| 7 | Dolostone, cryptalgal laminated, oolitic and cherty at top | 0.2 | 2.1 |
| 6 | Dolostone, thinly bedded, scour and fill structures | 0.4 | 1.9 |
| 5 | Dolostone, intraclastic | 0.2 | 1.5 |
| 4 | Dolostone, burrowed, thinly bedded | 0.4 | 1.3 |
| 3 | Dolostone, cryptalgal laminated | 0.2 | 0.9 |
| 2 | Dolostone, intraclastic | 0.2 | 0.7 |
| 1 | Dolostone, burrowed, thinly bedded | 0.5 | 0.5 |

000194

CENTRE FOR NFLD. STUDIES
OCT 5 1981
MEMORIAL UNIVERSITY
OF NEWFOUNDLAND

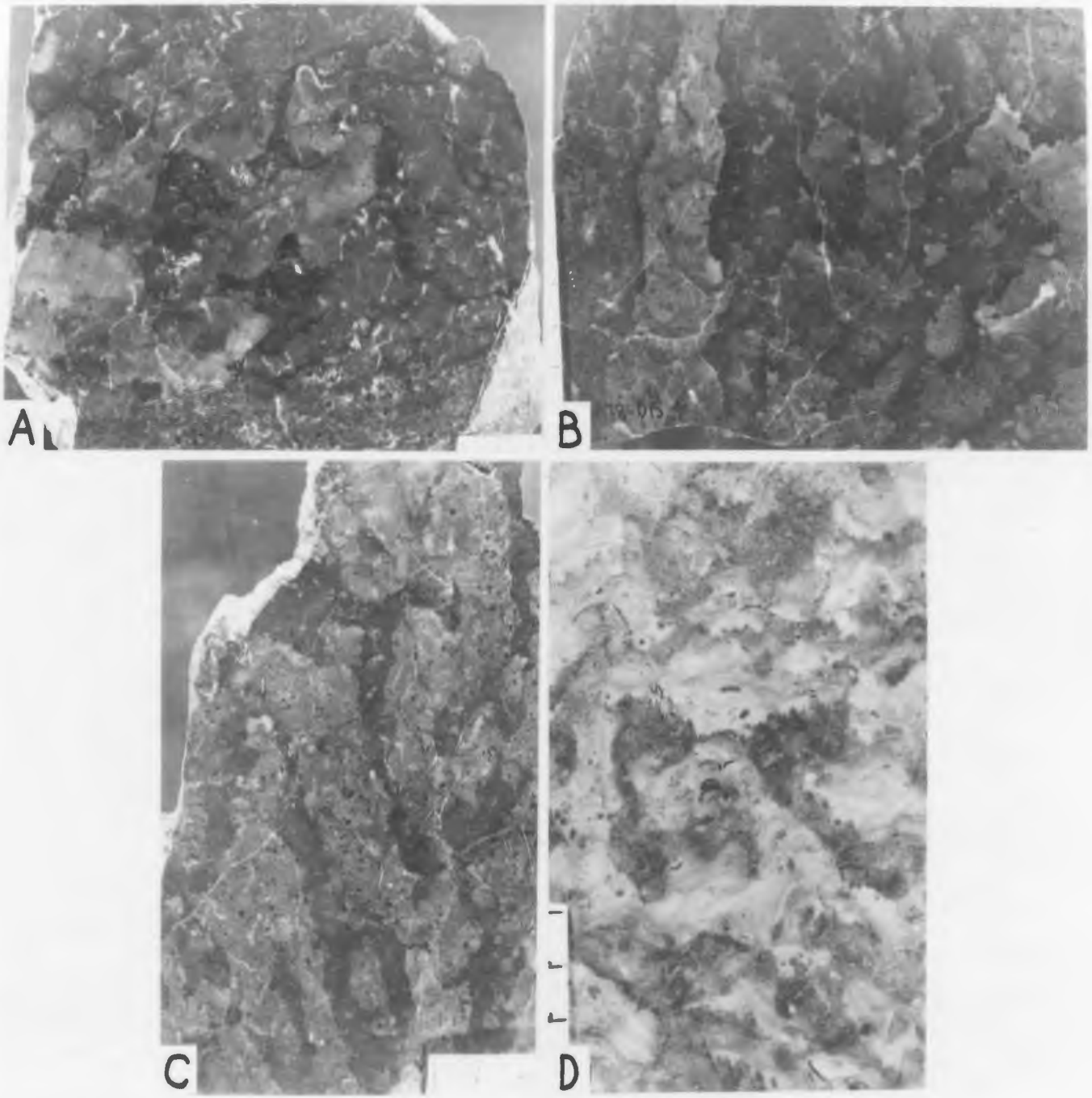
A
B
C
D